Improved dendritic cell therapy for cancer by enhancing *in vivo* lymph node migration using a novel chemokine-based sorting method

Paul Burgoyne

A thesis submitted to the College of Medicine, Veterinary and Life Sciences, University of Glasgow in fulfilment of the requirements for the degree of Doctor of Philosophy

August 2018

Institute of Infection, Immunity and Inflammation
College of Medical, Veterinary and Life Sciences
University of Glasgow

Abstract

Dendritic cells (DCs) are potent antigen presenting cells and are crucially involved in the induction of the adaptive immune response. Multiple DC subsets exist in the body at rest and during inflammation with unique tissue origins and development. The main function of DCs is the uptake of antigen from the peripheral tissue by endocytosis, and the transfer of this antigen to T cells within the lymph nodes (LNs) to generate an immune response against the antigen. Given the potency of the potential T cell response, DCs are an attractive cell type for therapeutic use in contexts such as cancer. Over 20 years of clinical trials have developed DCs for this purpose: although significant progress has been made, DC clinical trials still show subclinical and variable T cell responses in patients. Numerous strategies have been tested to improve this, including use of specific DC subsets, *ex vivo* activation and maturation of the cells using cytokines, different antigen loading strategies and different routes of injection. These, however, do not sufficiently take into consideration the migration capability of these injected cells, which severely limits the potential cell function.

CCR7 is the chemokine receptor crucially involved in DC homing to LNs and is a marker of DC maturity, but it has been shown that *ex vivo*-generated cells do not consistently express this receptor. Using a novel sorting methodology to isolate DCs expressing CCR7, it is possible to improve the maturity and function of the injected cells, as well as *in vivo* migration. CCR7-expressing cells are more capable of generating mature T cell responses *in vitro* due to the expression of co-stimulatory molecules such as CD80 and CD86 and the production of T cell-attracting chemokines. The B16F10 mouse melanoma was used to assess the potential improvement in therapeutic DC use following CCR7-sorting. In the subcutaneous model after a single injection, or multiple prophylactic injections, of CCR7-sorted DCs there was significant control of the tumour growth and this resulted in a longer survival duration. This was attributed to the increased T cell response induced by DCs reaching the LN, as more antigen-specific T cells were present in the CCR7-expressing DC-receiving animals and that the T cell phenotype was more mature by surface marker expression. In the metastatic model, however, there was no difference in the overall tumour burden between groups despite having a significantly improved antigen-specific T cell response following injection of the CCR7-sorted DCs. Finally, it was shown that this CCR7-sorting methodology is directly translatable to clinical use using the clinical grade MACSQuant Tyto cell sorter, and that CCR7-sorted human monocyte-derived DCs were also more potent activators of T cells *in vitro*.

Table of Contents

List of Tables

List of Figures

Author's Declaration

I declare that the work described in this thesis is original and was generated as a result of my own work. No part of this thesis has been submitted for any other degree, either at the University of Glasgow, or at any other institution.

Signature: ………………………………….

Printed name: ………………………………….

Acknowledgements

I would firstly like to thank my supervisors Professor John Campbell and Professor Gerry Graham for this opportunity and for your endless support along the way. I'm so grateful for everything I've been able to do during my time in Glasgow, thank you for the encouragement. John, you've always been an inspiration to me as a scientist and mentor - I am satisfied with my care. Please remember this when you start to regret employing Kayleigh and me together again.

To Kayleigh: know that meeting you has irreparably changed my life. I could write a thesis about all the ways you've helped me in the last four years (and I could fill at least ten with embarrassing stories), but I'll try to keep it short: thank you for giving me strength when I had none left - I can't wait until we rule the world. The next round of cucumber beers is on me!

To all the people I've worked with, not just in the CRG but on the whole of level 3: you are among the nicest, kindest people I've ever had the pleasure to meet. My friends in the CRG, in particular: Doug and Gill, for your guidance, adorable children and melting my heart by calling me Uncle Paul; Marieke, you are a queen for the people; Fabian, I adore you and can't wait to read your memoirs; and Frankie for dragging me out of the lab and into triathlon training. To the Thursday club, Jenny and Trish, if I could live these last three years on repeat (and not be killed at the end every time), I obviously would. Although we're split three ways across the world, remember that without the strength of our friendship we would still be stuck in that tomb in Egypt giving each other curly blow-dries to pass the time.

Thank you to my colleagues in the SNBTS, who've supported me through the majority of my academic life and (I hope!) will continue to now I'm a postdoc. I have to thank Rachel for her endless hours of work helping me sort and phenotype cells, and for only once requiring literal bribery to do so. Truly I am so grateful for all the time you gave to this project and my many side projects.

Thank you to my family for never really understanding what I do but listening intently when I describe it, and for literally never being able to explain it correctly to other people. Thank you, Dad, for understanding my passion for work and not being overly concerned

when I work the occasional 70hr week. Thank you, Mum, for being concerned when I needed it most, for feeding me when I forgot to eat and for the endless cups of tea.

Thank you finally to Alan for all your help in this last year. You've been an incredible help and I can't imagine having gone through this without you. Thank you for wanting to be with me even though I act like this and thank you especially for not strangling me in my sleep: I know you were tempted. I've been a nightmare, but I'll make it up to you for the rest of my life, I promise. Also, surprise to the people who didn't know we were together!

Definitions/Abbreviations

APC(s)	Antigen-presenting cell(s)
APC*	Allophycocyanin (fluorophore)
BCA	Bicinchoninic acid
BCMA	B cell maturation antigen
BMDC(s)	Bone marrow dendritic cell(s)
BSA	Bovine serum albumin
CAR	Chimeric antigen receptor
cART	Combined antiretroviral (drug) therapy
CD	Cluster of differentiation
cDC(s)	Conventional dendritic cell(s)
cDNA	Complementary deoxyribonucleic acid
CDP	Common dendritic cell precursor
cMoP(s)	Common monocytic progenitor(s)
CMV	Cytomegalovirus
ConA	Concanavalin A
CR	Complete remission
CSC(s)	Cancer stem cell(s)
CT	Cycle threshold (in QPCR assays)
CTL(s)	Cytotoxic T lymphocyte(s)
CTLA-4	Cytotoxic T-lymphocyte antigen 4
DAMP(s)	Damage-associated molecular pattern(s)
DAPI	4'-6'-diamidino-2-phenylindole
DC(s)	Dendritic cell(s)
DMEM	Dulbecco's minimal essential medium
DMSO	Dimethylsulphoxide
DNA	Deoxyribonucleic acid
DPX	Di-n-butyl phthalate in xylene
dsDNA	Double-stranded deoxyribonucleic acid
DTH	Delayed-type hypersensitivity
EBV	Epstein-Barr virus
ECM	Extracellular matrix
EDTA	Ethylenediaminetetraacetic acid
EFα	Elongation factor alpha
EMP(s)	Embryonic macrophage-erythrocyte precursor(s)
EMT	Epithelial-to-mesenchymal transition
ER	Endoplasmic reticulum
FACS	Fluorescence activated cell sorting

FCS	Foetal calf serum
Flt3-L	FMS-like tyrosine kinase-3 ligand
FMO	Fluorescence minus one
FSC	Forward scatter
GEMM(s)	Genetically engineered mouse model(s)
GFP	Green fluorescent protein
GM-CSF	Granulocyte macrophage-colony stimulating factor
GMP	Good manufacturing practice
GPCR(s)	G-protein coupled receptor(s)
H&E	Haematoxylin & eosin
HEPA	High-efficiency particulate arrestance
HEV(s)	High endothelial venule(s)
HIV	Human immunodeficiency virus
HLA	Human leukocyte antigen
HSCT	Haematopoietic stem cell transplant
ICOSL	Inducible T cell co-stimulator ligand
IDO	Indoleamine 2,3-dioxygenase
IF	Immunofluorescence (staining)
IFN	Interferon
IL	Interleukin
iLN	Inguinal lymph node
IMS	Industrial methylated spirits
IV	Intravenous
KLH	Keyhole limpet hemocyanin
LC(s)	Langerhans cell(s)
LLC	Lewis lung carcinoma
LN(s)	Lymph node(s)
LPS	Lipopolysaccharide
MAGE	Melanoma-associated antigen
MART-1	Melanoma-associated antigen recognized by T cells
MCM	Monocyte-conditioned media
M-CSF	Macrophage-colony stimulating factor
MDP(s)	Macrophage/dendritic cell precursor(s)
MEM	Minimal essential medium
MFI	Mean fluorescence intensity
MHC class I	Major histocompatibility complex class I
MHC class II	Major histocompatibility complex class II
mLN	Mediastinal lymph node
MoDC(s)	Monocyte-derived dendritic cells

MRI	Magnetic resonance imaging
NK	Natural killer
n-PEG	Polyethylene glycol (where *n* is the number of repeating structural units)
NTC	No template control (in QPCR assays)
NY-ESO-1	New York esophageal squamous cell carcinoma 1
OCT	Optimal cutting tissue
OR	Objective response
ORR	Objective response rate
OS	Overall survival
OVA	Ovalbumin
PAP	Prostatic acid phosphate
PBMC(s)	Peripheral blood mononuclear cell(s)
PBS	Phosphate-buffered saline
PCR	Polymerase chain reaction
PD	Programmed cell death
pDC(s)	Plasmacytoid DC(s)
PE	Phycoerythrin
PEB	Phosphate-buffered saline with 2mM ethylenediaminetetraacetic acid and 0.5% bovine serum albumin
PEG	Polyethylene glycol
PFA	Paraformaldehyde
PGE2	Prostaglandin E2
pLN	Popliteal lymph node
PolyI:C	Polinosinic:polycytidylic acid
PRR(s)	Pattern recognition receptor(s)
PyMT	Polyomavirus middle T
QPCR	Quantitative polymerase chain reaction
RBC(s)	Red blood cell(s)
RECIST	Response Evaluation Criteria in Solid Tumours
RNA	Ribonucleic acid
RPMI	Roswell Park Memorial Institute (medium)
RT	Reverse transcription
SAPE	Streptavidin-conjugated phycoerythrin
SLO(s)	Secondary lymphoid organ(s)
SNP(s)	Single nucleotide polymorphism(s)
SSC	Side scatter
STWS	Scotts tap water substitute
TAA(s)	Tumour-associated antigen(s)
TAE	Tris acetate ethylenediaminetetraacetic acid (buffer)
TAM(s)	Tumour associated macrophage(s)

TCR(s)	T cell receptor(s)
TGF-β	Transforming growth factor-beta
Th	T helper (cells)
TIL(s)	Tumour-infiltrating lymphocyte(s)
TLR(s)	Toll like receptor(s)
TME	Tumour microenvironment
TNFα	Tumour necrosis factor alpha
Treg(s)	T regulatory cell(s)
UV	Ultraviolet
VEGF	Vascular endothelial growth factor

Chapter 1

Introduction

1.1 Overview

The aim of this thesis is to investigate the mechanisms involved in dendritic cell (DC) migration, and in particular the expression of the chemokine receptor CCR7. This introduction will first discuss dendritic cell development, migration and function and the role that CCR7 plays in these. It will then discuss the development of tumours, in particular the immunological aspect of this process and why targeting the immune system is a viable route for therapy. Lastly, the current state of DC clinical use will be discussed in the context of cancer therapy with the potential improvements which could be made to DC therapies to increase their clinical efficacy.

1.2 Dendritic cells

DCs are the most potent antigen presenting cells (APCs) in the body and mediate the adaptive immune response between inflammation and tolerance. Since their discovery by Steinman and Cohn in the 1970s, several distinct subsets of DCs have been characterised (Steinman and Cohn, 1973). DCs can be identified by their expression of the haematopoietic lineage marker cluster of differentiation (CD) 45, major histocompatibility complex (MHC) class II, and CD11c in both mice and humans. DCs are environmental sensors: involved in the sampling and uptake of antigen in peripheral tissues and transfer of this antigen to secondary lymphoid organs (SLOs) such as the lymph nodes (LNs) by presentation to T cells, B cells and natural killer (NK) cells (Schmid *et al.*, 2000). Since their first description in the 1970s, DCs have been identified in almost all tissues in the body. Under homeostatic conditions, uptake of antigen from barrier tissues such as the skin and gut leads to the development of immune tolerance. This suppresses T cell responses to innocuous antigens from food or commensal microorganisms (Marelli-Berg *et al.*, 2008). In comparison, with accompanying inflammation such as infection or cancer, presentation of antigen can instead induce an immunogenic T cell response. While particular DC subsets are specialised for a role in homeostasis, including Langerhans cells (LCs), conventional DCs (cDCs) and plasmacytoid DCs (pDCs), most DC subsets can contribute to an inflammatory response and include 'emergency' monocyte-derived DCs (MoDCs). Ontogeny and function of these cells will be described in this section.

1.2.1 Development of DC subsets

1.2.1.1 Langerhans cells

The earliest appearance of cells in the body which resemble DCs is during embryonic development. LCs are exceptional among DC subsets, being derived by primitive myelopoiesis from the yolk sac and foetal liver (Romani *et al.*, 2003). Early embryonic macrophage-erythrocyte precursors (EMPs) respond to signals from interleukin (IL) -34 using the macrophage-colony stimulating factor (M-CSF) receptor during early embryonic development (Wang *et al.*, 2012). Since EMPs also give rise to tissue-specific macrophages during embryogenesis, there has been significant debate on whether LCs represent a tissue-specific macrophage or DC. The LC population is maintained by a pool of local self-renewing precursors in the dermis with some contribution of bone marrow-derived cells at rest (Kissenpfennig and Malissen, 2006). These precursors in the skin, explored in adoptive transfer studies using the Id2-/- knockout mice which prevent development of cells expressing the conventional LC marker langerin, are replaced by short-term monocyte-derived LCs (Seré *et al.*, 2012).

During homeostasis, LCs reside in the stratified epithelium of tissues such as the epidermis, cornea, oral cavity, esophagus and vagina in an immature state, and comprise between 2-3% of the total cells in these tissues. LCs have been historically identified in the tissue by the expression of the C-type lectin langerin, but also express E-cadherin, CD1a and CD1c; and lack the typical monocyte marker CD14 (Larregina *et al.*, 2001). The 'LC paradigm' describes the role of LCs in surveillance of the tissue; where they recognise potential exposure to pathogens through uptake and transfer of antigens to T cells in the cutaneous-draining LNs. Integration of pathogen antigens and inflammatory context of the tissue allows LNs to effectively instruct the magnitude and phenotype of the adaptive response to the antigen (Villadangos and Heath, 2005). In the absence of inflammation, LCs promote immune tolerance, but have been shown to be able to prime cytotoxic T cell responses in response to tissue inflammation (Kissenpfennig and Malissen, 2006).

While the phenotypic identity of LCs remains controversial, cell function more closely aligns them with true DCs than macrophages. As discussed, LCs uptake antigen in the periphery, undergo a classic maturation protocol resulting in migration to the LNs, and present antigen to T cells during both normal homeostasis and inflammatory conditions. This functionally aligns them with other DC subsets. Hierarchical clustering studies also align LCs with other conventional DC subsets by transcriptional profile (Carpentier *et al.*,

2016). In addition to this, it will be shown that LCs can be used for this purpose in a clinical context.

1.2.1.2 Conventional DCs

Conventional, or myeloid DCs (cDCs) are a population of blood-borne DCs which circulate both lymphoid and nonlymphoid tissue during homeostasis. cDCs are produced by the bone marrow, through definitive myelopoiesis from macrophage/dendritic cell precursors (MDPs). Signaling through FMS-related tyrosine kinase 3 ligand (Flt3-L) in the bone marrow microenvironment commits MDPs to the common dendritic cell precursor (CDP) lineage. This gives rise to both cDC1 and cDC2 subsets through a common pre-cDC precursor stage following granulocyte macrophage colony stimulating factor (GM-CSF) (Lutz *et al.*, 2017).

cDC1 and cDC2 subsets can be distinguished by surface marker expression, which in mice are CD103 and CD11b, respectively. In humans the same subset can be distinguished by CD141 and CD1c expression, respectively. CD103+ cDCs are present primarily in connective tissues, and express additional markers depending on the tissue in which they reside. In the Peyer's patches, lymphoid organs in the intestine, CD103+ cDCs express CD8 and relatively low levels of MHC class II (Varol *et al.*, 2009). In the lamina propria of the intestine, however, CD103+ cDCs coexpress CD11b. In other epithelial tissues such as the dermis of the skin, CD103+ cDCs can also express langerin (Merad, Ginhoux and Collin, 2008). CD11b+ cDCs are comprised of both true tissue cDCs and macrophages due to the expression of CD11b, although other markers such as CD64 can be used to distinguish the two in tissues such as the muscle (Langlet *et al.*, 2012).

Nonlymphoid cDCs in these tissues constantly migrate through the tissue to collect antigens and integrate inflammatory cues within the microenvironment to cells in the tissue-draining LNs (Randolph, Angeli and Swartz, 2005). This migration occurs in both the steady state and during inflammation, although uptake of antigen in the context of tissue inflammation highly upregulates MHC class II and T cell co-stimulatory molecules and produce inflammatory cytokines to induce a potent adaptive immune response. Significant experimental evidence suggests that cDCs may be superior at these processes than other DC subtypes (Villadangos and Schnorrer, 2007).

1.2.1.3 Plasmacytoid DCs

pDCs originate from myeloid and lymphoid precursors in the bone marrow, although the myeloid CDP lineage is the predominant mechanism. Along with Flt3-L, the transcription factor E2-2 favours the development of pDCs from CDP precursors (Cisse *et al.*, 2008). These cells can be identified by their unique surface marker profile; expressing CD4, CD303 (also known as BDCA2) and relatively low levels of CD11c (Cao, 2009). Unlike cDCs which at least partly develop during dissemination into tissues, pDCs exit the bone marrow as fully developed cells (Shortman and Naik, 2007). In the steady state, pDCs circulate the body through the blood and lymphoid organs, and can be detected in the LNs, spleen and thymus at rest (Takeuchi and Furue, 2007).

pDCs also express toll like receptors (TLRs) 7 and 9, which are specifically involved in recognition of viral RNA and DNA. While they make up only 0.2-0.5% of cells in the peripheral blood at rest, pDCs produce almost 95% of the total Type I interferon (IFN) (also known as IFNα) by PBMCs (Siegal *et al.*, 1999) to generate an antiviral defence. Antigen-inexperienced pDCs are already primed to respond rapidly upon detection of viral antigens, with IFN-production preceding maturation of the DC through production of IFNα. After exposure to antigen, pDCs undergo a classic DC maturation which includes upregulation of MHC class I and II and T cell costimulatory molecules, but lose the capacity to produce Type I IFN (Sozzani *et al.*, 2010). Mature pDCs are phenotypically and functionally comparable to cDCs (Grouard *et al.*, 1997; Shortman and Naik, 2007).

1.2.1.4 Monocyte-derived DCs

MoDCs, or inflammatory DCs, are a transient DC population derived by monocytic precursors in the blood or by emergency myelopoiesis from the bone marrow. As such, they are present in the blood at extremely low numbers at rest, but are detectable at a low level in the epithelia and mucosa (Jakubzick *et al.*, 2013). Unlike other DC subsets, which require the Flt3-L growth factor for development, Flt3-L and its receptor Flt3 are dispensable for development of MoDCs (Mckenna *et al.*, 2000). Instead, monocytes develop from common monocytic progenitors (cMoP) in the bone marrow using M-CSF and GM-CSF (Lutz *et al.*, 2017). While GM-CSF knockout mice display no loss of MoDC generation or function *in vitro*, the deficiency of the M-CSF receptor significantly impairs this (Greter *et al.*, 2012). In humans however, MoDCs do not require M-CSF for differentiation from PBMCs *in vitro*, making the role of these two growth factors difficult to fully elucidate (Lutz *et al.*, 2017).

Although the phenotype of MoDCs is likely context dependent, murine inflammatory DCs can be identified by expression of CD11b, MHC class II and intermediate levels of CD11c in addition to the Ly6C monocyte marker (Domínguez *et al.*, 2010). Extravasation into inflamed tissues downregulates Ly6C expression, making them difficult to distinguish from CD11b cDCs *in situ*. Inflammatory and infectious stimuli recruit monocytes into tissues, which can then differentiate into inflammatory DCs and can migrate to LNs and prime T cell responses (Zigmond *et al.*, 2012). Since monocytes can also give rise to macrophages under the appropriate conditions, there is a significant transcriptional overlap between MoDCs and macrophages, but functionally this results in a more versatile T cell stimulatory capacity in MoDCs than subsets of cDCs (Lutz *et al.*, 2017)

1.2.1.5 Summary

A summary of the development and function of LCs, cDCs, pDCs and MoDCs is shown in **Figure 1.1**, below.
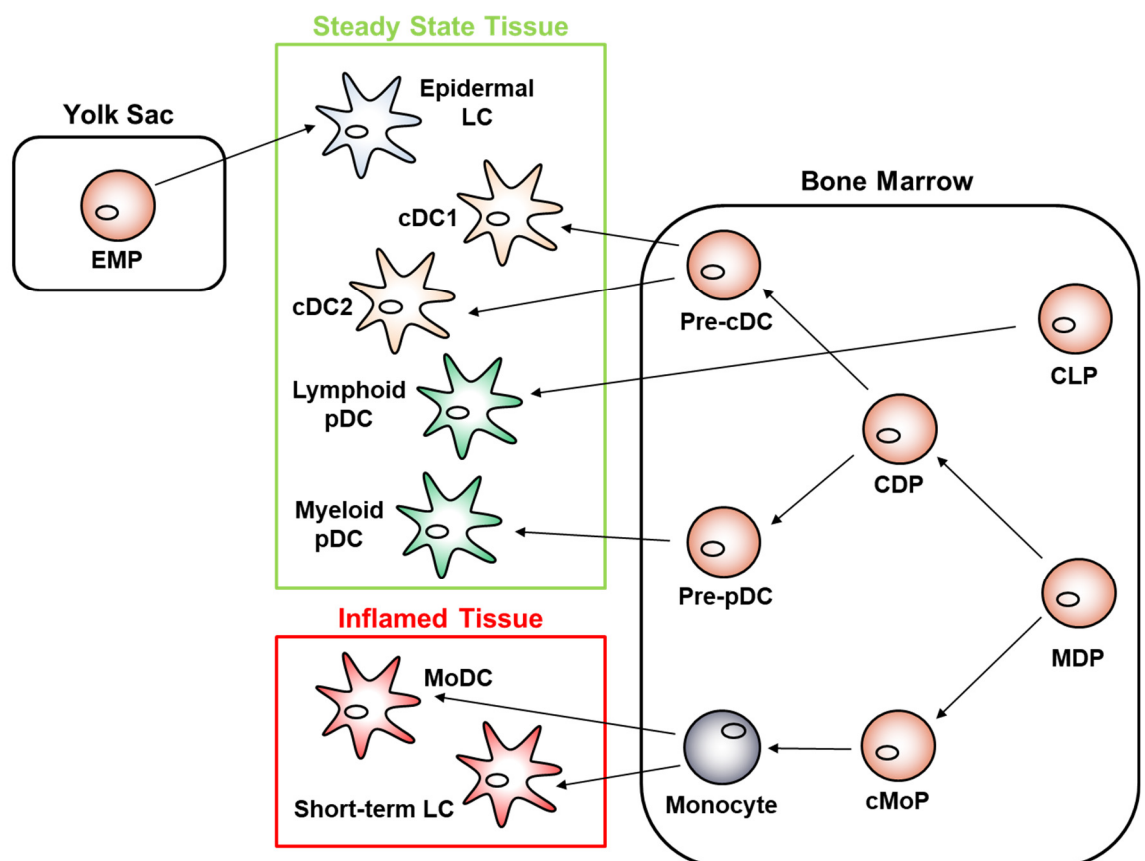
Figure 1.1 - Development of DC subsets from embryonic and adult tissues.
Abbreviations: cDC = conventional DC; CDP = common DC precursor; CLP = common lymphoid progenitor; cMoP = common monocyte precursor; LC = Langerhans cell; MDC = macrophage and DC precursor; MoDC = monocyte-derived DC; pDC = plasmacytoid DC (Adapted from: Lutz *et al.*, 2017).

1.2.2 Antigen uptake and presentation

DCs are the most potent APC in the body and can uptake antigens for presentation using a number of different mechanisms. Uptake of self or non-self antigens is followed by processing of the antigen by intracellular mechanisms and loading of the processed antigens onto MHC molecules presented on the cell surface. MHC molecules are subdivided into MHC class I and MHC class II, which are differentially expressed by DC subsets and stages of maturity, as described previously. DCs are capable of responding to a number of different potential antigen types, including pathogenic microorganisms, macromolecules such as proteins and other soluble antigens, and even cells undergoing apoptosis (Guermonprez *et al.*, 2002). Maturation of DCs involves downregulation of endocytosis to modulate the uptake of further antigens after activation and during migration (Kamphorst *et al.*, 2010).

Immature DCs exhibit the most variety in antigen uptake mechanisms, although these are modulated during maturation. Nonspecific antigen uptake is possible by macropinocytosis, where DCs can rapidly sample surrounding fluid and internalise it through macropinosomes (West *et al.*, 2000). Although significant *in vitro* evidence exists to support this phenomenon, its *in vivo* relevance is unclear as the majority of DC subsets sample antigen in the tissue with limited extracellular fluid. Phagocytosis is triggered by engagement of complement receptors, integrins or surface molecules such as CD36 for uptake of microorganisms, macromolecules and dying cells with varying efficiency between DC subsets (Guermonprez *et al.*, 2002). Both pinocytosis and phagocytosis require intracellular actin polymerisation and membrane ruffling for the formation of vacuoles containing the antigen.

Receptor-mediated endocytosis is another method of endocytosis which requires the expression of surface receptors such as lectins, scavenger receptors and pathogen receptors. Langerin, for example, is a C-type lectin expressed on LCs is a surface receptor used for phagocytosis (Valladeau *et al.*, 2000). Expression of langerin creates the characteristic LC organelle known as Birbeck granules, which improve capture and processing of antigens. In contrast to phagocytosis, expression of receptors involved in receptor-mediated endocytosis signal vesicle formation for internalisation through clathrin-coated pits (Slepnev and De Camilli, 2000).

After uptake of antigen, DCs must present this antigen in the context of MHC molecules on the cell surface to induce a T cell response in the LNs. DCs must therefore migrate from the site of the antigen uptake to the LNs, which they can do by entry into the lymphatics, or from the circulation.

1.2.3 DC migration

1.2.3.1 Chemokines and chemokine receptors

Migration of immune cells is crucial in developmental biology, activation of innate and adaptive immune responses, and the repair of damaged tissue (Griffith, Sokol and Luster, 2014). Leukocyte migration is primarily controlled by chemokines which are small molecules which orchestrate immune cell migration and positioning within the body. Almost 50 functional chemokines are functionally divided into two groups: inflammatory and homeostatic (Rot and von Andrian, 2004). Expression of the inflammatory, or inducible, chemokines is triggered through local release of inflammatory cytokines such as IFNγ and tumour necrosis factor alpha (TNFα) (Rollins, 1997), but can be triggered by infection, chronic tissue inflammation and autoimmunity (Gerard and Rollins, 2001). Many of these chemokines are also produced homeostatically by secretion from barrier tissues as a component of sweat, saliva and tears, which may take advantage of natural antimicrobial properties of chemokines such as CCL28 (Hieshima *et al.*, 2003; Söbirk *et al.*, 2013). The homeostatic chemokines, on the other hand, are expressed constitutively at discrete, typically lymphoid, sites within the body. Their expression allows migration of leukocytes within the lymphatic system, and is crucial for the development of primary, secondary and tertiary lymphoid structures (Ansel and Cyster, 2001). This group of chemokines, however, can also be upregulated during inflammation (Rot and von Andrian, 2004).

Chemokines exert their function through interaction with specific G-protein-coupled receptors (GPCRs) expressed on the surface which have seven transmembrane-spanning domains. There are 19 known chemokine receptors, which bind and internalise chemokines, and signal β-arrestin recruitment and typical downstream signalling for GPCRs (Zlotnik and Yoshie, 2000). There are also 5 'atypical' chemokine receptors, which bind chemokines but are defined by their lack of subsequent signalling; this allows the receptors to act as chemokine scavengers. Cells which express these receptors can sequester chemokines by internalisation; reducing local chemokine availability and thus controlling the course of an inflammatory response (Nibbs and Graham, 2013). Given that

very few chemokines interact exclusively with one receptor, this implies the binding of each chemokine to multiple receptors and therefore the ability to signal cell types with differential receptor expression, as well as to signal the same cell through different receptors. Although this would suggest a significant amount of redundancy within the system, studies using individual receptor knockout cells and neutralising antibodies have shown otherwise (Weber *et al.*, 2001; Zernecke *et al.*, 2006). Signalling through CCR7 will be discussed here; and is one of the best examples of differential signalling by the chemokines CCL19 and CCL21 acting through the same receptor.

Chemokines play a crucial role in the development of DCs. Signalling by receptor ligation does not appear to directly induce cellular differentiation in DCs, unlike T cells, which can use CCR2 and CXCR3 as differentiation signals (Luther and Cyster, 2001; Kurachi *et al.*, 2011), and non-haematopoietic cells such as astrocytes through CXCL12/CXCR4 interactions (Bajetto *et al.*, 2001). However, guiding the migration of haematopoietic cells to the microenvironments capable of supporting particular differentiation pathways is a potential indirect method by which chemokines control differentiation. Monocytes express classical inflammatory receptors including CCR1, CCR2 and CCR5 and use these to exit the vasculature into inflamed tissue (Vanbervliet *et al.*, 2002). These cells can go on to differentiate into inflammatory MoDCs in response to cytokines, and sample antigens present in the tissue, which triggers a downregulation of these chemokine receptors and a reciprocal upregulation of CCR7 (Sallusto *et al.*, 1998). Mature DCs, including MoDCs but also LCs and cDCs, can then respond to CCR7 ligands expressed by the lymphatic vasculature, allowing the cells to exit the inflamed tissue and move to the LNs where they can interact with T cells and facilitate the adaptive immune response (Randolph *et al.*, 1999).

1.2.3.2 Lymph node entry from the blood

pDCs have been shown to migrate directly from the blood into the LNs through specialised blood vessels known as high endothelial venules (HEVs). This haematogenous route is available almost exclusively to pDCs, and is accessed using chemokine receptors such as CCR5 and CCR7, the latter of which is expressed even on immature pDCs (Seth *et al.*, 2011). Once in the HEV, entry to the LN is achieved through expression of L-selectin (also known as CD62L) and E-selectin for attachment and to the endothelium with support of integrin ligation (Diacovo *et al.*, 2005).

1.2.3.3 Lymph node entry from the tissue

The function of DCs occurs in two stages and is regulated spatially and temporally by chemokine receptor expression. Both entry into and within the tissue is mediated by expression of chemokine receptors such as CCR1, CCR2 and CCR5 (Shi and Pamer, 2014). Antigen capture, along with inflammatory context-dependent cues induce maturation of the DC, which triggers downregulation of these chemokine receptors and upregulation of CCR7 (Sallusto, Palermo, *et al.*, 1999). Interaction of CCR7 with its ligand CCL21, produced by cells of the lymphatic vasculature, instructs DC LN migration and induces further cell activation by upregulating markers associated with T cell stimulation (Marsland *et al.*, 2005). Although both CCR7 ligands are involved in the migration of DCs to LN sinus, it has been shown in experimental models that only CCL21 is required for extravasation into the lymphatics due to its expression and presentation by lymphatic endothelial cells. CCL19, in comparison, is primarily involved in 'fine-tuning' cell migration within the LN proper (Weber *et al.*, 2013). This process is summarised in **Figure 1.2**, below.
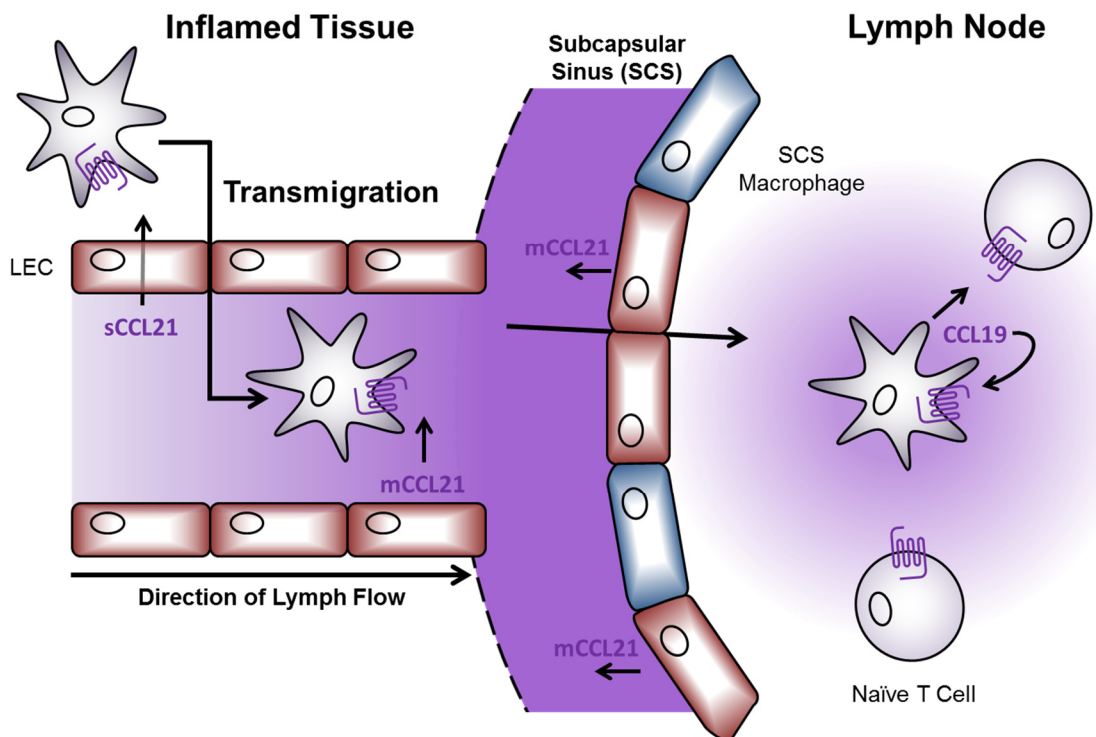
Figure 1.2 - The role of CCR7 in dendritic cell migration and function.
Mature, antigen-loaded DCs migration from the site of inflammation to the lymph nodes by transmigration into the lymphatic vessels and migration using chemotactic cues from CCL21. Once in the LN proper, DCs use CCL19 for positioning in proximity to T cells for activation.

In the absence of antigen uptake and inflammation, cells such as LCs remain restricted to the epidermis. Immature LCs constitutively express the chemokine receptor CCR6 which allows the cell to respond to CCL20 expressed by keratinocytes for intra-epidermal migration and surveillance (Spiekstra *et al.*, 2005). CCR6 expression is downregulated after antigen encounter and the induction of maturation. While migration of other DC subsets to the LNs after maturation is relatively fast, the migration of LCs to LNs is much slower. Unlike pDCs, cDCs and MoDCs which utilise CCR7 for migration to the LNs, the layered structure of the skin requires LCs to use both CXCR4 and CCR7 to access the lymphatics in a model of two-step migration (Villablanca and Mora, 2008). During LC maturation, upregulation of CXCR4 expression precedes CCR7, allowing migration from the epidermis to the dermis using CXCL12 produced by dermal fibroblasts (Ouwehand *et al.*, 2008). As CCR7 expression increases during this time, upon reaching the dermis LCs are primed to respond to lymphotactic chemokines and migrate into the lymphatic vasculature.

1.2.4 Induction of the adaptive immune response

Upon uptake of antigen and subsequent arrival in the LN microenvironment, DCs are critical for T cell activation and the development of an effector T response through induction of T helper (Th)-1, Th2, Th17 or regulator T cell (Treg) differentiation. During maturation, DCs upregulate the molecules necessary for this induction, and provide three distinct signals to T cells known as Signal 1, 2 and 3.

Antigen presentation by MHC molecules on the DC surface bind T cells which recognise the antigen through T cell receptor (TCR), which provides Signal 1. MHC class I molecules are expressed by all nucleated cells for the purpose of presenting endogenous peptides. These peptides are the result of cytosolic degradation of proteins produced by each cell and presented on MHC class I molecules by translocation into the endoplasmic reticulum (ER) (Vyas, Van der Veen and Ploegh, 2008). MHC class I-peptide complexes bind TCRs on CD8 T cells specific for the presented peptide and lead to stimulation. MHC class II presentation functions similarly to MHC class I although is primarily the role of professional APCs such as DCs. Exogenous antigens which are taken up by DCs are processed internally as described previously, and presented on MHC class II molecules through the ER (Neefjes *et al.*, 2011). MHC class II-peptide complexes bind TCRs on CD4 T cells. As DCs mature, their expression of MHC class I and II changes; MHC class I

complexes on the cell surface are rapidly replaced to reflect current antigen load, and MHC class II presentation is increased (Delamarre, Holcombe and Mellman, 2003). One other important presentation mechanism to discuss in this context is known as cross-presentation; where exogenous antigens are presented on MHC class I molecules instead (Sathe *et al.*, 2011). Most DC subsets have been shown experimentally to cross-present antigens, but cDC1s have superior cross-presentation function (Bachem *et al.*, 2010).

Upregulation of additional cell surface molecules in response to the inflammatory context allows DCs to give additional signals to T cells which can support or restrict T cell activation, which provides Signal 2. As the MHC-TCR interaction is transient, effective activation requires the integration of multiple signaling pathways through DC surface molecules. These molecules are known as co-receptors and can be broadly divided into two categories: the Ig superfamily, and the TNF receptor superfamily.

CD80 and CD86, which are expressed on the DC surface are members of the Ig superfamily, and interact with T cells through CD28 (Sharpe and Freeman, 2002). Ligation of CD28 on T cells augments the TCR signal by reducing the threshold of TCR engagement required for activation of the T cell but does not alone support phenotypic commitment of the cell (Lucas *et al.*, 1995). In addition to this, activated T cells can further respond to CD28 signaling by secretion of IL-2 which strongly supports T cell survival. In the absence of CD28 co-stimulation, T cells can become anergic, where T cells cannot effectively respond to stimulation, or undergo apoptosis (Alegre, Frauwirth and Thompson, 2001). Cytotoxic T-lymphocyte antigen 4 (CTLA-4) is another member of the Ig superfamily which, in comparison, binds CD80 with much greater affinity, but is strongly inhibitory unlike CD28. It inhibits T cell function by reducing expression of the IL-2 receptor, required for T cell survival, and arresting dividing T cells in the cell cycle (Teft, Kirchhof and Madrenas, 2006). *In vivo* ligation of CTLA-4 leads to the induction of T cell tolerance towards antigens and can programme T cell anergy and apoptosis (Greenwald *et al.*, 2001).

The TNF receptor superfamily involvement in the initiation of the T cell response is exemplified by expression of CD70, which binds CD27 constitutively expressed by naïve T cells. Interaction between CD27 and CD70 amplifies T cell activation, which shows a certain redundancy when compared to CD80/CD86, and has been shown to increase IL-2 and IFNγ production to increase cytotoxicity (Rowley and Al-Shamkhani, 2004). CD40 is another member of the TNF receptor superfamily and is an essential part of the T cell

response. In addition to stabilising the TCR for more potent cell communication, interaction of CD40 on the DC surface with CD40L (otherwise known as CD154) on the T cell surface has been shown to reciprocally activate cytokine production and co-stimulatory molecule upregulation by DCs (Elgueta *et al.*, 2013).

The secretion of pro- or anti-inflammatory cytokines by immature and mature DCs of each subset are different and are crucial in commitment to particular T cell phenotypes, which provides Signal 3. While most cytokines can support the development of the CD8 T cell response, the development of CD4 T cell subsets are cytokine-specific. IL-12, for example, is produced by cDCs activated by infectious agents and has been shown *in vitro* and *in vivo* to induce the development of T cells secreting high amounts of IFNγ for pathogen defence (Trinchieri, 2003). In particular, the IL-12p70 subunit can induce both cytotoxic (CD8) T lymphocyte (CTL) and Th1 responses which are strongly cytotoxic to pathogens and tumour cells (Zobywalski *et al.*, 2007). This has been shown to be produced by cDCs as well as MoDCs (Ratzinger *et al.*, 2004). In combination with transforming growth factor-beta (TGF-β), IL-6 has been shown to induce the development of a Th17 cell phenotype (Veldhoen *et al.*, 2006). Local IL-6 secreted by inflamed stromal tissue can be trans-presented by DCs to T cells, which requires expression of the IL-6 receptor (Heink *et al.*, 2017). Th17 cells can be identified by their production of IL-17, which is involved in the protection of mucosal barrier tissue and accumulation of neutrophils at sites of inflammation (Chen *et al.*, 2003; Liu *et al.*, 2016). In the absence of IL-6, TGF-β leads to the development of the anti-inflammatory Treg subset along with IL-2 (Golubovskaya and Wu, 2016). Unlike cytotoxic T cells, Tregs are involved in antigen tolerance and actively suppress the immune response against their cognate antigens (Jin *et al.*, 2010).

1.3 Tumour initiation and development

1.3.1 Primary tumour development

Tumour development has historically been thought to be a cell-autonomous disease, in which the driving force behind the induction and growth of the malignancy is genetic abnormality. In general, abnormalities are acquired by dividing cells, whether the cells acquire these by 'normal' means such as during cell division or are induced by infectious agents, chronic inflammatory processes, inhaled or ingested carcinogens, or even ultraviolet (UV) light (Blackadar, 2016). As a consequence of these abnormalities, cells are released from requiring extracellular control by the body and tumour development is

initiated. For many cancer types, the most common mutations are known and can be classified according to the six hallmarks of cancer, proposed by Hanahan and Weinberg (2000; revised 2011). This posits six key changes a cell must undergo for malignant growth: sustaining cell proliferation, evasion of growth suppressors, activation of invasion and metastasis, induction of angiogenesis, replicative immortality, and resistance to cell death by apoptosis (Hanahan and Weinberg, 2000).

Acquisition of these hallmark characteristics occurs differently between cancers, both in terms of the actual genetic changes and in the order in which they are acquired; in some cases, a genetic change may enable multiple capabilities simultaneously. An example of this is p53, encoded by the *TP53* gene, which is thought to be the most commonly mutated gene in human cancer (Kandoth *et al.*, 2013). p53 is a protein with potent tumour suppressor function which acts through modulation of the expression of genes involved in the repair of deoxyribonucleic acid (DNA), cell division and control of cell death by apoptosis (Carson and Lois, 1995). Both loss of this protein through mutation as well as gain-of-function mutations can lead to malignancy; resulting in changes in cell proliferation, invasion and metastasis, and angiogenesis (summarised in Muller and Vousden, 2014).

The developing tumour is comprised of more than just one proliferative mass of tumour cells. Tumours have been described as "wounds that do not heal" (Dvorak, 1987), and as such tumour growth is not tumour cell-intrinsic but is influenced by a number of cells types which are involved in wound repair and become functionally subverted by the tumour (Whiteside, 2008). After the first genetic changes that initiate tumour development, tumour-derived signals begin to affect the local stromal cells and immune cells responding to this tumour development. Fibroblasts within the tissue are normally activated during wound repair processes (Grotendorst, Rahmanie and Duncan, 2004), but this function can be subverted by tumour cells to induce remodelling of the extracellular matrix (ECM), angiogenesis or growth factor feedback loops to support tumour cell proliferation (Busch *et al.*, 2015). Cells representing the innate and adaptive immune system also respond, and include macrophages, NK cells, T cells and DCs, but also become either recruited to the tumour microenvironment (TME) or functionally suppressed (Grivennikov, Greten and Karin, 2011). Understanding and accounting for other cell types which exist in the TME is especially important in treatment success, as overlapping compensatory and tumour defence mechanisms may exist and lead to variable responses between patients.

As APCs, DCs are responsible for the induction of the adaptive immune response against developing tumours. After initial cell transformation, damage signals such as damage-associated molecular patterns (DAMPs) or cytokines can be produced which attract the attention of the innate immune system and patrolling DCs. Innate immune cells such as neutrophils and macrophages can protect against tumour development without requirement of the adaptive immune system, but this is dependent on the experimental model (Schreiber, Old and Smyth, 2011). At this stage, DCs can uptake tumour antigens and present these to T cells in the LNs. In most cases, production of IFNs and cytokines by activated cytotoxic T cells are capable of tumour elimination (Vesely *et al.*, 2011). Long-term control of tumour growth, known as the equilibrium phase, proceeds this phase if the tumour is not completely eradicated. The phase is a balance between tumour cell proliferation and destruction by the immune system, primarily mediated by T cells through production of IFNγ (Constantino *et al.*, 2017).

DCs function as immunogenic in early tumour development by presenting tumour antigens and activating tumour-specific T cell responses. In late tumour development, however, and despite their presence in the TME, antigen presentation and DC maturation becomes limited by the effect of the TME (Veglia and Gabrilovich, 2017). A number of different mechanisms contribute to this phenomenon. IL-10 produced by tumour-associated macrophages (TAMS) in the TME suppresses the maturity and production of IL-12 by DCs leading to a tolerogenic phenotype (Ruffell *et al.*, 2014). Expression of molecules like programmed cell death (PD)-1 by tumour infiltrating lymphocytes (TILs) and tumour cells themselves directly suppress DC function. Therapeutic block of either PD-1 or its ligand PD-L1 has been shown to reverse this suppressed DC phenotype and restore cytokine secretion in the TME (Salmon *et al.*, 2016). The presence of pDCs in the TME has also been shown to be immune tolerising through production of tumour-supporting T cell phenotypes through inducible T cell co-stimulator ligand (ICOSL). These cells then contribute to the suppressive TME milieu by producing cytokines such as IL-10 (Ito *et al.*, 2007).

1.3.2 Metastatic tumour development

Metastasis, the dissemination of cells from the primary tumour to a secondary site through the lymphatics or bloodstream, is a characteristic of malignant tumours and a major risk factor for cancer mortality. It is estimated that up to 90% of cancer-related deaths are caused by metastasis depending on the type of cancer (Chaffer and Weinberg, 2011). Sites

of metastasis tend to be specific to individual tumour types, such that secondary tumour sites can be predicted to a certain extent. Melanoma, for example, can readily metastasise to the lungs, brain, liver and distal skin (Eyles *et al.*, 2010); in comparison, colorectal and pancreatic cancer metastasise primarily to the liver and lungs (Nguyen, Bos and Massagué, 2009), but prostate cancer metastasis is confined to bone (Edlund, Sung and Chung, 2004). Despite some similarities in secondary site, there appear to be different genetic mechanisms directing metastases to these tissues between tumour types (Nguyen, Bos and Massagué, 2009). Temporal differences also exist between tumour types; although disseminating tumour cells can infiltrate secondary sites they may not immediately be able to successfully grow within this site. Lung cancers, for example, develop aggressive metastases quickly after diagnosis (Hoffman, Mauer and Vokes, 2000), but breast cancer metastases can present clinically years after complete remission as a result of the immune system eventually failing to control the tumour (Karrison, Donald and Meier, 1999). More effective treatments are being developed to treat primary tumours, but elimination of metastases remains challenging (Weigelt, Peterse and Veer, 2005).

To become metastatic a tumour cell must have several key characteristics, which have historically been thought to be acquired over successive mutation events but evidence from other cancer types challenges this. The process of metastasis requires local invasion of the primary tissue stroma, intravasation into the blood, survival in the blood, extravasation at the secondary site and establishment of tumour growth. The genetic changes and immune system interactions which contribute to these capabilities can be grouped into initiation, progression and virulence (Chiang and Massagué, 2008). It is likely that genetic changes supporting the invasion of tumour cells into the local stroma are maintained for infiltration of secondary sites. Changes and assistance in motility, transition of epithelial to mesenchymal cell morphology (epithelial-to-mesenchymal transition; EMT), degradation of the ECM or the process of angiogenesis can be involved in the acquisition of an invasive phenotype.

Mouse models have shown that T cells specific for the primary tumour can control dissemination of metastases and their growth in secondary sites (Eyles *et al.*, 2010). However, changes in the tumour as a result of chronic inflammation and genetic instability which lead to metastasis may affect the antigen presentation by metastatic lesions. This could be by antigen escape, where tumour cells downregulate antigen expression by presenting other antigens or through the downregulation of MHC molecules (Butterfield *et al.*, 2003; Constantino *et al.*, 2017). This limits the efficacy of pre-existing T cells,

requiring that DCs patrolling the secondary site recognise the metastatic lesion and initiate a second primary antigen response. In this late stage of tumour development however, as discussed previously, systemic immune suppression from the primary tumour may suppress this potential response (Nguyen, Bos and Massagué, 2009; Busch *et al.*, 2015).

1.4 Therapeutic use of dendritic cells

The inherent heterogeneity of tumours and tumour development between individual patients makes personalised medicine an attractive therapeutic approach. As the immune system is crucial to the anti-tumour defence, activation of the endogenous immune response or enhancing it with immune cell replacement has become a primary focus in the development of new therapies. Passive immunotherapy, such as the use of antibodies to activate immune cells or adoptive transfer of tumour-specific cytotoxic T cells, has been used successfully in several cancer scenarios (Palucka *et al.*, 2007). Although successful in the short-term, passive immunotherapy has not been shown to induce a lasting immunological response or the development of cellular memory for the target tumour associated antigens (TAAs). Active immunotherapy, in comparison, utilises antigen-loaded DC 'vaccines' to induce both a short- and long-term anti-tumour response (Boudreau *et al.*, 2009). DCs do not themselves directly target tumour cells but instead target cells of the immune system such as T cells and NK cells which are heavily involved in the anti-tumour response. Unlike conventional cancer therapies, cell vaccines may not result in significant reduction in tumour volume but instead apply an anti-tumour effect over a prolonged period of time (Gulley, Madan and Schlom, 2011).

DCs have been tested as immunotherapies in clinical trials for more than 20 years, particularly in cancer immunotherapy, primarily due their potency in processing and presenting antigens to activate T cells. The increasing understanding of DC biology during this time has been applied to clinical trials, which roughly separates them into 'generations'. The first generation of DC clinical trials used primarily patient-derived immature DCs, LCs or MoDCs from *ex vivo* culture but which were not matured before reinjection. The second generation of DC clinical trials used similar cells with addition of 'maturation cocktails' to prime DCs for function before reinjection. The third, current, generation (alternatively known as 'next generation') DC clinical trials still use these cells, but also natural DC subsets derived either in *ex vivo* cultures using specific growth factors or fully mature *in vivo* subsets derived by patient leukapheresis. The provision of antigen

to the DCs has also evolved between these generations. In this section, each generation will be summarised and the key successes for DC therapeutic use will be highlighted.

	First generation therapies	Second generation therapies	Third/Next generation therapies
Dendritic cell	• MoDCs • CD34+ cell-derived DCs • No maturation cocktail	• MoDCs Maturation cocktail e.g.: • IL-1β, TNFα, IL-6 and PGE2 • IFNγ, LPS, PolyI:C	• MoDCs • *In vivo* DCs e.g.: pDCs, cDCs Maturation cocktail (MoDCs) No maturation cocktail (pDCs, cDCs)
Cancer cell	• TAA peptides • Tumour cell lysate	• TAA peptides • Tumour cell lysate • Tumour RNA → electroporation	• TAA peptides • Tumour cell lysate • Tumour RNA → electroporation
Route of administration	Subcutaneous Intradermal	Intravenous Intranodal	Intratumoural **Combination of routes**

Figure 1.3 - Evolution of therapeutic DC use in cancer.
DC therapies can be subdivided into generations based on chronology and the prevailing trial methodology in each generation. DCs (purple) vary by source between each generation as does the use of cell maturation cocktails. Antigen from cancer cells (red) also vary by preparation between each generation. Route of cell administration doesn't necessarily change, with the same routes used in each generation. Abbreviations: cDCs = conventional DCs; IFNγ = interferon-gamma; IL-1β = interleukin-1beta; LPS = lipopolysaccharide; MoDCs = monocyte-derived DCs; pDCs = plasmacytoid DCs; PGE2 = prostaglandin E2; PolyI:C = polinosinic:polycytidylic acid; TAA = tumour associated antigen; TNFα = tumour necrosis factor alpha (Adapted from: Garg, Coulie, *et al.*, 2017).

1.4.1 First generation DC therapies

In the first generation of DC therapies, cells were derived from patient leukaphereses from which DC progenitors were cultured *ex vivo* or immature DCs were separated by density gradient. The tumour antigen in the first generation was typically a TAA peptide, or TAA proteins derived from tumour cell lysates, which targeted the *in vivo* T cell response towards antigens known to be expressed by particular tumours (Rosenberg, Yang and Restifo, 2004). In 1995, Mukherji *et al*. published data from a small study of dendritic cell use in patients with advanced metastatic melanoma (Mukherji *et al.*, 1995). The literature at the time described patient-derived peripheral blood mononuclear cells (PBMCs) cultured with GM-CSF as APCs, but retrospectively at least some of these cells can be described as DCs. Using a peptide of the common melanoma-associated antigen 1 (MAGE-1), a

cancer/testis antigen normally only expressed in the testis but reactivated in melanoma (van der Bruggen *et al.*, 1991), the DCs were loaded *ex vivo* and reinjected intradermally into 3 patients with advanced metastatic melanoma. Although no MAGE-1-specific CTLs were initially detectable in the blood or metastatic lesions of these patients, following 4 doses of peptide-loaded DCs, these CTLs did become detectable in both tissues. Despite showing no therapeutic efficacy, due to insufficiency in DC number, antigen presentation to T cells or the suppression of the immune system in these advanced stage patients, this study was one of the first to highlight the safety and potential for efficacy of DC therapy.

Development of DC culture protocols by the addition of IL-4 with the GM-CSF followed characterisation of the heterogeneity of cultures with GM-CSF alone, as well as in response to early reports of IL-4 improving DC phenotype and antigen presentation (Sallusto and Lanzavecchia, 1994). The first clinical trial to use this methodology in treatment was for melanoma in 1998 (Nestle *et al.*, 1998). In a small trial with 16 advanced metastatic melanoma patients, MoDCs generated with GM-CSF and IL-4 were loaded with multiple melanoma-specific antigens (highlighting a desire for a multiple-antigen strategy to prevent antigen escape) and injected weekly for a month, and then monthly following this up to 10 injections. Uniquely in this early trial, DCs were injected directly into an uninvolved peripheral lymph node to ensure T cell contact. Results of this trial supported the earlier Mukherji trial, showing safety in all patients and tumour regression in 5. This trial also made use of the keyhole limpet hemocyanin (KLH) adjuvant. KLH is a marine-derived glycoprotein commonly used as an immunostimulant, used in this context as an adjuvant for CD4+ T cell activation in particular (Wimmers *et al.*, 2017).

Other early trials used other DC sources, such as directly isolating DCs from peripheral blood by Hsu *et al.* (Hsu *et al.*, 1996). Separation of mononuclear cells, including myeloid progenitors but also monocytes and immature DCs, is possible by density gradient centrifugation. In this trial for low-grade follicular B cell lymphoma, tumour biopsies supplied the immunoglobulin expressed specifically by the tumour as the TAA and this was given to DCs in culture without GM-CSF or IL-4. 4 patients were each given 3 subcutaneous injections of this cell preparation: with a soluble antigen booster 2 weeks after the first DC injection, and the remaining DC injections 1 month after the first, and then again 6 months after this. All patients in this study completed the course of injections and developed T cell responses to the antigen leading to tumour regression and in one patient, complete remission.

Finally, in 2001, CD34+ progenitor cell-derived DCs were derived from patients by leukapheresis following GM-CSF mobilization of the bone marrow (Banchereau *et al.*, 2001). Culturing these cells with GM-CSF, Flt3-L and TNFα produces a myeloid cell population at different developmental stages but includes immature DCs, LCs and cDCs (Redman *et al.*, 2008). In this trial, 18 patients with advanced metastatic melanoma were injected subcutaneously with the cultured CD34+ cell population 4 times in total over a 2-month period. The cells were loaded with multiple melanoma-specific antigens including melanoma-associated antigen recognized by T cells (MART-1), MAGE-3 and gp100. Even in these heavily pre-treated patients, this study was the first to show a strong correlation between DC vaccination, particularly to multiple antigen preparations, and therapeutic outcome as 16 of these patients developed a T cell response against one or more of the antigens and 7 of these patients experienced either tumour regression or stable disease.

These first generation clinical trials, as they would later be known, were important in showing the safety and potential efficacy of DCs in a clinical context. In 2003, Ridgway published a review of the "first 1000 dendritic cell vaccinees", who were treated in 98 individual first generation trials between 1995 and 2001 (Ridgway, 2003). The majority of these patients were treated with peptide-loaded DCs for either metastatic melanoma or prostate cancer, reflecting the naivety of DC clinical use and the techniques available during that time. In summary, patients in 31 of these studies experienced a partial response to the vaccine, and patients in 17 experienced a complete remission (CR), defined differently by each trial. This review highlighted the potential benefit of DC therapy, despite only a modest success. It was also the first to draw attention to the variety of methods used for the generation of the cells, and antigen loading and injection strategies. This was, at the time and continues to be, a challenge in assessment of DC clinical trials: as most early clinical trials involved small numbers of patients with little option for multiple study arms, making combining and comparing data from these trials difficult (Butterfield, 2013).

Assessing efficacy of DC vaccination was also variable between trials, and it became apparent that conventional success measures for cancer therapy such as tumour regression may not be appropriate for DC trials. A review of immunotherapies was published by Rosenberg *et al.* in 2004, which compared first generation DC trials and other immunotherapies such as soluble protein or viral vaccination using both conventional oncological criteria and a newly developed criteria known as Response Evaluation Criteria in Solid Tumours (RECIST) (Rosenberg, Yang and Restifo, 2004). The standard

oncological criteria were established for global comparability of tumour treatment using a 50% decrease in patient tumour burden as the threshold for objective response (OR) (Miller *et al.*, 1981), compared to RECIST which uses a 30% decrease. Using these slightly more accommodating criteria, it was shown that peptide-loaded DCs resulted in tumour regression in 7.1% of patients, which was higher than alternative vaccination strategies, and was used to support the continued use of DCs in clinical trials.

1.4.2 Second generation DC therapies

The safety and potential efficacy shown in small first generation DC clinical trials opened the doors to larger clinical trials using more novel modifications of these basic clinical protocols. After the first generation of trials, insight into the control of DC development and function highlighted the need for fully mature DC to use in therapy (de Vries, Lesterhuis, *et al.*, 2003). A number of studies in the early 2000s showed key differences between immature DCs, cells which were used in many first generation trials, and cytokine-matured DCs. Successive studies in 1999 and 2000 from the same centre compared DCs generated by standard culture supplemented with monocyte-conditioned media (MCM) alone or MCM with TNFα (Thurner *et al.*, 1999; Schuler-Thurner *et al.*, 2000). Clinical responses to the vaccine were shown to be significantly better if the DCs were generated with TNFα in patients with metastatic melanoma following subcutaneous and IV injection, despite both DC groups expressing the basic conventional DC markers CD86 and the human leukocyte antigen (HLA)-DR, and CD83. Jonuleit *et al*. directly compared injection of immature DCs and mature DCs intranodally, each presenting different antigens for comparison of the T cell response (Jonuleit *et al.*, 2001). Only mature DCs, generated by the addition of IL-1β, TNFα, IL-6 and PGE2 into the culture media, were able to induce CTL formation *in vivo* despite both DC populations being able to induce this *in vitro*. Interestingly, patients receiving unpulsed immature DCs developed delayed-type hypersensitivity (DTH) responses, suggesting that these cells stay at the injection site or went on to potentiate unwanted inflammatory effects.

The Jonuleit maturation cocktail of IL-1β, TNFα, IL-6 and PGE$_2$ went on to become the standard maturation protocol used in clinical trials (Constantino *et al.*, 2016), but there were several alternative factors also assessed. While this common cocktail enhanced activity of DC vaccines, assessed by *in vitro* T cell stimulation, it was shown that these DCs do not secrete the cytokine IL-12. The role of IL-12 in the development of a T cell response was shown by Dubois *et al.* in 1998, and therefore was thought to be crucial to

DC efficacy (Dubois *et al.*, 1998). Rescue of the IL-12 secretory DC phenotype has been shown following ligation of CD40, and exposure to IFNγ or bacterial products such as lipopolysaccharide (LPS) or polyinosinic:polycytidylic acid (PolyI:C) which mimic environmental stimuli during endogenous maturation (Snijders *et al.*, 1998; Nicolette *et al.*, 2007; Fučíková *et al.*, 2011). Importantly, the mature DC phenotype was shown to be stable *in vitro* following cytokine removal, suggesting that the phenotype will not reverse when reinjected into the patients who may have a high level of inhibitory cytokines in the serum (Zobywalski *et al.*, 2007).

The second generation of DC therapies also began to expand the sources of tumour antigen, which in the first generation had been mostly antigenic peptides. Multiple sources of antigen such as antigen peptides, tumour ribonucleic acid (RNA), and tumour lysates were all shown to be capable of eliciting an antitumour response *in vitro* and *in vivo* when combined with DCs (Constantino *et al.*, 2016). It also highlighted the differences in downstream T cell responses as a result of different antigen sources, both improving the potential therapeutic response to DC vaccines and complicating comparison between studies. A number of trials during this period used bulk tumour cell RNA, or TAA-encoding RNA derived from tumour biopsies. RNA can be prepared from biopsies by simple molecular extraction techniques, amplified by polymerase chain reaction (PCR) and DCs can be electroporated with this RNA in place of natural antigenic peptide uptake. Expression of the tumour RNA in the cytosol allows the full polypeptide chain to be degraded and so multiple peptides can be presented (Schaft *et al.*, 2005). While this strategy relies on the accessibility of the tumour for biopsy, which is not always possible, it allows the presentation of multiple individual TAAs without the need for expensive molecular characterisation of TAAs.

Direct comparison between tumour RNA electroporation and irradiated tumour cells, which result in a mixture of apoptotic and necrotic cells, suggests that DCs with tumour RNA are more effective in animal models (Benencia, Courrèges and Coukos, 2008). In comparison to antigenic short peptides, which bind directly to MHC class molecules, other antigen sources rely on uptake and processing for presentation on these molecules. Protein sources, such as tumour cell lysates, require endocytosis by DCs for presentation, as described previously; apoptotic and necrotic tumour cells require the same process but can be affected by the method of inducing cell death. Both freeze/thaw and irradiation with UV light can induce tumour cell death and release of antigenic proteins, but apoptotic DNA produced during the process can bind directly to the MHC molecules on the DC surface

(Filaci *et al.*, 2002). UV irradiation can also lead to degradation of important antigen epitopes, but studies have shown the susceptibility is antigen-dependent (Labarrière *et al.*, 2002).

While the use of common melanoma TAAs such as the MAGE antigens, gp100 and New York esophageal squamous cell carcinoma 1 (NY-ESO-1) remained high (Bloy *et al.*, 2014), there was a shift in focus to developing new methods to target other tumours in the absence of a specific, defined antigen. A study by Hobo *et al.* published in 2013 showed that RNA encoding MAGE-3, Survivin and a B cell maturation antigen (BCMA) was a suitable TAA source for the induction of tumour-specific T cells by DC vaccination in a small cohort multiple myeloma patients after chemotherapy and autologous stem cell therapy (Hobo *et al.*, 2013). The DCs were injected intravenously and intradermally in this study and highly expressed conventional markers of DC activation such as CD40, CD86 and MHC class II. Although it was reported that more than 60% of the cells expressed CCR7, surface expression was shown to be low by flow cytometry. A third of the patients in this study had detectable anti-MAGE-3 and anti-BCMA T cells after the course of DC injections, and almost half of the patients in the study had a stable disease at the 26-month follow-up.

Bulk tumour RNA from glioblastoma biopsies was shown in 2013 to be able to induce a protective T cell response when presented by DCs (Vik-Mo *et al.*, 2013). This study by Vik-Mo *et al.* used RNA from autologous cultured glioblastoma biopsy organoids, containing cancer stem cells (CSCs), to load DCs. After a course of 7 intradermal injections, each a month apart, 5 of the 7 patients in the study survived for almost 2 years longer than the matched control patient cohort. 3 of these patients were alive almost 4 years after the therapy. Isolation of T cells from the blood showed an increase in the number of T cells specific for TAAs and control peptides in the DC treated patients, highlighting the role for these cells in control of the tumour growth. In addition, with the DCs targeting T cells directly to the CSCs and not the whole tumour, there was no significant initial decrease in the tumour volume when assessed by magnetic resonance imaging (MRI). As additional chemotherapy regimens were used, as part of the trial, the tumour volume did decrease over time as rapidly proliferating cells were destroyed and there were no CSCs to replace them. RNA electroporation subverts normal antigen presentation mechanisms; since RNA requires translation into proteins for presentation, this allows MHC class I presentation without the requirement for cross-presentation and

therefore does not necessarily require the most efficient cross-presenting DC subset (Bachem *et al.*, 2010).

Additional complexity arises from the observation that different antigen loading methods are affected by the maturation cocktail being developed in these clinical trials. Early elegant studies by Zobywalski *et al.* showed that although tumour RNA electroporation allowed successful antigen presentation by DCs matured using TNFα, IL-1β, IFNγ and PGE2, the addition of polyI:C to this cocktail inhibited presentation (Zobywalski *et al.*, 2007). There is also an implication for the timing of each step in the *in vitro* production of the cells. RNA transfection, for example, has been shown to be more effective in antigen presentation after cell maturation (Schaft *et al.*, 2005). Using the MAGE antigen family, it was shown that if transfected after DC maturation, the cells more strongly generated CTL responses. This closely reflects natural DC biology, where MHC-peptide complexes present on the immature cell surface are rapidly internalised and replaced during maturation (Lelouard *et al.*, 2002). This highlights RNA transfection as potentially superior antigen loading method since endocytosis is also reduced during maturation but is required for antigen presentation from TAA peptides or tumour lysates.

Most notably, novel maturation cocktails and antigen loading approaches introduced during the second generation improved the efficacy of DC therapy in clinical trials. The use of maturation cocktails in the treatment of prostate and renal cell carcinoma using DCs showed a significant number of patients had detectable TAA-specific T cells after the treatment (Draube *et al.*, 2011). Direct comparison between immature and mature DCs in these trials strongly supported the improved clinical efficacy of mature DCs. Comparative evaluation of clinical trial data from patients receiving antigenic peptide vaccines with patients receiving tumour lysate vaccines showed an increase in objective response rate (ORR) from 3.6% to 8.1% (Neller, López and Schmidt, 2008), which led to an increase of up to 20% in survival duration depending on the type of cancer against matched controls (Anguille *et al.*, 2014).

Sipuleucel-T was developed during this time for use in prostate cancer patients. This DC vaccine, also known and licenced as Provenge, is exceptional being the only one to be approved by the US FDA for clinical use. The majority of prostate cancer patients respond to hormone depravation therapy, but eventually become hormone refractory and go on to develop metastatic disease which leads to death in almost all cases (Small *et al.*, 2006). Sipuleucel-T is comprised of autologous PBMCs activated *in vitro* with a fusion protein

known as PA2024, which is a prostate-specific antigen (prostatic acid phosphatase - PAP) fused to the cytokine GM-CSF (Small *et al.*, 2000). Like many antigens used clinically, PAP is highly expressed in prostate tissue and prostate carcinoma with minimal expression in other tissues which limits potential off-target effects (Graddis *et al.*, 2011). DCs presenting PAP alone produce a weaker T cell response *in vivo* than DCs loaded with PA2024 suggesting that incorporation of GM-CSF during activation. In addition to this, DCs loaded with PA2024 have been shown to limit tumour development and prolong survival in animal models. In early clinical trials, Provenge was shown to be well-tolerated following intravenous (IV) injection in agreement with previous DC trials, as well as improving the anti-PAP T cell response and decreasing prostate cancer-associated antigen detectable in patient serum (Small *et al.*, 2006). These clinical responses correlated with therapeutic efficacy compared to control therapies, and Provenge has been able to improve overall survival (OS) of patients but has had no significant effect on delaying the time to disease progression (Kantoff *et al.*, 2010). Importantly, leukapheresis and the short 2-day culture time results in a significant number of T cells as well as B cells and NK cells in the bolus, which may limit efficacy (Wesley *et al.*, 2012). The approval of Sipuleucel-T for commercial healthcare use by the US FDA was a significant milestone in DC therapy and led to further modifications to cell production to improve efficacy.

1.4.3 Third/next generation DC therapies

The licencing of Sipuleucel-T by the FDA and the improved clinical responses to second generation therapies highlighted the potential of further improving DC vaccines. In concert with a better understanding of the complexities of DC biology, and the development of more sophisticated molecular techniques, the scope of the field was broadened.

One of the major focuses in the current generation of DC therapies is in the use of *in vivo* DC subsets – which have no requirement for costly *ex vivo* culture protocols. Transcriptional profiling of *in vitro* DCs such as CD34+ and CD14+ cell-derived DCs showed that although these cells are technically DCs based on phenotypic and functional criteria, they are transcriptionally different from their *in vivo* counterparts such as pDCs and cDCs, described previously (Lundberg *et al.*, 2013). Certain functionality may be unique to particular *in vivo* DC subsets: pDCs are strong producers of Type I IFNs, where myeloid cDCs have more potent uptake of apoptotic cells and debris and presentation of this antigen (Schreibelt *et al.*, 2010; Hagberg *et al.*, 2011). Given their more specialised functions, natural DC subsets have different surface and cytokine phenotypes when mature

and respond differently to inflammatory stimuli in maturation cocktails (Piccioli *et al.*, 2009). pDCs, for example, do not express common bacterial pattern recognition receptors (PRRs), which precludes maturation using bacterial products such as LPS. Natural DC subsets interact with T cells differently to one another and to *ex vivo* DCs. This can therefore implicate particular DC subsets as the most immunogenic in the context of cancer. While these DCs are relatively scarce in the blood at rest, clinical trial data has shown that both pDCs and cDCs can be reliably isolated in a sufficient number for therapeutic use when isolated using novel magnetic bead-based sorting methodologies.

pDCs are primarily involved in antiviral defence through the production of Type I IFNs, but have been shown to efficiently stimulate cytotoxic T cells in a melanoma context (Salio *et al.*, 2003). Despite their relative inefficiency in antigen uptake and presentation since their *in vivo* role is more immunomodulatory through cytokine secretion; experimental evidence has shown that pDCs can process TAAs for stimulation of CTLs (Villadangos and Young, 2008). In 2013, Tel *et al.* showed that natural pDCs can be isolated from melanoma patients by leukapheresis and cell sorting, loaded with gp100 peptides and reinjected a day later (Tel *et al.*, 2013). Compared to matched historical controls, pDCs were shown to significantly increase overall patient survival, with an increase in TAA-specific T cells in a number of the patients. While the efficacy of the therapy is difficult to confidently state in a small trial, the data presented are promising. pDCs are an example, however, of the importance of an appropriate route of injection. Circulating pDCs access the LN directly from the circulation through the HEVs as previously described, a unique route of migration among DC subsets. This precludes subcutaneous or intradermal injection strategies. Direct intranodal injection is possible (Tel *et al.*, 2013), although migration to downstream LNs is not consistently seen in patients.

Myeloid DCs, or cDCs as described earlier, are another *in vivo* DC subtype with a potential use in DC therapies. Like pDCs, cDCs have a specialised function and mainly migrate to the marginal zone of the LNs for surveillance of blood-borne bacterial and fungal antigens (Piccioli *et al.*, 2009). In contrast to pDCs which have poor antigen uptake and presentation capability, cDCs are much more capable at endocytosis than most DC subsets (Schreibelt *et al.*, 2010). This makes them a desirable DC subset to use therapeutically, on the rationale that improved antigen presentation may improve the resulting T cell response. cDCs can be further subtyped by expression of the surface markers CD1c and CD141, as described previously. CD1c+ cDCs are present in the blood at significantly higher numbers than CD141+ cDCs and have been used successfully in cancer clinical trials. Early phase I

clinical trials have supported the feasibility of isolating enough cDCs for therapeutic use, and that these cells are well-tolerated by patients (Prue *et al.*, 2015). Schreibelt *et al.* showed that CD1c+ cDCs were capable of inducing *de novo* antigen-specific T cell responses even when as low as $3x10^6$ cells were injected intranodally after overnight culture (Schreibelt *et al.*, 2016). The cells were immunogenic and expressed markers CD83 and CD86 highly, but CD80 and CCR7 more variably. T cells induced by the vaccine led to prolonged progression-free survival for up to a year longer in patients with detectable T cell responses to the DC vaccine compared to those without.

Given the variety of tumour types, cell sources, maturation and antigen loading techniques, and injection routes which have been described here, assessing the efficacy and the future of DC vaccination as an immunotherapy is difficult.

1.5 Improving dendritic cell therapies

It is clear that increased understanding of DC biology has been crucial in the progression through these DC therapy generations. Integrating this understanding into clinical trials has improved the breadth of antigen loading techniques for applicability to more cancer types, and correlation of DC phenotype to the desired T cell response through selection of appropriate DC sources and maturation cocktails (Garg, Coulie, *et al.*, 2017). Despite more than 20 years of improvements, DC clinical trials still show subclinical tumour responses and variable induction of T cell responses in patients. While DC phenotype has significantly improved, poor *in vivo* migration of cells to the LNs after injection remains a concern and is not yet sufficiently addressed in clinical trials. The threshold cell migration to the LN for activation of an anti-tumour response has been shown to be small (Lim *et al.*, 2007), however variable patient responses suggest even this number may not be being reached. Several strategies have been described which directly address improving cell migration post-injection, such as the route of injection, but novel strategies are clearly required to improve this.

1.5.1 Alternative injection strategies

After injection DCs must interact with T cells to exert their immunogenic function, which requires migration from the site of the injection into the LN. Appropriate injection strategies are a potential way of maximising LN migration from the injection site. It has been seen in numerous clinical trials that after commonly-used subcutaneous or intradermal injection, only a small percentage of the injected cells reach the LNs which is

crucial for their function. This was reportedly as low as 5% of the total injected cells (Verdijk *et al.*, 2009), a very commonly quoted figure in the DC literature. DC maturation state is a key factor in the ability of the cells to migrate, so incorporation of maturation cocktails into second generation DC protocols did improve migration (de Vries, Krooshoop, *et al.*, 2003).

The rationale for subcutaneous and intradermal injection strategies is in the direct access of the injected DCs to the lymphatic vasculature (Lappin *et al.*, 1999). As it reflects an endogenous migration by positioning mature DCs within the tissue and allowing natural migration, it was expected that these routes would provide the best route of injection to induce a T cell response. In comparison, as described previously, most DC subsets are not equipped to migrate from the blood into the LNs which precludes intravenous injection. It has been shown that intravenous injection leads to splenic T cell response as cells reach the spleen through the circulation (Mullins *et al.*, 2003). This study showed that, although inducing a T cell response which controlled melanoma lung metastases, intravenous injection failed to control a subcutaneously growing melanoma. Fong *et al.* showed a similar inability of intravenously-injected DCs to induce IFNγ-producing T cells in melanoma patients compared to intradermally-injected DCs (Fong *et al.*, 2001). While a splenic T cell response may be desirable in specific cancer types, the intradermal route was shown by Mullins *et al.* to also produce a splenic response in addition a response in the skin-draining lymph nodes.

Directly introducing DCs to the LN by intranodal injection is a potential strategy to ensure contact with T cells, but this methodology has shown a surprising comparable efficacy to intradermal injection despite the inefficiency of intradermally-injected cells to reach the LN (Lesterhuis *et al.*, 2011). Although intranodal DCs can immediately access T cells within the LN, there is some requirement for intranodal migration, as described previously, with no guarantee that injected DCs are capable of this. Additionally the surgery is technically complex and risks damaging the LN architecture, which severely compromises the potential immune response, and makes multiple injection strategies difficult (Tel *et al.*, 2013). Intradermally-injected DCs can also theoretically migrate to a number of LNs within the lymphatic branch, depending on the number and site of injections, but migration of intranodally-injected DCs through the efferent lymphatics has not been seen consistently (Quillien *et al.*, 2005; Tel *et al.*, 2013).

Taking these strategies into account, there is no clear superior injection strategy for maximising both appropriate DC migration and T cell communication. Each of these injection strategies have disadvantages and there is a clear need to develop new methodologies to improve migration. Given the current breadth of literature on DCs used clinically it was seen that DCs may be inherently incapable of migration upon injection by a lack of expression of the chemokine receptor CCR7.

1.5.2 DC chemokine receptor expression

In a number of trials discussed in this Chapter, DC surface marker expression was characterised prior to injection of cells. As discussed previously, the expression of CCR7 on mature DCs is crucial for migration into the lymphatics from either tissues or the bloodstream, however many of the cells used in these trials fail to express CCR7. In very early first generation DC trials, CCR7 expression was not quantified (Mukherji *et al.*, 1995; Hsu *et al.*, 1996; Nestle *et al.*, 1998). In the absence of cell maturation cocktails, however, expression would be unlikely (de Vries *et al.*, 2003). After the introduction of cytokine stimulation in the second generation of DC trials, assessment of CCR7 expression was more common (Zobywalski *et al.*, 2007; Hobo *et al.*, 2013) but is heterogenous in a mixed culture of mature and not-fully-mature DCs. This reflects *in vitro* evidence where CCR7 expression is not uniform in MoDC cultures using GM-CSF and IL-4. Taking these data into account, it possible that DCs prepared for clinical trials are not sufficiently equipped for migration to the LNs by heterogenous expression of CCR7.

In 2014, a study by Le Brocq *et al.* showed that it was possible to stain and sort cells expressing CCR7 using a novel chemokine-fluorophore conjugate in the place of an antibody (Le Brocq *et al.*, 2014). Given chemokine receptor structure, as described previously, specific, high-quality antibodies against chemokine receptors are difficult to produce. The study showed a reliable staining of CCR7-expressing cells which could be used to sort cells expressing the receptor to a high purity using magnetic beads; providing a methodology for isolation of these cells in a clinical setting. Expression of CCR7 is crucial for LN migration, so isolation of these cells would in theory isolate the DCs most capable of *in vivo* migration from a mixed culture.

1.6 Project aims

DCs have a significant potential for clinical use given their ability to stimulate the adaptive immune system against defined antigens. In a cancer context, targeting TAAs using DC

therapies can induce a robust, anti-tumour T cell response in patients. Although more than 20 years of improvement has been made to manufacturing, maturing and delivering DCs in this context, clinical responses are variable and do not yet meet expectation of efficacy. One potential issue in therapeutic efficacy is in the inability of the cells to reach the LNs following injection due to lack of expression of the chemokine receptor CCR7, which is not always upregulated following *ex vivo* culture. Using the methodology developed by Le Brocq *et al*., it may be possible to isolate only CCR7-expressing cells from culture, which may provide DCs with an improve LN homing capacity and therefore therapeutic efficacy. The aims of this project are to understand:

1. Does sorting DCs by expression of CCR7 improve their phenotype, migration and function?

2. Does sorting DCs by expression of CCR7 confer therapeutic efficacy in a mouse model of cancer?

In **Chapter 3**, sorting murine bone marrow dendritic cells (BMDCs) by CCR7 expression using CCL19 will be validated, and the cells characterised for surface marker phenotype, secretory profile, migratory capacity and immunogenic function. In **Chapters 4** and **5**, CCR7-sorted DCs will be challenged in the context of the subcutaneous and metastatic B16F10 melanoma models to assess their potential therapeutic benefit. Finally, in **Chapter 6**, human MoDCs will be generated and sorted for CCR7 expression using a good manufacturing practice (GMP)-grade clinical cell sorter to assess the potential for clinical translation of the methodology.

Chapter 2

Materials and methods

2.1 Cell culture

2.1.1 Maintenance of cell lines

The cell lines used and maintained in this thesis are described below. All cell culture and use were carried out under aseptic conditions i.e. within a tissue culture hood with a laminar High-Efficiency Particulate Arrestance (HEPA) filtration system and pre-sterilised equipment and reagents. 70% industrial methylated spirits (IMS) was used to sterilise equipment and hood surfaces before use. Centrifugation was performed at 300xg for 5min in a Biofuge primo centrifuge (Thermo Scientific) unless otherwise stated. All cultures were kept in an incubator at 37ºC / 5% CO_2 / 95% humidity.

The B16F10 murine melanoma cell line was maintained in Dulbecco's minimal essential medium (DMEM) (Sigma Aldrich, UK) supplemented with 10% foetal calf serum (FCS) (v/v), and 2mM L-glutamine, penicillin (100 U/ml) and streptomycin (100µg/ml; all Sigma-Aldrich) (complete DMEM).

2.1.2 Reconstitution of frozen cell lines

Cell lines were reconstituted from liquid nitrogen stocks prior to culture. Recovery of cells was performed by thawing vials in a 37°C water bath. Cells were washed once in 20ml of medium (pre-warmed to 37°C) followed by centrifugation. The supernatant was decanted, and the pellet of cells resuspended in 25ml of fresh culture medium for transfer into a 75cm^3 tissue culture flask.

2.1.3 Cell counting

Viable cells were counted using a Neubauer haemocytometer (Hawksley, UK) with dead cells assessed using 0.4% Trypan Blue (Sigma-Aldrich) staining. 5µl of trypan blue was added to an equal volume of cell suspension and briefly incubated at room temperature before loading into the chamber of the haemocytometer. The number of cells in each of the 4 x 4 grids was counted and an average cell number/grid was determined. Dead cells were identified by uptake of the Trypan Blue stain. Final cell number was obtained by multiplication of the average cell number with the dilution factor with Trypan Blue (x2) and a factor of 10^4 to give the number of cells/ml of cell suspension.

2.1.4 Passage of cell cultures

Cell lines used were routinely passaged upon reaching 80-90% confluence, which was assessed by inspection of cell cultures using a light microscope (Zeiss). To passage cells, medium was aspirated, and cells were washed with 5-10ml Phosphate-buffered saline (PBS) (Invitrogen). Adherent cells were detached from plastic flasks by enzymatic detachment with 0.5% trypsin (w/v) (Invitrogen) (1ml for 25cm^3 and 3ml for 75cm^3). Cells were incubated for up to 5min at 37°C and assessed for detachment using a light microscope. Trypsin was quenched by the addition of complete medium to a final volume of 10ml, and cells were resuspended by manual agitation with a pipette. The suspension was centrifuged and the supernatant decanted; cells were resuspended in an appropriate volume of fresh medium and split into a new tissue culture flask with a dilution factor between 1:20 and 1:40.

2.1.5 Freezing and storage of cell lines

Early passage cells from all cell lines were frozen down for future use. Cell suspensions were first washed once in PBS, centrifuged and resuspended at a density of up to 1×10^7 cells/ml in FCS with 10% dimethylsulphoxide (DMSO) (v/v) (Sigma-Aldrich) for freezing. 1ml of cell suspension was added to 2ml cryo-vials, which were cooled overnight at -80°C before transfer to vapour phase liquid nitrogen storage tanks.

2.2 Molecular methods

2.2.1 Cell lysate preparation

Cell lysates were prepared using the NP40 Cell Lysis Buffer (ThermoFisher Scientific). Cells were pelleted and washed twice with ice-cold PBS to remove the tissue culture medium. The cells were resuspended in cell lysis buffer at 5mg/ml as per the manufacturer's instructions. After 15min on ice with occasional vortexing, the lysate was transferred to the microcentrifuge tube provided and centrifuged at 14000rpm for 10min at 4°C. The lysate was transferred to a clean microcentrifuge tube for storage. Total protein concentration was determined by Pierce bicinchoninic acid (BCA) protein assay (ThermoFisher Scientific) as per the manufacturer's instructions.

2.2.2 RNA isolation

All techniques involving RNA were performed taking care to minimise environmental contamination by RNases. RNase-free or autoclaved plastic and glassware were used, as well as sterile filter tips and RNase-free water (Ambion). Work surfaces and equipment were decontaminated with RNAzap RNase decontamination solution (Ambion) before use.

RNA was extracted from cells using the RNeasy Mini Kit (Qiagen). Cells were pelleted, washed once in PBS and resuspended in an appropriate volume of RLT Buffer with β-mercaptoethanol for the expected cell number (350μl for $1\text{-}5\text{x}10^6$ cells; 600μl for $>5\text{x}10^6$ cells). The suspension was homogenized using a QIAshredder spin column before proceeding with the extraction as per the manufacturer's instructions. This included the on-column DNase digestion using the RNase-free DNase Kit (Qiagen) and the additional column drying step. The final elution volume was spun through the column twice to ensure optimal RNA concentration. The RNA concentration of each sample was determined by nanodrop (Nanodrop 1000, Thermo Scientific). RNA was stored for future use at -80ºC to maintain RNA integrity.

2.2.3 cDNA synthesis

RNA was converted to complementary DNA (cDNA) using a two-step Reverse Transcription (RT) process. The High Capacity RNA to cDNA Kit (Applied Biosystems) was used for all cDNA synthesis as per the manufacturer's instructions. Briefly, the reaction mix was prepared in 0.2ml PCR tubes as follows:

Ingredient	Volume (μl)
Template RNA	≤ 9
2x RT Buffer	10
20x RT Enzyme Mix*	1
Double-distilled Nuclease-free Water	Up to 20

* Substituted with nuclease-free water in control reactions.

The contents of each tube were mixed by pulse centrifugation. The RT process was carried out in a thermal cycler set to run at 37ºC for 60min to allow annealing of the RT enzyme to the template RNA, then 95ºC for 5min to initiate the reverse transcription of the RNA into cDNA. Product cDNA was stored at -20ºC until required.

2.3 Luminex

Cell lysates were collected for Luminex analysis as described in **2.2.1**. The Bio-Plex Pro™ Mouse Chemokine Assay (Bio-Rad) was used according to the manufacturer's instructions. All of the reagents and standards were included in the assay kit and were prepared as instructed. Briefly, all cell lysate samples were diluted in standard diluent to a final protein concentration of 200-900µg/ml for the assay. 50µl of magnetic beads were added to each well, followed by 50µl of the sample or the prepared standards and placed on an orbital shaker at 850rpm for 30min at room temperature. The plate was washed three times with 100µl of wash buffer, and then incubated following addition of 25µl of the detection antibody as previously. The plate was washed as previously, and 50µl of the anti-biotin detector antibody added to each well. After incubation on the orbital shaker at 850rpm for 10min at room temperature, the plates were washed three times again and 125µl of the assay buffer was added to each well. The plate was then immediately read using a Luminex 200 Bio-Rad analyser. The Luminex data were analysed as recommended by the manufacturer. Briefly, each microparticle bead region was designated as recommended, and doublet gates were set to between 8000 and 16500 to exclude aggregated beads detected by the lasers in the flow cell. The mean fluorescence intensity (MFI) was recorded for each sample, and the protein concentration of the samples determined using the standard curve acquired for each analyte.

CCL1	CCL24	CXCL1	IFNγ
CCL11	CCL25	CXCL10	IL-10
CCL12	CCL27	CXCL12	IL-16
CCL17	CCL3	CXCL13	IL-1β
CCL19	CCL4	CXCL16	IL-2
CCL2	CCL5	CXCL2	IL-4
CCL20	CCL7	CXCL5	IL-6
CCL22	CX3CL1	GM-CSF	TNFα

Table 2.1 - Chemokines and cytokines detected by the Bio-Plex Pro™ Mouse Chemokine Assay.

2.4 Quantitative polymerase chain reaction (QPCR)

2.4.1 Primer design

For QPCR, two sets of primers need to be designed for each gene of interest, known as 'inner' and 'outer' primers. Outer primers are used in the generation of standards for each gene by PCR; inner primers are designed to amplify a smaller region between the outer

primers and are used for gene quantification. To design accurate and efficient primers, the Ensembl software (www.ensemble.org) and Primer3 software (http://frodo.wi.mit.edu/) were used, with the following specifications:

Specification		Optimal Value	Range
Primer length (bp)		-	18 - 23
GC content		50%	40 - 65%
Melting temperature (Tm)		60ºC	59.5º - 61ºC
Max. self-complementarity		2	-
Max. 3' self-complementarity		1	-
Amplicon size (bp):	Inner primers	150	<150
	Outer primers	750	700 - 800

Additionally, primer sequences with more than two G or C bases within the last five bases at the 3' of each primer (creating a GC clamp), or with stretches of four or more G or C bases in a row were avoided to generate primers with low spontaneity to form primer dimers or hair-pin loops. The primer sequences were checked using the Basic Local Alignment Search Tool (BLAST) (https://www.ncbi.nlm.nih.gov/tools/primer-blast/) to ensure specificity for the gene of interest and no off-target binding potential. All primers were synthesised by Integrated DNA Technologies (IDT).

Primer Name	Primer Sequences	
Blasticidin resistance	Forward	5'- AGAACAGGGGCATCTTGAGC -3'
(Inner)	Reverse	5'- AGAGGGCAGCAATTCACGAA -3'
*CMV promoter (Outer)	Forward	5'- TGGCACCAAAATCAACGGGACT -3'
*eGFP (Outer)	Reverse	5'- CGTCGCCGTCCAGCTCGACCAG -3'
GAPDH (Outer)	Forward	5'- TGAACGGGAAGCTCACTGGC -3'
	Reverse	5'- TCCACCACCCTGTTGCTGTAG -3'
GAPDH (Inner)	Forward	5'- GTTGCTGTTGAAGTCGCAGGAG -3'
	Reverse	5'- ATGTGTCCGTCGTGGATCTGAC -3'
Kanamycin/Neomycin	Forward	5'- GAGGCTATTCGGCTATGACTGG -3'
resistance (Inner)	Reverse	5'- ACCGGACAGGTCGGTCTTGAC -3'
mRuby2 (Inner)	Forward	5'- TGGGAAAGAGTTACGAGATACGA -3'
	Reverse	5'- AACGAGACAGCCATCCTCAA -3'
OVA (Inner)	Forward	5'- CCAATCTGTCTGGCATCTCC -3'
	Reverse	5'- TGCTGACCCTACCACCTCTC -3'

Table 2.2 - QPCR primer sequences
*The CMV promotor and eGFP outer primers constitute a Forward and Reverse pair for plasmid cloning purposes.

2.4.2 Polymerase chain reaction (PCR)

PCR was performed using the Q5 High-Fidelity DNA Polymerase (Qiagen). The master mix for this PCR reaction was prepared as follows in RNase-free PCR tubes:

Ingredient	Volume (μl/reaction)
5x Q5 Reaction Buffer	5
Q5 High-Fidelity DNA Polymerase	0.25
dNTPs (10mM)	0.5
Primer Mix (10μM for each primer)	2.5
DMSO	0.75
BSA	1.25
Template cDNA*	1-2
Double-distilled Nuclease-free Water	Up to 25

* Substituted with nuclease-free water in control reactions.

Reactions were run in a 7900T thermal cycler (Applied Biosystems) with the following programme:

Step	Temperature (ºC)	Time	
Initial denaturation	98	3 minutes	
Denaturation	98	10 seconds	
Annealing	60	20 seconds	Repeated for 40 cycles
Elongation	72	40 seconds	
Final elongation	72	10 minutes	
Hold	4	Indefinitely	

2.4.3 Gel electrophoresis

PCR products were run on an agarose gel to determine the size of the product against a ladder of known DNA sizes. A 1% agarose gel was used unless otherwise specified. The gel was made by adding 0.5g of agarose (Sigma-Aldrich) to 50ml of tris acetate ethylenediaminetetraacetic acid (TAE) buffer, which was heated in the microwave until the agarose was fully dissolved. Ethidium bromide was added to the partially-cooled agarose solution. The solution was poured into a gel cassette to cool, with combs inserted into the gel to create wells in which to load samples. Upon cooling, the gel was place in an electrophoresis tank, which was filled up with TAE buffer until the surface of the gel was covered. Samples were loaded by pipette with a DNA ladder to allow determination of sample size. For samples ≤10kb in length, a type IV hyperladder (BioLegend) was used.

Samples were run for 60min at 100 volts, or until the loading dye had diffused to the end of the gel. The gel was then imaged by UV illumination using an Alpha 2200 Digital UV-Visphoto (Alpha Innotech, Santa Clara, California). To prepare specific PCR products to be QPCR standards, the band representing the product was carefully cut out with a scalpel blade and halved. From this, the product was extracted using the QiaQuick Gel Extraction

kit (Qiagen) as per the manufacturer's instructions. The DNA obtained was stored at -20ºC in the elution buffer provided in the kit.

2.4.4 QPCR assay

SYBR Green, a cyanide dye which binds double stranded DNA (dsDNA), is used to quantify gene expression in each sample in QPCR. The QPCR master mix was prepared as follows using SYBR Green Fast Mix (VWR-International):

Ingredient	Volume (µl)
SYBR Green Fast Mix	5
Double-distilled nuclease-free water	4
1:1 Primer mix	0.15

QPCR assays were performed with samples in quadruplicate, so volumes above were adjusted according to experimental requirements. Using a multichannel pipette, 9µl of the master mix was added to each well of a 384-well thin-walled PCR plate. To these, 1µl of the desired cDNA or standard DNA was added and mixed thoroughly. A 'no template control' (NTC) was also run for each primer pair with double-distilled nuclease-free water used in place of the DNA. Once the samples had been loaded, the plate was carefully sealed using an optical plastic film (Applied Biosystems), briefly centrifuged at 500g at 4ºC and run on a 7900HT thermal cycler (Applied Biosystems). The QPCR programme is described below:

Step	Temperature (ºC)	Time (s)	
1	95	20	
2	95	3	Repeated for 40 cycles
3	60	30	
4	95	15	
5	60	60	

*Steps 4-5 were added to produce a dissociation curve for the primers to confirm specificity.

2.4.5 Analysis of QPCR data

Cycle threshold (CT) was used as a metric of gene expression: describing the cycle of the QPCR at which replication of the gene by the enzymes in the master mix becomes significantly detectable above background by the machine reader. With this information, genes with low CT values are highly expressed, and vice-versa. For each gene, the R^2 value was considered: this uses the values from the standard curve constructed by dilutions of the

gene standard DNA to compare CT value consistency between replicates. The closer the R^2 value is to 1, the more accurately the gene expression in the experimental samples can be quantified using the standard curve. NTC control samples were also used to check for pipetting errors and are expected to have a very high or undetectable CT value. After these checks, the data were exported to Microsoft Excel and the expression of target genes normalised to the GAPDH housekeeping gene.

2.5 *In vivo* procedures

2.5.1 Animal welfare

Animals were housed in the Biological Services Central Research Facility at the University of Glasgow and the Beatson Institute and maintained in specific pathogen-free conditions with unrestricted access to food and water. All experiments were approved by the University of Glasgow Ethical Review Committee and performed under the auspices of a United Kingdom Home Office License.

2.5.2 Mice

C57BL/6 mice were bred and maintained in-house but were also purchased from Charles River laboratories as required. 8 to 12-week old mice were used in this project. These mice were allowed a week to acclimatise to the environment before being put on procedure if arriving from an external supplier. 8 to 12-week old mice of either sex were used for generation of BMDCs, unless cells were being used for injections, in which case female mice were used as a source of BMDCs. 8 to 9-week old female mice were used as recipients for injections under procedure. Specifically-modified mouse strains used in this project are described in **Table 2.3**. Briefly, OT mice were used as a source of ovalbumin (OVA)-specific T cells used in the validation of B16-ova transfectants and in T cell stimulation assays.

Genotype	Modification
OT-I	Transgenic TCR recognising MHC class I restricted OVA peptide
WT	C57BL/6 – no modification
WT albino	C57BL/6 – albino

Table 2.3 - List of mouse strains used in procedures.

2.5.2.1 Schedule 1

Mice were culled by exposure to rising concentration of CO_2, a recognised Schedule 1 procedure. The cull was confirmed by either cervical dislocation or by perfusion with a fixative such as 1% paraformaldehyde (PFA) in PBS (v/v) by injection into the circulation.

2.5.3 Dissection techniques

Mice were culled as described in **2.5.2.1**, and the body pinned out on a cork board for dissection. Mice were sprayed with ethanol and the viscera exposed by pinching the skin on the abdomen and making an incision up the midline to the neck using a pair of surgical scissors. At the top and bottom of the incision, further incisions were made along the midline of fore- and hindlimbs, respectively. The skin was then pulled back to fully expose the viscera and pinned as appropriate. The contents of the abdomen were exposed by making an incision up the midline to the diaphragm. The contents of the thorax were then exposed by excision of the diaphragm along the line of the ribcage, and then along either side of the ribcage towards the neck. The ribcage was then folded back to fully exposure the lungs and heart.

2.5.3.1 Bone marrow isolation

To extract the bone marrow, hindlimb skin was first cut above the ankle using surgical scissors and manually pulled back from the limb. The muscle and tendons were then cut away to expose the bone. The femur was cut as close to the hip joint as possible, and the paw removed from the tibia. In an air flow hood, both the tibia and femur were cut at the knee to expose the marrow. The bone marrow was then flushed from the cavity by flow-through of non-supplemented Roswell Park Memorial Institute medium (RPMI) (ThermoFisher Scientific) using a 20ml syringe and a 23G needle and collected in a $10cm^2$ culture dish. Cells were then homogenised by passing through a 70um filter using the insert of a 1ml syringe and were then centrifuged at 300xg for 5min to pellet the cells. Supernatant was decanted, and the cells resuspended at 10^7 cells/ml for culture as described in **2.6.1**.

2.5.3.2 Lymph node isolation

LNs were routinely isolated in this project for collection of T cells for culture and during tumour development, and collection of DCs in competitive migration experiments. The specific LNs taken and their location within the mouse are summarised in **Figure 2.1**.
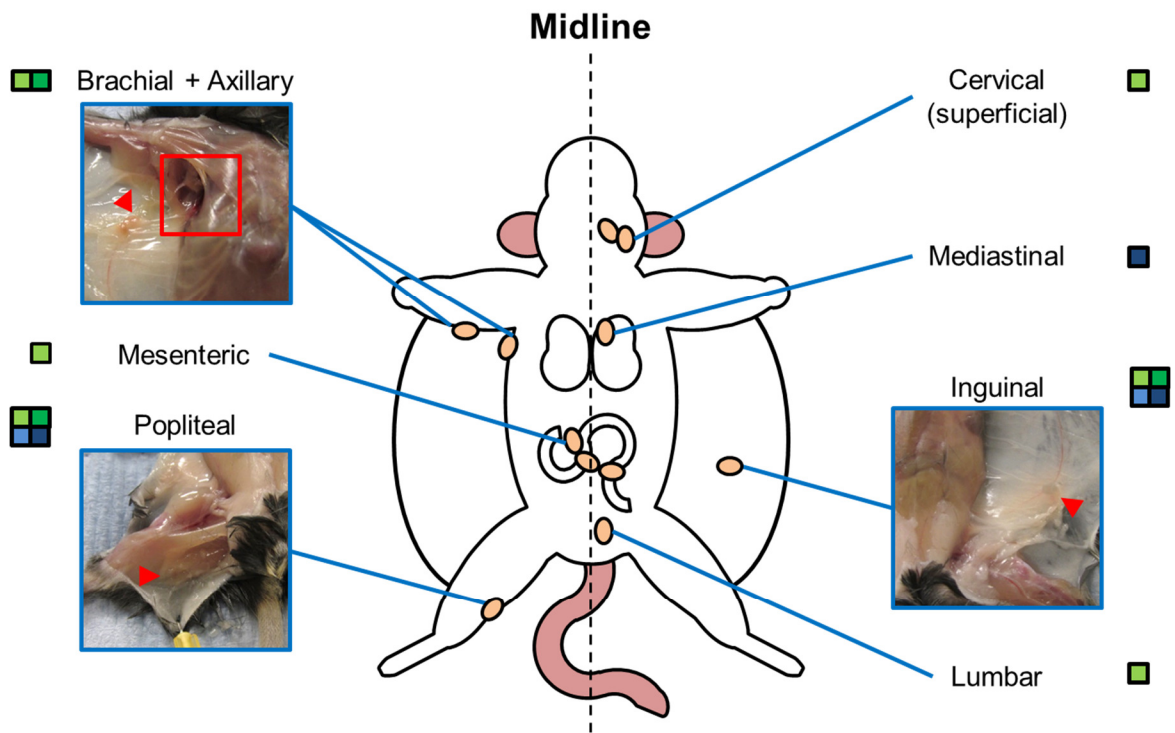
Figure 2.1 - Schematic diagram of mouse LN locations and their experimental use.
Inflammatory exudate from peripheral tissues and developing tumours drain into lymph nodes, such as those shown here, and except the mesenteric lymph nodes are reflected across the midline. The LNs in inset images are denoted by red arrows, with the axillary in the red box. LNs used in each experiment are identified by colour: T cell isolation/generation only (light green), competitive DC migration (dark green), and solid tumour (light blue) and metastatic tumour (dark blue) models.

Dissection of the individual lymph nodes are described below, and unless otherwise stated were removed using sharp watchmakers' tweezers:

- *Cervical* – The skin is cut up the midline towards the mouth using scissors and peeled back to expose this cluster of lymph nodes.

- *Mediastinal* (mLN) – This cluster of lymph nodes is partially visible at rest but become enlarged during inflammation in the lungs and lies along the trachea before the bifurcation to the lungs.

- *Inguinal* (iLN) – The inguinal lymph node (also known as the subiliac lymph node) is located within the mammary fat pad in the lower abdomen.

- *Lumbar* – Located along the midline and descending aorta, the lumbar LNs are a pair of LNs visible before the bifurcation of the aorta to the hindlimbs.

- *Popliteal* (pLN) – The popliteal lymph node is located in the popliteal fossa underneath the knee and is dissected by first pinning out the hindlimb at 90° to the body and peeling back the skin. The musculature is stripped away using tweezers until the lymph node is visible.

- *Mesenteric* – These lymph nodes lie in a chain within the mesenteric region of the gut and are visible following incision of the peritoneum and mobilisation of the gut.

- *Brachial and Axillary* – Both of these lymph nodes are located under the shoulder: the brachial lymph node lies directly below the upper forelimb if the mouse is pinned as described in **Figure 2.1**; the axillary LN is present sometimes as a cluster, in the musculature connecting the upper thorax to the skin when pinned.

For all T cell cultures, all of the lymph nodes except the mediastinal were removed. After footpad injections, DCs were isolated from the popliteal, inguinal and axillary/brachial lymph nodes on the left of the animal which drained the injection site. Following injection into the footpad, as described in **2.5.4.1**, the lymphatics in the hindlimb drain primarily into the popliteal LN, with some drainage seen into the inguinal, and axillary LNs via the efferent lymphatics (Harrell *et al*., 2008). In these experiments, the contralateral side LNs were dissected and retained as controls. In solid tumour experiments, the injection site-draining LN (popliteal), and tumour-draining LNs (inguinal in the solid tumour model; mediastinal in the metastatic model) were taken to analyse induction of tumour-specific T cells. Lymph nodes were homogenised by passing through a 70um filter using the insert of a 1ml syringe, the homogenate pelleted by centrifugation and resuspended as appropriate.

2.5.3.3 Spleen

The spleen is located in the posterior abdominal cavity and is located by mobilisation of the viscera following incision of the peritoneum and removal with surgical scissors. A single cell suspension was obtained from the spleen following manual cutting into small sections with scissors and passing through a 70um filter as described previously. The cells were pelleted by centrifugation at 350xg and the supernatant removed. Red blood cells (RBCs) were removed using the RBC lysis buffer (BioLegend) diluted to 1x concentration in PBS. Briefly, each pellet was resuspended in 5ml of RBC lysis buffer on ice for 5min,

and the reaction stopped by addition of 25ml of PBS. After centrifugation at 350xg, the supernatant was removed, and the cells resuspended in the appropriate buffer or medium and counted.

2.5.3.4 Lung lobe

For this protocol, mice were perfused with 10ml PBS using a 25G needle inserted into the left ventricle of the heart. This allowed the lungs to be fully perfused with PBS before dissection with surgical scissors and was important to remove blood from the circulation for subsequent imaging and flow cytometry. A single cell suspension was obtained from the lungs following manual cutting into small sections with scissors and transferring the tissue into 15ml tubes. 2.5ml of digestion mix was added to each tube, which contained 1.6mg/ml Dispase (Roche), 0.2mg/ml Collagenase P (Roche) and 0.1mg/ml DNase I (Invitrogen) in RPMI. The tissue was incubated at 37°C in a water bath for 40min, with manual agitation of the tube after 20min. Digested tissue was then passed through a 40um filter as described previously and washed with 10ml RPMI. After centrifugation at 350xg, the supernatant was removed, and the cells resuspended in the appropriate buffer or medium and counted.

2.5.4 Procedures

2.5.4.1 Footpad injections

BMDCs were generated and sorted using 23-PEG bCCL19 as described in **2.6.1** and **2.6.2,** respectively. In competitive migration experiments, albino mice were used. The cells were resuspended at $1x10^6$ total cells in 25μl in PBS/0.1% bovine serum albumin (BSA) (Millipore) for injection. Footpad injections were performed in one of the two following ways:

1. Mice were immobilised by the scruff by a member of staff, while the cells were carefully injected into the left footpad.

2. Mice were first fully anaesthetised using 30% isoflurane in oxygen in a Perspex chamber, as tested by cessation of movement and hindlimb reflexes, before transfer of individual mice to anaesthetic ventilator masks and performing the injection into the left footpad.

In both cases, the left footpad and associated contralateral draining lymphatics were left as an internal control for each injection.

To analyse the cells present in the footpad, mouse paws were removed and collected in 1ml of PBS in a 12-well plate. The skin was removed using surgical scissors and cut into small pieces. Both the skin and remaining paw were incubated with digestion mix which contained 2mg/ml Collagenase IV, 2mg/ml hyaluronidase and 0.1mg/ml DNase I (all Invitrogen) at 45°C for 20min in a shaking incubator. After incubation the tissue was removed and passed through a 100um filter as described previously and washed with 10ml PBS. Cells were washed twice by centrifugation, and then resuspended in the appropriate buffer or medium and counted.

2.5.4.2 Tumour models

B16F10 melanoma cells are a rapidly-metastasising subclone of the B16 murine melanoma cell line. In this project, the B16F10 line was transfected to express the ovalbumin cDNA and mRuby2 fluorescent reporter. Cells were grown to confluence in $75cm^3$ flasks and trypsinised as described previously and washed twice in PBS by centrifugation. The cells were resuspended at $5x10^6$ cells/ml in PBS and kept at room temperature before injections to prevent aggregation of cells.

Solid tumours

For better visualisation and measurement of subcutaneously growing tumours, mice receiving subcutaneous tumour cell injections were shaved on the flank using an electric razor (Wella) the day before tumour cell injection. To induce solid tumour formation, $5x10^5$ B16F10 cells were injected subcutaneously into the lower back of the mouse. Under Home Office guidelines tumour-bearing mice were weighed daily, their tumour growth measured daily using digital Vernier callipers (Sealey Professional Tools) and were monitored daily for any signs of sickness. This procedure typically ran for between 3 and 4 weeks before tumours reached maximal size and the mice were culled using an approved Schedule 1 procedure (see **2.5.2.1**).

Metastatic tumours

Mice receiving the intravenous injections of tumour cells were first placed into a heated Perspex box to allow the blood vessels to dilate and become more visible. Individual mice

were contained in a Perspex holding tube with an adjustable head restraint to minimise movement and risk of harm to the mouse. A magnifying lamp was also used to help visualise the tail vein for the injection. B16F10 cells were injected in a 100μl volume, with each mouse receiving 5×10^5 cells total. Mice were kept for no longer than 14 days with developing tumours and were both weighed and monitored daily, as discussed previously. On day 14 post-injection, mice were sacrificed using an approved Schedule 1 procedure (see **2.5.2.1**).

2.6 *Ex vivo* procedures

2.6.1 Generation of murine BMDCs

Bone marrow cells were cultured in 10cm^2 culture dishes at 10^7 cells/ml in RPMI supplemented with 10% FCS (v/v) and 2mM L-glutamine, penicillin (100 U/ml) and streptomycin (100μg/ml) (complete mRPMI). The medium was additionally supplemented with 20ng/ml recombinant murine GM-CSF (Peprotech) to support differentiation of the cells. On days 2 and 4 of the protocol, non-adherent cells in the medium were transferred to new culture dishes following manual agitation by pastette. New medium was added at these timepoints as necessary. On day 7, non-adherent cells were collected and resuspended at 8×10^6 cells/ml in complete mRPMI with 5mg/ml ovalbumin (Sigma-Aldrich). Cells in suspension were counted by haemocytometer as previously described in **2.1.3**. The suspension was plated on Ultra Low-Adherence 24-well plates (Corning) and incubated for 4 hours under normal culture conditions. After 4 hours, the supernatant was removed from the wells using a pipette and collected in a 50ml falcon tube. TrypLE (Life Technologies) (diluted from 10x to 1x concentration in PBS) was then added for a further 5-10min to detach the cells. After this the contents of the wells were manually agitated by pastette and collected with the non-adherent cells in the same 50ml falcon tube. The cells were washed by centrifugation and resuspended at 2×10^6 cells/ml in complete mRPMI. To stimulate the DCs to mature, 100ng/ml ultrapure LPS (Source Bioscience) and 50ng/ml murine recombinant TNF-α (Miltenyi Biotec) were added to the suspension, which was re-plated in 6-well plates and incubated for 24 hours under normal culture conditions. The cells were then collected as previously described using TrypLE as it maintains cell-surface molecule expression due to its non-enzymatic nature.

2.6.2 Chemokine-based sorting

Mature BMDCs were collected from culture and washed as described previously and resuspended at 10^7 cells/100μl in PBS with 0.5% (w/v) media-grade BSA and 2mM ethylenediaminetetraacetic acid (EDTA) (Ambion) (PEB buffer) for all sorting methodologies. Prior to staining, cells were blocked using FcR blocking reagent, as per manufacturer's instructions (Miltenyi Biotec). Cells were incubated at 4°C with either biotinylated CCL19 (bCCL19) with a polyethylene glycol (PEG) spacer residue set (400ng/ml; Almac Sciences, generated as described in Le Brocq *et al.*, 2014) tetramerised with streptavidin-PE (SAPE)(50μg/ml; Life Technologies) for 30min, or bCCL19 (400ng/ml) conjugated to anti-biotin PE (Miltenyi Biotec) as described previously (Le Brocq et al., 2014). 3-, 11-, and 23-PEG biotinylated CCL19 were used in this project, which describes the number of PEG residues in the chain separating the CCL19 molecule from the attached biotin residue. For cells being sorted by fluorescence activated cell sorting (FACS), an additional anti-CD45 antibody was added (1μl/10^7 cells), to further discriminate the cells cytometrically. After 30min cells were washed in PEB by centrifugation and resuspended in an appropriate volume of PEB. Cells were then sorted using either magnetic microbeads, the Aria II cell sorter (BD Biosciences) or the MACSQuant Tyto cell sorter, as described below.

2.6.2.1 Chemokine-based sorting using microbeads

For manual sorting, bCCL19-labelled BMDCs were resuspended at 10^7 cells/80μl in ice-cold PEB and stained with anti-PE microbeads (20μl/10^7 cells) for 20min at 4°C. The cells were then washed in PEB by centrifugation and resuspended. MACS LS columns (Miltenyi Biotec) were used for manual cell sorting. These columns were mounted on a magnetic stand using the Miltenyi QuadroMACS magnet and rinsed once with PEB prior to adding the magnetically-labelled cells. To sort the cells, a 25G needle was attached to the end of the column, and the cells added to the top in 3ml of PEB. After the cell volume had run through completely by gravity, the column was washed 3 more times with 3ml of PEB. To collect the labelled cells, the LS column was removed from the magnetic stand and washed with 5ml of PEB by gravity without using the plunger to preserve cell viability. The positive and negative sort fractions were washed by centrifugation and resuspended in PEB for counting, analysis of purity by flow cytometry, and further experiments.

2.6.2.2 Chemokine-based sorting using Aria II

Given the incorporation of a fluorescent conjugate into the sorting protocol for analysis of purity, the sorting method is amenable to translation to FACS. Two FACS sorters with unique sorting mechanisms were used during this project: the BD Aria II and Aria III (BD Biosciences) (which are functionally identical) and the MACSQuant Tyto (Miltenyi Biotec).

To sort cells on the Aria II, the sorter was first set up to run at 20ºC with autoclaved PBS at a neutral pH (7.4), instead of the BD Sheath solutions to omit sheath preservatives such as 2-phenoxyethanol, and the collection chamber pre-cooled to the same temperature to limit cellular metabolism without induction of cold shock apoptosis. If the cells were required to be sterile for further use, the aseptic cleaning process was also run. The sorter itself was fitted with an 85μm nozzle and was run at 45psi and a 52.3MHz frequency to produce a high frequency sort under minimal flow rate to maintain cell viability. Cells were filtered for sorting using 70μm filters (Greiner bio-one) and resuspended at 1×10^7 cells/ml in PEB. Forward scatter (FCS) and side scatter (SSC) gates were set using unstained cell controls, and the fluorescence gates set using single stained cell controls. For FACS, a dead cell discriminator was not used due to the fluidic sampling characteristics of the cells and potential intracellular activation as a result. The sorted cells were collected into sterile 15ml falcon tubes containing 3ml of complete mRPMI supplemented to 50% FCS (v/v) to preserve the cells following the sort. The collected cells were washed by centrifugation and resuspended at an appropriate concentration for their future use.

2.6.3 Cell labelling for *in vivo* tracking

2.6.3.1 PKH67 dye

PKH67 dye (Sigma-Aldrich) is a green fluorescent dye (ex: 490nm; em: 504nm) which intercalates into the lipid membrane of cells. Cells were labelled with this dye to allow *in vivo* tracking following injection, staining cells as per the manufacturer's instructions. Briefly, the PKH dye solution was prepared by dilution of the PKH dye to a concentration of 4μM in 500μl of diluent solution. Cells were prepared for staining by single cell suspension by washing in serum free RPMI and were resuspended in 500μl of diluent solution. The PKH dye solution and cell suspension were mixed by direct addition of the cell suspension to the dye solution, to a final concentration of 2μM PKH dye. Cells were incubated at RT for 5min before the dye was quenched with hRPMI and washed by

centrifugation. This washing step was repeated once before enumeration and resuspending the cells in an appropriate volume of PBS/0.1% BSA for injection (**2.5.4.1**). Samples of cells were routinely assessed for successful staining by flow cytometry.

2.6.3.2 CellTracker Red (CMTPX)

CellTracker fluorescent dyes, such as CellTracker Red (CMTPX) (Life Technologies) enter cells by passive diffusion and are converted into cell impermeant molecules by endogenous enzymes. This leads to red cytosolic staining of target cells (ex: 577, em: 602). A working solution of dye was prepared by dilution of the stock CMTPX solution in to a concentration of 2μM in serum free RPMI. Cells were prepared for staining by single cell suspension by washing in serum free RPMI and directly resuspended in the CMTPX working solution. The cells were then incubated at 37ºC for 30min, after which the dye was quenched by the addition of hRPMI and washed by centrifugation. Cells were counted and resuspended in an appropriate volume of PBS/0.1% BSA for injection (**2.5.4.1**). Samples of cells were routinely assessed for successful staining by flow cytometry.

2.6.4 Transwell migration assay

A transwell migration assay was used to determine migratory capacity of cells sorted using bCCL19 and PEG-variants. BMDCs were first sorted as described in **2.6.2**, retaining a small sample of unsorted, labelled cells as a control. Cells were first counted using a haemocytometer and resuspended at $1.5x10^6$ cells in chemokine buffer for each condition: unsorted, positive and negative sorted fractions. To ensure that no serum components were inducing migration of cells, the chemokine buffer used was RMPI supplemented only with 0.5% BSA (w/v). Dilutions of the CCL19 were also prepared in chemokine buffer at 0, 10, 100 and 500ng/ml. 24-well transwell plates were obtained from Corning and prepared as follows: first, 600μl of chemotaxis buffer was added to each well and incubated at 37ºC for 5min. This was then removed by pipette and replaced with chemokine solution in the relevant wells. Transwell inserts were then placed into the wells containing chemokine solution using tweezers, taking care to avoid the formation of bubbles which could hinder cell migration. 100μl of cell suspension, equivalent to $1.5x10^5$ cells per well, was then added carefully onto the filter of the well insert using a pipette. The plate was placed in a tissue culture incubator under normal culture conditions for 3 hours to allow migration. After this, the medium in the top of the insert was removed by pipette and the insert moved into an empty well using tweezers. The medium in the bottom of each well was then collected in an Eppendorf tube. The wells were then washed with PBS by pipetting 2-3

times and the PBS collected and added to the respective Eppendorf tubes. Although trypsin is commonly used to detach cells, it was not used in this protocol due to the potential damage to chemokine receptors that can be caused by enzymatic digestion. Additionally, the filters were not removed from the inserts and washed as there was a concern about the fragility of BMDCs having gone through maturation, activation and sorting within 24 hours. Cells were then prepared for counting by flow cytometry by spinning down in a microcentrifuge and resuspending in 200µl of FACS buffer. This protocol was repeated with cells allowed to rest for 4 hours in a tissue culture dish after labelling and sorting.

2.6.5 T cell cultures

Spleen cells were cultured in 12-well tissue culture plates at $2x10^6$ cells/ml in complete mRPMI. To induce antigen-specific activation of naïve T cells, ovalbumin-presenting mature BMDCs, generated as described in **2.6.1**, were added to the culture at a ratio of 1:25 BMDCs to spleen cells. On days 3 and 5 of the culture, half of the medium in each well was removed and replaced with complete mRPMI containing 100U/ml and 50U/ml recombinant murine IL-2 (Miltenyi Biotec), respectively. 100U/ml IL-2 allows expansion of activated T cells from the initial mixed cell culture, and 50U/ml is a maintenance dose of IL-2 for cell survival. After 7 days in culture, the cells were then collected using TrypLE for use.

2.7 Microscopy

2.7.1 Preparation of frozen tissue sections for microscopy

Immediately after dissection, tissues were immersed in 1% PFA overnight followed by immersion in 30% sucrose (Fischer) in PBS (w/v) overnight. After this, tissues were embedded in optimal cutting tissue (OCT) cryo embedding medium (Tissue Tek) within plastic tissue moulds by adding a small amount of OCT medium to the mould, placing the tissue down in the correct orientation using tweezers, and carefully covering in more OCT medium to ensure no bubbled formed. The tissue moulds were then chilled over dry ice until completely frozen and stored at -80ºC until required. Sections of these tissues were cut to 8µm thickness using an OTF5040 cryostat (Bright Instruments, UK), and mounted on polysine-coated SuperFrost slides (VWR, UK). These slides were stored at 4ºC until use.

2.7.2 Haematoxylin & Eosin (H&E) staining

Tissues for haematoxylin and eosin (H&E) staining were first prepared for frozen sections. Samples were first warmed to room temperature from -80°C storage and then fixed using ice-cold acetone. The sections were allowed to air-dry for 30min at room temperature. The remaining protocol is the same for both types of section. The tissues were taken to water through 100%, 90% and 70% alcohol for 10 dips each, followed by washing in running water. Slides were immersed in Haematoxylin Z (CellPath, UK) for 7min, and then washed in running water until clear. Slides were dipped in 1% acid alcohol for 12 dips, washed in running water, blued in Scotts tap water substitute (STWS; CellPath, UK) for 2min, washed again, and then immersed in Putts Eosin (CellPath, UK) for 4min. After this, cells were washed in running water for 2min, before dehydration through alcohol to Xylene by: immersion in 70%, 90%, and 100% alcohol for 10 dips each, followed by immersion in fresh Xylene 3 times for 1min each. Sections were then mounted using Di-n-butyl Phthalate in Xylene (DPX; VWR, UK) and coverslipped.

2.8 Flow cytometry

2.8.1 Flow cytometry staining procedure

Cells were prepared for flow cytometry by collection from culture or homogenisation from tissues, washed and resuspended at 1×10^6 cells in 200µl PEB in polystyrene FACS tubes (BD Biosciences). Non-specific binding of antibodies to cells, especially macrophages and dendritic cells, was blocked by incubating cells with FcR block (Miltenyi) at 5µl/sample for 20min at 4°C. The samples were then washed in PEB and resuspended in 200µl for staining with antibodies at the concentrations listed in **Table 2.4**.

For each fluorophore in a panel, a single stain was prepared using a drop of UltraComp beads (eBioscience) in place of cells. These single stained samples were used to set the compensation for the cytometers and limit fluorophore spillover between channels which could give false results. Fluorescence minus one (FMO) controls were also prepared using isotype control antibodies, described in **2.8.3**. After staining for 30min at 4°C, samples were washed with PEB and analysed using a MACSQuant (Miltenyi), LSR-II or LSR-Fortessa (both BD Biosciences) flow cytometer.

2.8.2 Flow cytometry antibodies

Target	Fluorophore	Clone	Dilution (if not 1/200)	Supplier
CD11c	PE	X9-15		BioLegend
CD8	FITC	5H10-1		BioLegend
CD44	APC*	IM7		BioLegend
CD62L	PE-Cy7	MEL-14		BioLegend
CCR7	PE	4B12		BioLegend
F4/80	FITC	BM8		BioLegend
MHC class I	AF647	AF6-88.5		BioLegend
CD40	PE-Cy5	3/23		BioLegend
CD86	PE-Cy7	GL-1		BioLegend
CD80	BV421	16-10A1		BioLegend
MHC class II	VioGreen	M5/114.15.2		Miltenyi Biotec
PD-1	PE	29F.1A12		BioLegend
CD25	PE	PC61		BioLegend
Tetramer	APC*		1/50	Caltag Medsystems

Table 2.4 - List of mouse antibodies used in flow cytometry.
APC* (fluorophore) = allophycocyanin; BV = Brilliant Violet™; CD = cluster of differentiation; FITC = fluorescein; PE = phycoerythrin; PE-Cy = phycoerythrin-cyanine (conjugate).

2.8.3 Analysis of flow cytometry data

Data were analysed using MACSQuantify (version 2.6) software (Miltenyi) or FlowJo (version 10) software (FlowJo). Cells were identified first by forward scatter (FSC) and side scatter (SSC) profile, which quantifies the size and shape of the cells in the sample. These cells are further gated by selecting single cells using SSC-A and -H parameters: if the sample contains cell aggregates these will lie off the y=x line. Dead cells were then excluded using a dead cell discriminator dye. This gating hierarchy is common to all flow cytometry analysis performed in this thesis and is summarised in **Figure 2.2**, below.
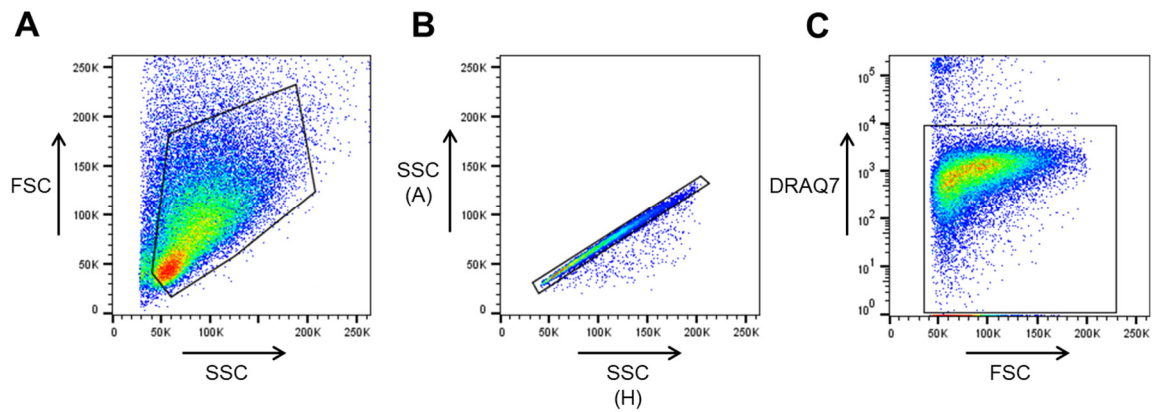
Figure 2.2 - Initial flow cytometry gating strategy.
Cells in each sample are gated first by size and shape using FSC/SSC (**A**), then by single cells (**B**), and finally by live cells (**C**).

To accurately analyse expression of surface markers and cytokines by antibody binding, it was important to use an FMO control. In each panel, an FMO control was made for every fluorophore, in which the fluorophore was replaced by an isotype control antibody bound to the same fluorophore. These FMOs acted as both negative controls for the fluorophore, allowing positive gates to be drawn for experimental samples and assessment of fluorophore spillover between channels.

Chapter 3

Characterisation of CCL19-sorted murine dendritic cells

3.1 Introduction and aims

Migration of DCs is crucial for their function and is almost exclusively controlled through chemokines and chemokine receptor expression. As briefly discussed in the **Introduction**, it is relevant to discuss the migration of the two main inflammatory DC subsets given their importance in DC therapy: steady-state, circulating DCs known as pDCs; and the typical inflammatory DCs (BMDCs in mice; MoDCs in humans). Ontogenically these subsets are quite different but are unified in their general function of uptake of both self and non-self antigens by endocytosis, and processing and presentation of these antigens to immune effector cells through MHC machinery.

Plasmacytoid DCs are a subset of DCs which exist in the body in the steady-state as fully-matured cells after development in, and egress from, the bone marrow. These cells can be identified by low expression of CD11b and CD11c, Siglec H and Ly6C in mice, and low or no expression of CD11c. pDCs highly express MHC class II and CD123 in humans (Rogers *et al*., 2013). Unlike their tissue-resident counterparts, pDCs circulate in the blood and are rarely found in the periphery with the exception of the intestine (Wendland *et al*., 2007) and appear to only enter tissues transiently to sample self-antigens and promote tolerance as shown in the context of tissue grafts (Ochando *et al*., 2006), or in response to an inflammatory signal from the tissue. They can secrete large quantities of IFNα in response to viral pathogens (Hagberg *et al.*, 2011). In both cases, pDCs can uniquely migrate back into the bloodstream after uptake of antigen and into the lymphatic organs through specialised venules called HEVs. pDCs express an unusual combination of canonically T cell-associated chemokine receptors (Seth *et al*., 2011) such as CXCR4, CXCR3 and CCR5. CXCL12, the ligand for the chemokine receptor CXCR4 is expressed constitutively by the lymphatics and was once thought to be the primary chemokine for steady state migration of pDCs into the LNs (Krug *et al*., 2002); with upregulation of the CXCR3 ligands CXCL9, CXCL10 and CXCL11 during viral infection potentially facilitating entry to the LNs during inflammation (Kohrgruber *et al*., 2004). Conflicting experimental evidence, however, suggests that these chemokine receptors do not induce pDC migration after activation (Penna, Sozzani and Adorini, 2001). In the steady state, these chemokine receptors may contribute more to the pDC surveillance of the periphery such as migration to the skin, or small intestine (Sozzani *et al.*, 2010). Interestingly, recent studies using CCR7$^{-/-}$ mice have shown intrinsic defects in the homing of pDCs, particularly after activation (Seth *et al.*, 2011) – highlighting this chemokine receptor as crucial for pDC migration, despite their expression of other chemokine receptors.

Inflammatory DCs are another subset of DCs, which are derived from myelomonocytic progenitors in the blood. These progenitors are released from the bone marrow as immature cells and migrate into tissues in response to inflammatory signals using the chemokine receptors CCR1, 2 and 5 (Fogg *et al.*, 2006). The process of extravasation from the blood into the tissues, and the subsequent inflammatory context in the tissue encourages maturation of the cells into DCs or macrophages depending on development stage of the progenitor cell (Liu, Victora and Schwickert, 2009). The cells sample antigen from the tissue, including cell debris and apoptotic cells, which, in concert with local cytokine production from other immune and stromal cells, induce maturation of the DCs and upregulation of CCR7 and co-stimulatory molecules such as CD80 and CD86 (Guermonprez *et al.*, 2002). Antigen uptake alone is sufficient to induce this upregulation and induce migration, in common with other DC subsets described here (Marsland *et al.*, 2005), but intravasating cells receive additional signals depending on the inflammatory context which can strengthen the immunogenicity of the final mature cell phenotype.

Migration of DCs to the lymph nodes using CCR7 is guided by expression of one of its ligands CCL21 by the lymphatic endothelium within the tissue (Saeki *et al.*, 1999), and by the fibroblastic reticular cells in the lymph node proper (Luther *et al.*, 2000). The highly-charged C-terminal extension of CCL21 allows the chemokine to be immobilised in components of the ECM, and helps guide haptotactic migration of DCs into the afferent lymphatics (Weber *et al.*, 2013). Once in the lymph node, mature DCs use CCL19 for fine migration control and have also been attributed as a source of CCL19. DCs present antigen primarily to T cells and provide 3 distinct signals for cell activation. Firstly, T cell recognition of the antigen-MHC complex provides Signal 1 (Bretscher & Cohn, 1970). Signal 1 in isolation is typically associated with T cell deletion or induction of a non-cytotoxic phenotype. This signal can be provided by a number of APCs, not exclusively DCs. Signal 2 refers to co-stimulatory signals from the cell presenting the antigen, and conventionally describes the interaction of CD80 and CD86 with CD28 on T cells (Keir and Sharpe, 2005). CD80 is expressed by APCs solely in response to maturation signals as described previously, whereas CD86 is present at low levels and expression is increased after stimulation. The physical proximity required for Signal 1 allows other cell-cell contacts such as CD80/86-CD28, as such these signals are referred to as co-stimulatory. A third signal, Signal 3, is derived from paracrine factors secreted by the APC which can skew T cell differentiation into a particular phenotype. One of the most potent and well-characterised 'signal 3' factors is IL-12, which specifically supports the production of CTLs and Th1 cells (Trinchieri, 2003).

In all DC subsets, expression of CCR7 is therefore crucial for cell function by allowing DCs to efficiently migrate to the lymph nodes following activation and induce the appropriate T cell response for their subset. Although DCs are utilised therapeutically, particularly in cancer therapy, the migratory capacity of the cells themselves are rarely taken in account and instead clinical trials use strategies such as intranodal injection (de Vries, Krooshoop, *et al.*, 2003) or simply large doses of cells to ensure adequate nodal accumulation of the DCs and therefore a therapeutic response. DCs generated in *ex vivo* cultures invariably display heterogeneous expression of CCR7, which limits potential migration, but isolating the CCR7+ cells is technically challenging given the paucity of antibodies against chemokine receptors in general. A novel sorting methodology developed by Le Brocq *et al.* (2014) may present an alternative method, as it uses a biotinylated CCL19 in place of an antibody and shows reliable and better staining for the CCR7+ cells by flow cytometry.

In this Chapter, DCs were sorted for expression of CCR7 using this CCL19-based sorting method and were characterised for their expression of co-stimulatory molecules on the cell surface, and their cytokine and chemokine expression profile. The migration of the cells was then assessed *in vitro* and *in vivo*, as well as an investigation into the kinetics of the receptor-ligand interaction. Finally, the ability of the sorted cells to induce functional T cell responses *in vitro* was explored using a co-culture system.

3.2 Optimisation of chemokine sorting protocol

3.2.1 Validation of chemokine staining

The use of biotinylated CCL19 (bCCL19) to detect the presence of CCR7 on the surface of DCs has been well characterised (Le Brocq *et al.*, 2014). Briefly, the bCCL19 is conjugated to phycoerythrin (PE) using streptavidin by first complexing streptavidin-PE (SAPE) into a tetramer, which is used as an antibody equivalent to stain cells expressing CCR7. This method was shown to identify the same population of cells as staining by a CCR7-specific antibody conjugated to PE. To ensure this protocol was reliably reproduced in this study, BMDCs were generated and stained with the bCCL19-SAPE conjugate. This is summarised in **Figure 3.1**, below. As shown, staining clearly identifies CCR7 expression on BMDCs as previously described.
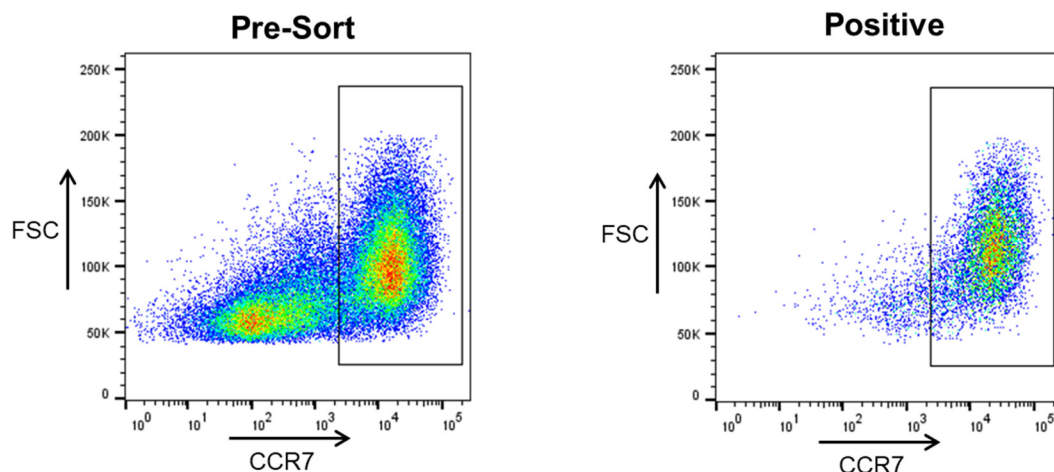
Figure 3.1 - Fluorescent discrimination of CCR7+ BMDCs using CCL19-SAPE conjugate.
BMDCs were generated using GM-CSF culture and stained using CCL19-SAPE. Cells were gated as shown in **Figure 2.2** prior to analysis. Following staining there is a clear CCR7-expressing population of cells, as shown in **Pre-sort** and effective separation of these cells by sorting, as shown in **Positive** (representative).

3.2.2 Optimisation of chemokine sorting

After confirmation of the staining protocol, next the sorting of cells using bCCL19 was validated. To reliably improve the protocol for a potential cell therapy, it was important to optimise the protocol for DC sorting. Le Brocq *et al.* (2014) used magnetic bead sorting to isolate DCs and T cells by CCR7 expression, and this was reproducible with respect to DCs in our hands (data not shown). To further improve sorting efficiency three modifications to the bCCL19 structure were also tested, which are described in **Figure 3.2**. The rationale for this modification was to accommodate the morphological change DCs undergo during maturation – an increase in the folded structure of the cell membrane known as spiculation, which increases the cell surface area to facilitate cell-cell contact (Xing *et al.*, 2011). Manual separation of cells using a magnetic bead system requires binding of the chemokine-SAPE-bead conjugate successively, so extending the biotin moiety and adjoined SAPE from the bCCL19/CCR7 interaction would allow more space for the α-PE microbeads to bind stably to the tetramer. Although staining with the conjugate alone was consistent, these modifications were expected to increase consistency and yield of DC sorts.
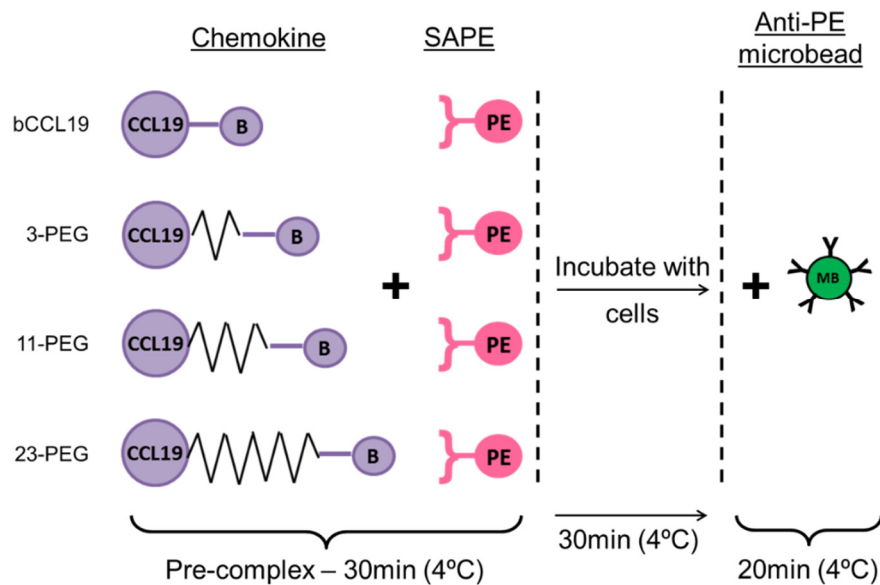
Figure 3.2 - Schematic representation of PEGylated bCCL19-SAPE conjugation and sorting.
bCCL19 is PEGylated to increase the distance between the peptide and the attached biotin moiety
and conjugated to SAPE for 30min before adding to the cells. After 30min the cells are washed and
incubated with anti-PE microbeads for sorting.

Dendritic cells expressing CCR7 were isolated from a mixed population of cells using the
bCCL19-SAPE conjugate with magnetic bead separation. The protocol was first tested by
comparing bCCL19, where the biotin moiety was conjugated directly to the chemokine,
with three PEG-chain variants where the distance between the biotin moiety and the
chemokine was increased using 3-, 11-, or 23-PEG residue-long chains. Firstly, the CCR7+
population in the unsorted fraction was compared to the positive and negative post sort
fraction for each of the four chemokine variants.
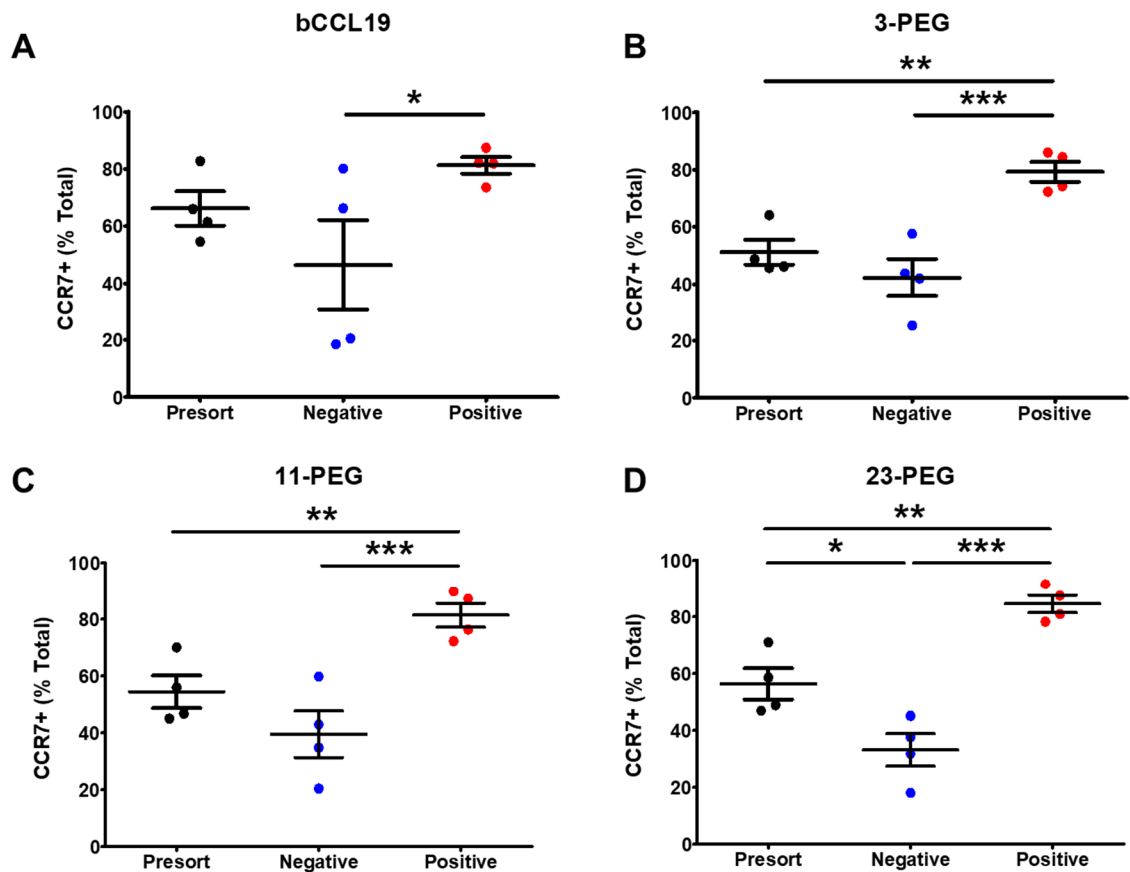
Figure 3.3 - Comparison of the CCR7-expressing population in the unsorted, positive and negative sorted fractions using bCCL19 variants.
BMDCs were sorted by magnetic column separation using each of the bCCL19 variants (bCCL19 (**A**), and 3-, 11-, and 23-PEG bCCL19; denoted as **B-D**, respectively) conjugated to SAPE to isolate the CCR7-expressing population. Tetramer-labelled, unsorted cells were retained as a control for initial populations and were compared to the negative and positive post sort fractions using flow cytometry. CCR7+ populations were gated first by size, single cells, and viability by DRAQ7. Data points represent individuals ± SEM. Statistical analysis was by one-way ANOVA with Bonferroni's Multiple Comparison Test: *P ≤ 0.05, **P ≤ 0.01, *** P ≤ 0.001 (n = 4/group).

All bCCL19 variants used were able to isolate CCR7-expressing cells to comparable levels, but statistical analysis of the individual variants highlights important individual differences. The only statistical difference in bCCL19 was between the negative and positive post sort populations, compared to any of the PEG-modified variants which all have additional significant differences between unsorted and positive sort populations (**Figure 3.3**). This suggests that bCCL19 can be used to sort BMDCs, however the positive population is not significantly enriched by the process (~66% in the presort to 81% in the positive). In comparison, PEG-modified bCCL19 was able to enrich the positive population for CCR7 expression from the starting population. 23-PEG bCCL19 was shown to be the most effective ligand for cell sorting based on the enrichment for CCR7-expression in the positive sorted fraction (~56% to 84%) and the coincident reduction of

the CCR7-expressing population in the negative sorted fraction compared to the unsorted fraction (~56% reduced to 33%). In all cases, the negative cell fraction still contained CCR7+ cells, although this was decreased from 46.35% (±15.77%) using bCCL19 to 42.17% (±6.626%), 39.5% (±8.21%), and 33.13% (±5.72% using 3-PEG, 11-PEG and 23-PEG CCL19, respectively, possibly highlighting the superior ability of the PEGylated variants to bind DCs preventing them from being lost in the negative fraction following sorting.
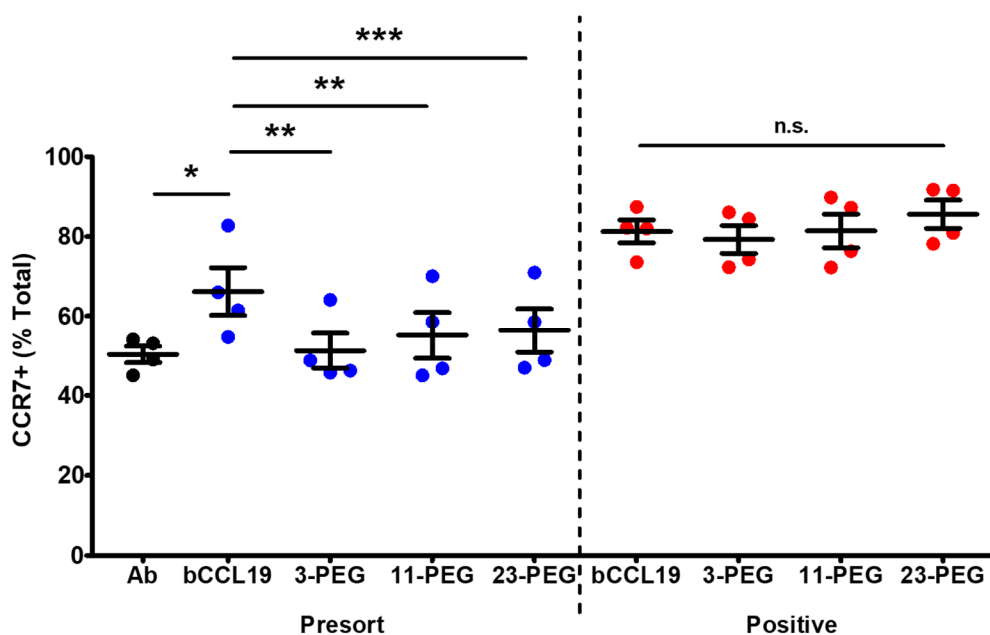
Figure 3.4 - Direct comparison of unsorted and positive sorted fractions using bCCL19 variants.
BMDCs were sorted by magnetic column separation using each of the bCCL19 variants (bCCL19 and 3-, 11-, and 23-PEG bCCL19) conjugated to SAPE to isolate the CCR7-expressing population. Negative and positive post sort fractions were compared using flow cytometry, with anti-CCR7 antibody-stained cells used as a control. Data points represent individuals ± SEM. Statistical analysis was by one-way ANOVA with Bonferroni's Multiple Comparison Test: *P ≤ 0.05, **P ≤ 0.01, *** P ≤ 0.001 (n = 4/group).

Direct comparison of staining for CCR7 (**Figure 3.4**) showed only a small but non-significant difference between the PEG-modified CCL19 variants in both pre-sort staining and isolation of CCR7+ cells. To allow comparison, one starting population was sorted using each of the four variants and should therefore have the same CCR7 expression. It can be seen, however, that bCCL19 may be overestimating the size of the CCR7+ population. Comparison of bCCL19 with a CCR7-specific antibody (**Figure 3.4 – Ab**) shows that it stained a significantly higher proportion of the cells (66.2% ±6% compared to 50.3

±2.1%). Although there was no statistical difference between the PEG-modified chemokine variants, the enrichment of the positive fraction described previously (presented in **Figure 3.3**) was an important consideration. Taking these data into account, 23-PEG bCCL19 was chosen for sorting BMDCs.

3.2.3 Improving cell viability and yield

While the CCL19 sorts routinely showed high purity of cells expressing CCR7 once the process was optimised for BMDCs, post-sort cell viability was the next key consideration. Magnetic column-sorting the cells requires all reagents and equipment to be at 4°C, as shown in **Figure 3.2**, and the protocol carried out swiftly in a tissue culture hood at room temperature (~22°C) or in a cold room (~4°C) depending on the level of sterility required. This temperature is crucial to prevent ligand-induced internalisation of CCR7 (Otero, Groettrup and Legler, 2006) and maintain accessibility of bCCL19 for subsequent microbead binding and therefore sorting. It was expected that DC viability following the magnetic sort would be reduced, given both the prolonged low temperature and mechanical stress from the magnetic column: if cell viability is low after the sort, this limits their potential viability *in vivo*. Although initial validation of bCCL19 was done using this separation, incorporation of a fluorophore conjugation step in the process allowed adaptation of the protocol for FACS as described in **2.6.2.2**. This sorting strategy also puts the cells under physical stress but was compared as a potential alternative. Routine cell viability was assessed after each sort described in **3.2.2**, and is summarised below.
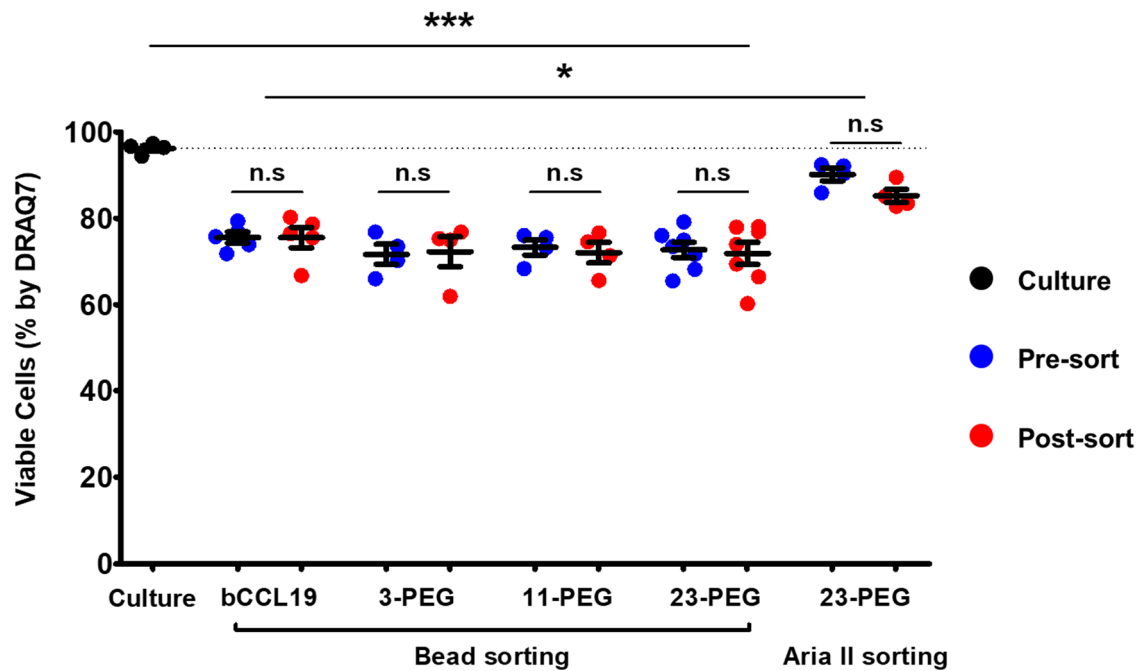
Figure 3.5 - BMDC viability remains high in FACS-sorted cells compared to column sorting.
BMDCs were taken from culture for chemokine sorting using each of the bCCL19 variants, or on the BD Aria II and were assessed for cell viability by flow cytometry using DRAQ7 compared to initial viability of cells in culture. Data points represent individuals ± SEM error bars. Statistical analysis was by one-way ANOVA with Bonferroni's Multiple Comparison Test: n.s. is not significant, *P ≤ 0.05, ***P ≤ 0.001 (n≥4/group).

There was a significant loss of cell viability from the initial isolation of the cells from culture (black dots) through the bCCL19-SAPE and bead staining steps to the pre-sorted cells (blue dots) and after sorting (red dots) (**Figure 3.5**). The cells started at above 96.2% (±0.62%) viability immediately after harvest and decreased to 70-80% viability by the start of the sort for each of the bCCL19 variants, but did not lose viability between the pre- and post-sort steps. Although the viability did decrease overall, there appeared to be no loss of cell viability as a result of the column sorting itself despite the cells being under mechanical pressure during the process. In comparison, there was no difference in viability between cells from culture and either the pre- or post-sort cells using the Aria II. The viability of the cells remained at 90.18% (±1.49%) viability prior to the sort and decrease to 85.23% (±1.5%) after the sort, but this change is non-significant. This suggests that separation of CCR7+ cells by FACS maintained the highest cell viability and may be the best sorting method for use of the cells post-sort. Cell yield was also seen to be a consistent issue with column-sorted cell populations, so was again compared to the yield of fluorescently-sorted cells.
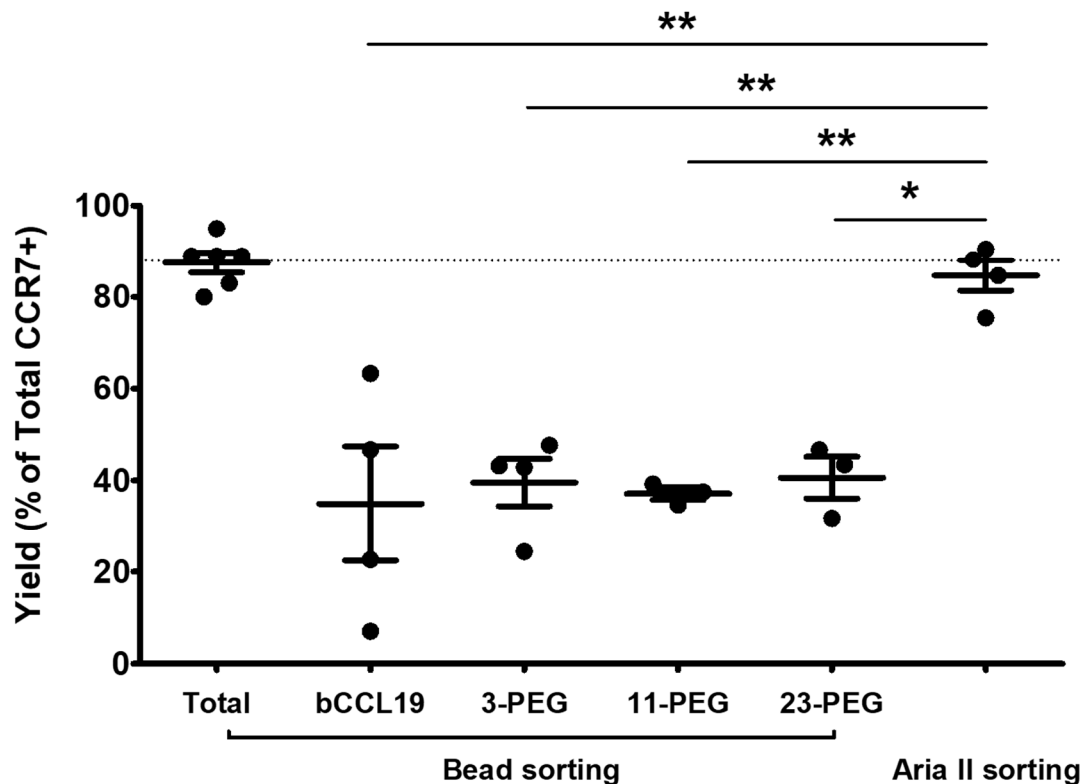
Figure 3.6 - BMDC post-sort yield is higher by FACS than column sorting.
Cultured BMDCs were magnetically sorted using each of the bCCL19 variants or using the BD Aria II and the CCR7+ cell yield was calculated as a proportion of the total CCR7+ cells in the initial population. Total cells recovered from the column is included as a positive control, but not included in the statistical analysis. Data points represent individuals ± SEM. Statistical analysis was by one-way ANOVA with Bonferroni's Multiple Comparison Test: *$P \leq 0.05$, **$P \leq 0.01$ (n = 3-5/group).

As shown in **Figure 3.6**, cell yield from the magnetic column sort was consistently only ~40% of the total starting CCR7+ cells regardless of the bCCL19 variant used. When comparing the four, however, the bCCL19 variant yield was very variable (34.91% ±12.49%) whereas the PEGylated variants showed a much lower variability in yield, suggesting that PEGylation of the chemokine improved the reliability of the sorting strategy. The remaining CCR7+ cells were present in the negative eluted fraction (as shown in **Figure 3.3**) or lost within the column itself. The total cell yield from the column was included here as a control, showing that up to 20% of the initial cell input can be lost just through the sorting process. The yield of the cells from the Aria II sort was significantly higher than any of the column-sorted groups, with almost double the number of returned cells (~40% for the column-sorted cells, and 84.7% ± 3.32% for the Aria II). Taking the viability and yield together, sorting cells by FACS was chosen for future use.

3.3 Sorted DCs migrate more efficiently to CCL19 gradients *in vitro* and *in vivo*

3.3.1 *In vitro* migration by Transwell Migration Assay

It is well-characterised in chemokine receptor biology that ligand binding to the receptor causes rapid internalisation and subsequent resistance to ligand signalling until the receptor is recycled back to the surface. If chemokine-sorted cells are to be considered a viable therapeutic product, then the migration capacity of the cells following sorting needs to be assessed. BMDC migration before and after sorting was tested using a transwell migration assay, which quantifies active cell migration in response to a cytokine gradient set up *in vitro*.
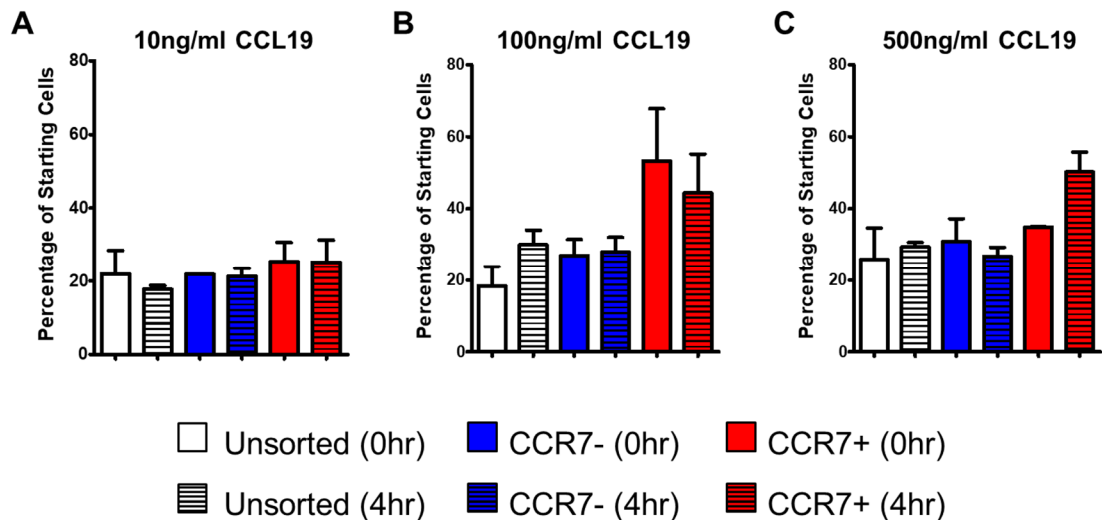
Figure 3.7 - CCR7-sorted DCs are capable of migration immediately after sorting.
CCR7-sorted cell migration was challenged using a transwell migration assay. **A** – 0hr post-sort. **B** – 4hr post-sort. Three concentrations of chemokine were used based on previous work by Le Brocq *et al.*, (2014) (n = 2).

It can be seen at both timepoints that BMDCs in the positive sorted fraction migrated more effectively than the others, as presented in **Figure 3.7**. Chemokine concentrations used here reflect a concentration too low to induce migration (10ng/ml), a biologically relevant chemokine concentration (100ng/ml), and a concentration too high to induce migration (500ng/ml) (based on the study by Haessler *et al.*, 2011). Chemokinesis has been shown to sharply decline with chemokine concentration above a functional maximum, during which the chemokine receptor is internalised and leads to cellular desensitisation and decline of cell migration. Up until this maximum, however, as the surface expression decreases, cell

sensitivity increases as the threshold signalling for migration is lowered (Petit, Chayen and Pease, 2008). Immediately after sorting, cells in the positive fraction migrated more strongly towards a 100ng/ml biological chemokine gradient compared to the other populations, with 53.3% (±14.5%) migrating through the transwell insert compared to the unsorted cells (26.9% ±4.5%) and the unsorted cells (18.4% ±5.4%). At the other concentrations there was little difference in migration capacity, if any. After 4 hours of rest, a similar trend in migration capacity was seen, however CCR7+ cells are also shown to migrate more than the other fractions at 500ng/ml CCL19. This data may be indicative of the bell-shaped curve of the chemokinesis response (Petit, Chayen and Pease, 2008). Immediately following sorting, the peak of the migration response appears to be between 100ng/ml and 500ng/ml, whereas after allowing the cells to rest and recycle the receptor, this peak appeared to have shifted to a higher concentration as the migration responses to 100ng/ml and 500ng/ml equalised.

Taken together, these data suggested that there may be some degree of receptor recycling occurring within the sorted BMDCs, however, this recycling did not appear to hinder the immediate migration of the cells *in vitro*. This is therapeutically relevant because it would allow the sorted cells to be used immediately, reducing the requirement for a rest, or "wash-out" period and therefore maintaining the quality of the final cell therapy product.

3.3.2 *In vivo* migration by footpad migration

To continue assessing the migratory capacity of CCR7-sorted DCs, the ability of the cells to migrate *in vivo* was quantified. BMDCs were sorted using 23-PEG bCCL19 and labelled with a fluorescent dye (either PKH-67 or CellTracker Violet, as described in **2.6.3**); a control population of unsorted cells was also labelled with the alternative dye. CCR7+ sorted cells were injected into one footpad, and unsorted cells containing the same number of CCR7+ cells were injected into the opposite footpad of the same animal. 48hr later, the footpads and pLN were removed for processing and flow cytometry to detect injected cells.
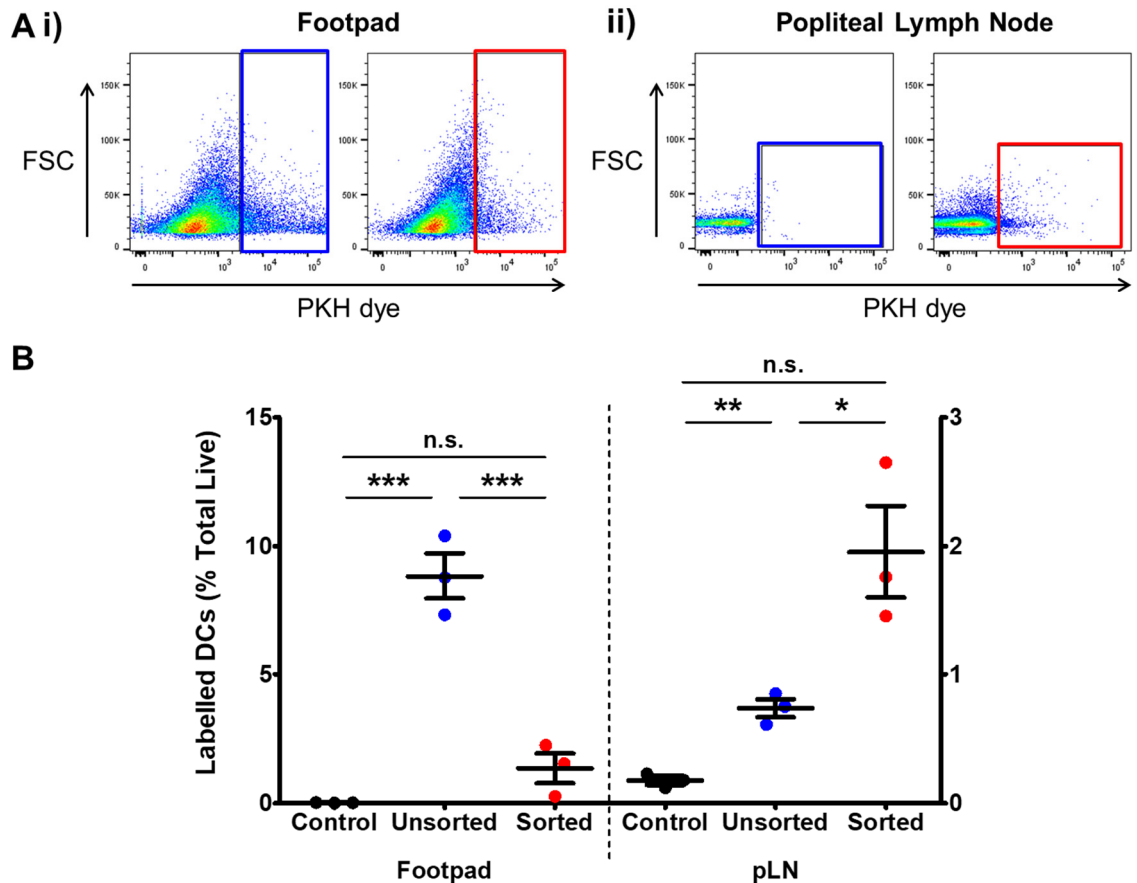
Figure 3.8 - CCR7-sorted BMDCs migrate more efficiently to the pLN following footpad injection but unsorted cells are retained at the injection site.
BMDCs were sorted for CCR7-expression or left unsorted as a control, differentially labelled using fluorescent tracking dyes. 48hr after injection into the footpad, the pLN was removed for analysis of cell migration. **A** – Representative flow cytometry plots showing labelled cells in the (i) footpad and (ii) popliteal lymph node, with unsorted cells gated in blue and CCR7-sorted cells gated in red. **B** – Quantification of the cells present in each tissue. Data points represent individuals ± SEM error bars. Statistical analysis was by one-way ANOVA with Bonferroni's Multiple Comparison Test: n.s. is not significant, $*P \leq 0.05$, $***P \leq 0.001$ (n = 3/group).

As shown in **Figure 3.8**, CCR7-sorted BMDCs effectively migrate from the site of the injection to the draining lymph node in 48hr compared to the unsorted comparison population. In the footpad, there is a significant difference in unsorted cells remaining in the tissue compared to sorted cells, which are almost 5 times fewer in number (**Figure 3.8B**). In contrast, in the footpad-draining pLN, there is almost double the number of CCR7+ cells in the sorted fraction. This highlights the importance of separating the migratory CCR7+ cells from the bulk population, as well as the removal of CCR7- DCs since they may contribute to retaining cells at the injection site.

3.4 Chemokine-sorted DCs represent a phenotypically distinct population of cells

3.4.1 Surface phenotype

Generation of murine BMDCs *in vitro* has been shown to yield a heterogeneous population of cells, comprising of both conventional DCs but also macrophages (Merad *et al*., 2013). This heterogeneity is evident in cultures using GM-CSF alone, a combination of GM-CSF and IL-4, or with Flt3-L. Recent work has begun to highlight the overlap in markers used to distinguish these two cell types, particularly with respect to the expression of CD11c on macrophages. To assess this complexity, bone marrow cultures with GM-CSF were stained for CCR7, the conventional DC marker CD11c, and the conventional macrophage marker F4/80.
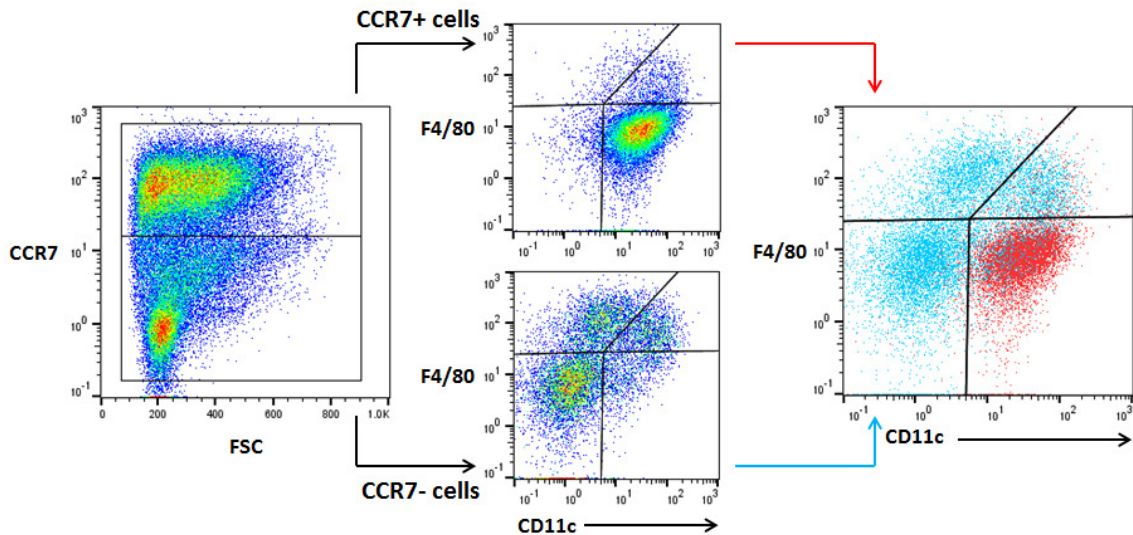
Figure 3.9 - Chemokine sorting effectively isolates a single cell population.
A heterogeneous GM-CSF-induced cell population has four populations identifiable by differential F4/80 and CD11c expression. bCCL19-stained cells (red) display an F4/80- CD11c+ phenotype; in comparison, cells not stained by bCCL19 (blue) display either an F4/80+ phenotype or express neither F4/80 or CD11c.

Staining with only CD11c and F4/80 identifies four cell populations in the culture. Cells were also stained for CD11b, the α-chain of the myeloid integrin Mac-1, which is expressed by monocytes and macrophages (Larson & Springer, 1990). CD11c discriminates DCs, as well as the final positive population following bCCL19-sorting (highlighted in red, **Figure 3.9**). This was expected since CCR7 is only expressed on mature DCs among mononuclear cells. F4/80 is a conventional macrophage marker, and F4/80+ cells here represent two populations further separated by expression of CD11c. *In*

vitro generation of mononuclear cells using only GM-CSF commonly produces this mixed population, which considering our interest in DCs in the culture is important to know to avoid assuming all CD11c+ cells in the culture are DCs. These two F4/80+ populations are thought to represent an M1 (CD11c+) and M2 (CD11c-) phenotype (Helft *et al*., 2015). The fourth population identified expresses neither F4/80 nor CD11c, and most likely represent undifferentiated cells in the myeloid lineage given the expression of CD11b (not shown). It is crucial to note that in mouse BM cultures derived using GM-CSF that only sorting by CCR7 expression results in a pure population of cells, with both alternative options (positive selection of cells expressing CD11c, and depletion of cells expressing F4/80) still resulting in a subtly heterogenous population. Crucially, the sorted CCR7+ population accounts for only ~60% of the total cell population (shown previously); highlighting the need for cell sorting to remove any immature cells from the product prior to injection which may result in development of unwanted T cell tolerance instead of proliferation (Hilkens *et al*., 2010).

Since CCR7 is upregulated on DCs only after maturation, its expression can be used to reliably identify mature DCs in a mixed CD11c-expressing population comprising both immature and mature DCs. As shown in **Figure 3.9**, only one CD11c+ population is present, after exclusion of F4/80 expression. Subsequent care was taken to exclude F4/80-expressing cells in future analyses to remove any influence of contaminating macrophages in the results. Cells were subsequently stained for markers of both DC activation status as well as receptors required for T cell costimulation to better characterise the cell phenotype.
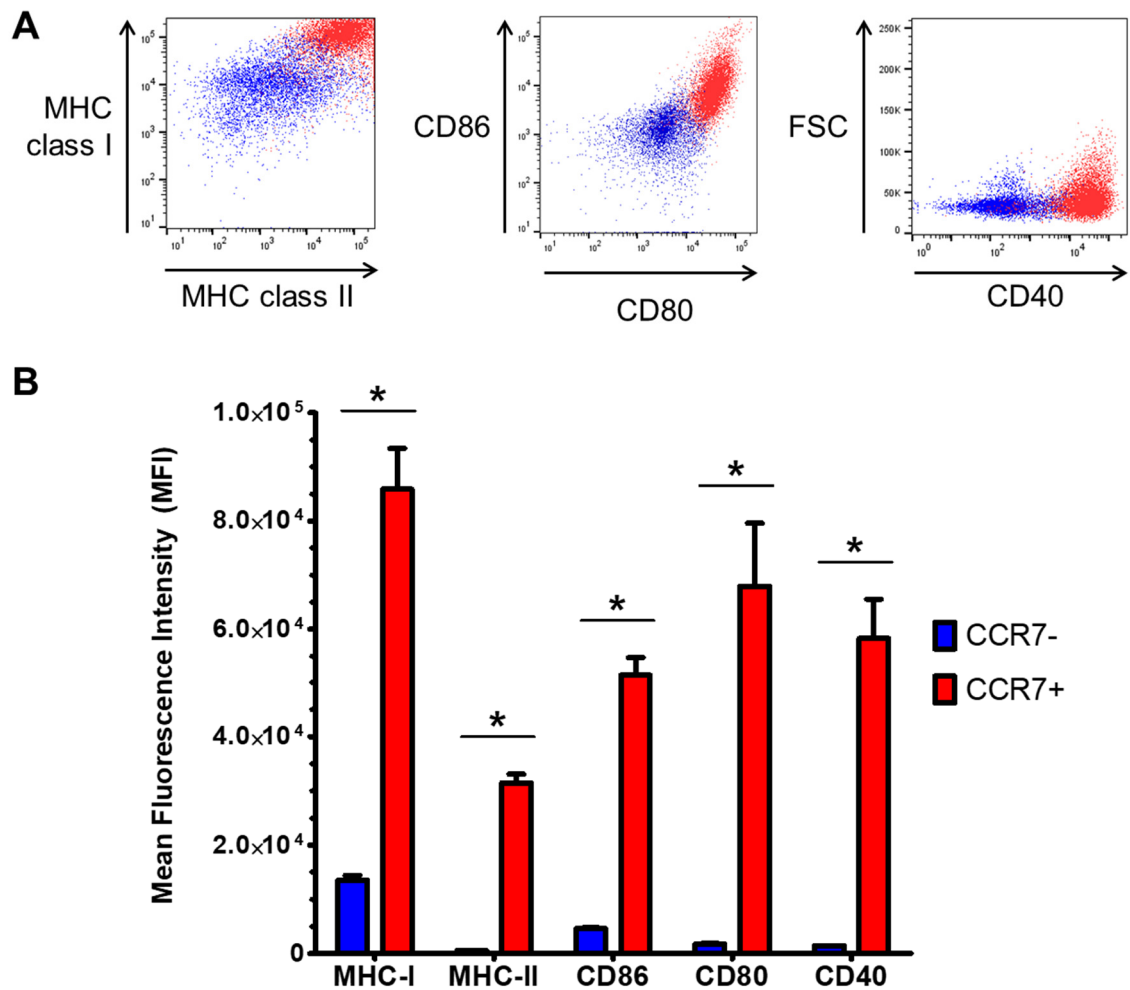
Figure 3.10 - CD11c+CCR7+ and CD11c+CCR7- BMDCs are distinct by surface phenotype.
A – Representative flow cytometry plots showing expression of activated DC markers in the CCR7-cells (blue) and CCR7+ cells (red). **B** – Quantification of expression shows these markers are significantly enriched in CCR7+ populations in comparison to CCR7- populations. Statistical analysis was by Students t test. * P ≤ 0.05 (n = 4).

As expected, sorted BMDCs more highly express markers required for effective T cell stimulation *in vivo* (**Figure 3.10**). CD40, CD80 and CD86 are required by BMDCs for strong and effective T cell activation; without this interaction BMDCs are likely to induce anergy in antigen-specific T cells instead of activation (Crespo *et al.*, 2013). CD80 and CD86 bind CD28 on T cells and induce activation in conjunction with TCR binding, as described previously. It is very important, therefore, for DCs to express these molecules for immune function, and CCR7+ DCs have been confirmed here to highly express them compared to the CD11c+ CCR7- DC population. CD40 functions similarly, interacting with CD154 on T cells and NK cells for induction of cytotoxicity (Grewal and Flavell, 1998). This interaction between DCs and NK cells has also been shown to support the generation of anti-tumour CTLs *in vivo* (Adam *et al.*, 2005). In addition to costimulatory molecules, CCR7+ DCs have an increased expression of MHC class I and class II

molecules, confirming the phenotype of this cell population as mature and immunostimulatory (de Vries *et al*., 2002). These data confirm the mature, sorted CCR7+ DCs are functionally capable of providing T cells with signals 1 and 2 for their activation.

3.4.2 Chemokine and cytokine profile

To further characterise the sorted and unsorted cells, the chemokine and cytokine secretion profile of the BMDCs was assessed by 33-plex Luminex analysis. BMDCs were generated and F4/80-CD11c+ cells were sorted using the BD Aria II. These cells were further sorted into CCR7+ and CCR7- cell fractions and lysed to collect proteins. Protein concentrations were determined using BCA assay prior to Luminex analysis to ensure an equivalent starting concentration (data not shown).

The expression of 33 analytes was assessed, although most of the chemokines and cytokines were below the level of detection suggesting that they are not produced by either immature or mature BMDCs. Of these 33, 9 are differentially produced by the two groups: CCL3, CCL4, CCL5, CCL17, CCL22, CXCL2, CXCL16, IL-1β, and IL-16. These data are summarised in **Figure 3.11**. All chemokines and cytokines assessed are listed in **Table 2.2**.
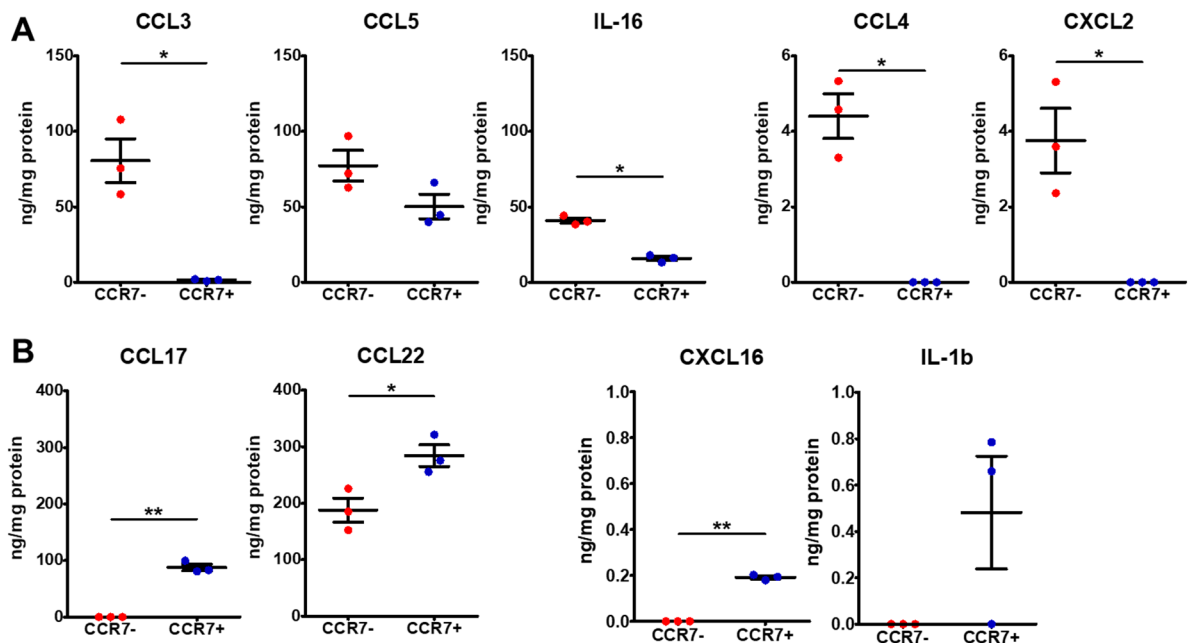
Figure 3.11 - Distinct chemokine and cytokine production by CCR7- and CCR7+ DCs.
CD11c+CCR7- and CD11c+CCR7+ DCs were sorted using the BD Aria III and lysed to extract the proteins for Luminex analysis. 33 chemokines and cytokines were analysed, with production of these 9 detectable, and different between the two groups. **A** – analytes more highly expressed by CCR7- DCs; **B** – analytes more highly expressed by CCR7+ DCs. Data points represent individuals ± SEM error bars. Statistical analysis was by Students t test. * P ≤ 0.05, ** P ≤ 0.01 (n = 3; 2 replicates each).

It is immediately apparent that CCR7- and CCR7+ DCs are phenotypically different by expression profile. As shown, CCR7- BMDCs produce at least 50-fold more CCL3 (80.59 ±25.1ng/mg protein), CCL4 (4.41 ±1.0ng/mg protein) and CXCL2 (3.76 ±1.48ng/mg protein), than CCR7+ DCs, with the latter two chemokines being undetectable in this group. Although there appeared to be a small decrease in CCL5 between the groups, this did not reach significance. CCR7- DCs, interestingly, produced more than double the amount of IL-16 than CCR7+ DCs (40.93 ±3.03ng/mg protein to 15.76 ±2.41ng/mg protein). In comparison, CCR7+ DCs expressed adaptive immune chemokines such as CCL22 and CCL17 more highly (284.0 ±33.73ng/mg protein to 187.8 ±36.76ng/mg protein, and 87.7 ±10.35ng/mg protein to undetectable, respectively) as well as more CXCL16 which was undetectable in the CCR7- DCs. The difference in IL-1β was only seen in 2 of the 3 samples tested so did not reach significance.

CCR7+ DCs therefore express an array of potent immune-stimulatory factors compared to CCR7- DCs also present in the cultured population. Flow cytometry data for surface marker expression, and analysis of chemokine and cytokine secretion by these cells supports the hypothesis that CCR7+ DCs alone are a potentially viable population for the generation of a CTL response; this was next confirmed using an *in vitro* co-culture system.

3.5 Sorted DCs induce an increased antigen-specific T cell response

Finally, the interaction of sorted and unsorted DCs with antigen-specific T cells was quantified and assessed using the OT-I mouse model. It has been shown that CCR7-expressing DCs highly express markers of T cell stimulation such as CD40, CD80 and CD86; exhibiting a more mature phenotype than CCR7- DCs. Additionally, CCR7+ DCs produced chemokines such as CCL17, CCL22, and CXCL16, suggesting these cells can potently attract T cells for activation. To quantify the ability of these cells to stimulate T cells, DCs were generated, fed ovalbumin and sorted as previously, with the addition of CD11c to separate immature (CCR7-) and mature (CCR7+) DCs. These cells were then cultured along with T cells recognising the MHC class I-ovalbumin epitope which were isolated from the lymph nodes of OT-I mice to assess changes in the T cell phenotype.

3.5.1 Conventional DCs (cDCs)

GM-CSF-derived BMDCs were sorted into two populations based on CD11c expression and differential expression of CCR7. The CCR7+ and CCR7- DCs were incubated with ova-specific T cells for 7 days, after which their surface phenotype was assessed by flow cytometry.
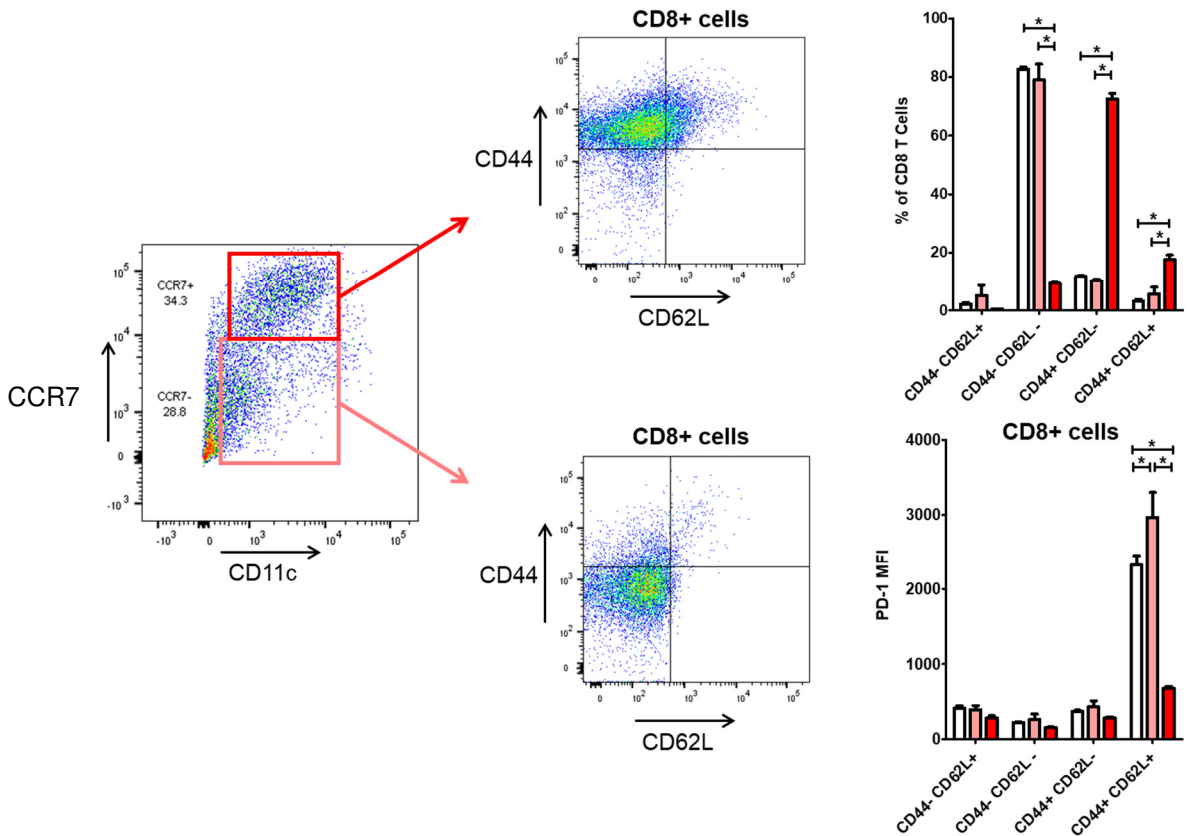
Figure 3.12 - CCR7+ and CCR7- DCs generated using GM-CSF induce distinct patterns of T cell maturity after co-culture.
GM-CSF- BMDCs were sorted for expression of CD11c and into CCR7+ (red box) and CCR7- (pink box) cell populations and cultured with OT-I T cells. After 7 days T cells were phenotyped for expression of CD44, CD62L and PD-1. Data points represent mean ± SEM error bars. Statistical analysis was by one-way ANOVA. * P ≤ 0.05 (n = 3).

After 7 days in culture with DCs, the T cells looked quite different in terms of surface marker expression. Using CD44 and CD62L to define cell maturity, T cells cultured with CD11c+ CCR7+ DCs expressed a more mature phenotype (defined by the CD44+ CD62L- phenotype). In comparison T cells cultured with CD11c+ CCR7- DCs were CD44- CD62L-, a less mature phenotype, with only a small percentage fully mature. This suggests that the phenotype associated with CCR7 expression on DCs is important for activation of antigen-specific T cells. PD-1 expression of these T cells was also assessed. PD-1 is a marker of functional exhaustion in T cells (Barber *et al*., 2006), so it was interesting to see

an increase in PD-1 expression in the most mature group of T cells exposed to either IL-2 alone (white bars), or CCR7- DCs (pink bars), but that this was not observed in T cells exposed to CCR7+ DCs.

3.5.2 Plasmacytoid DCs (pDCs)

As previously described, the expression of CCR7 is also crucial for the migration and therefore the function of pDCs *in vivo*. Flt3-L-derived DCs, which here are defined as pDCs but are generally accepted to represent a more *in vivo* DC-like phenotype than GM-CSF-derived DCs (Merad *et al.*, 2013), were generated and sorted for CD11c expression and split into CCR7+ and CCR7- cell fractions. These fractions were then co-cultured with ova-specific T cells for 7 days as previously (**3.5.1**).
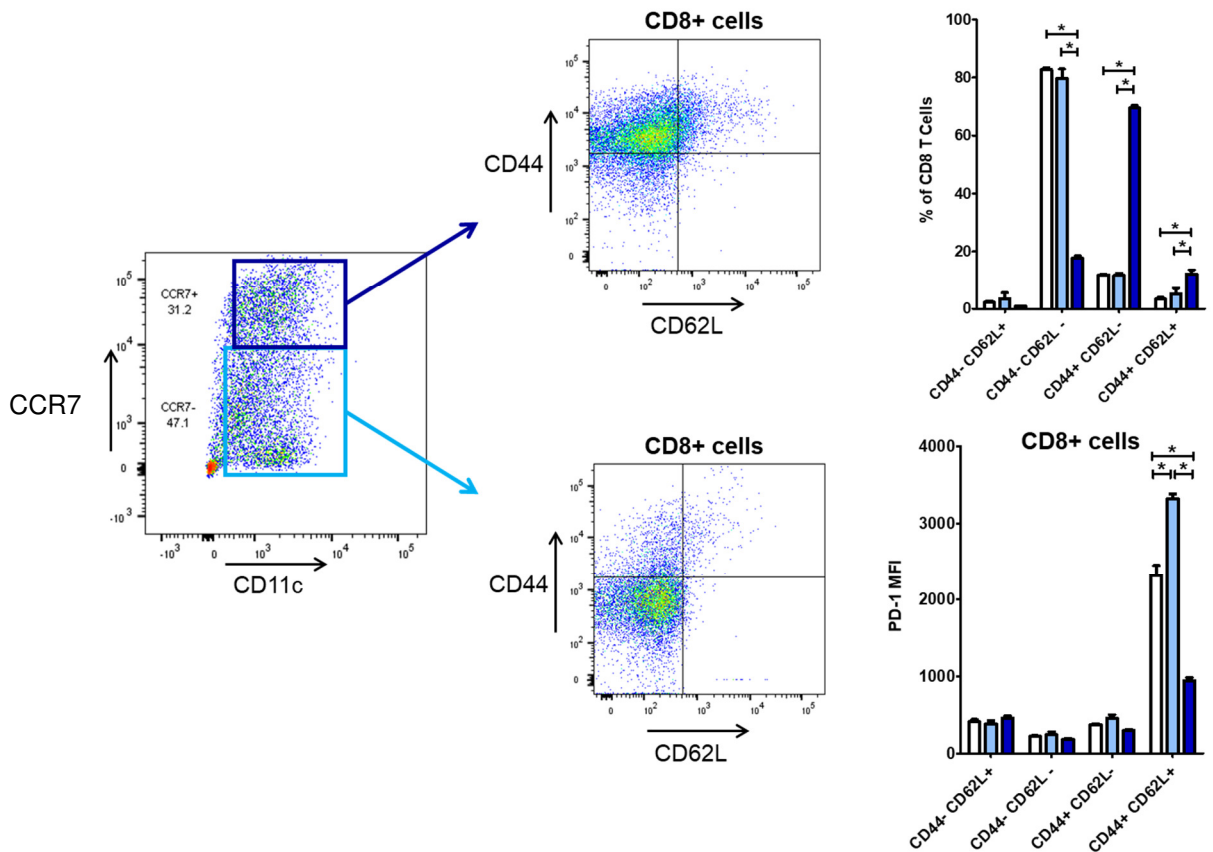
Figure 3.13 - CCR7+ and CCR7- DCs generated using Flt3-L induce distinct patterns of T cell maturity after co-culture.
Flt3-L-BMDCs were sorted for expression of CD11c and into CCR7+ (dark blue box) and CCR7- (light blue box) cell populations and cultured with OT-I T cells. After 7 days T cells were phenotyped for expression of CD44, CD62L and PD-1. Data points represent mean ± SEM error bars. Statistical analysis was by one-way ANOVA. * P ≤ 0.05 (n = 3).

Again, expression of CCR7 in pDCs seemed to correlate with the induction of a mature, response in antigen-specific T cells. CCR7+ DCs cultured with T cells lead to a mature T cell phenotype by expression of CD44 and CD62L compared to CCR7- DCs. Both IL-2 alone and CCR7- DCs led to a primarily early 'activated' phenotype (CD44-CD62L-) which may be in the transition to a mature phenotype but requiring longer than 7 days to do so. Similarly to GM-CSF DCs, IL-2 and CCR7- pDCs induced the expression of PD-1 more highly in the most mature T cell phenotype (CD44+CD62L+) suggesting exhaustion of these cells and a reduction in function or even senescence compared to T cells stimulated by CCR7+ pDCs.

In the absence of in-depth assessment of cytokine production by the generated T cells, it would be difficult to define the induced response as cytotoxic or otherwise, but these data confirmed that sorting DCs for CCR7 expression produces a population of cells which can potently stimulate T cells *in vitro*.

3.6 Discussion

The cell-sorting protocol published by Le Brocq *et al.* (2014) was first optimised for BMDCs using PEGylated variants of bCCL19. Although the original bCCL19 protocol was sufficient for staining of CCR7+ cells, it was shown to be variable compared to any of the PEGylated CCL19 variants. The variant with the longest space between the chemokine and the biotin moiety, the 23-PEG bCCL19, was seen to be consistent in both staining and magnetic column-sorting BMDCs by comparing the purity of the positive sort fraction and the positive cells remaining in the negative fraction. The yield of the positive cells in all cases was seen to be lower than ideal, so the incorporation of the PE fluorophore into the CCL19 conjugate was utilised to adapt the sort for FACS using the BD Aria II and Aria III (Aria III data not shown). This strategy was shown to reliably sort the BMDCs to a high purity of CCR7 expression with a consistently high yield. This sorting strategy did not affect cell viability as drastically as expected compared to magnetic column sorting, which was attributed to the physical stress experienced by BMDCs during the preparation for column sorting, which includes several centrifugation steps and incubations, as well as a consistent, controlled temperature of 4ºC for success. For FACS, this requirement is minimised by omitting the magnetic bead incubation step. As described in **2.6.2.2**, the settings of the Aria II itself can be adjusted to reduce shear stress experienced by the cells by controlling the flow rate and other parameters. In terms of cell viability, sorting the cells by FACS appears to have a smaller effect on cell viability than magnetic column sorting so

may be beneficial for cell survival and function after isolation. FACS was chosen as the sorting strategy for future experiments taking these data into account.

Compared to CCR7- DCs, CCR7+ DCs were shown to have a more mature surface phenotype, with a higher expression of MHC class I and class II molecules required for antigen presentation to cells of the adaptive immune system. Recognition of presented antigen by TCRs provides only 1 of 3 ideal signals to the T cell for generation of a cytotoxic response; the other signals come from interaction with co-stimulatory molecules such as CD80 and CD86 (signal 2), and concurrent paracrine signalling through cytokines such as IL-12 (signal 3). CCR7+ DCs described here express co-stimulatory molecules very highly in comparison to the CCR7- DCs, and also secrete cytokines more skewed towards activation of the adaptive immune response. CCR7+ DCs express chemokines commonly associated with naïve T cell and memory T cell chemoattraction such as CCL22 and CCL17, providing a potential mechanism for these cells to induce a cytotoxic T cell response and remodel an existing memory response *in vivo* (Adema *et al.*, 1997; Sallusto *et al.*, 1999). CXCL16 binds CXCR6 expressed by naïve, effector and NK T cells as well as a subset of memory CD4 T cells (Matloubian *et al.*, 2000). *In vitro* evidence has shown that IL-1β can induce production of IL-12 by DCs in conjunction with ligation of CD40 (Wesa and Galy, 2001), suggesting a potential autocrine effect of CCR7+ DCs inducing their own IL-12 secretion for generation of a potent CTL response. CCR7- DCs, in contrast, secrete mainly chemoattractants for innate immune cells, as well as DCs, and it would be interesting to investigate if these chemokines contributed to the retaining of injected DCs in the footpad. CCR7- cells secrete more CCL3, CCL4 and CCL5 than CCR7+ DCs, for example. CCL3 and CCL5 bind CCR1, and all three bind CCR5, which are expressed on macrophages and T_H1 cells (Weber *et al.*, 2001). CXCL2 is primarily a neutrophil chemoattractant through binding of CXCR2 (Lim *et al.*, 2015), but has also been shown to attract monocytes in humans (Geissmann, Jung and Littman, 2003). CCR7- DCs also secrete IL-16, which is a soluble ligand for CD4 and a chemoattractant for CD4-expressing T cells such as T cells, eosinophils and monocytes, but also DCs themselves (Kaser *et al.*, 1999). These data together suggest that CCR7- DCs attract primarily innate immune cells, with some contribution to a non-cytotoxic T cell subset and importantly, secrete IL-16 to control the migration of other DCs. This would highlight another reason for removal of these cells from a therapeutic regimen, as it would likely contribute to the poor migration of capable cells following injection.

Isolation of DCs expressing the chemokine receptor CCR7 is clinically relevant for two reasons. Firstly, CCR7 expression is crucial for efficient LN homing through CCL19 and CCL21 signalling (Hilkens *et al.*, 2010), so sorting CCR7+ cells using this method yields a therapeutically viable cell population. Secondly, as the upregulation of CCR7 occurs in mature DCs, the sorting process described also reduces the number of immature DCs from the final population. As described in previous literature and supported by data presented in this Chapter, in addition to generating both mature and immature DCs, GM-CSF alone also generates a complex mixture of macrophage phenotypes which express F4/80, CD11c and MHC class II in mice (Helft *et al.*, 2015). When considering sorting BMDCs to attain a pure cell population, both F4/80 and CD11c could be used, but would result in a mixture of cell types as summarised in **Table 3.1**.

	Depletion	Selection	
Cell Phenotype	**F4/80**	**CD11c**	**CCR7**
Uncommitted Progenitor Cells			
F4/80- CD11c- CCR7-	Y	N	N
Macrophages			
F4/80+ CD11c- CCR7-	N	N	N
F4/80+ CD11c+ CCR7-	N	Y	N
Dendritic Cells			
F4/80- CD11c+ CCR7- (immature)	Y	Y	N
F4/80- CD11c+ CCR7+ (mature)	Y	Y	Y

Table 3.1 - Cell populations remaining in GM-CSF bone marrow cultures after sorting strategies.
After sorting GM-CSF-derived bone marrow cultures using F4/80 depletion or selection for CD11c or CCR7 expression three distinct cell populations remain, showing that these sorting methods are not necessarily equivalent. Y = population remains in culture following sort; N = population does not remain following sort.

Both F4/80 and CD11c isolation strategies are currently available as GMP protocols, so it is important to consider both as potential alternatives to CCR7-sorting. Using F4/80 depletion to remove macrophages, the remaining F4/80- cells could still contain a mixture of immature/mature DCs and macrophages as well as uncommitted progenitors. Similarly, using selection of CD11c+ cells would remove a bulk CD11c- macrophage population and uncommitted progenitors, but could still retain CD11c+ macrophages and a mixture of

immature and mature DCs. Uncommitted monocytic progenitor cells within the culture are multipotent and could potentially differentiate into either macrophages or DCs after injection and should be removed. Macrophages should also be removed, as they can both uptake antigen and process it under these culture conditions. Experimental evidence has shown that although they are less potent than DCs at doing so, macrophages can present and activate T cells both *in vitro* and *in vivo* (Helft *et al*., 2015). Immature DCs lack a number of costimulatory surface molecules required for activation of T cells (Förster *et al*., 2008), so can instead lead to T cell anergy or tolerance towards presented antigens when introduced *in vivo* (Hilkens *et al*., 2010). The presented data support this: stimulation of T cells with CCR7- DCs leads to a large percentage of the immature CD44-CD62L- T cell phenotype which is no different to IL-2 stimulation alone. In addition to this, the mature CD44+CD62L+ T cell population also highly upregulates the exhaustion marker PD-1 in response to CCR7- DC stimulation. If these CCR7- cells are present within the initial cell injection, it is possible that further response to inflammatory signals from other injected cells or indeed at the injection site could promote upregulation of CCR7 and allow these cells to reach the lymph node. It is unknown at this time, however, if this upregulation might accompany a maturation of surface phenotype as seen *in vitro*. Voigtländer *et al*. showed that 'tolerogenic' DCs, which were only partially stimulated upon injection, became immunogenic following injection showing that DCs can undergo a second-wave of maturation in response to further stimulation (Voigtländer *et al*., 2006). This is an important therapeutic consideration, suggesting that the immature DCs have the potential to mature *in vivo* in response to endogenous signals but if these are insufficient to trigger a full mature phenotype then the DCs may develop as tolerogenic. Removal of these contaminating cell types are crucial for the production of a reproducible cell therapy. Although this wasn't addressed in the footpad migration experiments presented above, it would be interesting to assess the phenotype of the cells remaining in the footpad at 48hr to see any reduction in the number of cells expressing an immature CCR7- DC phenotype.

3.7 Chapter summary

In this Chapter, it was shown that it is possible to sort mature BMDCs, generated through either GM-CSF or Flt3-L with a novel chemokine-based sorting method based on expression of CCR7 as described by Le Brocq *et al* (2014). Using biotinylated CCL19, as well as three PEGylated versions of CCL19, the sorting methodology has been optimised for BMDCs and adapted for magnetic column sorting of the cells and fluorescence-based approaches such as the BD Aria II with high cell viability and improved cell yield. CCR7+

BMDCs represent a phenotypically mature cell population within the mixed cultures both in terms of surface phenotype and cytokine production suggesting that these cells are better equipped to attract T cells *in vivo* and potently activate them. Improved T cell stimulation was confirmed through co-culture with sorted or unsorted BMDCs using a model antigen. Additionally, it was shown that although utilising the CCL19-CCR7 ligand-receptor interaction for cell sorting may induce receptor internalisation, sorted cells still migrate more effectively to CCL19 gradients both *in vitro* and *in vivo* compared to a mixed cell population. Taking these data together suggest that improved migration of BMDCs to the lymph node after injection may induce a better antigen-specific T cell response which could be used for therapeutic benefit. In the next Chapter, the potential of CCR7-sorted BMDCs in a therapeutic context was assessed using an *in vivo* cancer model which expresses model antigen that can be targeted.

Chapter 4

Assessing CCL19-sorted dendritic cells in the subcutaneous B16F10.ova model

4.1 Introduction and aims

In the previous Chapter, the phenotype and function of CCR7-sorted DCs was compared to an unsorted DC population. It was shown that despite both populations expressing the classical DC marker CD11c, the CCR7-sorted population expressed markers associated with T cell co-stimulation more highly. The cells also expressed higher levels of T cell-specific chemokines, and this correlated with the stimulation of T cell memory formation maturation *in vitro*. Additionally, CCR7-sorted DCs (sDCs) were shown to have an advantage in CCL19-directed migration compared to unsorted DCs (uDCs), both in a transwell assay of chemotaxis *in vitro* and to the lymph node (LN) *in vivo*. Taking these data together, we have provided evidence that sorted DCs could be more functionally valuable in models of antigen-specific T cell induction.

Transplantable murine tumour models have been used extensively in the cancer field to understand tumour development and test novel therapeutics. As discussed in **Appendix I**, the B16 model is widely used for this purpose and is a particularly useful model with which to assess the therapeutic viability of CCR7-sorted DCs. Melanoma was the first clinical target of DC vaccines in 1995, as well as in many of the early clinical trials (Mukherji *et al.*, 1995). The high incidence of *de novo* protein formation in melanomas make them attractive therapeutic targets but not all can be used as tumour-associated antigens in the context of treatment due to similarities remaining to self-antigens and thus a potential endogenous tolerance (Overwijk and Restifo, 2001). In this respect, the B16F10 melanoma is a relevant model to use in cancer research. B16 cells have a deficiency in MHC class I machinery resulting in non- or low immunogenicity. MHC class I downregulation is a common immune escape mechanism (Seliger *et al.*, 2001) but this machinery can be upregulated by stimulation with IFNγ (as shown **Figure A**.7). Melanomas are one of the few tumours with consistent tumour-associated antigen expression between patients (Butterfield *et al.*, 2003) but animal models often fail to recapitulate this. B16 cells express some common melanoma-specific antigens such as tyrosinase and the MAGE family of antigens (Böhm *et al.*, 1998), but not BRAF kinase for example (Melnikova *et al.*, 2004) for potential immune targeting. To model a TAA in an experimental setting, the chicken egg protein, ovalbumin (OVA), was introduced to the cells by plasmid transfection. This allows expression of OVA by every B16F10 cell injected and mimics *de novo* protein expression by melanomas. In 1999 it was shown that adoptively transferred OVA-specific T cells could provide immune control in this tumour context despite poor MHC class I expression through initial recognition and subsequent

IFNγ signalling (Dobrzanski, Reome and Dutton, 1999). *In vivo* B16F10.ova tumours are quick-growing and generate a natural cytotoxic response following injection which fails to control tumour growth without intervention (Böhm *et al.*, 1998). In **Chapter 3**, DCs were given the whole ovalbumin protein *in vitro* to present fragments of the molecule to T cells using MHC class I and MHC class II, allowing stimulation and proliferation of T cells recognising these epitopes. It was also shown that CCR7+ DCs could stimulate the formation of a functional antigen-specific T cell response with the formation of memory T cells. Early DC clinical trials have shown the immunogenicity of injected DCs, with the detection of tumour specific T cells in the blood detectable as early as 7 days after DC injection (Mukherji *et al.*, 1995).

In this Chapter, the induction of an antigen-specific T cell response by CCR7+ and unsorted BMDCs was quantified in the context of the B16F10.ova melanoma. Three cell dosing strategies were assessed: one single DC injection at the same time as the tumour induction; two DC injections prior to the tumour induction, representing a true vaccination strategy; and two DC injections, the second of which was given after tumour initiation. In these models, tumour growth was monitored, and the antigen-specific T cell response was quantified by flow cytometry at the tumour end-point.

4.2 A single prior sDC injection is sufficient to control B16F10.ova subcutaneous growth.

To examine how the increased migration of CCR7-sorted dendritic cells to the lymph node could be affecting the induction of a T cell response, the B16F10.ova model was used. In this model, development of ovalbumin-specific T cells can be quantified by flow cytometry, but their function can also be assessed in terms of cell phenotype and tumour growth control.

In this first experiment, animals were injected with either sDCs or uDCs presenting the ovalbumin peptide into the footpad to generate an anti-ovalbumin T cell response. The footpad is a commonly used injection site in mice which is a combination of intradermal and subcutaneous injection (Kamala, 2008) and mimics the use of these routes in human therapy. PBS/0.1% BSA injections were used as controls. The following day, animals were injected with the B16F10.ova cells into the flank to induce subcutaneous melanoma. The timings of these injections were chosen to allow development of the immune response

concurrently with early tumour growth, as clinical trial data suggest that DC vaccination is less effective against fully-developed tumours (Constantino *et al.*, 2016). Immunotherapeutic strategies are rarely used in late-stage tumours without combination surgery or chemotherapy, but this experimental modality was chosen to first assess the basic results of DC vaccination. The first DC injection strategy was as detailed in **Figure 4.1**.
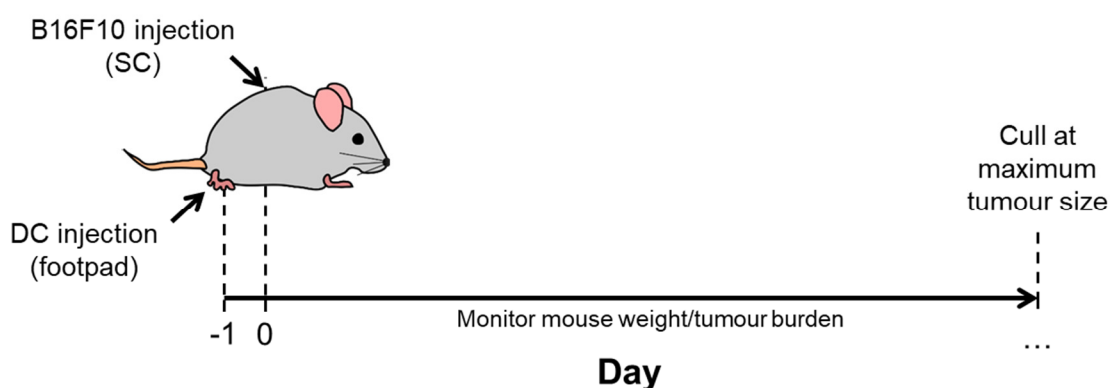
Figure 4.1 - Experimental timeline of single prior DC injection in the B16F10.ova tumour model.
Mice were first injected with either PBS/0.1% BSA, unsorted DCs (uDCs) or sorted DCs (sDCs) into the left hind footpad under isofluorane anaesthetic. The following day (d0), all mice were injected with B16F10.ova cells subcutaneously into the flank and allowed to grow to maximum tumour diameter.

4.2.1 Tumour growth and survival

B16F10.ova cells were injected subcutaneously into the flank and the mice were monitored daily and tumour growth was quantified using digital skin-fold callipers. The end-point of this experiment was the PBS control group reaching the maximum tumour diameter of 12mm; on this day (d17), all mice in the experiment were culled and the relevant tissues processed as described previously.
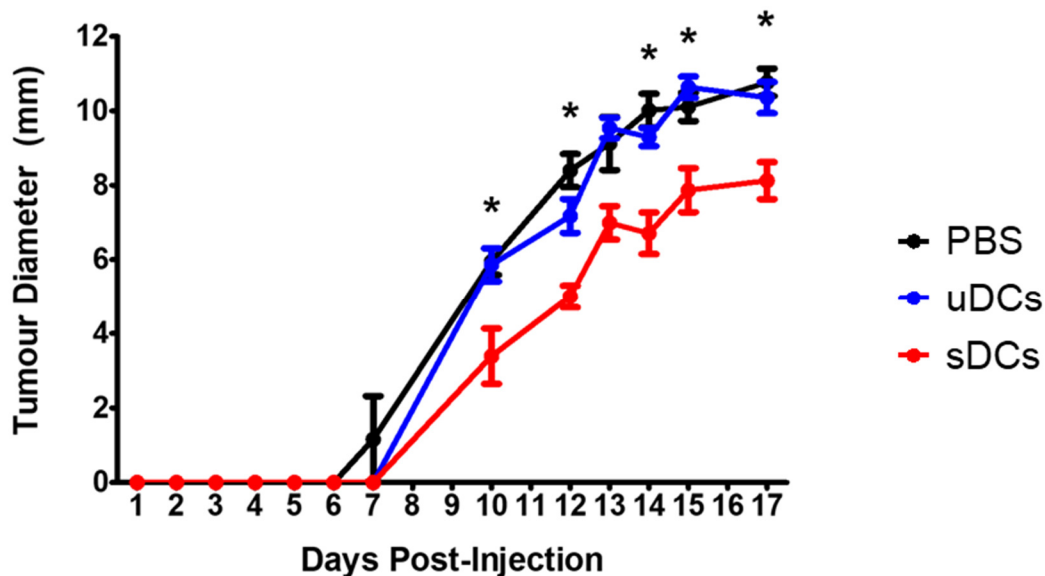
Figure 4.2 - B16F10.ova tumour growth following a single DC injection.
Mice receiving B16F10.ova tumours by subcutaneous injection into the flank were also injected with either PBS/0.1% BSA (black bars), unsorted DCs (uDCs – blue bars) or sorted DCs (sDCs – red bars), and the tumour growth monitored daily until the maximum tumour diameter had been reached. Statistical analysis was by one-way ANOVA with Bonferroni's Multiple Comparison Test: *$P \leq 0.05$ for both PBS vs. sDCs and uDCs vs. sDCs (summary of 2 experiments with n = 5-6/group).

When mice were injected with uDCs there was no difference in tumour growth compared to the mice receiving only PBS/0.1% BSA into the footpad. In comparison, when mice were injected with sDCs there were significant differences in the tumour growth at 10, 12, 14, 15 and 17 days post-injection compared to both uDC and PBS/BSA-receiving mice (**Figure 4.2**). Importantly, the tumour growth in the PBS control group is consistent with the rate of growth shown by other groups, making these data comparable to previous studies (Overwijk and Restifo, 2001).

4.2.2 Antigen-specific T cell distribution

To assess the effect of injected DCs on the generation of an antigen-specific immune response, T cells were isolated from the injection site-draining and tumour-draining lymph nodes, the pLN and iLN respectively, and the spleens from tumour-bearing mice. Antigen specificity was assessed using a fluorophore-conjugated tetramer of the MHC class I-restricted OVA peptide SIINFEKL bound to MHC class I molecules (Caltag Medsystems). This tetramer binds TCRs specific for this epitope and allows identification of these cells by flow cytometry.
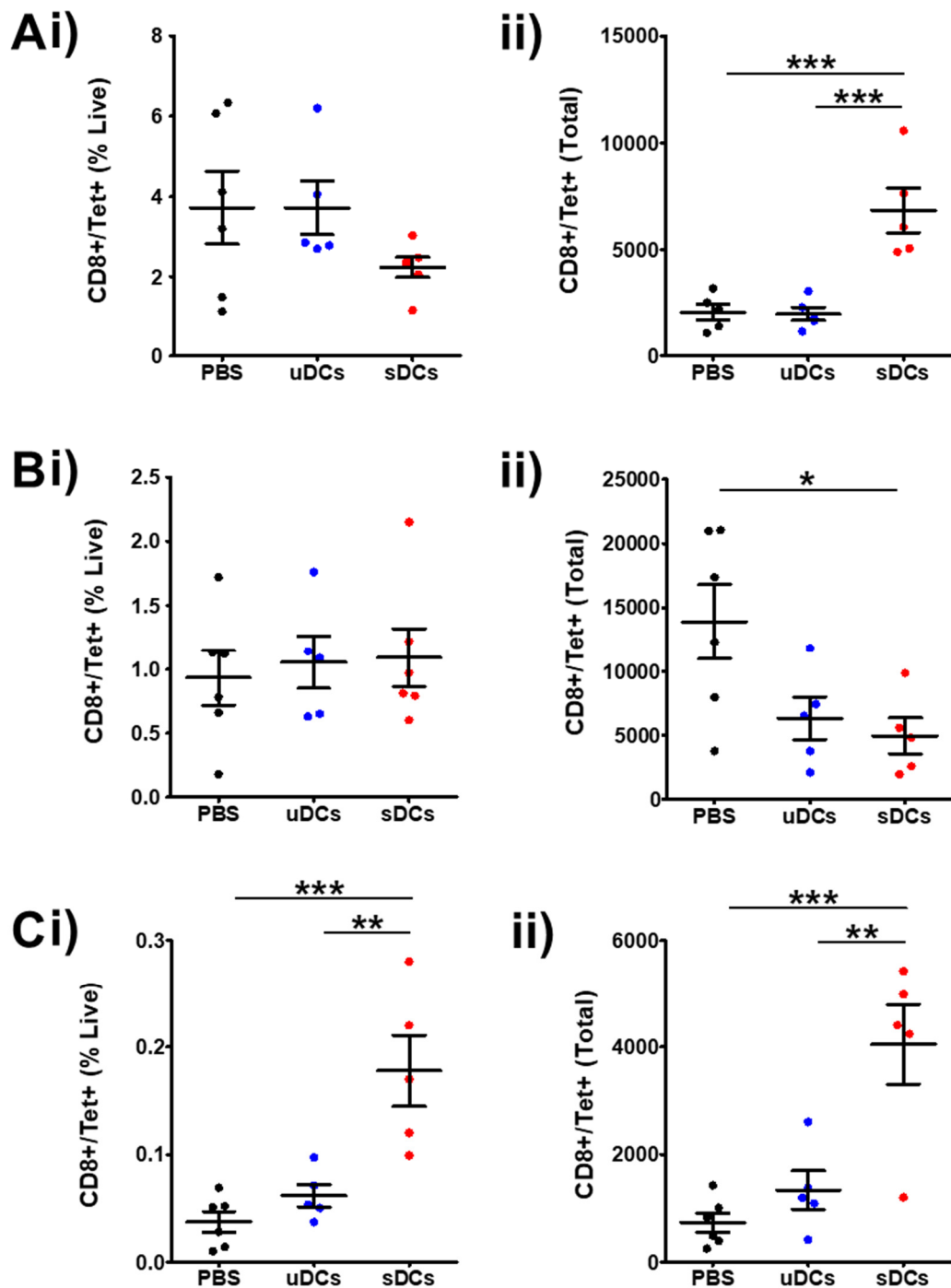
Figure 4.3 - sDC vaccination increases the magnitude of the antigen-specific T cell response in the lymphatic system.
Mice receiving the B16F10.ova tumours by subcutaneous injection were assessed for the antigen-specific T cell response to DC vaccination in the (**A**) popliteal LN (pLN); (**B**) inguinal LN (iLN); and (**C**) spleen by flow cytometry. Cell number was quantified by either percentage of live cells (**i**) or total cell number (**ii**) for each tissue. Data represent individuals ± SEM error bars. Statistical analysis was by one-way ANOVA with Bonferroni's Multiple Comparison Test: *P ≤ 0.05, **P ≤ 0.01, ***P ≤ 0.001 (n = 5-6/group).

Induction of an antigen-specific T cell response in the injection site-draining lymph nodes

was first assessed using the pLN, which drains the footpad (**Figure 4.3A**). Mice receiving

a single injection of sDCs had a 3-fold increase in T cell number compared to either PBS or uDC-receiving mice (6852 ±1051 to 2083 ±381.7 or 1997 ±324.2, respectively; **Figure 4.3Aii**). These mice also had enlarged LNs compared to the control mice (data not shown). Although there was no difference in the response as a percentage of the cells in the LN, cell number clearly showed an increase in total cell number – which could be from an increased initial infiltration of DCs into the LN, or an increased capacity for T cell stimulation of these DCs as shown previously (**Figure 3.13**) or a combination of the two. In the iLN, the opposite was seen: mice receiving no DCs at all had the highest number of antigen-specific T cells (13907 ±2908) compared to the other two groups (6330 ±1671 or 4954 ±1397 for uDC and sDC, respectively; **Figure 4.3Bii**). This 3-fold increase in cell number in one of the tumour-draining LNs suggests that this is an important site for the T cell response in untreated animals (Marzo *et al.*, 1999), but is not directly accessed by DCs following footpad injection. In comparison, there was only a modest response in this LN by mice receiving either DC vaccination. In the spleen, the site of central T cell memory and a secondary site of cell proliferation, there was an increased response to the sDC vaccine in both percentage of the total cells (0.178% ±0.033%; **Figure 4.3Ci**) and the actual cell number (4052 ±742.5; **Figure 4.3Cii**). This could be migration of the DCs themselves into the spleen after injection, or as a secondary effect of the increased T cell production. There was no difference between the T cells in the spleen of mice receiving either PBS or uDCs.

4.2.3 Antigen-specific T cell phenotype

To understand the phenotype of the T cells present in the lymphatics, antigen-specific T cells from the pLN, iLN and spleen were further characterised by the expression of CD44 and CD62L to determine the maturity and function of these cells.
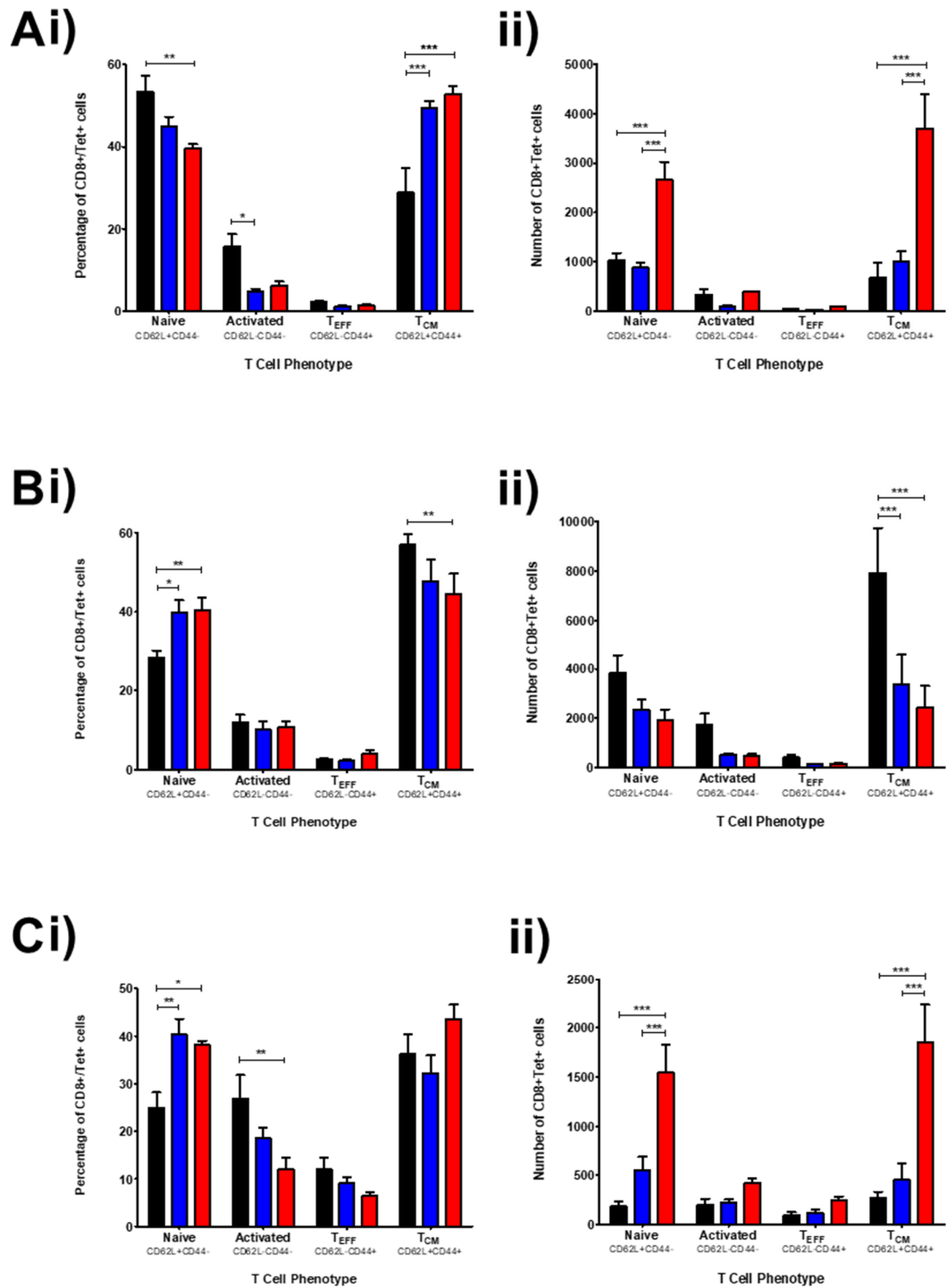
Figure 4.4 - DC vaccination increases tumour antigen-specific T cell proliferation and maturity in the lymphatic system.
Mice receiving B16F10.ova tumours by subcutaneous injection were assessed for the antigen-specific T cell response to DC vaccination in the (**A**) popliteal LN (pLN); (**B**) inguinal LN (iLN); and (**C**) spleen by flow cytometry. Expression of CD44 and CD62L was used to phenotype the T cells, which were quantified by either percentage of live cells (**i**) or total cell number (**ii**) in each tissue. Data represent mean ± SEM error bars. Statistical analysis was by one-way ANOVA with Bonferroni's Multiple Comparison Test: *$P \leq 0.05$, **$P \leq 0.01$, ***$P \leq 0.001$ (n = 5-6/group).

In the pLN (**Figure 4.4A**), there was a significant decrease in the naïve T cell (CD62L+CD44-) compartment as a percentage of the antigen-specific T cells after vaccination with either uDCs (44.9% ±2.37%) or sDCs (39.52% ±1.03%) compared to the PBS-receiving mice (53.27% ±3.99%). The primary phenotype in the DC-receiving mice was the mature, T_{CM} phenotype characterised by expression of both CD62L and CD44, which was significantly increased compared to the PBS-receiving mice (49.30% ±1.83% and 52.86% ±1.95% compared to 28.82% ±6.10%). This may be indicative of DC-T cell interactions in the LN. Cell number also showed the magnitude of difference between sDCs and uDCs, with both the naïve and T_{CM} cell numbers being between 3- and 4-fold higher than either control group (**Figure 4.4Aii**). In the iLN, there was a significant difference in the production of naïve T cells by the DC-receiving mice, but this was not supported by the actual cell number (**Figure 4.4B**). The PBS control group had a significantly increased T_{CM} phenotype by both proportion and total cell number, suggesting that although antigen-specific T cells are generated in response to the tumour challenge, they may not contribute to tumour rejection. Finally, in the spleen there was an increase in the number of naïve cells produced by the spleen of DC-vaccinated mice by proportion (**Figure 4.4Ci**), but sDC-receiving mice had a significantly higher cell number compared to the other two groups. Interestingly, there was also a significant increase in the number of T_{CM} cells compared to the other groups.

4.3 Multiple prior injections of sDCs led to tumour control and increased survival duration.

In this experiment, animals were injected with either sDCs or uDCs presenting the ovalbumin peptide, or PBS/0.1% BSA into the footpad as previously. After a week, injections were repeated to boost the primary immune response from the first injections. The following day, animals were injected with the B16F10.ova cells into the flank to induce the model of subcutaneous melanoma as previously. This injection strategy is summarised in **Figure 4.5** below.
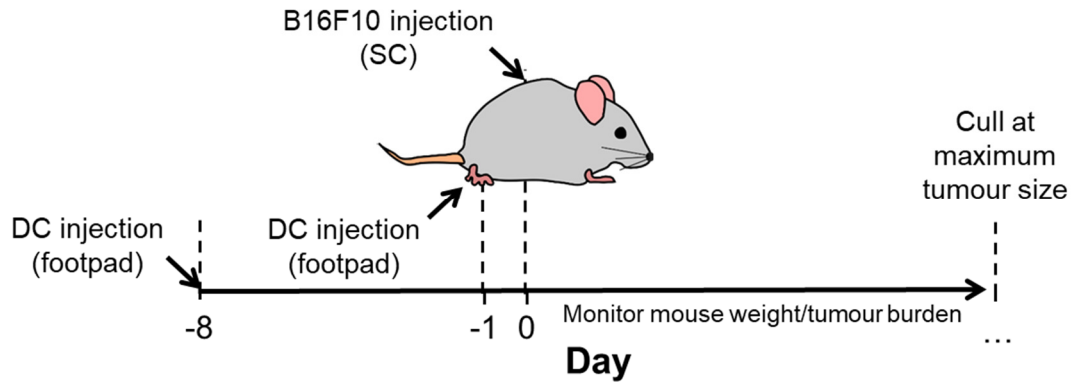
Figure 4.5 - Experimental timeline of multiple prior DC injections in the B16F10.ova tumour model.
Mice were first injected with either PBS/0.1% BSA, unsorted DCs (uDCs) or sorted DCs (sDCs) into the left hind footpad under isofluorane anaesthetic. A week later (d-1), mice were injected again and then the following day (d0) all mice were injected with B16F10.ova cells subcutaneously into the flank, and tumours allowed to grow to maximum tumour diameter.

4.3.1 Tumour growth and survival

Mice were monitored daily and tumour growth was measured at their largest diameter using digital skin-fold callipers after injection of the B16F10.ova tumour cells. In this experiment, tumours reaching the maximum diameter of 12mm was the end-point, and animals were culled as they reached this point and relevant tissues taken for analysis. This is in contrast to **4.2.1**, in which all experimental animals were culled at the same time.
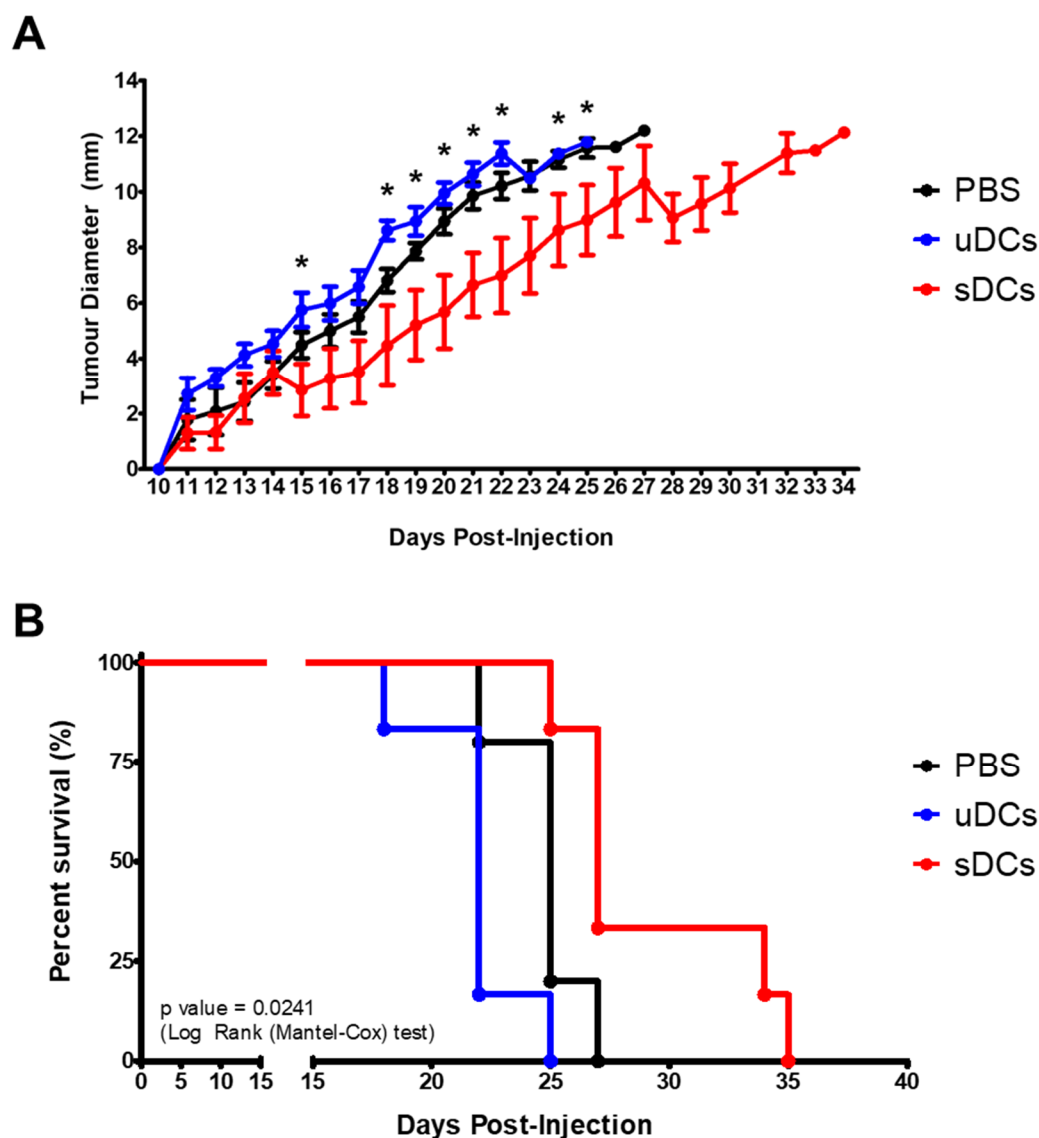
Figure 4.6 - B16F10.ova tumour growth and survival after 2 prophylactic DC injections.
Mice were injected with either PBS/0.1% BSA (black bars), unsorted DCs (uDCs – blue bars) or
sorted DCs (sDCs – red bars), and week later these injections were repeated. The following day
mice received B16F10.ova tumours by subcutaneous injection into the flank and the tumour growth
monitored daily until the maximum tumour diameter had been reached. Decreased tumour growth
(**A**) and increased individual survival (**B**) was seen in the sDC-receiving mice but not the control
groups, uDC and PBS. Statistical analysis was by one-way ANOVA with Bonferroni's Multiple
Comparison Test: *$P \leq 0.05$ for both PBS vs. sDCs and uDCs vs. sDCs (n = 5-6/group).

Tumour survival was slightly longer in this experiment compared to in **4.2**. This may have
been as a result of culling individual animals at their maximum tumour burden instead of
as a group as was done previously. This also reflects the slight variability in tumour
development between individual animals. From day 18, there was a significant difference
between the tumour growth in sDC-receiving mice and the control groups, with a
difference of as much as 4mm in diameter (**Figure 4.6A**). Following this, the sDC-
receiving mice had significantly smaller tumour sizes compared to the controls and this
had a significant effect on survival. Mice injected twice with sDCs prior to tumour

development survived for 27 days compared to uDC-receiving mice which survived for 22 days or PBS/0.1% BSA-receiving mice which survived for 25 days (median survival; shown in **Figure 4.6B**), and had a 17-30% increase in mean survival duration compared to the control groups. There was also a small significant difference in the mean survival of the uDC and PBS groups, despite there being no difference in mean tumour growth.

4.3.2 Antigen-specific T cell distribution

The injection-site draining pLN, tumour-draining iLN, and spleen was removed from tumour-bearing mice and assessed for induction of tumour antigen-specific T cells by flow cytometry.
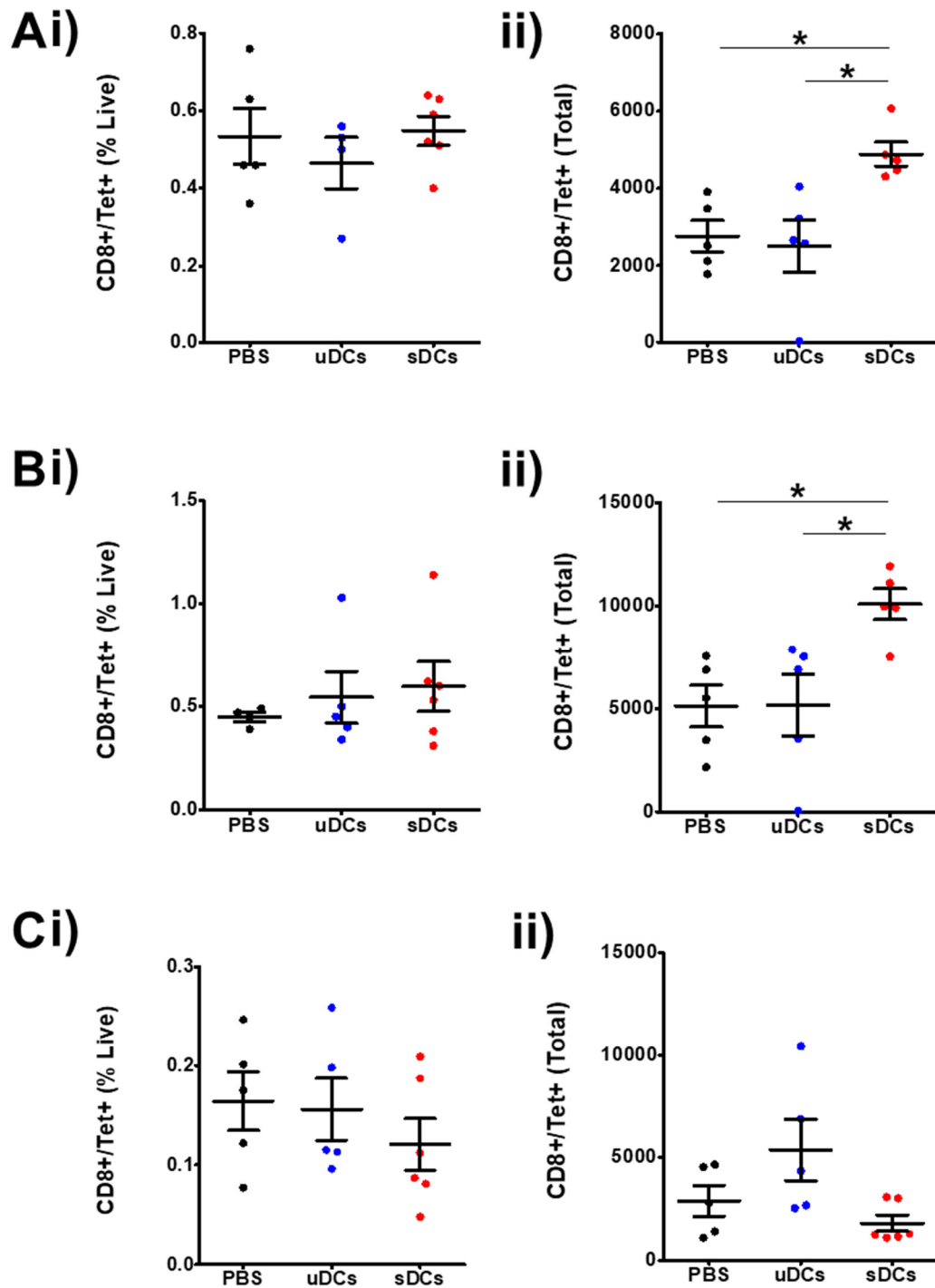
Figure 4.7 - Prior sDC vaccination increases the magnitude of the antigen-specific T cell response in the lymphatic system.
Mice receiving the B16F10.ova tumours by subcutaneous injection were assessed for the antigen-specific T cell response to DC vaccination in the (**A**) popliteal LN (pLN); (**B**) inguinal LN (iLN); and (**C**) spleen by flow cytometry. Cell number was quantified by either percentage of live cells (**i**) or total cell number (**ii**) for each tissue. Data represent individuals ± SEM error bars. Statistical analysis was by one-way ANOVA with Bonferroni's Multiple Comparison Test: *P ≤ 0.05 (n = 6/group).

As seen previously, sDC-receiving mice had a greater magnitude of T cell response in the injection-site draining pLN compared to either control group (**Figure 4.7A**). Although

there was no difference in cell number by percentage of live cells, there was a 2- to 3-fold increase in antigen-specific cells by total number (4887 ±309 compared to 2764 ±403 and 2506 ±603 for PBS and uDC, respectively; **Figure 4.7Aii**). This agreed with data shown in **Figure 4.3**, and supports the hypothesis that increased migration of DCs to the draining LN can improve T cell stimulation. A similar pattern was seen in the tumour-draining iLN (**Figure 4.7B**), where sDC-receiving mice had a higher total number of antigen-specific T cells (10087 ±742.6) compared to the uDC (5182 ±1492) and PBS-receiving groups (5125 ±1014). This data could be indicative of T cell memory development as a result of the second DC injection. In the spleen, in comparison, there was no difference between any of the treatment groups (**Figure 4.7C**). The PBS control group had a similar response as in the single injection experiment, however the sDC-receiving group had fewer cells than previously (1820 ±392 to 4052 ±742). Although there appears to be a difference in cell number after uDC injections, this difference did not reach significance.

4.3.3 Antigen-specific T cell phenotype

To assess the function and maturity of the T cells produced in the lymphatic system in response to DC injection, T cells from the pLN, iLN and spleen were stained using CD44 and CD62L for flow cytometry analysis.
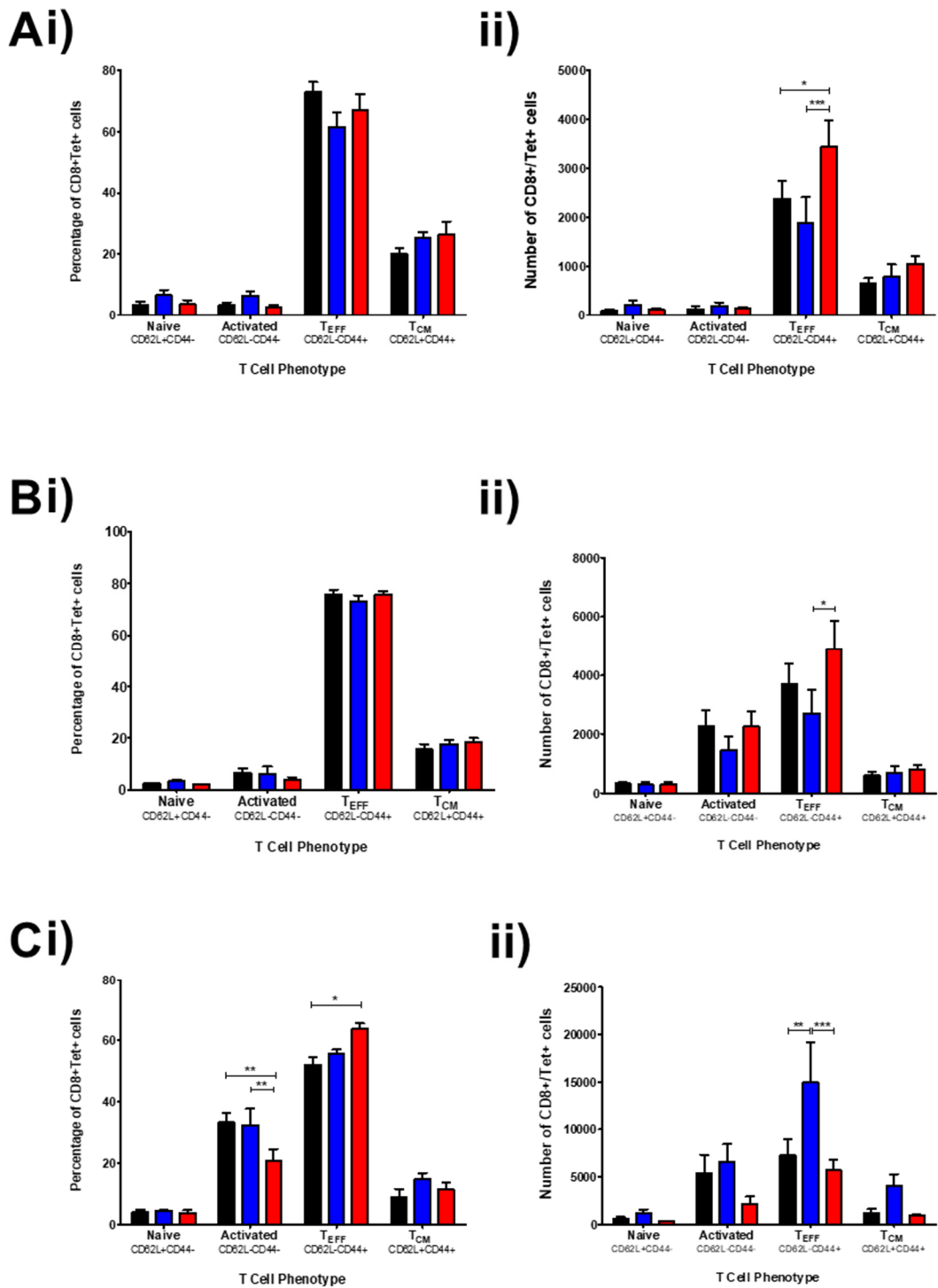
Figure 4.8 - Prior DC vaccination increases tumour antigen-specific T cell proliferation and maturity in the lymphatic system.
Mice receiving B16F10.ova tumours by subcutaneous injection were assessed for the antigen-specific T cell response to DC vaccination in the (**A**) popliteal LN (pLN); (**B**) inguinal LN (iLN); and (**C**) spleen by flow cytometry. Expression of CD44 and CD62L was used to phenotype the T cells, which were quantified by either percentage of live cells (**i**) or total cell number (**ii**) in each tissue. Data represent mean ± SEM error bars. Statistical analysis was by one-way ANOVA with Bonferroni's Multiple Comparison Test: *P ≤ 0.05, **P ≤ 0.01, ***P ≤ 0.001 (n = 6/group).

In both the pLN and iLN there are more antigen-specific T cells after sDC injections, and the phenotype of these cells was primarily a T_{EFF} CD62L-CD44+ phenotype (**Figure 4.8A and B**). The response was between 1.5- and 2-fold higher compared to the uDC- and PBS-receiving groups, although in these groups the primary response was also skewed towards the T_{EFF} phenotype which had previously not been seen. In the spleen, there was a significant decrease in the presence of activated antigen-specific T cells in the sDC group by percentage, but this did not reach significance by total number (**Figure 4.8C**). Similarly, although the proportion of T_{EFF} cells in the spleen is highest in the sDC-receiving mice, the uDC mice have more by total cell number (**Figure 4.8Cii**). This may suggest that more antigen presentation is occurring in the spleen in the uDC-receiving mice as a result of poor DC trafficking to the initial LNs. There is some evidence suggesting that immature DCs migrate preferentially to the spleen (Emmanouilidis *et al.*, 2006) and could be contributing to this phenotype.

4.4 A second sDC injection after tumour initiation does not control growth

To better model the treatment of solid tumour growth with DC therapies as the strictest test of DC potential, tumours were allowed to develop first before the second DC injection. In this experiment, animals were injected with either sDCs or uDCs, or PBS/0.1% BSA into the footpad as previously. The following day, animals were injected with the B16F10.ova cells into the flank to induce the model of subcutaneous melanoma. A week into tumour development, as tumours were becoming palpable as observed previously, animals were injected with the same treatment a second time. This injection strategy is summarised in **Figure 4.9** below.
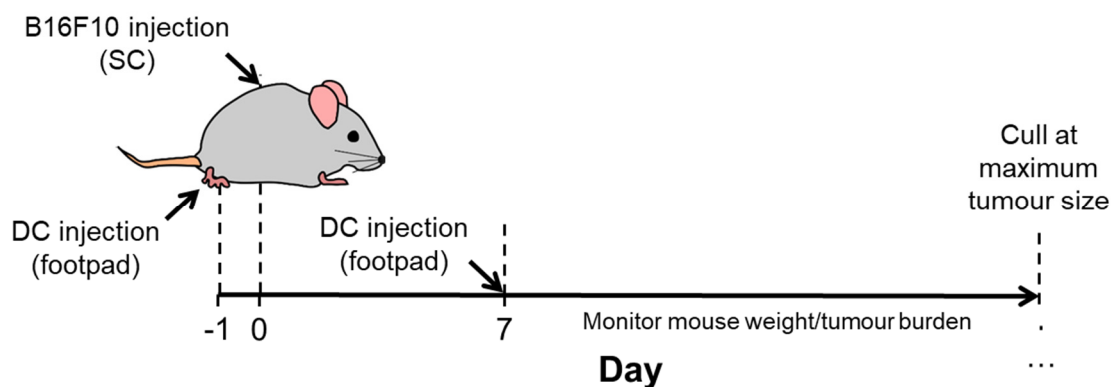
Figure 4.9 - Experimental timeline of multiple DC injections in the B16F10.ova tumour model.
Mice were first injected with either PBS/0.1% BSA, unsorted DCs (uDCs) or sorted DCs (sDCs) into the left hind footpad under isofluorane anaesthetic. The following day (d0), all mice were injected with B16F10.ova cells subcutaneously into the flank, and one week later (d7) were injected with PBS/0.1% BSA, uDCs or sDCs into the footpad again, and allowed to grow to maximum tumour diameter.

4.4.1 Tumour growth and survival

Tumour growth was measured using digital skin-fold callipers after B16F10.ova tumour injection. In this experimental setup, maximum tumour diameter was 12mm as previously, and individual mice were culled as they reached this end-point. The draining LNs and spleens were removed for flow cytometry analysis.
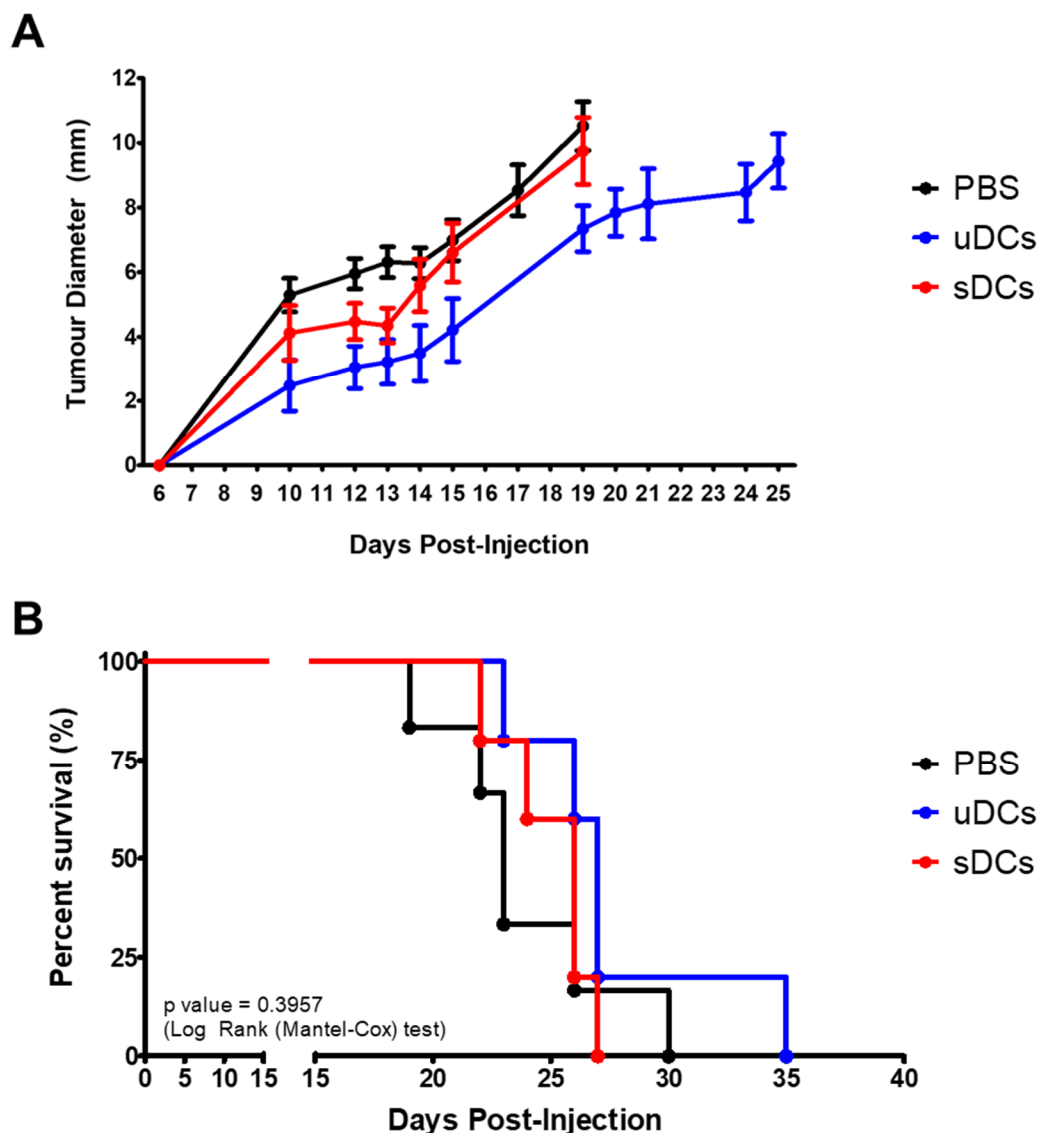
Figure 4.10 - B16F10.ova tumour growth and survival after multiple DC injections.
Mice were injected with either PBS/0.1% BSA (black bars), unsorted DCs (uDCs – blue bars) or sorted DCs (sDCs – red bars), and the following day the mice received B16F10.ova tumours by subcutaneous injection into the flank. A week later the DC or control injections were repeated. Tumour growth was monitored daily until the maximum tumour diameter had been reached. No difference in tumour growth (**A**) and or individual survival (**B**) was seen in the sDC-receiving mice or the control groups, uDC and PBS (n = 5-6/group).

Unlike previous experiments, injection of sDCs after establishment of the tumour growth does not lead to differences in tumour growth or to overall survival of the animals (**Figure 4.10**). From the development of a palpable tumour mass around day 7 until the end of the study, the three experimental groups showed no difference in the rate of tumour growth (**Figure 4.10A**). In this experiment, uDC-receiving mice had the longest duration of survival post-injection of the B16F10.ova tumour (27.6 ±2 days) compared to either sDC-receiving mice (25 ±0.9 days) or the PBS control mice (23.8 ±1.5 days) but this difference does not reach significance (**Figure 4.10B**). The median survival duration of the sDC

group (26 days) was also no different compared to the controls (PBS – 23 days; uDCs – 27 days).

4.4.2 Antigen-specific T cell distribution

To assess the effect of injected DCs on the generation of an antigen-specific immune response, T cells were isolated from the injection site-draining and tumour-draining lymph nodes, the pLN and iLN respectively, and the spleens from tumour-bearing mice.
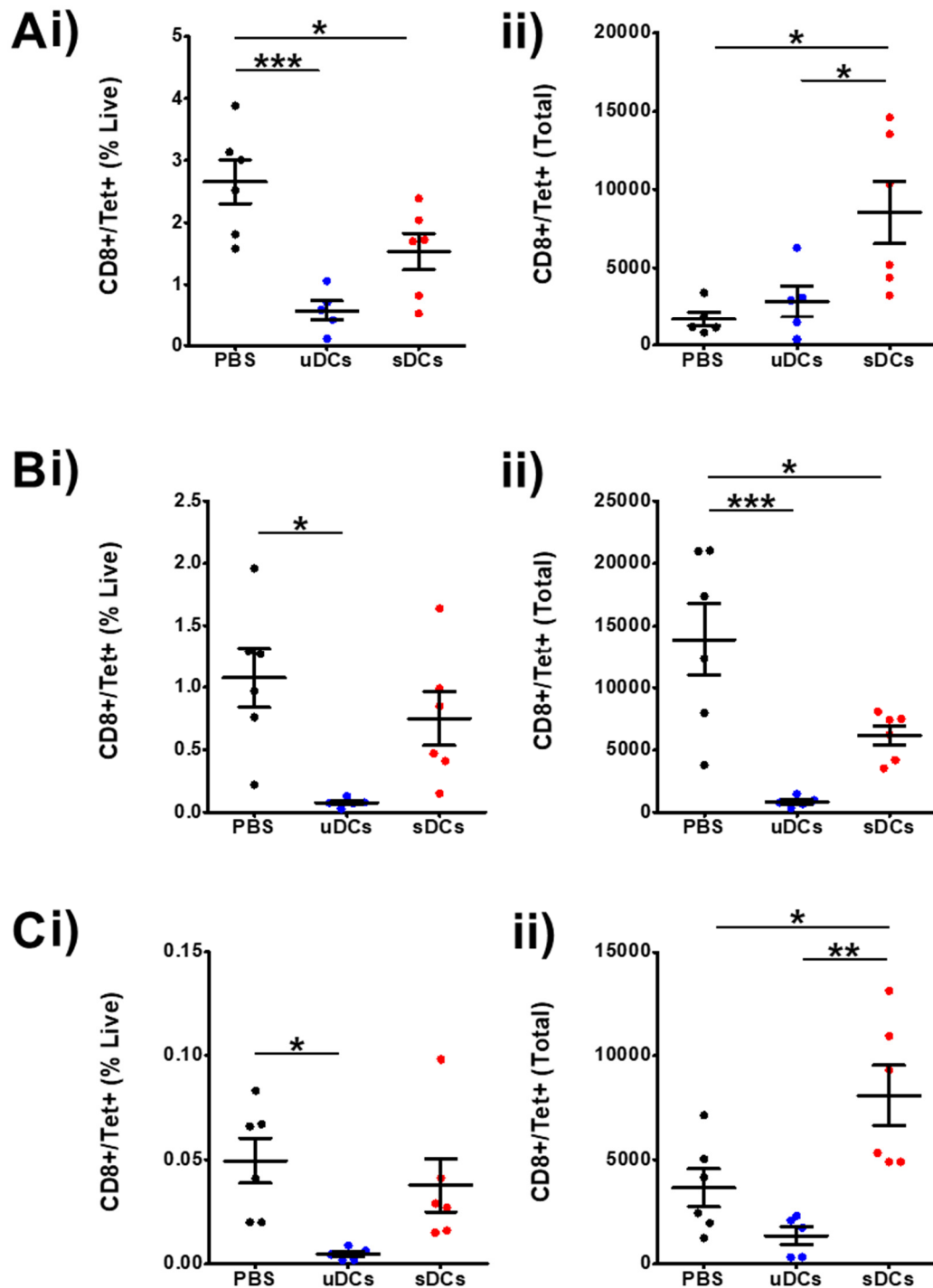
Figure 4.11 - sDC vaccination after tumour development increases the magnitude of the antigen-specific T cell response in the lymphatic system.
Mice receiving the B16F10.ova tumours by subcutaneous injection were assessed for the antigen-specific T cell response to DC vaccination in the (**A**) popliteal LN (pLN); (**B**) inguinal LN (iLN); and (**C**) spleen by flow cytometry. Cell number was quantified by either percentage of live cells (**i**) or total cell number (**ii**) for each tissue. Data represent individuals ± SEM error bars. Statistical analysis was by one-way ANOVA with Bonferroni's Multiple Comparison Test: *P ≤ 0.05, **P ≤ 0.01, ***P ≤ 0.001 (n = 6/group).

In agreement with previous experiments, injection of sDCs effectively induced an antigen-

specific T cell response in the injection site-draining LN which was significantly higher

than either uDC-receiving mice or the PBS control (8541 ±2013 to 1675 ±464 and 2823 ±996 for PBS and uDC, respectively; **Figure 4.11Aii**). Up to a 3-fold difference in total cell number was seen in the sDC-receiving mice, consistent with previous data. In the iLN, however, the PBS-receiving mice had a significantly higher number of antigen-specific cells (13907 ±2908) than either of the DC-receiving groups (830 ±185 or 6150 ±770 for uDC and sDC, respectively; **Figure 4.11B**). This was much higher than previously seen in the PBS control groups and may be due differences in tumour cell preparation or cell viability before injection. Interestingly, the DC-receiving animals had fewer antigen-specific T cells than seen before (**Figure 4.3Bii; Figure 4.7Bii**). The spleen, again, had a higher number of antigen-specific T cells following sDC injection (8075 ±1444; **Figure 4.11Cii**). There was at least a 2-fold difference between the sDC-receiving and PBS control groups (3660 ±902), and up to a 3-fold difference between the sDC and uDC groups (1356 ±429).

4.4.3 Antigen-specific T cell phenotype

Antigen-specific T cells in the pLN, iLN and spleen were further phenotyped by flow cytometry using CD44 and CD62L as markers of cell maturity and *in vivo* function.
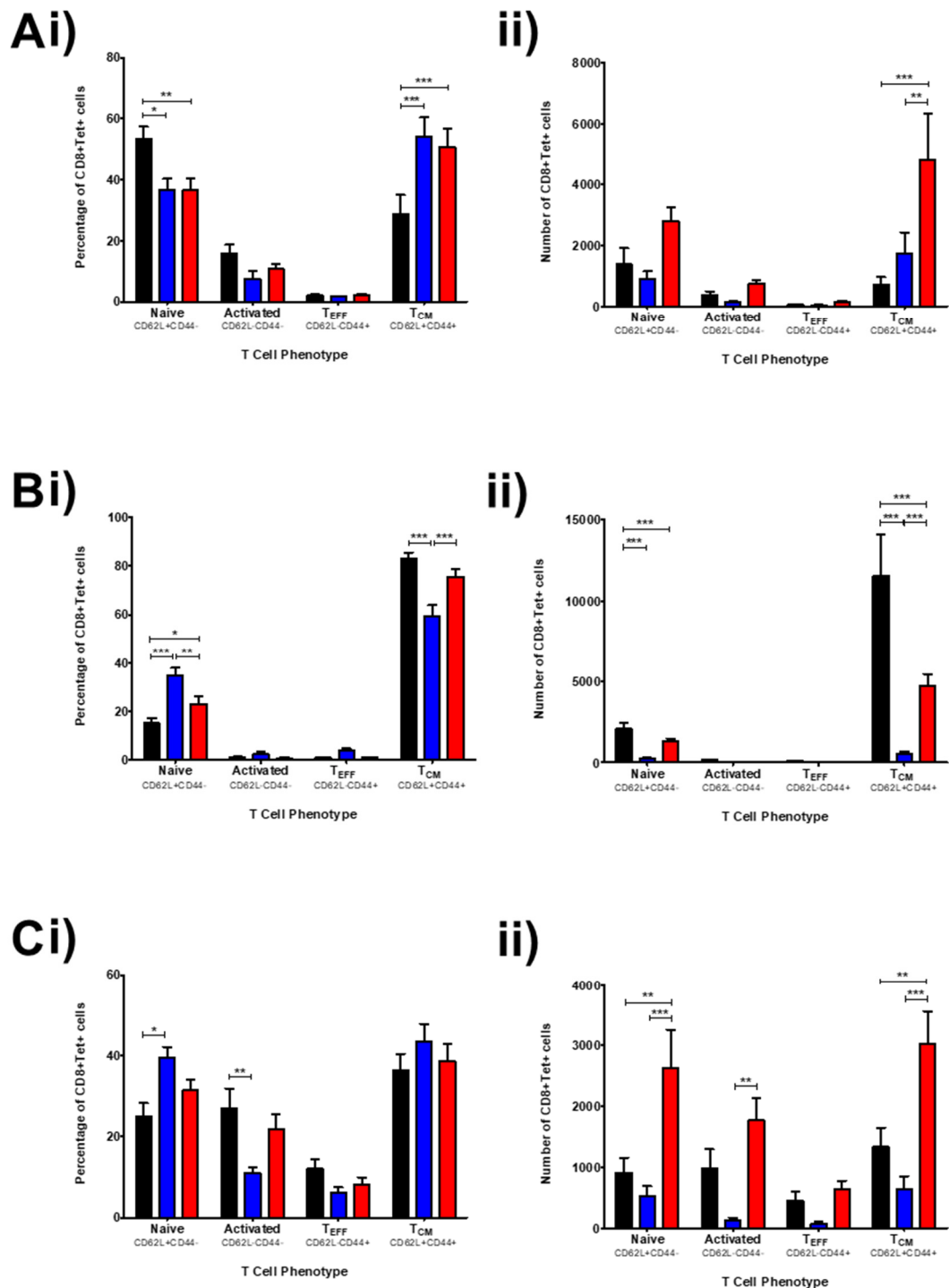
Figure 4.12 - sDC vaccination after tumour development increases tumour antigen-specific T cell proliferation and maturity in the lymphatic system.
Mice receiving B16F10.ova tumours by subcutaneous injection were assessed for the antigen-specific T cell response to DC vaccination in the (**A**) popliteal LN (pLN); (**B**) inguinal LN (iLN); and (**C**) spleen by flow cytometry. Expression of CD44 and CD62L was used to phenotype the T cells, which were quantified by either percentage of live cells (**i**) or total cell number (**ii**) in each tissue. Data represent mean ± SEM error bars. Statistical analysis was by one-way ANOVA with Bonferroni's Multiple Comparison Test: *P ≤ 0.05, **P ≤ 0.01, ***P ≤ 0.001 (n = 6/group).

Antigen-specific T cells in the pLN in DC-receiving animals were mostly mature memory

T cells, compared to the PBS controls which were primarily naïve by phenotype. In terms

of total cell number, the mice receiving 2 injections of sDCs had a significantly higher T_{CM} number than the uDCs despite having no difference by proportion (**Figure 4.12Ai**). In the iLN the PBS control group has a very high antigen-specific T cell number compared to the DC-treated groups, which was unexpected but shows a similar trend to the single DC injection experiment (**Figure 4.4Bii**). The sDC-receiving mice showed a significant increase in TCM cells in comparison to the uDC group. In the spleen, sDC-receiving mice had significantly higher antigen-specific T cells of naïve, activated and T_{CM} phenotypes compared to the uDC and PBS controls. This suggests that although tumour growth was not controlled in this experiment, there is a quantifiable immune response in response to the sDC injections.

4.5 Discussion

This Chapter presents data supporting the efficacy of CCR7-sorted DCs in the induction of a T cell response and in control of tumour growth *in vivo*. This confirms two important hypotheses described in the **Introduction**. Firstly, ensuring migration of injected antigen-presenting DCs to the lymph nodes can improve an antigen-specific T cell response *in vivo*. This is consistent in all three of the DC injection strategies presented here, shown by a significant increase in T cell number in the injection site-draining lymph node. The phenotype of these cells is injection strategy-dependent, with a single injection of sorted DCs or with a second DC injection after tumour induction resulting in a production of both naïve, antigen-inexperienced T cells and mature memory T cells. Injection of multiple doses of DCs prior to antigen from the tumour as a traditional vaccination strategy, however, resulted in development of a more effector memory phenotype (**Figure 4.8A**). The same T cell response was not seen in the unsorted DC group despite the animals being given the same number of CCR7+ cells in the injection bolus. It is important to highlight the difference between T cell responses of the uDC and sDC groups is typically 2- to 3-fold in magnitude in the pLN, even though the two groups were given the same total number of CCR7+ cells. Taking these data together with the cell phenotyping from **Chapter 3**, there is evidence that the CCR7- cells within the population are negatively affecting the ability of the CCR7+ DCs to induce a T cell response, whether this is by limiting cell migration to the lymph nodes or suppressing the T cell response itself. The second hypothesis was that this improved T cell response could be beneficial in the context of DC therapies. Treatment of late-stage solid tumours is clinically difficult as the tumour invades the stroma and subverts the systemic immune response, and rare in clinical trials

since most patients will have undergone a number of surgeries and treatments before being considered for DC therapy (Constantino *et al.*, 2016). The data presented here highlights the potential benefits of CCR7-sorted DCs in a model system which is more extreme than would be seen in clinical use of these cells. In two of three injection strategies, CCR7+ DCs could control tumour growth and improve survival duration with no other interventions compared to the unsorted DC population.

A single injection of sDCs at an early point in tumour development was shown to be effective in controlling tumour growth and extending survival duration of treated animals. Tumour growth was not controlled by an endogenous immune response in mice receiving only PBS/BSA, or by injection of an unsorted DC population containing an equivalent number of CCR7-expressing DCs. In the pLN, up to a 5-fold increase was seen in the number of T cells which recognise the antigen presented by the DCs in mice treated with sDCs compared to uDCs. The phenotype of pLN antigen-specific T cells was similar between these treatment groups, however, suggesting that there had been some infiltration of injected DCs. Since the uDC group does not control tumour growth as effectively, it is possible that although some DCs may reach the LN, the number of cells is too small to reach the T cell threshold required for control or rejection (Lim *et al.*, 2007). Without an earlier timepoint this cannot be determined. The same was seen in the spleen, where the phenotype of T cells induced by DC vaccination was mostly naïve compared to PBS controls but no different between the DC-receiving groups. Actual cell number higher was 3-fold higher in the mice receiving sDCs compared to the uDC group, suggesting that although the induced phenotype is similar between the two groups there is an increased magnitude of the response in the sDC-receiving group. Antigen-specific T cell presence in the spleen was unsurprising after sDC injection, but whether this was due to migration of the DCs themselves to the spleen for antigen presentation, or as a secondary effect of T cell production within the lymphatics is unknown.

The dose of DCs given in these experiments is higher than in previous literature, and LNs have a limited capacity for cell infiltration (Mullins *et al.*, 2003); it is possible, therefore, that increased migration of DCs into the draining lymph node causes spillover into the vasculature as LN capacity is reached. In the iLN, in contrast, tumour-bearing mice receiving only PBS had the highest induction of antigen-specific T cells of the three experimental groups. In the absence of a therapeutic intervention, the primary immune response occurs in the tumour-draining lymph nodes as tumour antigens are presented by endogenous APCs (Marzo *et al.*, 1999). It is possible, however, that the presence of cells in

the iLN does not necessarily correlate with cytotoxicity due to tumour-derived immune suppression mechanisms (Fransen, Arens and Melief, 2013). Generation of a natural immune response in the iLN appears to have no effect on the growth of the tumour, which suggests a suppressive mechanism may be involved. In DC-receiving mice the immune response is higher in the spleen and injection site-draining lymph nodes and is sufficient to slow tumour growth without involvement of the tumour-draining lymph nodes. Single therapeutic DC injections are rarely given, however, to better assess CCR7+ DCs in a therapeutically relevant model, multiple DC injections were given to B16 tumour animals.

When multiple DC injections are given prior to the induction of tumour growth, CCR7+ DCs are again able to slow tumour growth compared to the control groups. This was thought to be due the formation of an antigen-specific memory, due to the high number of T_{EFF} cells present in both the pLN and iLN of sDC-receiving mice. The generation of T_{CM} cells seen after a single injection of DCs (**Figure 4.4A**) could be supporting the rapid expansion of antigen-specific effector cells in the lymph nodes after a second injection of the same DCs (Fearon, Manders and Wagner, 2001). Multiple uDC injections promoted a different pattern of T cell expansion, with the primary T_{EFF} response occurring in the spleen. This was interesting as it reproduces the development of a T cell response seen in IV but not subcutaneous injection of DCs. Route of immunisation has a well-characterised effect on the biodistribution of DCs (Eggert *et al.*, 1999): after IV injection, DCs accumulate within the spleen by being unable to access the lymphatics from the bloodstream. In comparison, DCs injected subcutaneously preferentially migrate to the LNs, if they express CCR7 (Mullins *et al.*, 2003). This data may be indicative, therefore, of an increased migration of uDCs into the spleen and cause an increased effector response within that tissue.

It is possible that this injection strategy could result in complete tumour prevention using a smaller tumour cell number. Previous studies use varying numbers of tumour cells, between $2x10^5$ and $1x10^6$ cells (Kline *et al.*, 2012; Neubert *et al.*, 2014), but this may be too high to allow effective rejection in this model. Multiple DC injections prior to tumour growth may not seem therapeutically viable, however this traditional vaccination strategy could be viable in preventing small metastases after tumour resection or reducing recurrence after complete cure. The latter strategy has been attempted clinically in AML, a cancer in which relapse is common after complete remission and often fatal (Ravandi, 2013). Instead of treating a solid tumour, intradermally-injected DCs were used to control the recurrence of AML in patients following complete remission through chemotherapy

(Anguille *et al.*, 2017). Induction of AML-specific T cell responses in patients correlated with increased survival, and the study achieved a 43% clinical response rate. Similarly, recurrence of cancer in patients with resected metastatic colorectal cancer can be delayed using DC vaccination (Morse *et al.*, 2013). This could be replicated using the B16F10.ova model if tumour resection was a possibility, or by a reduction in initial tumour number to prolong the duration of the tumour growth. Generation of a T cell response against a tumour antigen can therefore be a viable treatment strategy for prevention of relapse; this could be improved in a clinical context using CCR7 sorting as described here.

When the second DC injection is given after induction of the tumour growth, the T cell response does not control tumour growth as seen previously with the other injection strategies. In sDC-receiving mice, there was a significant increase in T cells in the pLN compared to the PBS and uDC controls. Most of these cells were of the T_{CM} phenotype, which were 3 times higher in sDC-receiving mice than either control. In the iLN, PBS control animals had the highest antigen-specific response by total number. Again, this is likely to be the natural immune response in the tumour-draining lymph node. There is a difference in magnitude of response compared to previous experiments, but this may be as a result of increased immunogenicity of the tumour cells through passage or a lower cell viability between experiments which could stimulate the immune response. In the spleen there was a significant difference in naïve, activated and T_{CM} cell numbers after sDC injection compared to the controls which mirrors the single DC injection. Although there is a clear increase in T cell number in both the pLN and spleen of sDC-treated mice, there was no control of the tumour growth in this experiment.

It may be that directing the immune response to a LN distal to the tumour has a detrimental effect to protection giving the aggressive growth of this particular tumour model, a concept first described by Brown *et al.* (Brown *et al.*, 2001). The reduction in T cells in the tumour-draining lymph node (**Figure 4.3Bii** and **Figure 4.12Bii**) after a single dose of DCs or a second injection after tumour establishment is apparent compared to the natural T cell response seen in the PBS controls (**Figure 4.12**). Another possibility is that the tumour cells downregulate expression of ovalbumin, which is supported by the experimental evidence of a significant anti-ovalbumin response being unable to control the tumour growth. A study in 2013 showed that multiple 'boosts' of T cell activation by DC vaccines were actually detrimental in both the B16F1 model and a transgenic prostate adenocarcinoma model if used therapeutically (Ricupito *et al.*, 2013) One hypothesis for this is overstimulation of the T cells if the doses of DCs are too close together, given that

the tumour itself provides antigen to further prime the response to the first dose of cells. This study used DCs presenting a single antigenic peptide. This is an important consideration for the therapeutic use of DCs: particularly in the selection of the antigen used.

In this Chapter, only a single antigen is used to allow accurate quantification of the induced T cell response, however may not allow for a strong enough response, or conversely a response which is too strong, for complete tumour rejection. Analysis of the tumours themselves for expression of ovalbumin would be able to show the extent of tumour sculpting by the immune response by quantifying the proportion of cells which retain expression of the antigen. Single-antigen DC preparations do have clinical relevance, exemplified by Sipuleucel-T against PAP (Kantoff *et al.*, 2010). In clinical trials, and since approval for clinical use, these therapies can prolong patient survival by increasing tumour antigen-specific T cells, but do not lead to striking tumour regression compared to equivalent T cell immunotherapies (Rosenberg *et al.*, 2011). Tumour cells expressing alternative antigens can also arise under this immune pressure. Some clinical evidence does exist to support multiple therapeutic vaccines with a single antigen leading to immunosuppression and decreased survival (Eggermont, 2009); so care must be taken in clinical trial design, particularly if CCR7-sorted DCs prove to be significantly more immunogenic than current DC vaccines. To induce a more complete tumour response, multiple tumour antigens derived from tumour cell lysates or mRNA can be used; which could be done in this model given the availability of tumour cells prior to treatment. Using the melanoma cell-derived mRNA, clinical evidence showed detectable T cell populations recognising different tumour antigens following DC therapy (Benteyn *et al.*, 2012). Although this method is outwith the scope of this study, this is a potential consideration for future work.

To fully characterise the response of the immune system to this DC vaccine, it would be beneficial to understand the response of other cell types to treatment. The CD8+ T cell response is invariably important in the anti-tumour response (Kirkwood *et al.*, 2012), but is not the only potential immune response from DC therapy. CD4+ T cells support the development of CD8 responses through cytokine production, but are stimulated by presentation of antigen by MHC class II instead of class I (Ossendorp *et al.*, 1998). The presence and activation of CD4+ T cells in tumour immunology is understood to be both supportive of the CD8 response as well as in the production of IFNγ and TNFα for tumour killing (Shklovskaya *et al.*, 2016). Cytokine production by CD4+ T cells leads to

downstream activation of other cell types, including cytotoxic eosinophils which can be recruited to the tumour (Hung *et al.*, 1998). Uptake of exogenous whole-protein antigen by DCs allows presentation of antigen by both the MHC class I and II, compared to direct peptide loading which is specific for one of the two (Delamarre, Holcombe and Mellman, 2003). Understanding of the CD4 response, and its potential downstream effectors, may be a novel outcome for DC therapy for cancer. Interactions of DCs with B cells in the lymph nodes is also a potential anti-tumour mechanism. Canonically B cell function is in the production of antibodies, and there is some evidence to support the importance of this in the B16F10 model (Guy *et al.*, 2016). Production of cytokines by B cells within the lymph nodes can tailor the T cell response towards an antigen, making them relevant in tumour biology. Both positive and negative outcomes of B cell function in tumour development have been reported. B cell depletion in experimental knockout models has been shown to augment the anti-tumour response (Qin *et al.*, 1998), but depletion of B cells in adulthood conversely inhibits the anti-tumour response (DiLillo, Yanaba and Tedder, 2010). DCs are capable of activating B cells and transferring antigen to them (Wykes, Pombo and Jenkins, 2018), so it would be interesting to understand if increasing migration of DCs to the lymph node has any effect on these processes.

4.6 Chapter summary

In the previous Chapter, it was shown that sorting DCs by CCR7 expression is viable and beneficial to both cell migration and phenotype. Induction of a more mature T cell response *in vitro* was also seen, and to expand on this in a therapeutic context, the B16F10.ova model of melanoma was used. Three injection strategies were used to understand the consequences of improved migration in this tumour model: one single injection at the same time as tumour induction, or two injections with the additional injection before tumour induction to mimic a traditional vaccination, or after tumour induction to replicate therapeutic use. In all cases, CCR7-sorted DCs led to a significantly increased antigen-specific T cell number in the injection-site draining lymph nodes compared to the unsorted DC, and PBS control groups, which is proposed to be as a result of improved migration of the DCs. This agrees with the common hypothesis that a deficit in cell migration limits the efficacy of DC therapy (de Vries, Krooshoop, *et al.*, 2003; Sabado and Bhardwaj, 2015). There was no difference in cell number between the uDC and PBS controls, suggesting that removal of the CCR7- cells from the injection bolus is beneficial in addition to just improving cell migration. After a single injection or two

injections after tumour development, cells in the pLN were antigen-inexperienced naïve T cells and developing memory T cells, suggesting clonal proliferation of DC-stimulated T cells in the lymph nodes. There was also a splenic response higher than the control groups. After two injections prior to tumour development, the primary response was in effector T cells which is proposed to be a second wave of antigen response after initial memory development. In the iLN, the PBS control group showed the highest antigen response which was expected as it drains antigen from the tumour and is the primary site of the endogenous immune reaction. In the single and vaccination strategies, sDCs slowed tumour growth and increased survival compared to the controls, but this was not seen in the treatment injection strategy. This was potentially due to diversion of the primary immune response to a non tumour-draining LN, but this hypothesis requires further assessment. In summary, sorting DCs by CCR7 expression does improve migration to the lymph nodes and increase the antigen-specific T cell response *in vitro*, and that these properties can be beneficial in a therapeutic context.

Chapter 5

Assessing CCL19-sorted dendritic cells in the metastatic B16F10.ova model

5.1 Introduction and aims

In **Chapter 4**, CCR7-sorted DC function was assessed in the control of subcutaneous melanoma growth. After a single injection, or multiple injections, prior to the initiation of tumour growth, sDCs were able to control tumour growth and increase survival times compared to the injection of an unsorted DC population. sDC injection led to the production of mature, antigen-specific T cells within the injection site-draining lymph node and in the spleen whereas this response was minimal after unsorted cell injection. Although survival duration was increased by 20-30% in this model, animals did still reach maximal tumour size after sDC injection. This suggests that DCs alone are not sufficient to control the rapid growth of subcutaneous tumours in this model even with prophylactic injection strategies.

In a clinical setting, the majority DC therapies are given after removal of the bulk tumour mass by surgery or chemotherapy (Francia *et al.*, 2011). Secretion of immunosuppressive factors such as TGFβ, IL-10 and indoleamine 2,3-dioxygenase (IDO) by the tumour reduces DC and T cell cytotoxicity, so removal of tumour mass is beneficial to the development of a therapeutic response (Gulley, Madan and Schlom, 2011). Multiple clinical trials with patient cohorts subdivided by tumour stage, and therefore tumour size, show that patients with less advanced tumours respond better to DC therapies (Hanna *et al.*, 2006; Kantoff *et al.*, 2010). Even after traditional interventions, residual tumour cells from the primary tumour or from developing metastatic lesions may remain in the patient, which may lead to relapse. In addition to control of primary tumour growth, enhanced antigen-specific T cell numbers can also help control the development of metastatic lesions after removal of the primary tumour.

Metastasis, which is the occurrence of secondary tumour lesions distal to the primary tumour, is a complicated process and still not fully understood. It is thought to account for up to 90% of cancer mortality, depending on the type of cancer (Chaffer and Weinberg, 2011). As described in the **Introduction**, there are a number of steps involved in metastasis including invasion of local tissue, escape into the blood, adherence within the vasculature, extravasation and survival within this secondary site. The initial anti-tumour response in the primary tissue site is often an innate mechanism. Macrophages are important in the development of many tumours and can comprise a large proportion of the actual tumour mass (Pollard, 2004). Macrophage knockout or inhibition can delay the development of angiogenesis within the tumour and invasion of the tumours into the local

stroma (Wyckoff *et al.*, 2004). Tumour-associated neutrophils are also becoming better characterised as promotors of tumour metastasis (Fridlender *et al.*, 2009).

Although cytokines secreted by the tumour, such as TGFβ as described previously, subvert the immunogenicity of macrophages and neutrophils (Courau *et al.*, 2016), a strong anti-tumour T cell response can revert these cells back to a cytotoxic state and help prevent metastasis development systemically in addition to being directly cytotoxic to the primary tumour themselves (Governa *et al.*, 2017; Hoves *et al.*, 2018). The circulating T cell response against the primary tumour helps control early metastatic growth in distal tissues, a phenomenon known as concomitant immunity which was first described in 1986 (Dye, 1986). The adaptive immune response does not effectively control tumour cells in the blood, as more than 80% of tumour cells have been shown to survive and extravasate to secondary sites (Koop *et al.*, 1995). As the tumour grows and develops immune escape mechanisms, the protection of concomitant immunity decreases with the dearth of activated tumour-specific T cells (Janssen *et al.*, 2017). Even removal of the primary tumour can trigger activation of dormant metastases if T cell protection decreases from inactivity. Reactivation or replacement of these T cells is therefore a viable and potentially necessary strategy for the control of metastatic development at secondary sites

The ability of DC vaccination to induce significant anti-tumour T cell responses makes them an attractive target as cancer immunotherapeutics. Their viability in a solid tumour context have been described in **Chapter 4** but primary, and secondary, metastatic tumours may both benefit from DC therapy. Despite the efficacy of novel treatments for primary tumour growth, there is an absence of effective anti-metastatic treatments, even given the high mortality attributable to cancer metastasis (Weigelt, Peterse and Veer, 2005). In the 4T1 orthotopic model of breast cancer in mice, DC vaccination with dasatinib support was able to reduce metastasis from the primary tumour through expansion of CD8+ T cells (Song *et al.*, 2018). In the B16 and Lewis lung carcinoma (LLC) models, DC vaccines have also shown efficacy in reduction of metastasis (Markov *et al.*, 2015). Current clinical trials in metastatic tumour contexts have shown some success, such as improved survival of metastatic uveal melanoma (Bol *et al.*, 2014). Dendritic cell vaccines have also been shown to have a significant effect on survival of metastatic melanoma, with almost double the survival duration compared to alternative treatments (Dillman *et al.*, 2018). DCs are, therefore, a clearly viable therapy for metastasis.

The B16F10.ova model can be used as a solid tumour model (**Chapter 4**) but is most commonly used as a metastatic model. Multiple repeated isolations of the parental B16F0 and F1 clones within lung tumour lesions have selected the F10 clone for lung-metastatic properties. This clone was then modified to express ovalbumin as a tumour-associated antigen (**Appendix I**). As in **Chapter 4**, the induction of an antigen-specific T cell response following either sDC or uDC was quantified in the context of the B16F10.ova metastatic melanoma model. Given the limited duration of this model, two injection strategies were assessed: one single DC injection at the same time as the tumour induction; and two DC injections prior to the tumour induction. Tumour lesion growth within the lungs was quantified at the experimental end-point, and the antigen-specific T cell response was analysed by flow cytometry.

5.2 A single prior sDC injection does not fully control metastases-like lesions in the lung

To examine the control of small, metastasis-like tumour lesions, the B16F10.ova model was used. Metastasis in this model is mimicked by intravenous injection of the tumour cells, as an alternative to the subcutaneous injection model (**Chapter 4**). This approach is slightly more limited in analysis due to the difficulty in monitoring and quantifying tumour growth over time and the shorter experimental duration.

In this experiment, uDCs or sDCs were injected into the footpad, using PBS/0.1% BSA as a control as previously. The following day, B16F10.ova cells were injected intravenously into the tail vein and the animals were monitored for 14 days (**Figure 5.1**).
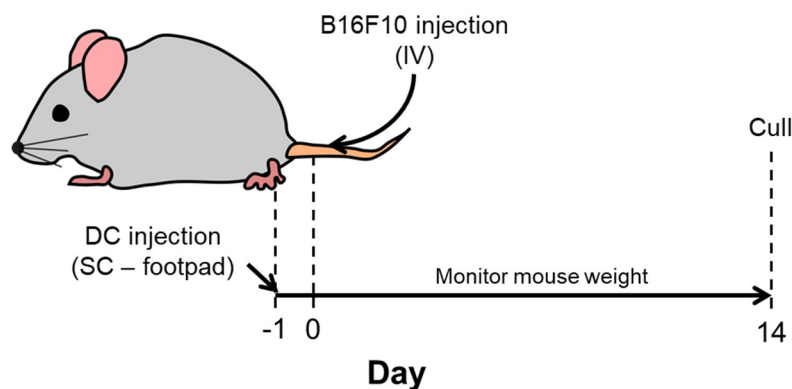
Figure 5.1 - Experimental timeline of single prior DC injection in the B16F10.ova metastatic tumour model.
Mice were first injected subcutaneously with either PBS/0.1% BSA, unsorted DCs (uDCs) or sorted DCs (sDCs) into the left hind footpad. The following day (d0), all mice were injected with B16F10.ova cells intravenously into the tail vein and culled at d14.

5.2.1 Tumour burden

After 14 days, animals were culled and the lungs perfused with PBS and removed. Metastatic lesions within the lungs were identified by their dark melanin colour, with large external lesions visible by eye and smaller external lesions visible using a dissecting microscope. The lesions are melanin-positive in this model (spontaneous amelanic clones and cultures were discarded) and can be quantified without the need for secondary detection measures. The tumour burden was quantified by counting the total number of lesions visible in the lungs.
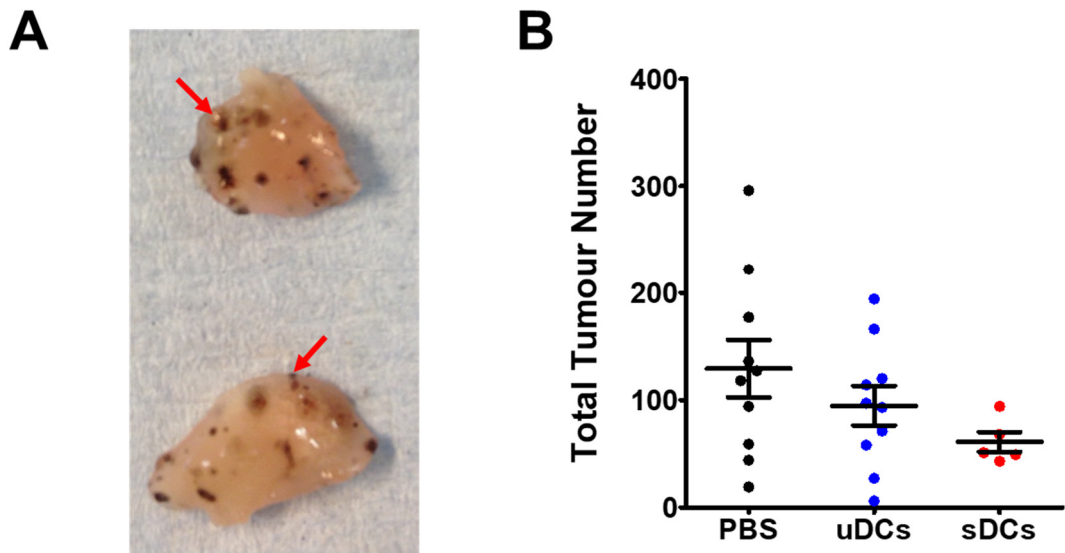
Figure 5.2 - B16F10.ova external metastatic tumour burden following a single DC injection.
14 days after DC injection and B16F10.ova tumour induction, lung metastases were quantified by microscopy. **A**) Melanic tumour lesions are visible (red arrow – examples). **B**) No significant difference was seen between either DC-receiving groups or the PBS controls (individual data points represent one animal, with mean ± SEM error bars). Statistical analysis was by one-way ANOVA with Bonferroni's Multiple Comparison Test (n = 10/group for PBS and uDC; n = 5 for sDC).

There was no significant difference in tumour burden observed between the experimental groups after 14 days. After sDC injection, there did appear to be a reduction in tumour burden, although this does not reach significance. The large variability in external tumour numbers in the PBS and uDC-receiving groups made statistical analysis difficult, so internal tumour burden was also quantified. This variability may result from the numbers of tumour cells engrafting in the lungs after injection and may not represent a rejection response in these animals. The largest lung lobe was prepared for histology and sections were cut using a cryotome. For each animal, three non-serial sections were stained using H&E staining and tumour lesions were counted by microscopy.
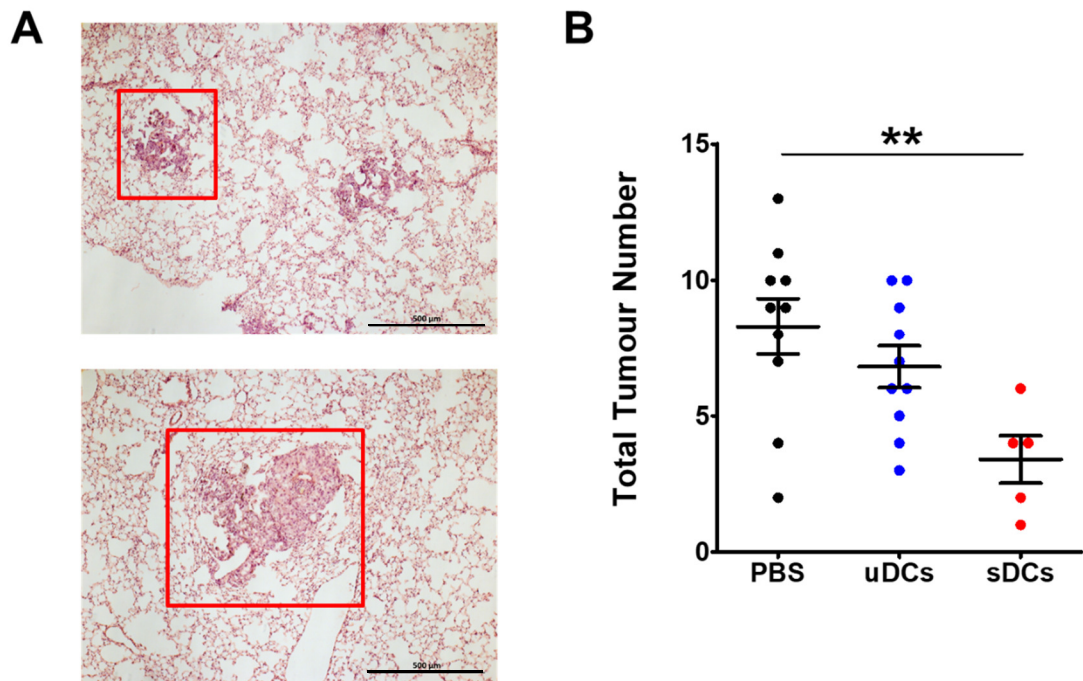
Figure 5.3 - B16F10.ova internal metastatic tumour burden following a single DC injection.
14 days after DC injection and B16F10.ova tumour induction, lung metastases were quantified by microscopy after H&E staining. **A**) Melanic tumour lesions are visible (red boxes – examples). **B**) sDC-receiving mice had fewer internal tumours than the PBS controls, but not the uDC-receiving mice (data points represent average tumour number between 3 lung sections per animal, with mean ± SEM error bars; scale bar is 500µm). Statistical analysis was by one-way ANOVA with Bonferroni's Multiple Comparison Test: **P ≤ 0.01 (n = 10/group for PBS and uDC; n = 5 for sDC).

Lesions were quantified across the whole section for each animal and an average value of three sections per animal was taken (**Figure 5.3**). Tumour lesions within the tissue itself are distinguishable from the lung parenchyma (red boxes, **Figure 5.3A**). In agreement with the external tumour data there was a large variability between internal tumour numbers (**Figure 5.3B**), however internal burden did significantly decrease after sDC injection (3.4 ±0.87) compared to the control groups (8.3 ±1.0 and 6.8 ±0.77 for PBS and uDCs, respectively).

5.2.2 Antigen-specific T cell distribution

To assess the induction of an ovalbumin-specific T cell response, T cells were isolated from the injection site-draining pLN and from the spleen, as well as from the lungs, and analysed by flow cytometry.
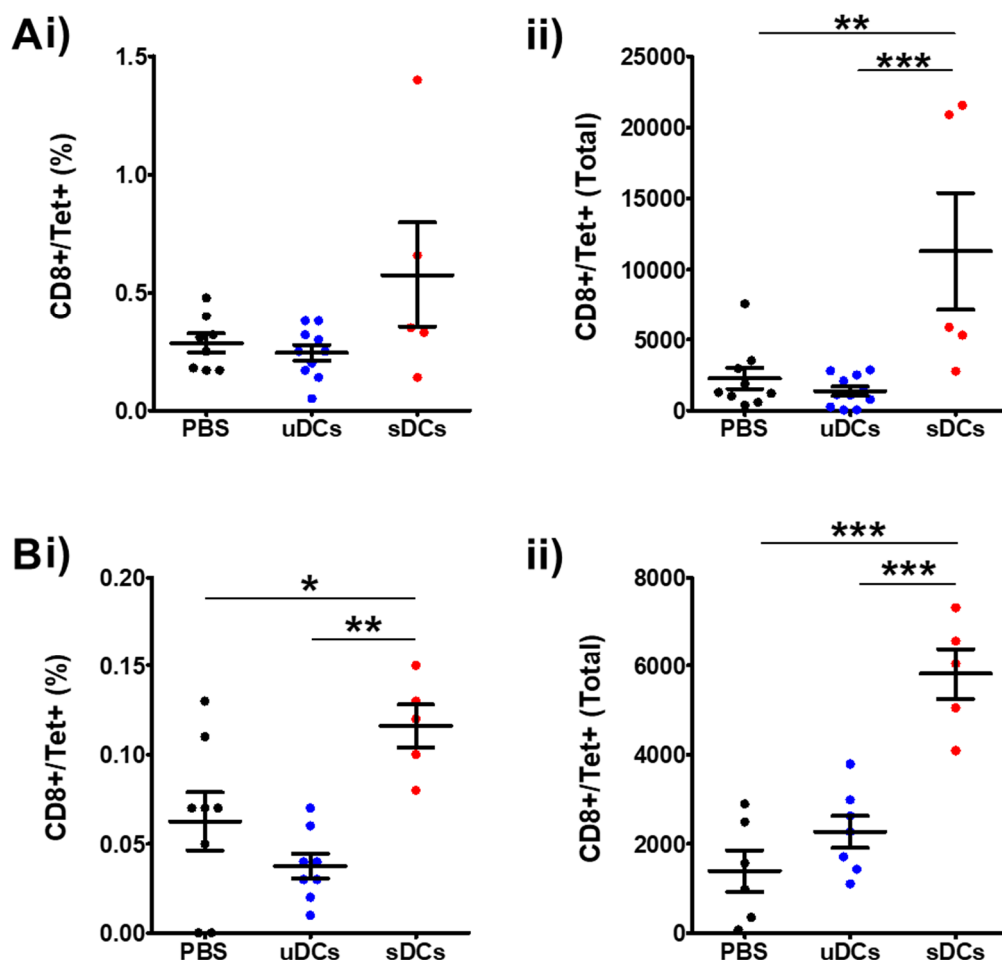
Figure 5.4 - sDC vaccination increases the magnitude of the antigen-specific T cell response in the pLN and spleen.
Mice receiving the B16F10.ova tumours by intravenous injection were assessed for the antigen-specific T cell responses to DC vaccination in the (**A**) popliteal LN (pLN) and (**B**) spleen. Cell number was quantified by either percentage of live cells (**i**) or total cell number (**ii**) for each tissue. Individual data points represent one animal, with mean ± SEM error bars. Statistical analysis was by one-way ANOVA with Bonferroni's Multiple Comparison Test: *P ≤ 0.05, **P ≤ 0.01, ***P ≤ 0.001 (n = 5-10/group).

In agreement with previous data from solid tumour models, injection of sDCs resulted in an increased antigen-specific T cell response (**Figure 5.4**). In the pLN (**Figure 5.4A**), sDC-receiving mice had an increased total number of antigen-specific T cells (11280 ±4100), compared to either PBS (2266 ±751) or uDC (1365 ±322) control groups. The total cell number was more variable than previously seen, however. A similar result was seen in the spleen (**Figure 5.4B**), with sDC injection resulting in the highest T cell response in both percentage and total cell number. The response was between two and three times higher after injection of sDCs (5815 ±568) in comparison with either control groups (1391 ±465 or 2271 ±356 for PBS or uDCs, respectively).
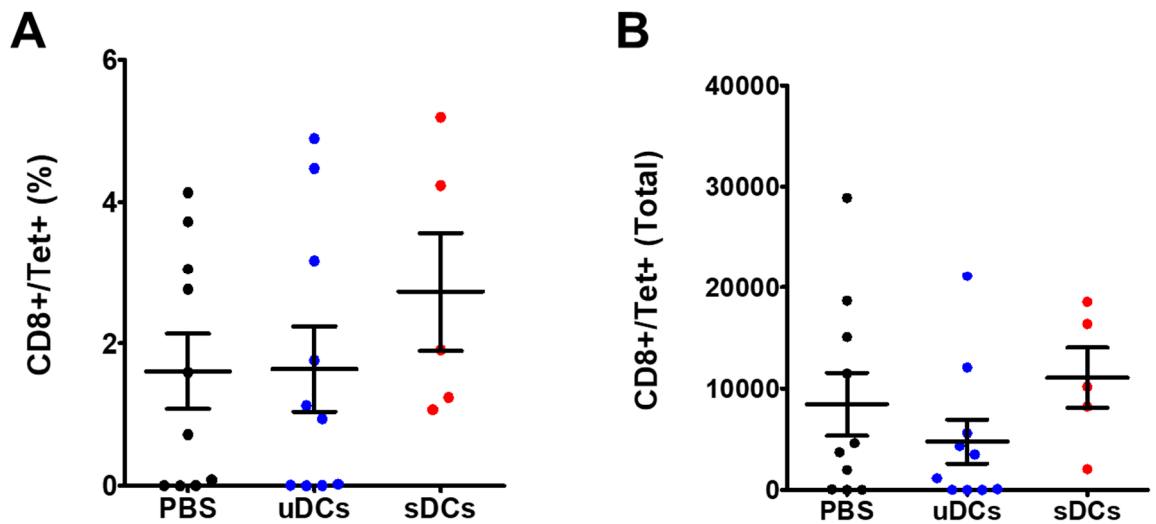
Figure 5.5 - sDC vaccination does not increase the magnitude of the antigen-specific T cell response in the tumour-bearing lungs.
Mice receiving the B16F10.ova tumours by intravenous injection were assessed for the antigen-specific T cell responses to DC vaccination in the tumour-bearing lungs. Cell number was quantified by either percentage of live cells (**A**) or total cell number (**B**) for each tissue but show no difference between experimental groups. Individual data points represent one animal, with mean ± SEM error bars. Statistical analysis was by one-way ANOVA with Bonferroni's Multiple Comparison Test (n = 5-10/group).

In the tumour-bearing tissue, however, sDC injection resulted in no difference in the antigen-specific T cell response compared to the control groups (**Figure 5.5A**). There appeared to a decrease in the detectable cells after uDC injection, however this did not reach significance in this experiment. In the sDC-receiving animals, there was an average of 11071 cells (±2948 cells) specific for the tumour antigen, compared to 8452 (±3104) in the PBS-receiving animals and 4788 (±2175) in the uDC-receiving animals (**Figure 5.5B**). Since the antigen-specific response is not significantly different between the sDC groups and the controls, although there is a decrease in the internal tumour burden (**Figure 5.3**), these data may be indicative of the importance of other immune cells in the protection against the metastatic lesions in this model.

5.3 Multiple injections of sDCs do not lead to tumour control in the metastatic model

Despite detectable antigen-specific T cells in the pLN and spleen in sDC-receiving mice, there was no difference in the T cell number in the lungs. Although there was no difference in external lung tumour burden, there was a significant decrease in the internal tumour burden after sDC injection when analysed histologically. To better understand the

involvement of T cells in the anti-tumour response in the lungs, an additional injection of either DCs or PBS was given before induction of tumour growth. In this experiment, the additional injection of either sDCs or uDCs or PBS/0.1% BSA into the footpad was given a week before the second set of injections and the tumour induction. This strategy is summarised in **Figure 5.6** below.
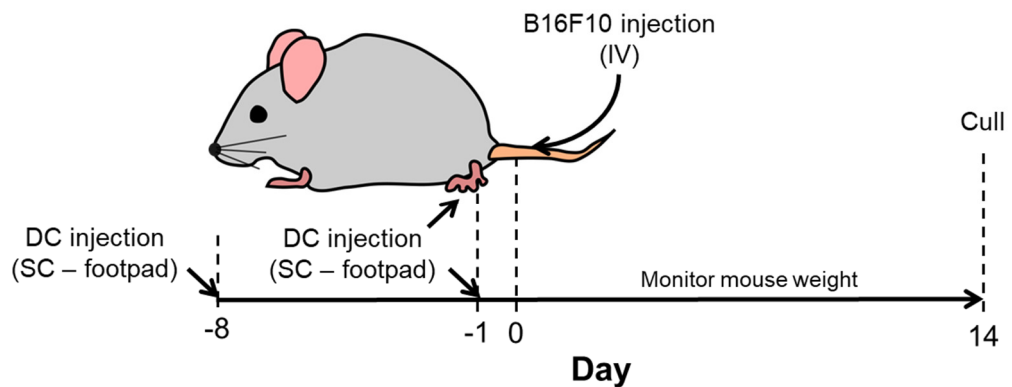
Figure 5.6 - Experimental timeline of multiple prior DC injections in the B16F10.ova metastatic tumour model.
Mice were first injected subcutaneously with either PBS/0.1% BSA, unsorted DCs (uDCs) or sorted DCs (sDCs) into the left hind footpad under isofluorane anaesthetic. A week later (d-1), mice were injected again and then the following day (d0) all mice were injected with B16F10.ova cells subcutaneously into the flank and culled at d14.

5.3.1 Tumour burden

14 days after IV tumour injection, melanic lesions on the surface of the lungs were counted by light microscopy.
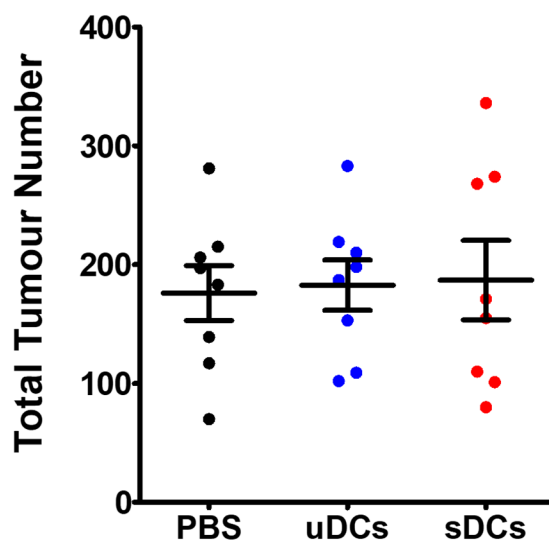
Figure 5.7 - Multiple sDC injections have no effect on the number of external metastatic lesions in the lungs.
Melanin-producing tumour lesions in the lungs after 14 days were quantified by light microscopy but show no difference between the experimental groups. Individual data points represent one animal, with mean ± SEM error bars. Statistical analysis was by one-way ANOVA with Bonferroni's Multiple Comparison Test (n = 8/group).

As shown in **Figure 5.7**, there is no difference in the total lesion count across all lung lobes between the experimental groups, although the range of counts within each group again highlight the variability inherent in the model. In the PBS control there was an average of 176 ±23.1 tumour lesions, whereas in the uDC and sDC-receiving animals the average was 182 ±21.2 and 186.9 ±33.4, respectively.

5.3.2 Antigen-specific T cell distribution

T cell responses in the lymph nodes were again assessed using flow cytometry. In this experiment, both the injection site-draining pLN and tumour-draining mLN were taken, as well as the lungs and spleen.
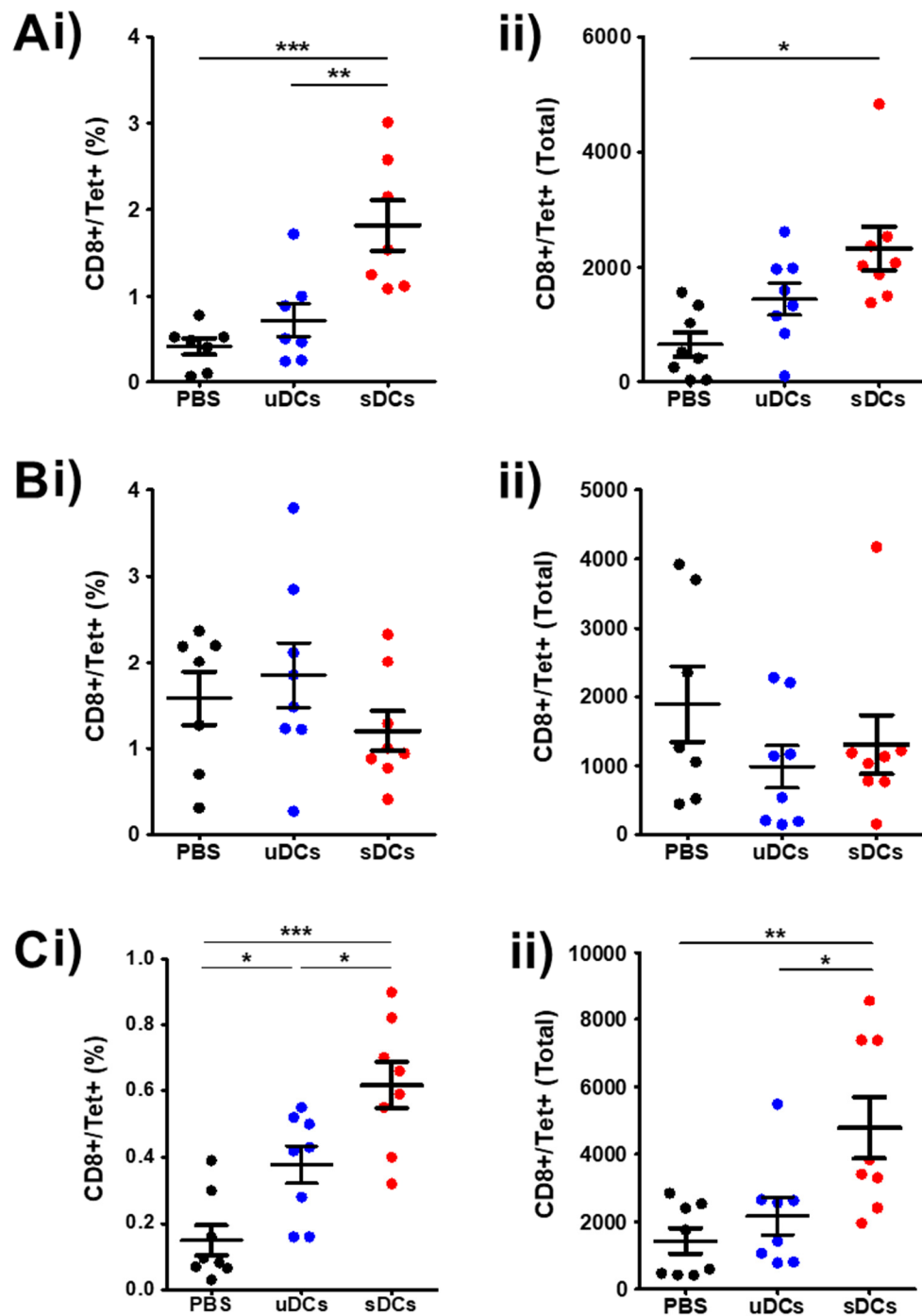
**Figure 5.8 - Prior sDC vaccination increases the magnitude of the antigen-specific T cell response in the lymphatic system.**
Mice receiving the B16F10.ova tumours by intravenous injection were assessed for the antigen-specific T cell responses to DC vaccination in the (**A**) popliteal LN (pLN); (**B**) mesenteric LN (mLN); and (**C**) spleen by flow cytometry. Cell number was quantified by either percentage of live cells (**i**) or total cell number (**ii**) for each tissue. Individual data points represent one animal, with mean ± SEM error bars. Statistical analysis was by one-way ANOVA with Bonferroni's Multiple Comparison Test: *$P \leq 0.05$, **$P \leq 0.01$, ***$P \leq 0.001$ (n = 6-8/group).

In agreement with all previous data, sDC injection resulted in the highest induction of T

cell responses in the pLN and spleen as both a percentage of live cells and in total cell

number (**Figure 5.8A** and **C**, respectively). In the pLN (**Figure 5.8Aii**), sDC-receiving mice had twice as many antigen-specific T cells as the uDC-receiving mice (2328 ±383.5 to 1454 ±275) and four times as many as the PBS control group (650 ±209.9). In the spleen there was a very similar trend (**Figure 5.8Cii**), as sDC-receiving mice had 4776 ±909 ovalbumin-specific T cells compared to 1432 ±375.4 in the PBS controls and 2174 ±552.7 cells in the uDC group. In the mLN, however, there was no difference between any of the groups (**Figure 5.8B**). Mice receiving unsorted DCs appeared to have the lowest T cell response (982 ±308.7) when compared to the PBS control (1893 ±549.8) or the sDC-receiving mice (1305 ±427.5), but this difference is not significant.
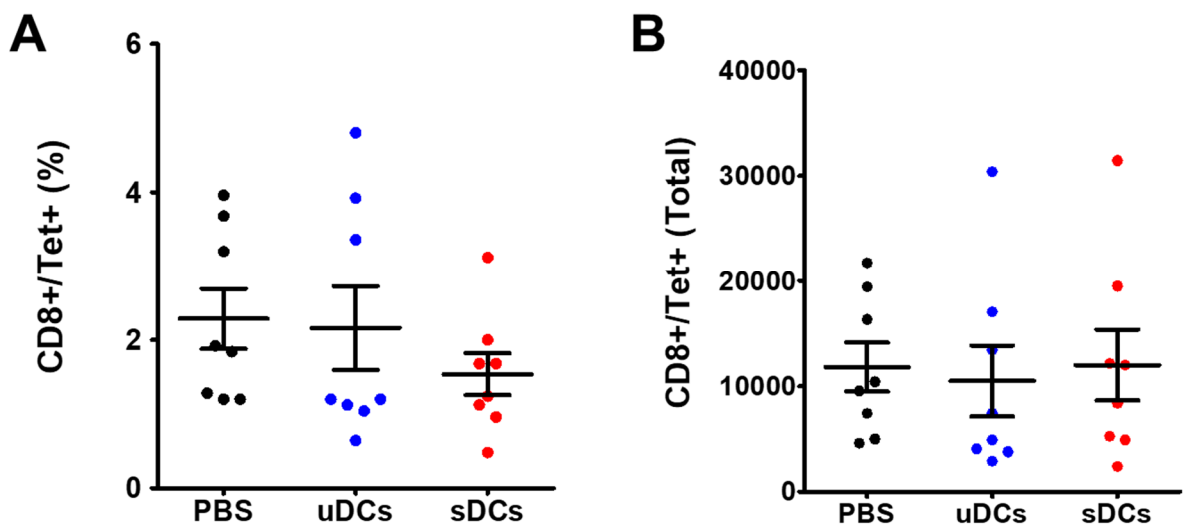
**Figure 5.9 - Multiple sDC injections do not increase the magnitude of the antigen-specific T cell response in the tumour-bearing lungs.**
Mice receiving the B16F10.ova tumours by intravenous injection were assessed for the antigen-specific T cell responses to DC vaccination in the tumour-bearing lungs. Cell number was quantified by either percentage of live cells (**A**) or total cell number (**B**) for each tissue but show no difference between experimental groups. Individual data points represent one animal, with mean ± SEM error bars. Statistical analysis was by one-way ANOVA with Bonferroni's Multiple Comparison Test (n = 6-8/group).

Figure 5.9 shows the number of tumour antigen-specific T cells detectable within the lungs of tumour-bearing mice. In agreement with the single injection strategy, there was no difference between DC-receiving mice and PBS controls in the prevalence of T cells within the lungs during development of metastases. In the sDC group, the average T cell response is 12002 ±3370 cells, compared to the uDC group which had 10494 ±3363 cells and the PBS control group which had 11809 ±2321 cells.

5.3.3 Antigen-specific T cell phenotype

To further phenotype the antigen-specific T cells in each of these tissues (**5.3.2**), antigen-specific T cells were also characterised for expression of CD44 and CD62L.
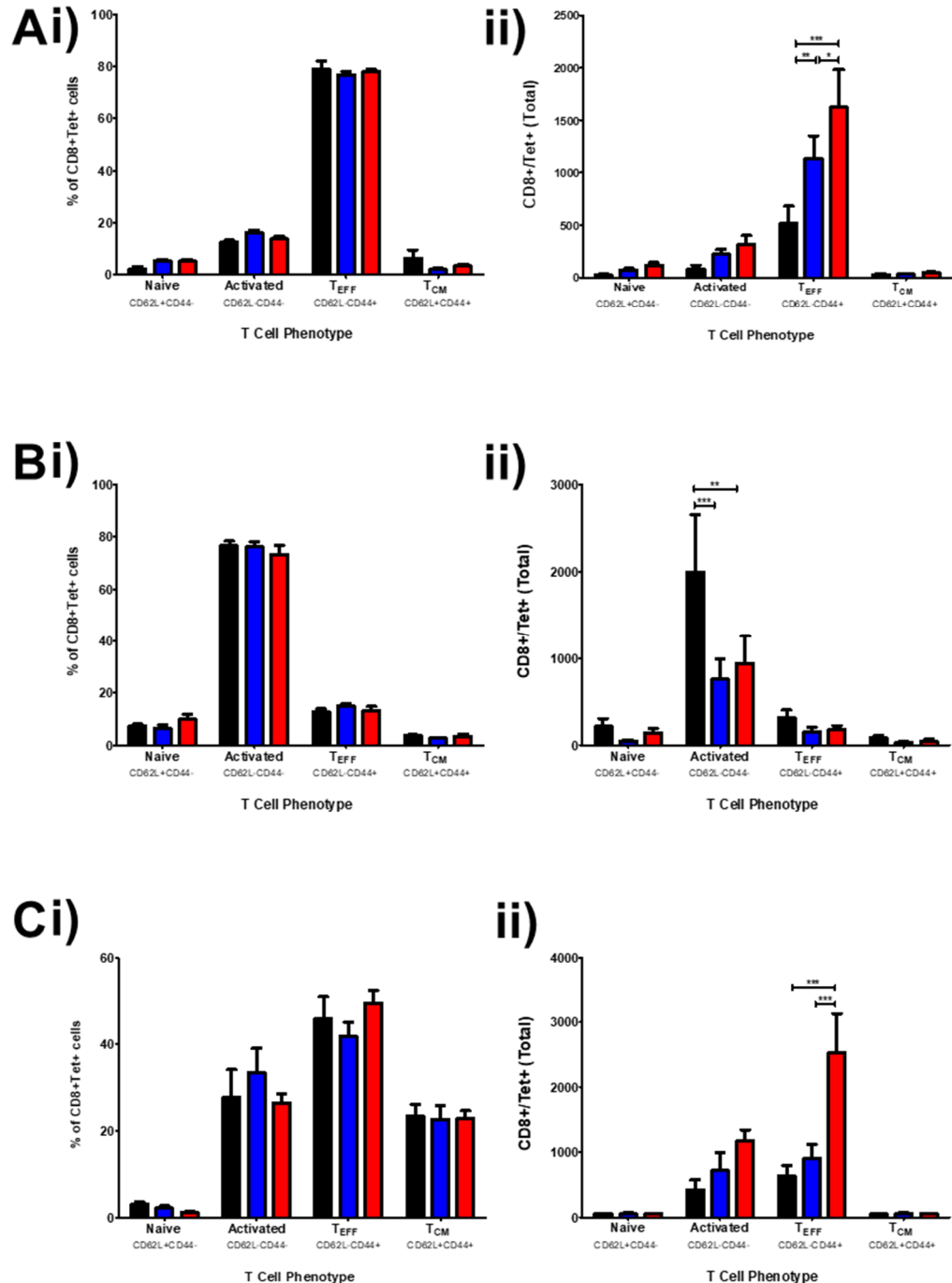
Figure 5.10 - Prior sDC vaccination increases the tumour antigen-specific T cell maturity in the lymphatics.
Mice receiving the B16F10.oca tumours by intravenous injection were assessed for the antigen-specific T cell response in the (**A**) popliteal LN (pLN); (**B**) mesenteric LN (mLN); and (**C**) spleen by flow cytometry. Expression of CD44 and CD62L was used to phenotype the T cells, which were quantified by either percentage of live cells (**i**) or total cell number (**ii**) in each tissue. Data represent mean ± SEM error bars. Statistical analysis was by one-way ANOVA with Bonferroni's Multiple Comparison Test: *P ≤ 0.05, **P ≤ 0.01, ***P ≤ 0.001 (n = 6-8/group).

Antigen-specific T cell phenotype in the lymph nodes and spleen is shown in **Figure 5.10**. The primary phenotype of the cells in the injection site-draining pLN is effector T cells, in agreement with prior DC vaccination in the solid tumour model (**Figure 4.8A**). The sDC-receiving mice had an average of 1623 ±355.8 T cells with a CD62L- CD44+ effector phenotype (**Figure 5.10Aii**). The PBS-receiving mice had only 514 ±167.2 cells, and the uDC-receiving mice had 1129 ±221.3 cells in comparison. There was no difference between any of the other T cell phenotypes in this LN (**Figure 5.10B**). In the spleen, a similar trend was seen to the pLN (**Figure 5.10C**). The sDC group had almost four times more antigen-specific effector T cells compared to the PBS controls (2525 ±603.7 to 633 ±164.5) and three times the number in the uDC group (903 ±210.5). There was a slight increase in the number of activated T cells (CD62L- CD44-) but this does not reach significance. In the mLN, the LN which drains the lungs, there was a higher activated T cell response in the PBS controls than either of the DC-receiving groups (1997 ±657.6 to 753 ±234.8 and 940 ±31.3 for uDC and sDC, respectively).

5.4 Discussion

Control of subcutaneous B16F10.ova tumour growth by sDC injection was shown in **Chapter 4**, so metastatic B16F10.ova tumour growth was assessed to better understand the role the increased T cell response may have in the development of experimental metastasis. After a single sDC injection there was a significant increase in tumour antigen-specific T cell number in both the pLN and spleen compared to controls as seen previously (**Chapter 4**). Similarly, after multiple sDC injections prior to the initiation of metastatic tumour development, there was a significant increase in antigen-specific effector T cells in the pLN and spleen compared to the uDC and PBS controls. This supports the hypothesis that DC vaccination augments the endogenous T cell response suggested in **Chapter 3**, although the extent to which the endogenous response controls the tumour response is uncertain. In comparison to the solid tumour model, T cells in this model didn't reach the final T_{CM} phenotype (**Figure 5.10**). The smaller tumour cell number in the absence of a bulky primary tumour may provide less antigen for endogenous antigen presentation and T cell activation. In mice, the development of T cells to this final memory phenotype appears to be progressive through the three other stages described (naïve, activated, T_{EFF}) so it is possible that the short duration allowed by this model may not allow the full development of the memory phenotype (Sallusto, Geginat and Lanzavecchia, 2004) unlike in **Chapter 4**

which was up to 2 weeks longer in duration. Other groups allow tumour development for longer, up to 21 days post-injection, although by this point there may be pulmonary complications (Overwijk and Restifo, 2001). These data further support the first aim of this project: that by ensuring initial migration of sDCs to the LNs the T cell response can be enhanced.

Despite the induction of a quantifiable antigen-specific response in the pLNs and spleens of sDC-receiving mice, however, a single therapeutic injection or multiple prior injections of DCs was not sufficient to control tumour growth. In both injection strategies, there was no significant difference in the number of metastatic lesions on the surface of the lungs. This disagrees with a number of studies using the B16F10.ova melanoma model which see tumour number decrease (Mac Keon *et al.*, 2015), although care needs to be taken when comparing methodologies and results. There was a difference in internal tumour burden though after a single injection (**Figure 5.3**), confirming that sDC injection can contribute to tumour control even if this is minimal when compared to other studies and may represent an insufficiency in this DC injection strategy. If this decrease in internal tumour burden was similarly seen after multiple DC injections, the lack of a difference in the antigen-specific T cell infiltration seen in the lungs (**Figure 5.9**) could be indicative of alternative mechanisms of tumour rejection, but this would require further experiments. A number of immune cell types including NK cells (Grundy, Zhang and Sentman, 2007) and neutrophils (Jablonska *et al.*, 2010) have been proposed to help control metastatic growth in this model. DCs can activate NK cells *in vivo* (Zobywalski *et al.*, 2007), so this could be a potential anti-tumour mechanism.

Even after multiple sDC injections there was no change in the numbers of antigen-specific T cells within the lung-draining mLN or within the lungs themselves. In this model, although useful to be able to quantify the immune response in an injection-site draining lymph node, it may have been beneficial for tumour control to inject the DCs to a lymphatic branch which can directly access the lungs. When considering the peripheral and central compartments as distinct, it was shown in 2003 that injection of DCs into the periphery, such as subcutaneously, is insufficient to control tumours growing centrally without development of memory T cells within the spleen (Mullins *et al.*, 2003). Although a T cell response was quantifiable within the spleens of the sDC-injected group in these experiments, this was not seen to be fully mature when the phenotype was determined by flow cytometry (**Figure 5.10Ci**). A mature T cell response was seen previously, however, in a model of longer duration (**Figure 4.4 and 4.8**) which may suggest that sDC injection

induces a T cell response but after only 14 days is insufficient to control tumour growth. It is significantly increased compared to uDC injection however, which further addresses the first aim of this project. The prior vaccination strategy was also shown in the solid tumour model to slow tumour growth (**Figure 4.6**), so it was unexpected that no comparable tumour control was seen in this model. This may be attributable to the injection strategy, so using an alternative method of DC injection in this model may clarify the potential benefit of sorting DCs by CCR7 expression. One common alternative is the intravenous injection of DCs. Studies using pre-vaccination with tumour mRNA-loaded, or tumour lysate-loaded, DCs showed efficacy in reducing B16F10.ova melanoma lesions within the lungs, but used multiple intravenous injections instead of subcutaneous as used here (Matheoud *et al.*, 2011; Markov *et al.*, 2015). While intravenously-injected DCs will reach the spleen by circulation in the blood, expression of CCR7 is crucial for effective intrasplenic migration. Previous studies have shown that in the absence of CCR7, endogenous DCs in the spleen fail to migrate to the T cell zone to effectively present antigen and this significantly reduces antigen-specific T cell proliferation (Calabro *et al.*, 2016). Although requiring a different injection strategy, there is some evidence that CCR7-sorted DCs may also be more effective than unsorted DCs in intrasplenic migration.

Antigen selection for loading DC vaccines is another key consideration, particularly in melanoma. Each cancer patient has a cancer specific to themselves, with growing evidence showing variable TAAs between patients in addition to the individual growth and metastatic potential between patients. In melanoma, several well-defined TAAs exist, including the MAGE family of antigens which are melanocyte-specific and frequently used for tumour targeting; however, both primary and metastatic melanomas are associated with hundreds of neoantigens (Lennerz *et al.*, 2005). While these may not represent tumour-driving mutations, they can result in *de novo* protein formation that can act as TAAs. Appropriate antigen selection is required especially if the goal is prevention of metastasis. A clinical trial of metastatic melanoma therapy using DCs showed superior protection using patient-derived tumour cells as a source of antigen (Dillman *et al.*, 2018). Tumour-derived mRNA or tumour cells themselves provide a large pool of potential TAAs and circumvent the need for molecular characterisation of *de novo* produced proteins for peptide synthesis, with experimental evidence showing that even single amino acid changes in proteins can be targeted for tumour control (Castle *et al.*, 2012). While MHC/peptide complexes have short half-lives, limiting the potential presentation of antigen to native T cells by peptide or even lysate-loaded DCs, mRNA-loading extends the duration of antigen availability. This occurs through synthesis of all possible antigenic

proteins by the DCs, including multiple epitopes of the same antigen, and provides an internal source of peptides for further presentation (Schaft, Dörrie and Nettelbeck, 2006). It is possible, therefore, that a stronger and more effective response could be elicited using these methods of antigen loading.

There is a clear variability in development of B16F10.ova metastatic tumour formation in this model. Although it is possible that variability may arise for experimental considerations such as cell aggregation over time before injection, or small differences in individual IV injections, there are other reasons to pursue future experiments with alternative models (Timmons, Cohessy and Wong, 2016). As described previously, the B16F10.ova model is used as an "experimental" melanoma and is not without limitations. Intravenous injection into the tail vein itself is difficult in mice can introduce variability. Over 10 generations of *in vivo* selection in the lungs, the B16F10 clone was selected for metastasis to the lungs, at detriment to MHC class I expression and immunogenicity which makes them difficult to target experimentally (Ishiguro *et al.*, 1996; **Figure 7.6**). An earlier or alternative clone, such as the parental B16F1 or bladder-metastasising B16-BL6, could be used instead. Outwith experimental considerations, there is disagreement over how representative the B16F10 model is of clinical metastatic melanoma. Rapid growth of tumours from cell lines is a poor equivalent to human cancer development, and these models fail to recapitulate the, often significant, existing tumour burden and treatment history in patients with late stage cancers participating in clinical trials (Francia *et al.*, 2011). Introduction of a large number of tumour cells into the bloodstream is highly unlike human metastasis, which is a more gradual (Eyles *et al.*, 2010). Disseminated tumour cells can even become dormant in the secondary tumour site, and the B16 model fails to recapitulate this. Intravenous introduction of these cells also skips important steps in the acquisition of tumour metastatic capability: acquisition of an invasive phenotype, shedding from the primary tumour and escape into the vasculature (Chaffer and Weinberg, 2011). The B16F10 model more closely represents the formation of multiple primary tumours lesions than true metastasis, by definition.

To overcome this, subcutaneous B16F10 tumours could be allowed to develop until the occurrence of spontaneous metastasis, but this would be much less predictable than the metastatic model which is still likely to introduce variability between animals. The 4T1 model of breast cancer has been shown to reliably metastasise within a few months post-injection, so could be a potential alternative to the B16F10 model (Song *et al.*, 2018). Genetically engineered mouse models (GEMMs) can be used to supplement experimental

metastasis models. GEMMs develop metastases through comparable mechanisms to human tumours through alteration of specific genetic pathways, especially those which are relevant in human biology. Mice which are transgenic for the Polyomavirus middle T (PyMT) gene develop spontaneous hyperplasia in the mammary gland, which is very similar to atypical human hyperplasia (Maglione *et al.*, 2001), and progress to metastasis (Siegel, Hardy and Muller, 2000). Tumour-associated genes such as *Brca* and *Pten* can be manipulated to reflect germline BRCA1/2 mutations in metastatic breast and ovarian cancer (Gourley *et al.*, 2010), and abrogation of PTEN in metastatic prostate cancer (Margue *et al.*, 2006). These 'knockdown' models, however, showed limited similarity to the high metastatic potential of the human equivalents. More recent models using tissue-specific genetic alterations may be more viable. For metastatic melanoma in particular, one possibility is a melanocyte-specific expression of a mutated BRAF proto-oncogene combined with PTEN knockout (Dankort *et al.*, 2009). BRAF modification alone did not lead to melanoma progression in this mouse model, but addition of PTEN silencing resulted in melanoma with metastatic lesions and is therefore an attractive spontaneous model for future study. Another advantage of these models is the slow tumour development in association with local stroma and vasculature, which further increases the similarities to human tumours.

5.5 Chapter summary

In **Chapter 4**, it was shown that CCR7-sorted DCs were capable of reducing the rate of subcutaneous melanoma tumour growth, improving survival duration and significantly increasing the anti-tumour T cell repertoire of vaccinated mice. To assess the potential of this anti-tumour response in the development of secondary tumour growth, the B16F10.ova model was used to induce metastatic lesions in the lungs by intravenous injection. Two injection strategies were used to compare the tumour burden following DC injection: one injection at the same time as tumour induction, and two injections prior to tumour induction as a true vaccination strategy. In both cases, CCR7-sorted DCs led to a significantly increased tumour antigen-specific T cell number in the injection site-draining lymph nodes and spleen compared to the unsorted DC control and PBS control groups, which agrees with data presented in **Chapter 4** and supports the first aim of this project. Similarly, cell phenotype was shown to be mostly mature T effector cells although the short duration of this model may limit the full maturation of the T cells combined with the absence of a large antigen source from a solid tumour mass for T cell memory

establishment (Ricupito *et al.*, 2013). In this model, however, there was there was no control of external metastatic lesion growth and only a small reduction in internal lesion growth between the sDC group and the controls after either single or multiple DC injections. There was no difference in the mediastinal T cell response either, suggesting that the subcutaneous DC injection strategy was insufficient to generate a beneficial anti-tumour immune response in this context. In summary, despite a conserved increase in cell migration to the lymph nodes and increase in the anti-tumour T cell response, in the B16F10.ova model, CCR7-sorted DC injection does not result in the reduction in tumour burden compared to the unsorted DC controls.

Chapter 6

Development of CCL19-sorted human dendritic cells for therapy

6.1 Introduction and aims

Dendritic cells are becoming increasingly valuable therapies for cancer and other diseases, but poor *in vivo* migration of the cells could limit their efficacy. The data presented thus far support the use of CCL19-sorting as a methodology for isolating functional BMDCs from non-functional or immature DCs present following the conventional GM-CSF culture method. This protocol resulted in consistent, high-purity sorting of CCR7-expressing DCs using both manual and FACS-based sorting strategies to optimise cell yield and viability to enable their therapeutic use. Expression of CCR7 is a marker of maturity, and CCR7+ cells were shown to also express other markers of maturity such as T cell costimulatory molecules and antigen-presentation machinery. It was then shown that CCR7+ DCs can induce a more mature T cell response *in vitro*, and using this response translates to a decrease in tumour growth and increase in survival in a mouse subcutaneous melanoma model. Improvement in the anti-tumour response is thought to be a combination of improved DC migration to the lymph nodes and mature phenotype, as well as the removal of potential immunosuppressive cells from the injection bolus. Taking these data together, increasing DC migration to the lymph node using CCL19 sorting is a viable and potentially beneficial therapeutic strategy.

Current GMP generation protocols for human monocyte-derived DC production use GM-CSF and IL-4, especially in cancer vaccination. Given the low prevalence of mature endogenous DCs in the blood, CD14+ monocytes, which represent ~10% of PBMCs, are extracted from the donor by apheresis and used as a cellular source in the majority of clinical trials (Constantino *et al.*, 2016). These cells are cultured over 7-10 days, depending on the lab and protocol, in GMP-compliant media supplemented with GM-CSF and IL-4 to make MoDCs (de Vries *et al.*, 2002). CD34+ progenitors from the blood have also been used, and culture with GM-CSF or Flt3-L as well as other cytokines can generate a heterogenous mixture of antigen-presenting cells including MoDCs (Ratzinger *et al.*, 2004). Although most commonly this is done in culture flasks, it has been shown that the entire process is amenable to a closed-bag culture system (Zobywalski *et al.*, 2007; Macke *et al.*, 2010): this is the most GMP-applicable protocol, as it provides enclosure and scalability of the protocol. Isolation of natural DC subsets such as pDCs (Tel *et al.*, 2013) and cDCs (Schreibelt *et al.,* 2014) is a more recent development in DC therapy but is also possible at GMP level.

Maturation protocols also vary but are an extremely important consideration to fully activate cells required for migration, as discussed previously. The most common maturation cocktails used in clinical trials include TNFα, IFNγ, polyI:C, and PGE2 in varying combinations. PolyI:C, a TLR3 agonist (Okada *et al.*, 2011), is normally paired with PGE2 because although PGE2 increases CCR7 expression on DCs it has been shown experimentally to reduce production of inflammatory cytokines such as IL-12p70 which may increase migration to the detriment of T cell stimulation (Lee *et al.*, 2002; Scandella *et al.*, 2002). These maturation cocktails are all suitable for GMP use.

The aim of this Chapter is to develop the CCL19-sorting protocol for human translation in as a GMP process. bCCL19, including the PEGylated variants, are synthesised chemically to high quantity and purity; and are already amenable to GMP use (Le Brocq *et al.*, 2014). As described, all secondary reagents including cytokines and media have been developed by the manufacturers to GMP-grade use. The MACSQuant Tyto is a FACS-based cell sorter being adapted for GMP compliance through single-use sterile cartridges as a closed-system cell sorter. Translation of the CCL19-protocol to the Tyto was first done using BMDCs, before using human MoDCs derived from buffy coats. Sorted MoDCs were analysed for surface phenotype by flow cytometry, and their function was assessed through co-culture with matched donor T cells. The T cell response was then characterised by surface staining for flow cytometry, and assessment of cytokine production after antigen re-challenge.

6.2 Materials and methods

6.2.1 Isolation of PBMCs from buffy coat

Human buffy coats were obtained from the SNBTS under appropriate sample governance and were used as a source of white blood cells. To isolate these cells, the whole blood volume, typically 45-50ml, was first diluted to 200ml in PBS. 50ml Leukosep tubes (Greiner bio-one) were prepared by adding of 15ml of Histopaque (Sigma-Aldrich) and centrifuging the tubes at 1000xg for 1min. The diluted blood was then added to these prepared tubes and was centrifuged at 450xg for 40min to separate the blood layers over the Histopaque gradient. After this, 20ml of the top fraction was removed by pastette, and the remaining volume above the filter was pooled into new Falcon tubes. This collected fraction was washed in PBS and spun down at 350xg for 7min. After this, the supernatant was discarded and the cell pellets pooled as a single buffy coat PBMC sample. The pooled sample was washed in PBS and spun down again before use.

6.2.1.1 CD14+ cell isolation

PBMCs were separated into CD14+ and CD14- cell fractions using anti-CD14 microbeads (Miltenyi Biotec), using a protocol similar to **2.6.2.1**. Briefly, PBMCs were resuspended at 10^7 cells/80µl in cold PEB and stained with anti-CD14 microbeads (20µl/10^7 cells) for 20min at 4ºC. Unlike the previous protocol, anti-CD14 do not require additional staining steps for sorting. After 20min the cells were washed in PEB by centrifugation, resuspended and run through a MACS LS column (Miltenyi Biotec) as described previously. The positive and negative fractions were collected and washed by centrifugation and resuspended in PEB for counting, purity analysis by flow cytometry and further experiments. Pre-sort, positive and negative sorted fractions were routinely assessed for purity of CD14 expression by flow cytometry.

6.2.2 Generation of human dendritic cells (MoDCs)

Human dendritic cells were generated from monocytes present in the purified CD14+ buffy coat PMBCs as described in **6.2.1**, and are known as MoDCs. Monocytes were cultured in 24-well plates at a concentration of $2x10^6$ cells/ml in RPMI supplemented with 5% human AB serum (SNBTS), and 2mM L-glutamine, penicillin (100 U/ml) and streptomycin (100µg/ml) (hRPMI). The medium was additionally supplemented with 50ng/ml recombinant human GM-CSF (Miltenyi Biotec) and 15ng/ml recombinant IL-4 (Miltenyi

Biotec) to induce differentiation of the cells. On days 2 and 4, half of the medium in each well was replaced with fresh hRPMI containing GM-CSF and IL-4. On day 6, immature DCs were loaded with Epstein-Barr Virus (EBV) antigen using the EBV Consensus Peptivator (Miltenyi Biotec) at a concentration of 20µl peptide per 10^7 cells. On day 7, the dendritic cells were matured by the addition of 20µg/ml PolyI:C (Miltenyi Biotec) and 1µg/ml PGE2 (Sigma-Aldrich) to the wells, but the media was not replaced at this time to avoid removing any EBV antigen. The cells were incubated with these cytokines under normal culture conditions for a further 48hr before collection of the cells for further use using TrypLE as described previously.

6.2.3 Generation of short-term human T cell cultures

Human T cells were cultured from the purified CD14- buffy coat PMBCs as described in **6.2.1**. The CD14- fraction was cultured in 24-well plates at a concentration of $2x10^6$ cells/ml in complete hRPMI supplemented with 1µl/ml concanavalin A (ConA) (Sigma-Aldrich) to encourage T cell outgrowth over the other cells present in the CD14- fraction. On day 4, 1ml of medium containing 40U/ml human IL-2 (Miltenyi Biotec) was added to each well to give a final IL-2 concentration of 20U/ml. On day 8, cells were spun down at 300xg for 5min and resuspended in hRPMI containing 20U/ml IL-2 at a concentration of $2x10^6$ cells/ml. These cells were plated overnight, after which they were collected by pipetting for further use.

6.2.4 Chemokine sorting using MACSQuant Tyto

6.2.4.1 Cartridge and sample preparation

To maintain a completely closed-system cell sort, the Tyto uses unique a sorting cartridge, shown in **Figure 6.1**, below.
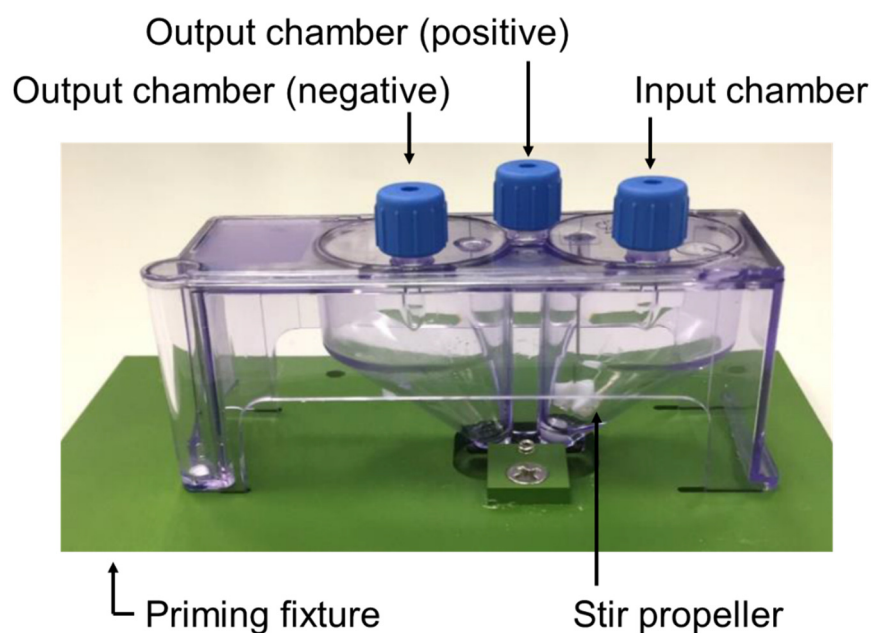
Figure 6.1 - Schematic diagram of the MACSQuant Tyto sorting cartridge.
A visual description of the MACSQuant Tyto cartridge, showing the input/output chambers, the stir propeller in the input chamber and the external priming fixture.

These cartridges are first prepared by loading the cartridge into a priming fixture inside a sterile tissue culture hood and introducing ~500µl of Tyto Running Buffer (Miltenyi Biotec) using a luer lock syringe to cover the stir propeller. After this, sterile air is introduced using a syringe to pressurise the chamber and prime the cartridge filter. Excess running buffer was then removed. MoDCs were stained with CCL19-SAPE as described in **2.6.2** and CD45-VioBlue (Miltenyi Biotec). Cells were resuspended in running buffer at a concentration no higher than 5×10^6 cells/ml in a maximum volume of 10ml (the cartridge limit). The cells were introduced to the input chamber using a luer lock syringe which was attached to the input valve with the plunger removed. Cells were added to the syringe barrel after filtering with a 70µm pre-separation filter (Miltenyi Biotec) and ejected into the chamber by inserting the plunger of the syringe into the barrel.

6.2.4.2 Sorting protocol

The loaded cartridge was inserted into the Tyto by first scanning the cartridge barcode using the barcode scanner peripheral attachment, opening the instrument door, and locking the cartridge in place in slot in the instrument stage within. To set-up the cytometer for the CCL19 sort, the 'trigger' was set to PE fluorophore as this is the defines the target cell population. The cells were initially analysed to set trigger and gating parameters using cell size and expression of CD45 to identify the bulk cell population and exclude debris, and

discrimination of the target cell population using expression of CCR7 by CCL19-SAPE before initialising the sort.

6.2.4.3 Cell retrieval

Cells were retrieved from the cartridge by first removing it from the instrument stage in the Tyto, and then from the cartridge by pipette with gel-loading pipette tips. For chambers with larger volumes, such as the negative output chamber, cells were collected by attached a luer lock syringe to the valve and inverting the cartridge. The positive and negative fractions were washed by centrifugation and routinely enumerated and assessed for cell yield and purity using the MACSQuant. Cells in the positive and negative chambers were kept separate for further analysis by flow cytometry or culture with T cells.

6.2.5 T cell stimulation assay

T cells were generated as described in **6.2.3** and co-cultured with CCR7+ or CCR7- MoDCs from chemokine sorting. The cells were collected as appropriate and mixed at a ratio of 1:25 DCs:T cells in hRPMI supplemented with 20U/ml IL-2 and plated in round-bottomed 96-well tissue culture plates. Cultures were maintained for 10 days and media was replenished as necessary by the replacement of half of the media with fresh hRPMI containing IL-2. Cells were recovered by manual agitation and collection using a pipette, and their phenotype analysed by flow cytometry.

To assess the production of cytokines in response to EBV antigen re-challenge, T cells were recovered from the 10-day culture and resuspended at 5×10^6 cells/well in hRPMI in a 12 well plate. 1μg/ml of the EBV Consensus Peptivator (Miltenyi Biotec) was added to each experimental well, using 2μl/ml of PMA and ionomycin per well for the positive control wells and nothing in negative control wells. Cells were incubated at 37ºC for 2 hours before addition of 1μl/ml of Brefeldin A was added to each well. The cells were then incubated for a further 3 hours. After this, cells were recovered by manual agitation and collection using a pipette and prepared for flow cytometry.

6.2.6 Flow cytometry

6.2.6.1 Flow cytometry staining procedure

Flow cytometry staining for surface markers was performed as described previously in **2.8**.

To assess the production of intracellular cytokine, cells were first stained for surface marker expression as appropriate, before being fixed and permeabilised using cytofix/cytoperm solution (BD Biosciences). Briefly, 500µl of cytofix/cytoperm solution was added to each sample and these were incubated at 4ºC for 20min. After this, samples were washed in perm wash buffer (BD Biosciences), diluted from 10x concentration to 1x in distilled water, and centrifuged at 350xg for 5min. The cells were resuspended in 200µl perm wash buffer and intracellular antibodies were added at dilutions shown in **Table 6.1**. Samples were incubated at 4ºC for 20min before washing and resuspending in PEA buffer for analysis by flow cytometry.

6.2.6.2 Flow cytometry antibodies

Target	Fluorophore	Clone	Dilution (if not 1/200)	Supplier
CD11c	PE	X9-15		BioLegend
CD14	VioBlue	M5E2		BioLegend
CD25	BV421	BC96		BioLegend
CD45Ra	PE-Vio770	T6D11		Miltenyi Biotec
CD45Ro	PerCP-Vio700	UCHL1		Miltenyi Biotec
CD8	VioGreen	BW135/80		Miltenyi Biotec
CD80	FITC	2D10		BioLegend
CD83	PE	HB15e		BioLegend
CD86	APC*	IT2.2		BioLegend
IFNγ	eF450	45.B3	1/50	eBioscience
IL-2	APC*	MQ1-17H12	1/50	BioLegend
MHC class II	FITC	L243		BioLegend
TNFα	PE-Cy7	REA636	1/50	Miltenyi Biotec

Table 6.1 - List of human antibodies used in flow cytometry.
APC* (fluorophore) = allophycocyanin; BV = Brilliant Violet™; FITC = fluorescein; PE = phycoerythrin; PE-Cy = phycoerythrin-cyanine (conjugate)

6.3 Results

6.3.1 Both BMDCs and MoDCs can be sorted using CCL19 on the MACSQuant Tyto

6.3.1.1 BMDC sorting

In this study, BMDCs were readily accessible and were first used to optimise the Tyto sorting protocol before more valuable human samples were used. Purity of the cell sort was first assessed by staining the cells with the CCL19-SAPE conjugate, sorting the cells, and assessing the expression of CCR7 in each of the sort fractions.
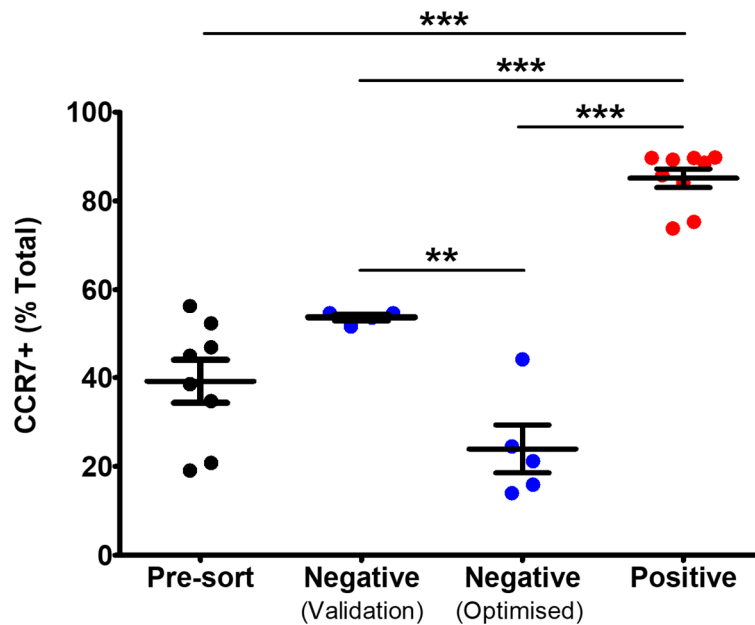
Figure 6.2 - BMDCs can be effectively sorted for CCR7 expression using the MACSQuant Tyto.
BMDCs were sorted using the MACSQuant Tyto and the CCR7 expression of each sort fraction was compared to the initial pre-sort (black) by flow cytometry. The negative fraction (blue) is split into pre- and post-optimised groups, compared to the total positive samples (red). Data points represent mean ± SEM error bars. Statistical analysis was by one-way ANOVA with Bonferroni's Multiple Comparison Test: **P ≤ 0.01, ***P ≤ 0.001 (n = 9/group; negative groups are n = 4 and n = 5/group).

Figure 6.2 shows clearly the ability of the fluorophore to identify and be utilised of the sorting for both BMDCs and MoDCs. With BMDCs, this sorting protocol increased the purity of CCR7 expression from 39.16% (± 4.85%) in the pre-sort fraction, to 85.13% (± 2.11%) with high consistency. The lack of a significant reduction in the negative fraction in the early optimisation (validation), however suggested that although the sorted cells

were ~90% CCR7+, the yield of these cells from the initial sorting population was low. After optimisation of the sorting parameters such as transit time and valve opening frequency there was a significant reduction in percentage of CCR7+ cells in the negative fraction, decreasing from 53.6% (± 0.76%) to 23.94% (± 5.37%). As previously with Aria II sorting, the cell yield and viability were next assessed.
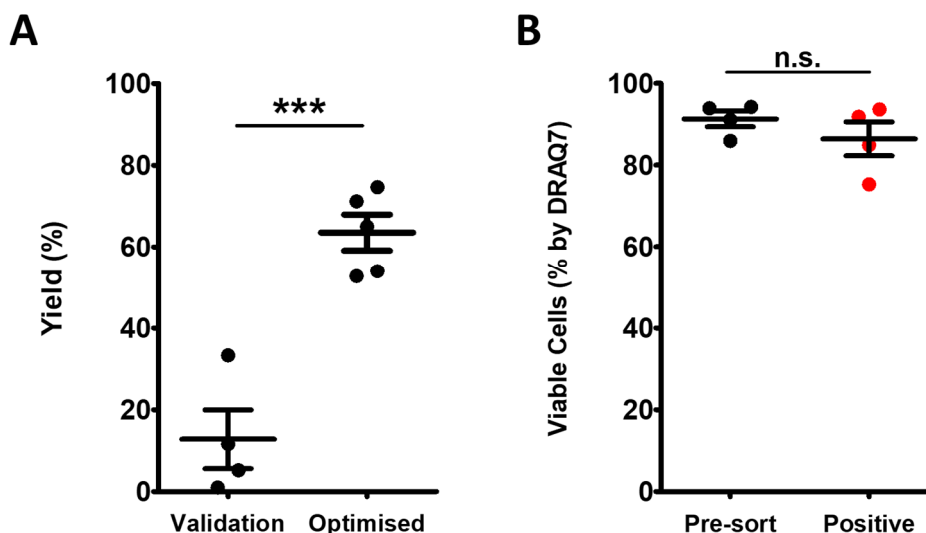
Figure 6.3 - High yield and viability of Tyto-sorted BMDCs using CCL19.
After optimisation of the sorting protocol for the BMDC CCL19-SAPE strategy, there was a difference in (**A**) cell yield (n = 4-5/group) from the total CCR7+ cells in the pre-sort sample, whereas (**B**) cell viability always remained high and was not affected by the sorting protocol (n = 4/group). Data points represent mean ± SEM error bars. Statistical analysis was by unpaired Student's t test: n.s. = non-significant, ***P ≤ 0.001.

Yield of the CCR7+ cells in the positive fraction was shown to be low in the initial cell sorts, as predicted by the lack of depletion of the negative fraction. The initial sorts were all less than 40% yield (12.8% ± 7.18%) but increase significantly to 63.51% (± 4.42%) after optimisation. This approached the cell yield from the Aria II as shown previously (**3.2.3**). Cell viability, in comparison, remained consistently high between the pre-sort and sorted cells. Taken together with viability assessment (**3.2.3**), FACS-based sorting had no immediate effect on the viability of BMDCs.

6.3.1.2 MoDC sorting

Once optimised, the protocol was extended to MoDCs to explore the feasibility of using the Tyto for GMP-like sorting with CCL19-SAPE. MoDCs were generated from buffy

coat-derived monocytes as described above and labelled with CCL19-SAPE for sorting using the update parameters from the BMDC optimisation.
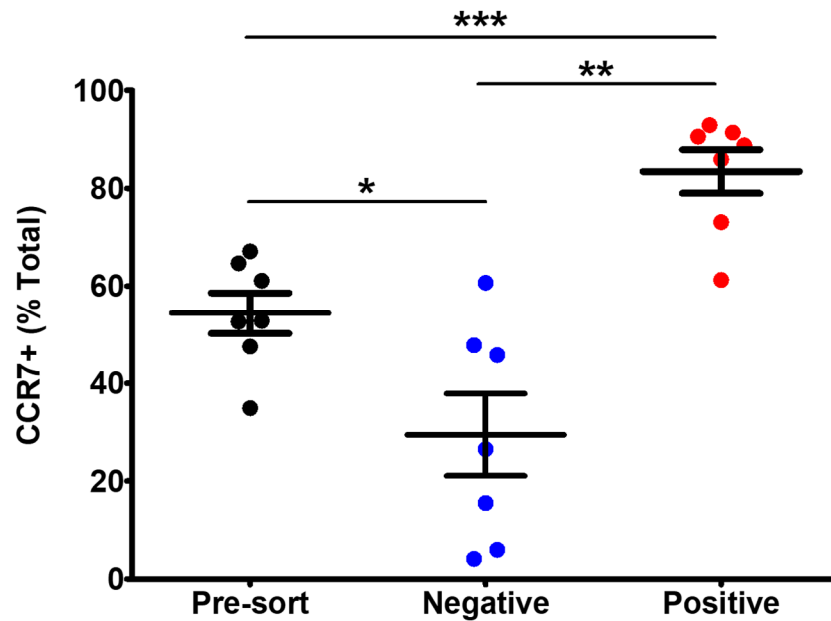
Figure 6.4 - MoDCs can be effectively sorted for CCR7 expression using the MACSQuant Tyto.
MoDCs were sorted using the MACSQuant Tyto and the CCR7 expression of each sort fraction was compared to the initial pre-sort (black) by flow cytometry. The negative fraction (blue) is split into pre- and post-optimised groups, compared to the total positive samples (red). Data points represent mean ± SEM error bars. Statistical analysis was by one-way ANOVA with Bonferroni's Multiple Comparison Test: **P ≤ 0.01, ***P ≤ 0.001 (n = 8/group).

Using the optimised parameters from the BMDC sorts, MoDCs can be sorted for high purity of CCR7 expression using the Tyto (**Figure 6.4**). The pre-sort population were enriched from 54.37% (± 4.2%) to 83.42% (± 4.48%) expression of CCR7, reaching higher than 90% on three occasions. Additionally, as shown previously, there was a significant depletion of the negative fraction which drops to 29.47% (± 8.4%), with three of these samples lower than 10%.
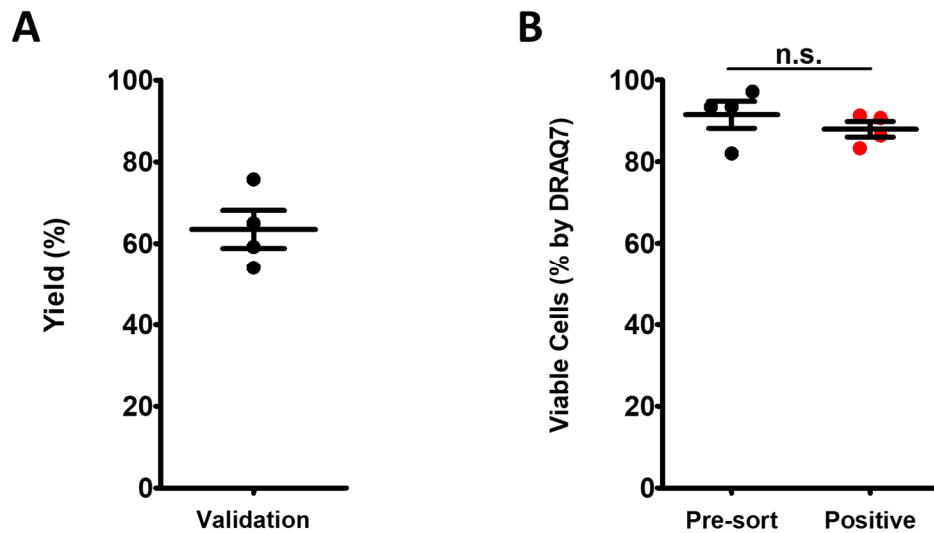
Figure 6.5 - Yield of Tyto-sorted MoDCs is high and cells maintain viability during the protocol.
Using an optimised sorting protocol, MoDCs could be sorted on the Tyto using CCL19 with (**A**) high cell yield from the pre-sort fraction and (**B**) cells remained highly viable after sorting. Data points represent mean ± SEM error bars. Statistical analysis was by unpaired Student's t test: n.s. = non-significant (n = 4/group).

The optimised sorting protocol resulted in a high yield of CCR7+ cells from the pre-sort sample (**Figure 6.5**), which is 63.48% (± 4.67%). Although this was lower than seen with the Aria II (84.7%; **Figure 3.6**), it is comparable and higher than the column yield. There was no decrease in cell viability immediately after the sort (**Figure 6.5B**) by DRAQ7 staining; which was again consistent with previous FACS-based sorting on the Aria II. These data together support the use of the MACSQuant Tyto for adaptation of the CCL19-sorting protocol to a GMP-compliant protocol.

6.3.2 CCL19-sorted MoDCs are phenotypically distinct

Like BMDCs, inflammatory MoDC migration *in vivo* is tightly regulated as a function of cell maturity: MoDCs undergo a distinct shift in chemokine receptor expression and therefore migratory capacity after exposure to antigen and maturation signals such as cytokines. Surface phenotype of CCR7+ and CCR7- MoDCs was analysed after sorting using flow cytometry and compared.
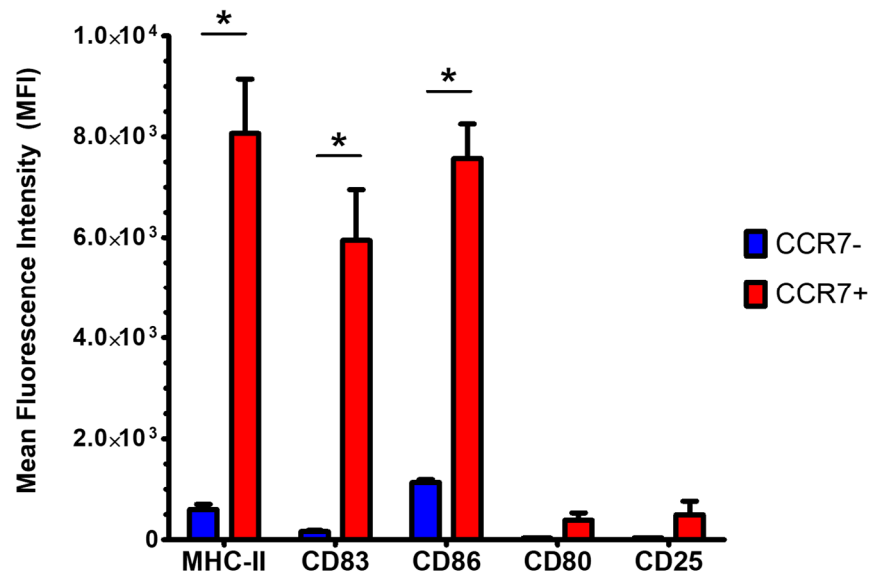
Figure 6.6 - CCR7+ and CCR7- MoDCs are distinct by surface phenotype.
Expression of activated DC markers were significantly enriched in CCR7+ populations (red bars) in comparison to CCR7- populations (blue bars). Statistical analysis was by Students t test. * P ≤ 0.05 (n = 3).

As expected, CCR7+ MoDCs expressed more highly several markers of cell maturity including MHC class II, CD83 and CD86 (**Figure 6.6**); which was consistent with the phenotype of CCR7+ BMDCs (**Figure 3.10**). This data was consistent with characterisation of therapeutic DCs previously described (de Vries *et al.*, 2002), as expected. There was also a small but non-significant increase in expression of CD80 (MFIs: 36 ± 5 to 389.63 ± 145.9) and CD25 (MFIs: 39.33 ± 3.28 to 494 ± 271). CD25 is the IL-2 receptor, and is expressed on DCs maturing in response to PGE2 (von Bergwelt-Baildon *et al.*, 2006). DCs lack the signalling pathways to functionally respond to IL-2 stimulation like T cells do but CD25 expression has been suggested to enhance T cell activation alongside traditional immunogenic markers CD80, CD83 and CD86 (Velten *et al.*, 2007). Although not particularly novel, it was important to again highlight the variability of the GM-CSF and IL-4 culture system and that CCR7-expressing cells within this system were phenotypically distinct in agreement with mouse *in vitro* data.

6.3.3 CCL19-sorted MoDCs induce a distinct T cell phenotype after co-culture

To confirm the function of MoDCs after sorting and compare CCR7- and CCR7+ MoDCs in T cell stimulation, sorted DCs were co-cultured with donor-matched buffy coat T cells. After 10 days of culture, T cells were collected and analysed by flow cytometry.
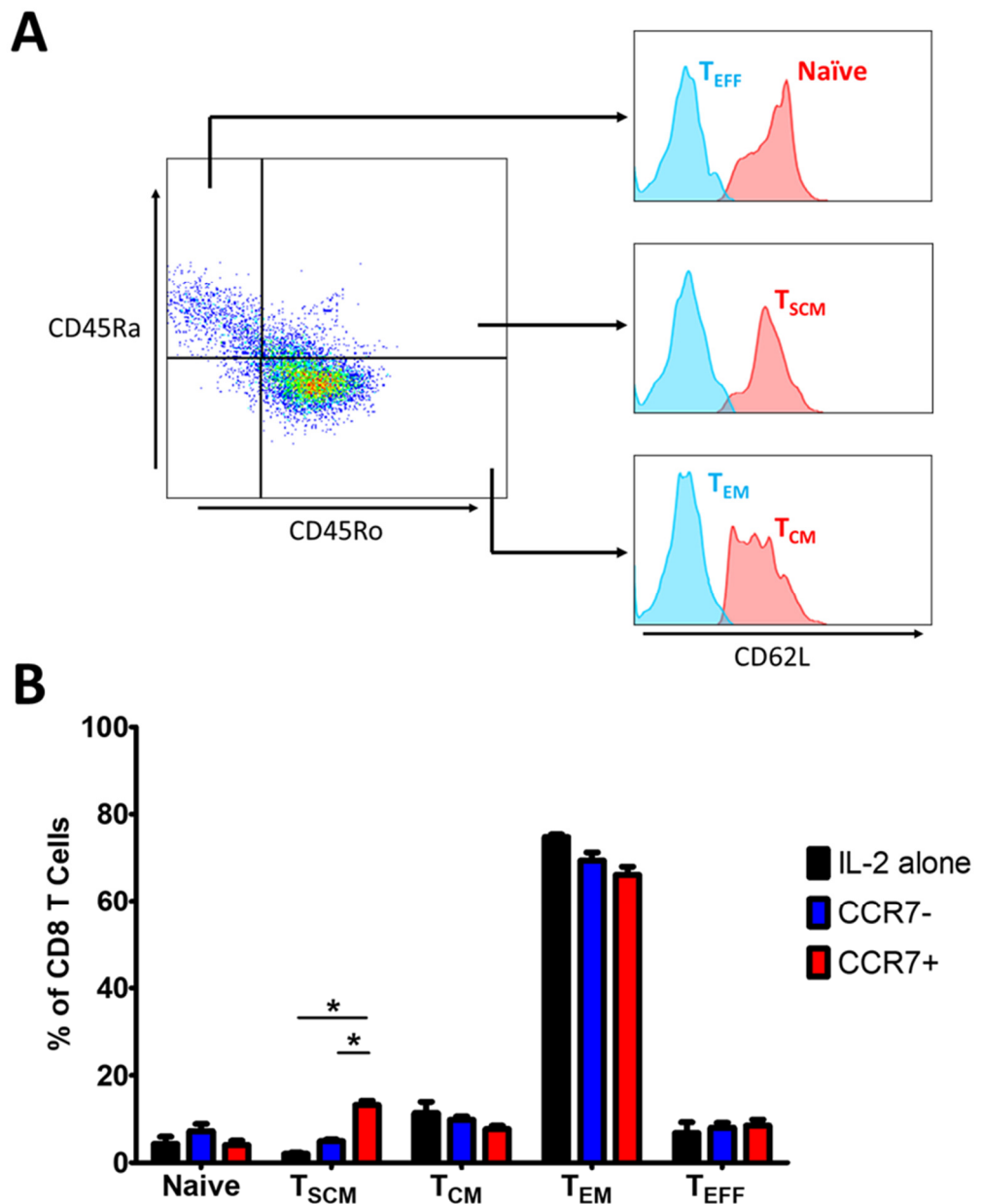
Figure 6.7 - CCR7+ MoDCs stimulate expansion of stem memory T cells but no other subset. (**A**) T cell subset gating strategy. (**B**) After 10 days of culture together, CCR7+ MoDCs (red bars) stimulated more expansion of stem cell memory T cells but did not affect other subsets compared to controls (IL-2 alone – black bars; CCR7- DCs – blue bars). T cells were classified by surface marker expression analysed by flow cytometry. Abbreviations: T_{CM} – central memory T cell; T_{EFF} – effector T cell; T_{EM} – effector memory T cell; T_{SCM} – stem cell memory T cell. Statistical analysis was by Students t test. * P ≤ 0.05 ($n = 3$).

T cells in this experimental set-up showed little stimulation in response to CCR7+ DCs compared to the IL-2 alone control, or CCR7- DCs (**Figure 6.7**). T cell subsets were identified using the surface markers CD45Ra, CD45Ro and CD62L. The common leukocyte antigen in humans, CD45, has two isoforms which can be used to discriminate naïve (CD45Ra) and memory (CD45Ro) T cells (Faint *et al.*, 2001). CD62L, also known as L-selectin, is involved in T cell migration, and shed during the acquisition of lytic,

effector function (Yang *et al.*, 2011). Using these markers, T cell subsets were defined phenotypically as described in **Figure 6.7A**, with increasing differentiation as follows: Naïve, T_{SCM}, T_{CM}, T_{EM}, and T_{EFF}. CD45Ra-CD45Ro- cells were excluded from analysis despite expression of CD8, as these cells could be NK or NK T cells (Baker *et al.*, 2001). Similarly, CD45Ra+CD45Ro+ cells were excluded as they may be a transitional phenotype not accommodated by these defined subsets (Golubovskaya and Wu, 2016). Taking this into consideration, it was seen that CCR7+ MoDCs only increased the proportion of T_{SCM} cells in the culture (13.44% ± 1.29%) compared to CCR7- MoDCs and IL-2 alone (4.94% ± 0.66%, and 2.06% ± 0.22%). No difference in total T cells by cell number was observed, however (data not shown), suggesting that CCR7+ MoDCs are skewing the cell response towards a memory phenotype. There was also no difference in expression of CD28 or CD57 between the groups (data not shown).

To better understand the induction of antigen specific cells, and not the maintenance or induction of T cells by MoDC cytokines alone, T cells were re-challenged with the EBV peptide and assessed for production of three important T cell cytokines: IL-2, IFNγ and TNFα.
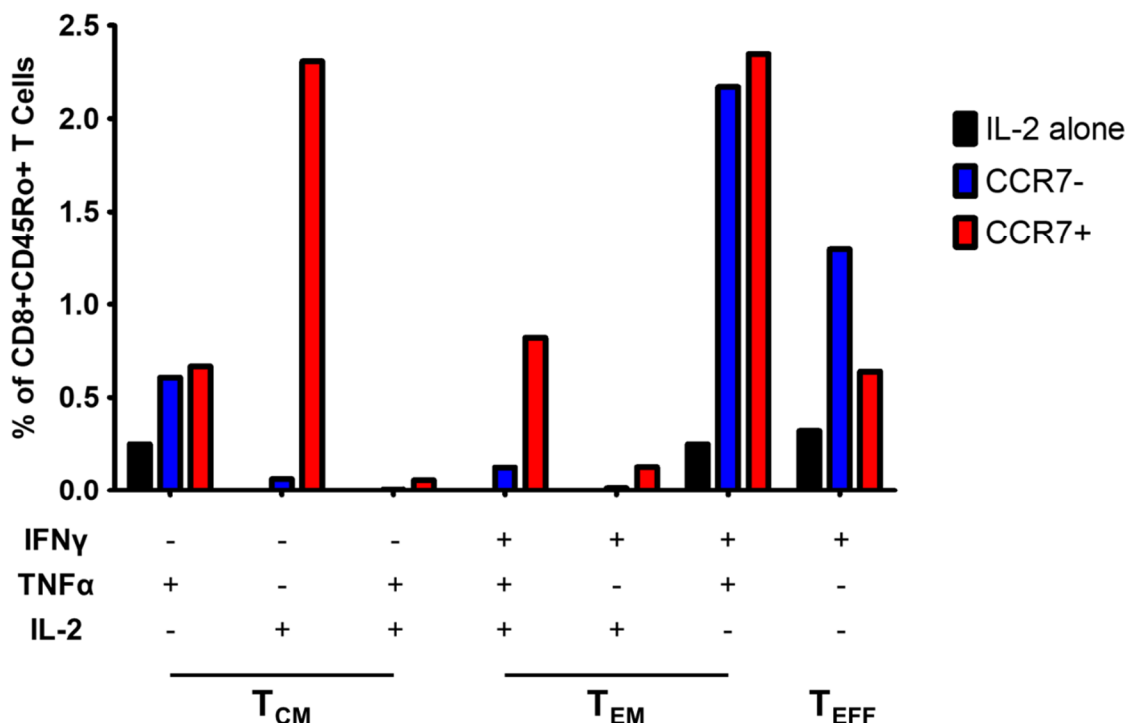
Figure 6.8 - CCR7+ MoDCs induce T cell memory phenotypes by cytokine production.
After 10 days of culture, CCR7+ MoDCs (red bars) stimulated the development of antigen-specific T cells with memory phenotypes compared to CCR7- cells and IL-2 alone. T cells were assessed by intracellular flow cytometry after restimulation with peptide. Abbreviations: T_{CM} – central memory T cell; T_{EFF} – effector T cell; T_{EM} – effector memory T cell (*n* = 1) (Kwak *et al.*, 2013).

Although only one buffy coat donor responded to peptide restimulation detectable above the background response, it was still possible to distinguish different cell phenotypes using cytokine production (**Figure 6.8**). In agreement with earlier surface phenotyping, CCR7+ cells resulted in the stimulation of T_{CM} cells which secrete IL-2, as well as T_{EM} cells secreting all three cytokines. T_{SCM} cytokine phenotype is less well-defined than the other T cell phenotypes, but may be represented here by the IL-2+ cells (Roberto *et al.*, 2015). In contrast, CCR7- cells resulted primarily in the production of more terminal effector cells such as IFNγ+ TNFα+ cells and cells secreting IFNγ+ alone. This agreed with the surface phenotype shown in **Figure 6.7**. Overall this suggests that CCR7+ cells can activate robust antigen-specific memory cell proliferation which may lead to an increased downstream effector response, compared to CCR7- cells which activate only the effector response.

6.4 Discussion

In this Chapter, it was shown that sorting MoDCs by CCR7 expressing using bCCL19 is translatable to a GMP-grade protocol, and results in an inflammatory MoDC population capable of stimulating T cells *in vitro* and induction of a memory response.

Using a GMP-grade protocol, it was possible to sort both BMDCs and MoDCs to high yield and cell purity for expression of CCR7 using bCCL19-sorting as described in **Chapter 3**. Although the MACSQuant Tyto was used for optimisation of this protocol, the adaptation of the protocol for flow-based cell sorting allows the methodology to be broadly applied to other clinical grade cell sorters. It is likely that additional instrument-specific modifications will be required to achieve a consistent high purity and cell viability as shown here with the Tyto system. With these modifications, the protocol presented here is immediately applicable to human delivery if required.

Characterisation of the MoDC phenotype shows that, as seen in BMDCs, CCR7 is expressed on cells along with markers of cell maturity and immunogenicity such as CD80, CD83 and MHC class II. As described previously, enrichment of these cells is beneficial in the induction of a T cell response. In BMDCs, removal of immature, CCR7- cells from the bulk population enhanced T cell maturity after co-culture (**Figure 3.13**). In comparison the CCR7- cells alone produced only immature T cells by surface phenotype and potentially the induction of early cell anergy. Preliminary T cell phenotyping shown here show a similar trend in activation, with CCR7+ MoDCs inducing the production of more mature T

memory cells when compared to CCR7- cells and IL-2 alone. Interestingly, this response was seen in each of the three buffy coats used despite only one of these showing a significant antigen-specific response by cytokine production (**Figure 6.8**). This suggests that in addition to providing strong antigen presentation to cognate T cells, CCR7+ MoDCs may also produce other signals for expansion of the memory response in the absence of direct TCR recognition. Production of cytokines such as IL-15 and IL-2 can support expansion of memory T cells specifically both *in vitro* and *in vivo* (Klebanoff *et al.*, 2004). Previous experimental evidence shows that activated MoDCs can secrete IL-15 in culture (Gorvel, Korenfeld and Tung, 2017), making it possible to promote the expansion of memory T cells in a paracrine manner. It would be interesting to further analyse MoDCs for cytokine production as done with BMDCs in **Chapter 3** to confirm this potential mechanism of T cell stimulation.

Unlike with the OT-1 T cell model used in **Chapter 3**, the prevalence of EBV-responsive people within the human population had to be used to quantify an antigen-specific T cell response in human MoDC/T cell co-cultures. In mice, it is possible to engineer a culture system where almost 100% of T cells are reactive against one antigen, ovalbumin in the OT-1 model, and use this to quantify a bulk response to a stimulus such as ovalbumin-presenting DCs. In humans, the small proportion of circulating EBV-specific T cells had to be used instead, as donor T cells recognise a multiplicity of antigens in comparison. It is expected that 90% of the world's population will have been exposed to EBV by adulthood (Lennon, Crotty and Fenton, 2015); with lifelong, latent infection being maintained by low grade replication after exposure. Using EBV as a model antigen requires careful analysis to not over-interpret observations, so to confirm this finding the T cells were further phenotyped for cytokine secretion to quantify a true antigen-specific response by restimulation with the EBV peptide. As shown in **Figure 6.8**, one buffy coat donor was responsive to the EBV peptide, which was determined by cytokine production above the background of T cells maintained in IL-2 alone. Through analysis of three important T cell cytokines, IFNγ, TNFα and IL-2 it was possible to identify cell phenotypes within the antigen-responding population only (Seder, Darrah and Roederer, 2008).

IFNγ is a potent cytotoxic cytokine, involved in the defence against pathogens and tumour cells alike (Shankaran *et al.*, 2001). Coordinated secretion of IFNγ and TNFα has been shown to increase cytotoxicity (Bogdan *et al.*, 1990); as well as upregulate MHC class I and II on both tumour cells and endogenous APCs (Restifo, Dudley and Rosenberg, 2012). IL-2 production is a determinant of T cell function after exposure to antigen: naïve CD8+

T cells expressing IL-2 is closely associated with the formation of antigen memory, whereas failure to express IL-2 after activation tends the cell towards effector function (Malek and Castro, 2010). IL-2 as a cytokine is an extremely potent T cell growth factor, usually produced by CD4+ T cells, but to a lesser extent CD8+ T cells too. T cell polyfunctionality through production of these three cytokines has been shown to increase efficacy of these cells in an antiviral and antitumour context (Klebanoff, Gattinoni and Restifo, 2006; Precopio *et al.*, 2007). In addition to the superior cytotoxicity of IFNγ and TNFα together compared to IFNγ alone, these T cells also produce more IFNγ per cell which further increases cytotoxicity (Precopio *et al.*, 2007). Production of IL-2 by these cells also promotes the expansion of both effector and memory T cells, supporting further expansion of the antigen-specific T cell response in this context. Analysis of these phenotypes in future buffy coat samples will be vital to ensure reliability and allow accurate statistical analysis, but the initial data are encouraging.

Although preliminary, this analysis supports the expansion of mature, memory T cells by CCR7+ human DCs and not by CCR7- cells. The T_{SCM} phenotype shown by flow cytometry have been characterised *in vivo* as an early memory phenotype, which is highly proliferative and effective in the antitumour defence (Gattinoni *et al.*, 2012). These cells can also give rise to T_{CM} and T_{EM} cells as differentiated progeny, expanding the multifunctional antigen-specific response (Flynn and Gorry, 2014). As described previously, characterisation of T_{SCM} cells by cytokine production is difficult given the production of IFNγ, TNFα and IL-2 transiently in healthy human blood (Roberto *et al.*, 2015). In a number of studies, the generation of more T_{CM} cells by vaccination strategies has shown superior protective immunity (Klebanoff, Gattinoni and Restifo, 2006). In a cancer context, transfer of T_{CM} cells compared to T_{EM} cells has the potential to induce not only an increased effector cell proliferation but to also support the formation of durable antigen memory with correction of the endogenous memory (Kaech, Wherry and Ahmed, 2002). The generation of this response endogenously by vaccination could have the same beneficial effect, in particular the benefit of overcoming endogenous immune suppression as a result of persistent tumour antigen exposure.

6.5 Chapter summary

This Chapter presents data which supports the viability of bCCL19-sorting as a GMP-grade clinical protocol, with immediate clinical applicability. In **Chapter 3** it was shown

that it was possible to sort murine BMDCs for expression of CCR7 using a novel CCL19-sorting strategy (Le Brocq *et al.*, 2014). While originally a magnetic bead-based methodology, incorporation of a fluorophore conjugate into the chemokine tetramer allowed translation of the strategy to FACS using the BD Aria II. In this Chapter, data presented show that the strategy can be further modified to near-GMP compliance by sorting using the MACSQuant Tyto. After optimisation of the sorting parameters, MoDCs generated using GM-CSF and IL-4 were shown to be sorted by expression of CCR7 to greater than 90% purity and a high yield from the initial starting population. Preliminary flow cytometry analysis agreed with previous mouse *in vitro* and *in vivo* data that CCL19-sorted cells had improved surface phenotype, however further phenotyping needs to be done to characterise the CCR7+ MoDC population. Finally, CCR7+ MoDCs were capable of inducing more memory T cells, both by direct antigen presentation but possibly also cytokines, which was assessed by flow cytometry of T cells after co-culture. Function of the T cells was also assessed following antigen restimulation with peptide antigen by intracellular cytokine production, confirming, importantly, that these T cells can produce cytotoxic and immune-enhancing cytokines such as IFNγ, TNFα and IL-2 which are beneficial in a cancer context. Taking these data together, CCL19-sorting of MoDCs is a viable clinical protocol which could have therapeutic benefit in a cancer context.

Chapter 7

General discussion

7.1 Introduction

7.1.1 Dendritic cell therapies

Dendritic cells are the most potent antigen-presenting cell in the immune system, which makes them an attractive cell type for utilising therapeutically. DC therapy is currently a safe and feasible immunotherapy in a number of clinical contexts including cancer. T cells can be used in cancer therapy for their antigen-specificity and cytotoxicity (Rosenberg *et al.*, 2011); DCs can be used to induce this *in vivo* T cell response against a specific target antigen expressed by tumour cells. These antigens can be neoantigens, such as those from genetic changes and resulting in *de novo* protein formation, viral antigens in the case of oncogenic viruses, overexpression of tissue-specific antigens or even the re-expression of developmental proteins not normally subjected to immune control (Bol, Schreibelt, *et al.*, 2016). Although more than 20 years of clinical trial data show that the induction of an immune response is possible, DC therapy still fails to elicit consistent anti-tumour effects which lead to survival in cancer patients. In comparison to the clear effect of alternative immunotherapy approaches such as chimeric antigen receptor (CAR) T cells, the early potential of DC therapy has not yet been realised. However, significant progress has been made in the improvement of DC therapies since the first reported DC clinical trial in 1995 (Mukherji *et al.*, 1995). Three generations of DC therapies have explored a variety of alternative DC sources, methods of delivering of antigens to target the immune response to tumours, 'maturation cocktails' to influence DC phenotype and the resulting immune response, and injection strategies to influence cell migration *in vivo*. Competent migration is integral for DC function, and crucially has been shown to be variable in clinical trials and is therefore only recently becoming adequately addressed in this context as will be described in the following sections.

7.1.2 Source of DCs

Early trials used heterogenous cell populations which included DCs, whether this was the whole mononuclear fraction from patient blood, or culturing DC progenitors. More recent trials have used naturally occurring DC subsets for their specific immune qualities. Each of these cell sources pose different challenges for therapeutic use and have different potential benefits. Culturing DC progenitor cells such as cytokine-mobilised CD34+ bone marrow progenitors or CD14+ monocytic progenitors is desirable because of the large cell number that can be derived from *ex vivo* differentiation (Nestle, 2000). Transcriptomic data, however, distinguishes these cells from 'true' *in vivo* DC populations such as circulating

pDCs and cDCs (Lundberg *et al.*, 2013). The paucity of *in vivo* DCs makes them challenging to use therapeutically, but despite this small circulating cell number both pDCs and cDCs can be isolated in sufficient number for therapeutic use by positive selection for BDCA4 (CD303) expression for pDCs (Tel *et al.*, 2013) or BDCA1 (CD1c) for cDCs (Schreibelt *et al.*, 2016) from patient leukapheresis. Different DC subsets have been trialled primarily to improve the anti-cancer immune response, although it is interesting to note that migration of all of these subsets is strongly dependent on expression of CCR7 (Förster, Davalos-Misslitz and Rot, 2008).

As described in the **Introduction**, upregulation of CCR7 is intrinsic to the process of DC activation. Immature DCs increase expression of CCR7 following uptake of antigen and exposure to local inflammatory stimuli and use this receptor to migrate to the lymph nodes via the lymphatics between 24hr and 48hr (Huang *et al.*, 2001). This change is seen in *ex vivo*-generated DCs as well as cDCs, although heterogeneous CCR7 expression can limit potential migration (Sabado, Balan and Bhardwaj, 2017). pDC migration is slightly different, however. Expression of CCR7 on pDCs has been reported in the steady state, although lower than the other DC cell types, and contributes to lymph node migration without prior antigen exposure (Penna, Sozzani and Adorini, 2001; Seth *et al.*, 2011). Natural and *ex vivo* generated pDCs do also upregulate CCR7 after cytokine and antigen exposure, accompanying upregulation of conventional markers of DC maturity such as CD80 and CD86 (Krug *et al.*, 2002) (**Figure 3.11**). In comparison to the migration of other DCs, which is through tissue and lymphatics to the lymph node, pDCs utilise CCR7 and CD62L to enter the lymph nodes from the circulation through the high endothelial venules (Seth *et al.*, 2011). Taking these studies into account, CCR7 can be used as both a marker of cell maturity and migratory capacity. Isolation of DC expressing CCR7 is therefore a potential benefit for DC therapy regardless of the source of DCs used in clinical trials.

7.1.3 Maturation of DCs

Most DC maturation cocktails focus on strengthening DC-T cell interactions *in vivo,* although there are some used specifically to enhance CCR7 expression. Human MoDC cultures can be supplemented with PGE_2, which increases the expression of CCR7 through prostaglandin receptors leading to downstream cAMP signalling and metalloproteinase activity to further support migration (Scandella *et al.*, 2002). Some early studies suggest that PGE_2 skews the T cell response to DC stimulation to a more regulatory or T_H2 phenotype through suppression of IL-12p70 production, which limits its use as a cancer

therapeutic (Jongmans *et al.*, 2005). IL-12p70 induces CTL development and its production by DC vaccination correlates with increased time to progression and survival (Carreno *et al.*, 2013). The production of IL-12p70 has been shown to be largely recoverable with the addition of other maturation stimuli such as PolyI:C, a TLR3 agonist (Krause *et al.*, 2009). There is evidence supporting the transient nature of CCR7 upregulation, and the suppression of DC CCL19 secretion which attracts naïve T cells within the lymph node (Muthuswamy *et al.*, 2010). Other studies show conflicting evidence of the ability of PGE_2 to enhance T cell proliferation by DCs, and therefore immunogenic function.

In addition to this, the timing of the maturation protocol during *ex vivo* manipulation is important to DC function. In clinical trials, DCs are most commonly matured for between 24 and 48hr to ensure the mature phenotype prior to injection into recipients (Sabado, Balan and Bhardwaj, 2017). This has been shown, however, to have a potentially negative effect on DC function. After the initial maturation stimulus, including cytokine stimulation *in vitro*, there is a complex change over time in the ability of the DC to secrete cytokines which support T cell activation such as IL-2 (Dohnal *et al.*, 2009). While these longer maturation times seen in clinical trials allow maximum cell maturity, and the desirable expression of CCR7 (de Vries, Krooshoop, *et al.*, 2003), this can lead to 'exhaustion' of cytokine production and may be disadvantageous overall (Langenkamp *et al.*, 2000). Upregulation of the CCR7 mRNA has been shown as early as 4hr post-stimulation, and the receptor detectable on the surface as early as 10hr post-stimulation (Sallusto, Palermo, *et al.*, 1999; Jin *et al.*, 2010) The combined use of shorter cytokine stimulation times and isolation of sufficiently matured cells by expression of CCR7 may therefore be beneficial to ensuring and improving DC T cell stimulation. This would also shorten the culture time and cost required for clinical preparation of DCs for therapy in addition to potentially improving efficacy.

7.1.4 Routes of injection

Finally, different injection strategies have be explored to ensure DC migration to the target tissues. Most of these focus on localising DCs within the lymph node for stimulation of T cells, but intra-tumoural injection has been attempted. The rationale for this strategy allows direct tumour sampling by the injected DCs, which can uptake and then present tumour-targeting antigens to T cells either *in situ* or after migration to the draining lymph nodes. Injected DCs would have to then overcome the overwhelmingly immunosuppressive TME

for function (Galluzzi *et al.*, 2012). In practice, this injection strategy is also technically challenging since not all tumours will be easily accessible for direct injection, and if they are accessible, tumour biopsy and *ex vivo* DC preparation may be a more feasible strategy. Other injection routes include subcutaneous, intradermal, intravenous, intralymphatic and intranodal.

Subcutaneous, intradermal or intravenous injection comprise the three most frequently used injection strategies (Constantino *et al.*, 2016). Subcutaneous and intradermal injections both facilitate the access of injected cells to the lymphatic system, allowing natural migration to the lymph nodes after injection (Lappin *et al.*, 1999). This strategy, however, has been shown to limit the number of cells reaching the lymph nodes after injection, which has been reported as less than 5% in cell tracking studies (Verdijk *et al.*, 2009). Compared to intravenous injection strategies, DCs require receptors such as CCR7 for active migration into the lymphatic vessels; as discussed previously, however, CCR7 is not expressed by all cells generated *ex vivo*. Increasing the injected cell number is not a feasible approach, as this can lead to cell death *in situ* and have an effect on the potential generation of the T cell response. Under significant cell influx, LN congestion also prevents the entry of more cells via the lymphatics to protect the LN architecture and the developing immune response (Förster *et al.,* 2012). The use of multiple, smaller doses at different injection sites can potentially overcome these issues (Sabado, Balan and Bhardwaj, 2017), although crucially these cells still require expression of CCR7 for this migration.

Intravenously injected cells, in comparison, are less limited in number than either subcutaneous or intradermal injection, but there is still debate over the migration pattern of IV-injected cells. Most types of DCs used clinically are less capable of LN entry from the blood due to their maturity and downregulation of tissue-homing chemokine receptors (Hauser and Legler, 2016), the exception being pDCs which are fully capable. This leads to sequestering in tissues such as the spleen or non-lymphoid tissues such as the lungs which negatively effects their function (Butterfield, 2013). Biodistribution of mature DCs can influence the immune response, so IV injection may be beneficial if the target is metastatic lesions which can be more effectively controlled by splenic memory T cells than by those resulting from e.g. subcutaneous injection (Mullins *et al.*, 2003). Although natural circulatory flow can direct IV-injected DCs to the spleen, it was shown by Calabro *et al.* that expression of CCR7 is required for intra-splenic migration to the T cell zone for function (Calabro *et al.*, 2016).

In each of these injection routes, CCR7 expression is important for direct migration. Direct injection of DCs into the lymph nodes themselves has been tried to overcome the need for *in vivo* migration, but this technique is technically challenging and may not be performed consistently between patients (Verdijk *et al.*, 2009). Although it was expected to show superior clinical response as a result of the immediate access of injected DCs to T cells within the lymph node, intranodal injection has at best shown comparable efficacy to intradermal injection (Quillien *et al.*, 2005; Lesterhuis *et al.*, 2011). There are some studies, however, which show superior immune responses to intranodally-injected DCs compared to other routes (Bedrosian *et al.*, 2003); although at least highlights the potential for inconsistency between clinical trial centres.

Intradermal injection strategies facilitate the migration of DCs to multiple LNs via lymphatic drainage, while single intranodal injections have not been shown to facilitate this consistently. Potential hydraulic disruption of LN architecture can limit both the immune response and DC migration to adjacent LNs via the lymphatics. The technical complexity of intranodal injection also precludes multiple LN injections (Tel *et al.*, 2013). Taking this into account however, a role for CCR7 expression can still be proposed – both to ensure subsequent migration of the cells to other LNs through the lymphatics, and to isolate the mature population from the immature population which is normally retained at the injection site after intradermal injection and does not reach the lymph node.

7.1.5 Project aims

Using the novel cell sorting methodology first described by Le Brocq *et al.* (2014), the aim of this thesis and the experiments within was to develop CCL19-based DC sorting as a potential improvement for therapeutic applications. The first aim was to show that CCL19 sorting can isolate a mature, migratory DC subset expressing the chemokine receptor CCR7 from a bulk population. The sorted cells should display a more effective lymph node migration. This aim was addressed in **Chapters 3 and 6**. Mouse and human DCs were generated using appropriate, clinically-relevant protocols (human cells), and sorted for CCR7 expression using an optimised chemokine sorting method. These DCs were characterised by flow cytometry for markers of DC maturity, and the production of immune-activating chemokines and cytokines to predict *in vivo* function. Migration of the sorted DCs was also compared to unsorted DCs using transwell migration as well as *in vivo* LN chemotaxis assays. Finally, the antigen-presenting function of these cells was assessed *in vitro* by culturing them with T cells. The second aim was to show that this

sorting protocol alone can improve the generation of an antigen-specific response and as a result improve an anti-tumour response in a mouse model of melanoma. In **Chapters 4 and 5**, the B16F10.ova model was used to determine the potential benefit of CCR7-sorted DCs in the induction of an antigen-specific T cell response in solid tumour growth or metastasis models respectively. To support the translation of this protocol to clinical use and other potential cell therapies, work in **Chapter 6** also adapted the sorting protocol for future GMP compliance.

7.2 CCL19-sorted DCs have improved *in vitro* migration and function

Discovery of novel DC subsets or improved culture conditions has improved *in vivo* DC function and potential efficacy as a cancer immunotherapy, but this efficacy is still limited if DCs do not migrate sufficiently to lymph nodes after injection. As previously discussed, multiple methods have been tested to improve migration to the lymph nodes, where DCs can contact and activate T cells, whether by using an alternative DC subset (Lundberg *et al.*, 2013), adapting the culture methods to increase expression of surface molecules involved in migration such as CCR7 (Krause *et al.*, 2009), or simply by different routes of injection such as directly into the lymphatics or lymph nodes themselves (Lesterhuis *et al.*, 2011). The advantages and disadvantages of these methods have also been discussed.

To allow the data generated during the project to have the widest relevance, the most commonly-used DC generation protocols for mice and humans were chosen. In mouse models, bone marrow progenitors were expanded in *ex vivo* culture with GM-CSF alone, and stimulated using TNFα and LPS (Mac Keon *et al.*, 2015). This culture produced a heterogeneous population of myeloid cells including uncommitted progenitors, macrophages and BMDCs (Helft *et al.*, 2015), which can then be separated by expression of common DC markers such as CD11c but are most commonly used as a bulk population. These cells were characterised and used for experiments in **Chapter 3**. In humans, the majority of DC clinical trials use DCs manipulated *ex vivo*, with most of these developed from CD14+ progenitors using GM-CSF and IL-4 (Constantino *et al.*, 2016). The cells in this study were matured using PolyI:C and PGE$_2$. These cells were characterised and used for experiments discussed in **Chapter 6**. Although many novel protocols exist for improving DC function, these are not easily compared and difficult to standardise within

the current literature. In addition to this, *in vitro* functionality does not necessarily translate to *in vivo* functionality if DCs do not sufficiently migrate to the lymph nodes.

In both **Chapters 3 and 6**, DC generation protocols resulted in at least one population of mature, activated DCs as determined by expression of CCR7, as well as MHC class II, CD86, and CD80 (in mouse) and CD86 (in humans) (de Vries *et al.*, 2002). As shown in **Chapter 3**, DCs can be sorted for expression of CCR7 using both magnetic and flow cytometry-based bCCL19-sorting methods. CCR7+ cells were capable of immediate response to ligand after sorting and show greater migratory capacity to the lymph nodes draining the injection site. Using an unsorted DC population as a control, it was also shown that 10 times more unsorted cells were retained at the injection site than following CCR7+ DC introduction, and only half as many DCs reached the lymph node despite an equivalent cell number being injected. This is clinically relevant for two reasons. Firstly, expression of CCR7 on DCs is indicative of cell migratory capacity, given that only CCR7+ DCs are responsive to its ligand CCL19 both *in vitro* and *in vivo*. This is in agreement with findings by Le Brocq *et al.* in the original literature for this methodology (Le Brocq *et al.*, 2014). Separation of these cells from a bulk population isolated the most capable cells for immediate migration to the lymph nodes. Secondly, the presence of CCR7- cells in the injected population which were retained at the injection site highlights the need to remove these cells from the bulk population. In mice, these cells are macrophages with some immature DCs (**Figure 3.10**), which were shown to actively produce innate-attracting chemokines as well as IL-16 (**Figure 3.12**). Not only did these cells not move to the LNs within their lifespan, limiting their therapeutic function, they may in fact have had a detrimental effect on migration of capable CCR7+ cells by competing for chemotactic signals. This was seen following footpad injection, where after injection of CCR7+ DCs alone there were very few cells still in the footpad at 48hr, but when unsorted cells were injected containing the same number of CCR7+ DCs more than 10 times the number of cells were found in the footpad (**Figure 3.9**).

Retention of cells at the injection site was not thought to be simply due to an excess of cells as other studies have injected up to 5-fold more cells into the footpad with no apparent consequences to the viability of the injected cells *in situ* or in their migration to lymph nodes (Martin-Fontecha *et al.*, 2003). In humans, CCR7- cells are primarily immature DCs which may not undergo subsequent maturation *in vivo* after injection due to tumour suppressing factors. Data presented here show that CCR7- cells produced innate immune-attracting chemokines, which could chemotactically confine DCs to the injection

site and therefore provide some mechanistic insights for retention other than physical constraint and poor cell survival in both mouse models and human clinical conditions (Verdijk *et al.*, 2009). This may provide additional rationale for removal of the CCR7- cell population.

Expression of CCR7 is also a marker of functionally mature DCs, and it was shown that only the CCR7+ DC population was capable of inducing a mature T cell response *in vitro* but not the CCR7- population. Using expression of CD44 and CD62L, it was shown that T cells stimulated by CCR7+ DCs were mature effector T cells and memory T cells, which showed almost no expression of the exhaustion marker PD-1 (**Figure 3.13**). In comparison, although the CCR7- cell population could stimulate T cells, these cells were primarily activated naïve T cells. The few mature T cells present in the CCR7- DC culture also expressed PD-1 as highly as the T cells stimulated with IL-2 alone, suggesting the activation of these cells without the development of memory observed in the CCR7+ cell culture. These data are consistent between DCs generated by both GM-CSF, and Flt3-L suggesting that *in vitro* expression of CCR7 on the cells, regardless of ontogeny, leads to the development of a more clinically relevant T cell phenotype.

The benefit of DC therapy in comparison to other immunotherapies is the potential for both priming naïve T cell development as well as restimulating chronically activated and functionally inactive memory T cells (Klebanoff, Gattinoni and Restifo, 2012). Newly formed naïve and memory T cells generate CTLs, which are directly anti-tumourigenic (Palucka and Banchereau, 2013). These cell types were both produced *in vitro* only in response to CCR7-expressing DCs, suggesting that these cells might produce this desirable immune phenotype *in vivo*. Reactivation of endogenous memory T cell function is not assessable in the murine system, however, since freshly isolated T cells have not yet encountered the model antigen in this system so as a result have no existing memory of the antigen. In a human system, this can be assessed using EBV as a model antigen. Exposure to EBV is expected in up to 90% of the population, and as is associated with a prolonged latent infection and development of an immune memory against the antigen (Lennon, Crotty and Fenton, 2015). In **Chapter 6**, MoDCs presenting the EBV peptide were co-cultured with T cells from 3 individual buffy coat donors to replicate the murine culture system. Although only one donor was reactive to the EBV antigen, expansion of a central memory T cell secreting IL-2 and an effector memory T cell secreting IFNγ, TNFα and IL-2 was noted in response to the CCR7+ DCs alone (**Figure 6.8**). The generation of T cells expressing these three cytokines may confer superior cytotoxicity in an antitumour context,

as suggested by previous studies (Klebanoff, Gattinoni and Restifo, 2006). Taking care to not over-extrapolate the data, there is some evidence that CCR7+ DCs can therefore lead to expansion of therapeutically desirable T cell phenotypes, although it is clear that more replicates would be required for confirmation.

Taking these *in vitro* data together, it has been shown that isolating CCR7-expressing DCs from a mixed culture was beneficial to both DC migration and functional activation of T cells. In confirmation of previous literature, CCR7+ DCs migrated more effectively to CCL19 *in vitro* as well as to the popliteal LN following footpad injection than cells lacking expression of the receptor. The CCR7- cells in the injection bolus were shown by flow cytometry to comprise immature progenitors, macrophages and immature DCs, and using Luminex analysis were shown to produce large amounts of innate immune cell-attracting chemokines which could cause an unwanted inflammatory effect or and led to retention of cells at the injection site. In addition to this, *in vitro* data suggest that these cells do interact with T cells. This has also been reported from *in vivo* studies (Helft *et al.*, 2015). Combined immune stimulation data from mouse and human studies highlighted the production of CTLs and memory T cells to *de novo* antigens, as well as the reactivation of memory T cells in a recall response by CCR7+ DCs but not CCR7- cells. Both of these qualities are described as the 'ideal' T cell response to immunotherapy (Palucka and Banchereau, 2013). In a cancer context, CTL generation is required for efficient rejection of the primary or secondary tumours (Durgeau *et al.*, 2018). Memory T cells both support CTL function and provide a prolonged antigen-specific response to control occult metastases which may develop later in life (Klebanoff *et al.*, 2005). These data, therefore, show that CCL19-sorted DCs would have several benefits in a tumour context.

7.3 CCL19-sorted DCs can improve the anti-tumour T cell response in the B16F10.ova model

7.3.1 Solid tumour model

The B16F10.ova model was used in this project to assess the effect of improving therapeutic DC migration on the anti-tumour immune response using single or multiple injection strategies in both solid and metastatic tumour development. The solid tumour model, in which tumour cells were subcutaneously introduced into the flank, is a widely used model for the study of novel therapies; although it doesn't mimic the slow growth seen in many types of cancer (Mac Keon *et al.*, 2015). In control animals, there is a

detectable tumour antigen (anti-ova) response primarily in the tumour-draining lymph nodes (**Figure 4.3A**, **4.7A**, **4.11A**). Similarly to human tumour data, tumour-specific T cells exist in the tumours, lymph nodes and circulation but do not sufficiently control tumour growth. This may be due to the immunosuppressive pressures of the TME in the human context - whether this is inhibiting their cytotoxicity or triggering cellular exhaustion (Thommen and Schumacher, 2018). After injection with CCL19-sorted DCs but not unsorted DCs, a significant increase in the development of antigen-specific T cells in both the injection-site draining lymph nodes and the spleen was seen suggesting a robust T cell stimulation by the sorted cells. Between 2 and 3-fold more T cells were seen in these tissues compared to the either the control or unsorted DC-receiving animals. This T cell expansion was also consistent regardless of the injection strategy: a single DC injection, or a second prior to or after tumour initiation. In the human setting this replicates quite well the development of a *de novo* response to a novel antigen (Butterfield, 2013). Early proof-of-principle studies have shown that DCs can elicit *de novo* antigen-specific responses to a number of melanoma-associated antigens such as gp100 and MAGE-3, even in late-stage patients (Schuler-Thurner *et al.*, 2000; Banchereau *et al.*, 2001). This is supported by numerous later studies showing inducible responses to neoantigens presented by DCs (Carreno *et al.*, 2015).

After injection of unsorted DCs into the footpad there was no difference in immune response compared to the untreated controls, despite both the sDC and uDC-receiving mice having the same total number of CCR7-expressing cells in the injection bolus. It was shown in **Chapter 3** that these cells can reach the LNs, but may fail to reach the threshold required for T cell activation (Kaech, Wherry and Ahmed, 2002). Taking these data together again confirms the first aim of the project that CCL19-sorting of DCs can improve their migration to the lymph nodes and induction of a T cell response *in vitro*. Despite injection of the same number of CCR7-expressing cells, the number of DCs reaching the injection site-draining LNs was not the same following injection of sorted or unsorted cells. In each of the injection strategies, injection of CCL19-sorted cells strongly supported the development of new naïve and memory T cells in the injection site-draining lymph nodes and spleen. Consistent with *in vitro* data presented in **Chapter 3**, these T cells were both naïve antigen-specific T cells and central memory T cells as determined using CD44/CD62L discrimination. Additionally, a second injection of DCs prior to induction of the tumour growth resulted in a largely effector T cell response, suggesting the expansion of an initial memory population (Palucka and Banchereau, 2013).

In both the single injection, and double pre-tumour injection 'booster' strategy, it was seen that injection of CCR7+ cells slowed the tumour growth rate and increased survival of the animals. Tumours did still reach the maximum tumour size. One mechanism of tumour escape from the immune system is downregulation of antigen presentation machinery or antigen shedding under immune pressure (Schreiber, Old and Smyth, 2011). It would be interesting to assess the antigen presentation of the tumour cells at the tumour end-point to see if any differences were seen in the mice receiving CCL19-sorted DCs compared to the control groups. Use of multiple TAAs, through tumour mRNA or lysate loading, has been shown to provide a more comprehensive anti-tumour T cell response (Garg, Vara Perez, *et al.*, 2017) and prevent, for example, the survival of tumour cells which have lost surface expression of ovalbumin being used for tumour targeting (Neller, López and Schmidt, 2008). This strategy has been shown to be feasible and effective in a number of clinical trials for cancers such as melanoma (Redman *et al.*, 2008). When the second injection was given after the tumour development, however, no benefit in slowing tumour progression was seen (**Figure 4.10**) despite the strong induction of the same T cell distribution and phenotype seen previously. This is striking since almost all clinical trials using DCs utilise multiple injections to sustain the T cell response to reach clinical efficacy (Santos and Butterfield, 2018). Introduction of 1 or 2 injections of CCL19-sorted DCs prior to tumour development are both efficacious, but data here suggest that further DC injections after tumour development are not, despite an equivalent induction of T cell response in the injection-site draining lymph nodes and a higher number of antigen-specific T cells in the spleen.

The second injection of DCs was closer to the first than is commonly seen in clinical trials, which are more likely to be 2 weeks or even months apart (Constantino *et al.*, 2016). Injections in proximity to the same lymph node have also been shown experimentally to be detrimental to prevention of tumour growth in the B16 model (Ricupito *et al.*, 2013) when the transplantation of the tumour itself can be considered an adjuvant to the generation of an anti-tumour immune response. Given that there is a quantifiable T cell response in the lymph nodes and the spleen, it could be possible that diverting the T cell response to an LN uninvolved in the tumour response allows early development of the early tumour, after which it is less susceptible to CTL control. This hypothesis is supported by early data from studies using this model (Brown *et al.*, 2001). Stimulation of Treg generation by CD8+ T cells is another important possible mechanism for this unexpected detrimental effect of repeated T cell stimulation (Spranger *et al.*, 2013). In summary the solid tumour model did

provide insights into the potential superiority of CCL19-sorted DCs which is applicable to a number of clinical tumour contexts.

7.3.2 Metastatic tumour model

In comparison to the subcutaneous model, there was no significant effect on the development of experimental metastasis after single or multiple DC injections. Treatment of metastasis is a major focus of novel cancer therapies as it represents up to 90% of cancer mortality depending on the type of cancer (Chaffer and Weinberg, 2011). In this project, the B16F10.ova model was used to induce 'experimental' metastatic lesions by intravenous injection. DC injection was given once or twice prior to induction of tumour formation, and the effect on metastatic development was assessed. In contrast to the solid tumour model, neither DC injection strategy had any significant effect on the number of lesions in the lungs of recipient mice compared to the controls. After a single injection of DCs, there were significantly fewer internal tumours within the lungs which may suggest a non-T cell-mediated immune control of these tumours when taken together with the T cell data. These data were surprising given the wealth of clinical trial data showing efficacy in delaying metastasis as measured by overall survival particularly in melanoma (Bol *et al.*, 2014; Alvarez-Dominguez *et al.*, 2017; Dillman *et al.*, 2018).

Similarly to the solid tumour model, however, antigen-specific T cells were quantifiable in the injection-site draining lymph nodes and in the spleen; although this was not observed in the tumour-bearing lungs themselves. This is partially agrees with clinical trial data for metastases, in which patients receiving DCs had a measurable induction of antigen-specific T cells (Lim *et al.*, 2007). T cell phenotyping was only done in the two-injection experiment, but the phenotype agreed with previous data from the same strategy in the solid tumour model. The injection-site draining lymph node and spleen both showed primarily an effector T cell response, but a very small number of memory T cells (**Figure 5.10A**). The shorter experimental duration may be the cause of this, as murine T cells develop sequentially through these stages of maturity (Sallusto, Geginat and Lanzavecchia, 2004)

In addition to the considerations discussed in the previous section such as antigen selection and tumour-derived immune suppression, route of injection potentially contributes to the subclinical response observed in this model. For direct analysis of the draining lymph node T cell population, the popliteal LN-draining footpad injection strategy was again

performed. As part of the peripheral lymphatics, migration of DCs to the popliteal LN may not allow T cells access to the central compartment which drains the lungs (Mullins *et al.*, 2003). Intravenous injection of DCs is commonly used in this model and has been shown to induce protective T cell immunity against metastatic B16F10 challenge (Matheoud *et al.*, 2011; Markov *et al.*, 2015), so appropriate alternative injection strategies would be worth pursuing to confirm the potential for clinical efficacy. Most DCs arrive in the spleen following IV-injection by the circulation without the need for active chemotaxis, but previous studies support a role for CCR7 in correct positioning within the spleen for T cell stimulation (Calabro *et al.*, 2016). As discussed previously, CCL19-sorted DCs may still be superior in this case, but this would need to be addressed in future experiments.

7.3.3 B16F10.ova as a model of human cancer development

Human tumours develop through three immune phases, distinguishable by the characteristics of the tumour cells themselves and by their interaction with the host immune system: these are the elimination, equilibrium and escape phases. These stages were described in more detail in the **Introduction** but are relevant here to understand the role of T cells and the relevance of the DC therapy in this project. In the elimination phase, T cells and other immune cells can effectively control tumour growth through endogenous cytotoxicity mechanisms. This phase is difficult to observe in humans, but is supported by prevalence of tumour-specific T cells at clinical presentation as well as experimental mouse models in which cancer development can be induced (Vesely *et al.*, 2011). Immune pressure alone can prevent this small initial lesion from developing further, but failure in control at this phase leads to further growth into tumour equilibrium. In this phase, proposed to be the longest stage due to slow proliferation, tumour cells continue to be subjected to immune pressure but undergo the process of editing and acquisition of the hallmarks of cancer as proposed by Hanahan and Weinberg (Hanahan and Weinberg, 2011). The adaptive immune system is primarily responsible for restricting tumour growth during this phase as shown by experimental suppression of CD8 and CD4 T cells in a model of chemical carcinogenesis (Koebel *et al.*, 2007).

Under constant immune selection pressure, an evolution occurs in the presentation of antigen by tumour cells, presentation of antigen through MHC class I molecules is downregulated, or cells with less immunogenic antigens are selected for (Dunn *et al.*, 2002). Through the acquisition of further mutations and development of an immunosuppressive TME, tumours progress to the escape phase (Schreiber, Old and

Smyth, 2011). As a result, tumour growth becomes uncontrolled and leads to the presentation of detectable tumour masses and often, clinical presentation and diagnosis. By production of TGF-β or IDO, for example, or the upregulation of PD-1 expression, the tumours can directly suppress the function of T cells, even those introduced therapeutically (Vesely *et al.*, 2011). The control of the T cell response is crucial to each of these phases and understanding of these mechanisms in both the murine model and human setting is important. Experimental murine models of tumour development are useful but not completely indicative of tumour development in the human clinical setting. The B16F10.ova model used in this project is a murine melanoma transduced to express the 'neoantigen' ovalbumin. T cells generated *in vivo* in response to this tumour developing have not been subjected to the same thymic selection pressures which a human T cell might have been in the same context (Mac Keon *et al.*, 2015). The tumour model also does not mimic the slow tumour growth seen in many types of cancer, with an extremely quick growth to the maximum size between 15 and 20 days post-transplant (Overwijk and Restifo, 2001). In the three-stage model of tumour development, the B16F10.ova model therefore reflects the initial elimination phase and progresses rapidly to the uncontrolled growth escape phase.

To assess the T cell response in the absence of tumour-intrinsic suppressive mechanisms, DC injections were given prior to tumour development in both the solid (**Chapter 4**) and metastatic (**Chapter 5**) B16F10.ova model. It is likely, therefore, that T cells produced by CCL19-sorted DCs used here augment the natural anti-tumour response. This is apparent from the differences in solid tumour growth at the earliest detectable stage, where mice receiving CCL19-sorted cells showed significantly smaller subcutaneous tumours than either control group. Since no further DC injections were given in these dosing strategies, T cells induced by the DC injections have a similar function to those in the elimination phase when the tumour immunosuppressive mechanisms have not yet developed. Clinical use of DCs in patients at high risk of metastatic tumour occurrence has been shown to be up to 3 times more effective in the induction of an immune response compared to those with active metastatic disease (Bol, Aarntzen, *et al.*, 2016). *In vitro*, or immediately after injection, B16 cells do not express common immune suppressive mechanisms such as IDO or PD-L1 but these do increase with increasing CD8+ T cell infiltration into the tumour mass (Spranger *et al.*, 2013). This is indicative of the tumour escape phase, as described previously. Given the rapid progression of the tumour to this stage it is technically challenging to assess DC function in this context, although it would be more clinically viable. It has been shown by meta-analyses of clinical data that increasing tumour volume

negatively correlates with the success of immunotherapeutic approaches (Gulley, Madan and Schlom, 2011).

The increased magnitude of the T cell response, both in the production of antigen-specific T cells and the development of antigen memory, was shown in these experiments to prolong animal survival in the solid tumour model, although it did not prevent tumour growth. Without a timepoint earlier in the tumour development, such as 1 or 2 weeks post-transplant, it is difficult to suggest a reason for this other than T cell insufficiency against the rapidly growing tumour. Since it can be seen that sorted DC-receiving mice still have significantly more antigen-specific T cells at the maximum tumour growth (**Figure 4.3, 4.7, 4.11**), the hypothesis is that at this point the tumour milieu is actively suppressing T cell function (Fransen, Arens and Melief, 2013). This is consistent with the significant number of antigen-specific T cells present in the tumour-draining lymph node in the control mice which have no apparent effect on the progression of tumour growth . To clarify this, profiling the tumour for expression of IDO or PD-L1 (Spranger *et al.*, 2013), or other more general immune suppressors such as TGF-β or vascular endothelial growth factor (VEGF) known to be important in the B16 melanoma model (Courau *et al.*, 2016), may help clarify the mechanism of suppression to allow therapeutic manipulation. Future tumour models could explore the immune response earlier in the tumour development to assess the effect of CCL19-sorted DC therapy at earlier stages in the tumour progression, and correlate this with progression of the tumour between the elimination, equilibrium and escape phases.

Taking this into consideration, these *in vivo* data may not fully recapitulate the human cancer context and it would be important to fully characterize the response to CCL19-sorted DCs in a more clinically relevant model. Other mouse models of tumour development may lead to mechanistic insights into the development of an immune response following DC injection, and how the suppressive tumour milieu interacts with this immune response. As described in **Chapter 5**, a number of alternative models exist which could better replicate the human cancer context. The ideal model would consist of a primary tumour which can be treated with the DC therapy at this stage but could continue on to develop metastatic lesions which could also be used to assess DC function. Our current *in vivo* data support the development of a supplemented primary immune response, which could be relevant in a human context using tumour neoantigens or whole tumour lysates to target antigens more poorly expressed by the primary tumour or expressed by occult metastatic lesions (Dillman, 2017).

7.3.4 Combination therapies using CCL19-sorted DCs are a potential future strategy to increase therapeutic efficacy

Although DC function and migration to lymph nodes is crucial to the improvement of DCs as a cell therapy for cancer, in many of these contexts the subversion of the immune system by the tumour still limits the therapeutic T cell response induced. The combination of DC vaccination with chemotherapy may seem counterintuitive given the leuko-depletive effect of many chemotherapeutic agents but has been shown to improve survival in a number of clinical trials. Cytotoxic regimens using chemotherapy such as the alkylating agent, dacarbazine or an antimetabolite such as methotrexate can have beneficial effects in this context, releasing tumour antigens from dying tumour cells and increasing their expression of danger signals and deletion of immune suppressing immune cells such as Tregs within the TME (Butterfield, 2013; Bracci *et al.*, 2014). Use of these regimens in combination with DC therapy is becoming more common, defined as a chemoimmunotherapy (Anguille *et al.*, 2014). As a standard-of-care treatment, many patients enter into DC clinical trials having previously undergone chemotherapy, and those undergoing next generation trials are already being treated with the combination of therapies (Garg, Vara Perez, *et al.*, 2017). A similar chemotherapeutic approach could be used in future animal models to assess the benefit of CCL19-sorted DCs in this more clinically-relevant context.

T cell suppressive mechanisms are highly involved in late stage cancer and further limit the efficacy of adoptively transferred T cells and DC therapies alike. Future advances in the immunotherapeutic approach may, therefore, require blocking these pathways to ensure consistent T cell activation. CTLA-4 was one of the original targets chosen for this use in metastatic melanoma using the monoclonal antibody Ipilimumab (Hodi *et al.*, 2010). CTLA-4 is expressed by T cells, is structurally similar to CD28 and binds the same ligands; CTLA-4, however, acts as an agonist to CD28 and prevents its signaling during TCR engagement, and suppresses T cell activation (Teft, Kirchhof and Madrenas, 2006). Increased expression of CTLA-4 occurs on T cells following frequent TCR stimulation, and functionally limits T cell proliferation (Melero *et al.*, 2007). Conversely this is desirable in cancer, reactivating the exhausted tumour-specific T cell response and allowing recovery of cytotoxicity (O'Day, Hamid and Urba, 2007). Prolonging the T cell response by combination therapy of CCL19-sorted DCs with anti-CTLA-4 antibodies is therefore a viable treatment strategy and ensures that the threshold of T cell responses is consistently reached. Interestingly, in early use of anti-CTLA-4 antibodies in poorly

immunogenic tumour contexts, prior vaccination strategies, including using DCs, were required for maximum efficacy (Chambers *et al.*, 2001). This regimen has been tested in several small clinical trials, showing that the combination of anti-CTLA-4 antibodies and DCs lead to CR in 20% of the treated patients and PR in 18% compared to matched control patients, with anti-tumour T cells detectable in the peripheral blood (Ribas *et al.*, 2009; Wilgenhof *et al.*, 2016). Another mechanism for T cell suppression discussed in the previous section is expression of PD-L1 by tumour cells, which interacts with PD-1 on T cells to inactivate them (Zarour, 2016). Blockage of PD-1 on T cells (Brahmer *et al.*, 2012), or PD-L1 on the tumour cells (Brahmer *et al.*, 2012) using specific monoclonal antibodies are similarly viable strategies to CTLA-4 blockade. A number of clinical trials using either anti-PD-1 or anti-PD-L1 antibodies in combination with DC therapies are currently recruiting (Bol, Schreibelt, *et al.*, 2016). As PD-1 has been shown to be expressed by B16F10 tumour cells, blocking this T cell checkpoint may be of benefit in this model in both the control and CCL19-sorted DC-receiving animals which have a robust but non-functional T cell repertoire. The combination of both anti-CTLA-4 and anti-PD-1 antibodies has been used successfully in the B16 model and resulted in expansion of antigen-specific T cells and depletion of immune suppressive cells, suggesting that incorporation of DCs might further improve this (Curran *et al.*, 2010).

7.3.5 Summary of dendritic cell therapy

Evidence presented in this project shows the benefit of sorting CCR7+ DCs for cancer therapy, given the decrease in tumour burden and increased survival in these *in vivo* models. This highlights the CCL19-sorting protocol as potentially beneficial in these regimens and confirms the hypothesis that focusing on cell migratory capacity alone can improve therapeutic outcome. Although it is clear many studies focus on strengthening the phenotype of the DC to improve the generation of an anti-tumour T cell response using novel strategies (Constantino *et al.*, 2016), such as the source of DCs, maturation cocktails, and route of injection, limited cell migration will always limit therapeutic efficacy if DCs cannot reach T cells to activate them. Data presented in **Chapters 3-5** show that CCL19-sorted DCs are more capable of migrating and stimulating anti-tumour T cells, which can slow tumour growth and improve survival in the subcutaneous B16F10.ova model. In **Chapter 6** it was shown that this protocol is adaptable to GMP DC production as required for use in clinical trial vaccinations, using GMP-compliant reagents for development of the DCs *ex vivo* and the MACSQuant Tyto (Miltenyi Biotec) - a closed-system clinical-grade cell sorter. With the ability to purchase chemically-synthesised CCL19 and other

chemokines at GMP-grade, these preliminary data support the benefits of CCR7-sorting human MoDCs and growing efficacy data on the superiority of CCR7-sorted BMDCs in a melanoma model, this project offers the direct applicability of the CCR7-sorting methodology to future clinical trials using DC vaccines.
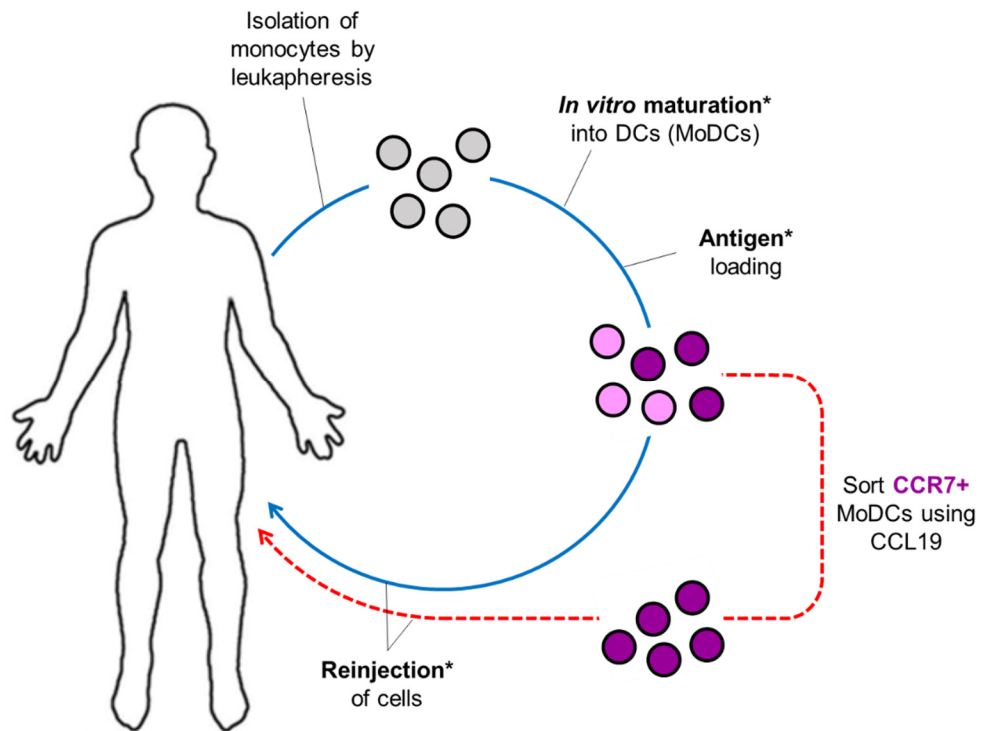
Figure 7.1 - Modifying current clinical protocols for dendritic cell production to include CCR7-sorting.
The CCR7-sorting methodology described here can be easily adapted into current clinical trial methodologies using patient-derived monocytes (grey) to separate CCR7+ DCs (purple) from CCR7- DCs (pink) (*: general steps which are variable between studies).

7.4 Improved DC migration is relevant in non-cancer clinical contexts

7.4.1 Antiviral therapies

There are a number of alternative contexts in which DC vaccination may be of benefit in addition to cancer; DC therapies can induce strong and durable antigen-specific responses in patients with chronic infections such as Human immunodeficiency virus (HIV). HIV is most commonly treated with combined antiretroviral drug therapy (cART), which suppresses viral replication and allows reconstitution of the depleted CD4+ compartment

specifically targeted by the virus (Vrisekoop *et al.*, 2015). Although able to lower viral titres to undetectable and non-transmittable levels, cART cannot induce an HIV-specific immune response and therefore cannot completely 'cure' the infection requiring patients to be on cART indefinitely(van den Ham *et al.*, 2018). This is reported to be due to incomplete distribution of cART through the body, which leads to continued replication in restricted anatomical sites such as the gut and LNs (Lorenzo-Redondo *et al.*, 2016). Alternative, or complimentary, strategies focus on this aspect of treatment; with DC therapy a potential option. In particular, the ability of DCs to cross-present antigens to CD8+ T cells without requirement for CD4+ cooperation (Fonteneau *et al.*, 2003) makes them especially attractive as a therapy because CD4+ T cells are depleted in untreated HIV patients or those beginning cART. In completed clinical trials, DC vaccines show a modest success but broad conclusions again are limited by the variety of DC preparations and maturation cocktails, cell number, antigen selection, and injection strategy (Miller and Bhardwaj, 2014). Importantly, migration of cells post-injection has been highlighted as a potential concern – resulting, in part, in the need for different injection strategies (García and Routy, 2011) or indeed, methods to improve cell migration to the lymph nodes such as sorting for CCR7 expression. One of the first of these studies in 2004 showed that 3 intradermal injections of HIV-mRNA loaded MoDCs was able to elicit HIV-specific CD4+ and CD8+ T cells in patients, with half of those experiencing these responses for at least 1 year (Lu *et al.*, 2004). Interestingly, the investigators measured draining lymph node size which could be used a surrogate measurement of DC migration following injection, but for obvious medical reasons were unable to quantify this migration. DC phenotype was assessed for quality control purposes but did not include analysis of CCR7 expression – although other markers of maturity such as CD80, CD83 and CD86 were upregulated to greater than 70% expression in the injected bolus.

A more recent study using ASG-004, an MoDC product with electroporated HIV-specific mRNA encoding HIV-1 Gag, Nef, Rev and Vpr genes, has also shown the ability to induce functional anti-HIV immune responses in patients with chronic HIV infection in a small trial (Gay *et al.*, 2017). In this study, it was shown that conversion of the existing central CTL immunity to an effector CTL immunity may be influential in viral control, but in neither this study nor previous studies using ASG-004 (Routy *et al.*, 2010) was the migration of DCs to the lymph node assessed. Development of a measurable anti-HIV immune response is typically seen, although control of viraemia is not consistent between trials (García and Routy, 2011). In the absence of migratory information of anti-HIV DC therapies, it would be interesting to explore if the quality of cell migration is limiting

therapeutic efficacy as is the leading hypothesis in cancer vaccination, and if improving this leads to efficacy as shown here.

In chronic Hepatitis C infection, a strong antiviral T cell response has been shown to be able to clear the virus again making DC vaccination a viable therapeutic option (Zhou *et al.*, 2012). Current treatment includes interferon and ribavirin but this is only effective in about half of patients (Poynard *et al.*, 2002), and with a third of patients eventually progressing to cirrhosis and then liver failure, hepatitis C is a major public health risk. DC vaccines have been shown to induce strong anti-hepatitis C T cell responses in a mouse hepatitis C antigen-expressing tumour, resulting in control of tumour growth and validating the efficacy of the generated T cell response (Encke *et al.*, 2005). This study uses peptide-pulsed, subcutaneously-injected DCs for therapy, but did not assess migration of the DCs. It also showed a prophylactic benefit to the tumour challenge, as shown with the prophylactic injection strategy presented in **4.3**, which opens up an interesting avenue for the use of DCs prophylactically in addition to use as a treatment option to support conventional vaccines. In human hepatitis C infection, DC clinical trials have shown detectable antigen-specific T cell induction but no viral clearance, suggesting insufficiency of T cell induction to be the primary reason for the lack of efficacy (Zabaleta *et al.*, 2015), and not immune suppression as seen in cancer. This study also highlighted the differences between patient-derived and healthy control-derived DCs in function, which may require identification of an alternative source of cells for therapy depending on the disease context of the individual.

7.4.2 Antifungal therapies

Finally, DCs have been used as anti-fungal therapies in the context of stem cell transplantation. Aspergillosis, infection by fungi of the *Aspergillus* genus particularly *A. fumigatus*, occurs insidiously in approximately 10% of haematopoietic stem cell transplant (HSCT) recipients as side effect of immune suppressive regimens (Marr, 2008). The highest risk period for Aspergillosis is 60-90 days post-transplant even with prophylactic anti-fungal drug treatment. Despite occurring in up to 10% of HSCT recipients, Aspergillosis symptoms are difficult to diagnose and the infection still has a high mortality rate (Miceli *et al.*, 2017). Uptake of fungal spores and components induce a potent anti-tumour function in DCs, shown experimentally as an increase in IL-12 production and a subsequent induction of Th1-mediated anti-fungal immunity *in vivo* (Bozza *et al.*, 2002). In T-cell depleted mice, anti-fungal DC vaccination induced accelerated reconstitution of

aspergillus-specific T cell responses compared to the slow recovery of the response in the untreated group (Bozza *et al.*, 2003) which prevent infection upon subsequent challenge. Cell migration in this study showed limited migration to the lungs, and lymphoid tissue including thoracic lymph nodes and thymus. During T cell reconstitution, it may be of benefit to guide more DCs to the thymus and lymph nodes for direct T cell education than to the periphery; for which CCR7-sorting could be useful. This response can also be replicated in a human *in vitro* context, supporting the translation of this strategy to the clinic (Grazziutti *et al.*, 2001). Induction of IL-12 production by DCs using mRNA has been shown to enhance defence against intracellular pathogens such as *Leishmania* as both a prophylactic and therapeutic treatment (Ahuja *et al.*, 1999; Roy and Klein, 2012). Both MoDCs and pDCs (Matsuse *et al.*, 2017) have been shown to contribute the anti-fungal response, particularly in the lungs, but crucially require LN migration to transfer fungal antigens to LN-resident DCs for this function (Ersland, Wuthrich and Klein, 2010). In combination with the development of anti-fungal DC preparations, it is possible that CCR7-sorting cells could be used to direct cell migration to the LNs.

7.5 Chemokine-based sorting can be adapted to other cell therapies

7.5.1 Cytotoxic T cells

Finally, the chemokine system is relevant to not only DC migration, but to the migration of several immune cell types with a potential for therapeutic use. Chemokine receptors are expressed by most, if not all cells of the immune system, and control migration to specific tissues in addition to having functional implications (Stein and Nombela-Arrieta, 2005). Of these immune cells, T cells may be the most therapeutically viable cells, and are currently used as therapies in a number of clinical contexts such as metastatic melanoma (Rosenberg *et al.*, 2011). Tumours, and tumour-associated stroma, actively secrete chemokines and attract both pro- and anti-tumourigenic immune cells. In breast cancer for example, secretion of CCL2 and CCL5 is one of the initial driving mechanisms behind recruitment of macrophages to the developing tumour which become pro-tumourigenic TAMs and are prognostically very poor (Ben-Baruch, 2006). The same chemokines in ovarian cancer and melanoma, however, attract T cells and expression is beneficial to tumour control and regression (Harlin *et al.*, 2009). T cells express a number of cancer-relevant chemokine receptors which control their tumourigenicity to a certain extent, including CCR1, 2, 3, 4,

5, 6, 7 and 8 and CXCR1, 2, 3, 4 and 5 (O'Garra, McEvoy and Zlotnik, 1998). Despite isolation of TILs from the actual tumour milieu, migration of these cells to primary or secondary sites after expansion and reinjection is lower than expected (Fisher *et al.*, 1989). If tumour biopsies were analysed for their chemokine production, it could be possible to sort *ex vivo*-derived therapeutic T cells for expression of the matching chemokine receptors to target them directly to the tumour for function. This concept was first proposed by Kershaw *et al.* in 2002, who showed that matching cell expression of CXCR2 with secretion of CXCL1 by melanoma cells was sufficient to induce tumour tropism (Kershaw *et al.*, 2002).

This matching strategy was also shown to be successful in the directed migration of activated T cells expressing CCR2 to tumours highly expressing CCL2 in models of lymphoma and melanoma (Brown *et al.*, 2007). In response to these studies, chemokine receptor upregulation by transduction has been highlighted as a potential improvement to therapeutic T cell homing to tumours: both CCR2 and CXCR2 have been transduced in T cells for successful treatment of melanoma (Garetto *et al.*, 2016; Idorn *et al.*, 2018). Idorn *et al*. also showed that the chemokine receptor repertoire of *in vitro*-expanded TILs stays relatively consistent over culture suggesting that cell sorting methods could be beneficial since the pre-expansion receptor expression is maintained during culture. Sorting T cells for the chemokine receptors which bind chemokines produced by the tumour, for example, CCL2 or CCL5, may help increase T cell migration to the tumour following injection and also remove T cells which cannot reach it (Ben-Baruch, 2006). The limited trafficking of engineered CAR T cells to tumours (Kakarla and Gottschalk, 2015) could also be supplemented with selection of cells for chemokine receptor expression. Current novel CAR therapies have used lentiviral transduction of CCR2 expression for CAR T cells to improve migration to the tumour as it was seen that after extended culture only 7% retained expression of the receptor (Moon *et al.*, 2013). This improved tumour-specific migration, as the non-transfected control cells remained in the blood. Sorting the cells by expression of the receptor may prove beneficial, however, in overcoming the technical limitations of multiple rounds of lentiviral transfection for addition of the chimeric receptor, and then addition of the chemokine receptor; or may even be beneficial for isolating only the successfully transfected cells after these steps.

7.5.2 NK cells

To circumvent the need for *in vitro* availability of a specific antigen, NK cells have become a recent attractive target for therapeutic use. In the context of cancer, NK cells are directly cytotoxic independent of MHC-recognition and contribute to tumour surveillance (Imai *et al.*, 2000). Intratumoural NK cell infiltrate is associated with a good prognosis in gastric carcinoma (Ishigami *et al.*, 2000), lung cancer (Villegas *et al.*, 2002) and renal cell carcinoma (Geissler *et al.*, 2015). Interestingly, T cell infiltrate into renal carcinoma lesions has been observed to be a poor prognostic factor (Igarashi *et al.*, 2002), justifying the development of non T cell-based immunotherapies. Again, however, poor migration of NK cells derived from *in vitro* expansion to tumours limits their efficacy, although NK cells have been shown to express a number of relevant chemokine receptors for tumour-specific migration including CCR2, CCR5, CXCR1 and CX3CR1 (Bernardini *et al.*, 2016). Additionally, expression of particular chemokine receptors is linked to cytotoxicity such as CXCR1 (Cooper, Fehniger and Caligiuri, 2001) so application of a chemokine sorting methodology may be beneficial to not only cell migration but cell function as shown here with dendritic cells. Directed expression of chemokine receptors such as CXCR2 by viral transfection has been shown to improve cell homing to CXCL1 and CXCL5 produced in renal cell carcinoma (Kremer *et al.*, 2017), which supports a focus on the chemokine receptor of potential NK cell therapies.

7.6 Conclusion

Dendritic cells are a valuable potential cancer therapy, although their efficacy is currently limited outside of a small percentage of clinical trials. A number of factors may account for this, but the lymph node migration of cells generated *in vitro* is poor and insufficient cell numbers reach the lymph node to induce an effective anti-tumour T cell response. Sorting dendritic cells for expression of the chemokine receptor CCR7, crucial for lymph node migration, allows more cells to reach the lymph node, improves cell function and the T cell response and this leads to a reduction in tumour growth in a model of subcutaneous melanoma. This modification to current clinically-used protocols may therefore inform and be incorporated into future clinical trials to help ensure a robust T cell response in all patients and may improve tumour survival as shown here. In addition to this, the chemokine sorting methodology presented in this thesis is broadly applicable to a number

of cell therapies in different disease contexts outside of DC therapy and has been shown to be relatively easy to accommodate at a GMP-compliant level.

Appendix I

Generation and characterisation of the B16F10.ova cell line

A.1 Introduction and aims

As described in the **Introduction**, a mouse model of metastatic melanoma was used to assess the potential benefit of CCL19-sorted DCs as a therapy for cancer. The main aims of this Chapter are to describe the generation of this cell line, its validation and characterisation as a model before use in the experiments detailed in **Chapters 4** and **5**.

Mouse models of cancer are an extremely valuable tool for the development of new therapies and have been used in the field from as early as 1943 (Gross *et al.,* 1943). The B16 melanoma is an example of one such model, which was first isolated from the C57BL/6 mouse strain and gave rise to two tumour cell lines known as B16F1 and B16F10. These lines are widely used as both solid primary tumour and secondary metastatic tumour models. The original cell line, B16F1, can produce subcutaneous tumours but very variable systemic metastases compared to the B16F10 cell line which has been selected over 10 generations for metastatic potential to the lung after IV injection in addition to subcutaneous tumour formation by injection into the skin (Ishiguro *et al.*, 1996). The B16F10 model was used in this study to allow study of both primary and secondary tumour development and will be the model discussed for the rest of this Chapter. The tumour is described as syngeneic given its C57BL/6 background, and as a result grows quickly in these mice receiving the tumour cells by injection either intravenously or subcutaneously. To allow *in vivo* targeting of the tumour by potential therapies, the cell line is commonly transduced to express a known foreign protein.

For use in this project, the B16F10 cell line was engineered to express the chicken egg protein ovalbumin. Several methodologies exist for introduction of this antigen including transfection of the MHC-restricted epitopes of ovalbumin - $OVA_{257-264}$ and $OVA_{323-339}$ for MHC class I and II respectively - or an MHC-fused epitope, but in this project transfection of the whole protein coding sequence (cDNA) was chosen to elaborate the whole protein to allow processing and presentation of antigen by endogenous APCs during the progression of tumour development because this mirrors the clinical context (Huang *et al.*, 1994). The transfection was validated also using microscopy, QPCR, flow cytometry and a functional T cell cytotoxicity assay.

A.2 Generation of B16F10.ova

A.2.1 OVA gene source

The plasmid vector pOVA, which encodes the full-length cDNA sequence of chicken ovalbumin, was a kind gift from Shoshana Levy (Addgene plasmid #31598). The plasmid was given transformed into *Escherichia coli* (E. coli), which were first expanded by streaking the bacteria along agar plates containing 50ng/ml ampicillin and incubating overnight at 37ºC. Colonies were then picked from the agar plates using sterile pipette tips and introduced into a conical flask containing 50ml of liquid agar broth containing 50ng/ml ampicillin. The flask was incubated at 37ºC overnight on a moving plate mixer. The plasmid was then extracted from the bacterial cells using the PureLink HiPure Plasmid DNA Purification (Midiprep) Kit (Invitrogen) according to the manufacturer's instructions, and the DNA content of the eluted fraction was quantified by nanodrop (Nanodrop 1000, Thermo Scientific).

A.2.2 Subcloning OVA gene into an expression vector

PCR outer primers for amplifying ovalbumin cDNA were designed to incorporate the EcoRI and ApaI restriction sites to allow ligation of the DNA fragment into the pEGFP-N3 mammalian expression vector (BD Biosciences) under the control of the cytomegalovirus (CMV) gene promotor. As shown below, the ApaI reverse primer was additionally designed to include a STOP codon to prevent ligation of the ovalbumin cDNA sequence to the green fluorescent protein (GFP)-tag present in the plasmid during transcription. Primer sequences were designed based on the ovalbumin and primer sequences from Maecker *et al.*, (1997) and McReynolds *et al.*, (1978). These sequences are listed in **Table A**.1 below.

Primer Name	Primer Sequence
EcoRI-OVA (*Forward*)	5'- CCCCGGAATTCATGGGCTCCATCGGCGCAGC - 3'
ApaI-OVA (*Reverse*)	5'- TTATAGGGCCCTTAAGGGGAAACACATCTGC - 3'

Table A.1 - PCR primers used in cloning OVA into pEFGP-N3. Restriction sites for the specified restriction enzymes are highlighted in red.

Ovalbumin cDNA was amplified from the pOVA eluate (**A1.1**) by PCR using the Q5 High-Fidelity DNA Polymerase (Qiagen) as described in **2.4.2**. The reactions were run in a thermal cycler using the following program, and are specific for amplification of the longer ovalbumin gene fragment:

Step	Temperature (ºC)	Time	
Initial denaturation	98	3 minutes	
Denaturation	98	10 seconds	
Annealing	63*	30 seconds	Repeated for 35 cycles
Elongation	72	55 seconds**	
Final elongation	72	10 minutes	
Hold	4	Indefinitely	

* Specific melting temperature of the primers designed, ** Extension time was for the 1200bp DNA fragment at a rate of 40 seconds/kb of DNA.

The ovalbumin cDNA was then purified from the PCR reaction mixture using the PCR Purification Kit (Invitrogen) according to the manufacturer's instructions. To validate the size of the fragment, the PCR product described previously was run on a 1% agarose electrophoresis gel which was prepared as described in **2.4.3**. The fragment was sequenced for confirmation (Eurofin Genomics).

To incorporate the cloned fragment into the plasmid, both the fragment and recipient plasmid (pEGFP-N3) were digested using the EcoRI and ApaI restriction enzymes. The digestion was prepared using the following enzyme mix, with one sample used as a no enzyme control reaction:

Ingredient	Volume (µl/reaction)
Restriction enzyme – EcoRI and ApaI	1
Reaction buffer	10
Template DNA	
OVA gene fragment	Up to 100
or Plasmid	5
Double-distilled Nuclease-free Water	Up to 100

ApaI was added first; the samples were vortexed briefly and incubated at 25ºC for 8 hours, after which EcoRI was added and the samples incubated at 37ºC overnight. Digestion of fragment and plasmid was validated by electrophoresis on a 0.8% agarose gel. Prior to introduction of the ovalbumin gene fragment, the plasmid prep was treated with phosphatase enzyme to reduce re-ligation of the plasmid before introduction of the plasmid. The enzyme mix for the ligation was set up as described below, with one sample used as a no insert control to assess for spontaneous re-ligation of the plasmid:

Ingredient	Volume (μl)/Concentration
Plasmid	100ng
OVA gene fragment	76.13ng*
Ligase enzyme	0.5
Reaction buffer	1
Double-distilled Nuclease-free Water	Up to 10

* OVA gene fragment concentration was determined using the following formula:

$$ng_{insert} = \left(ng_{pl\,DNA} \times \frac{Kb_{insert}}{Kb_{pl\,DNA}} \right) \times 3$$

The samples were then left at 4ºC for 20 hours to allow ligation.
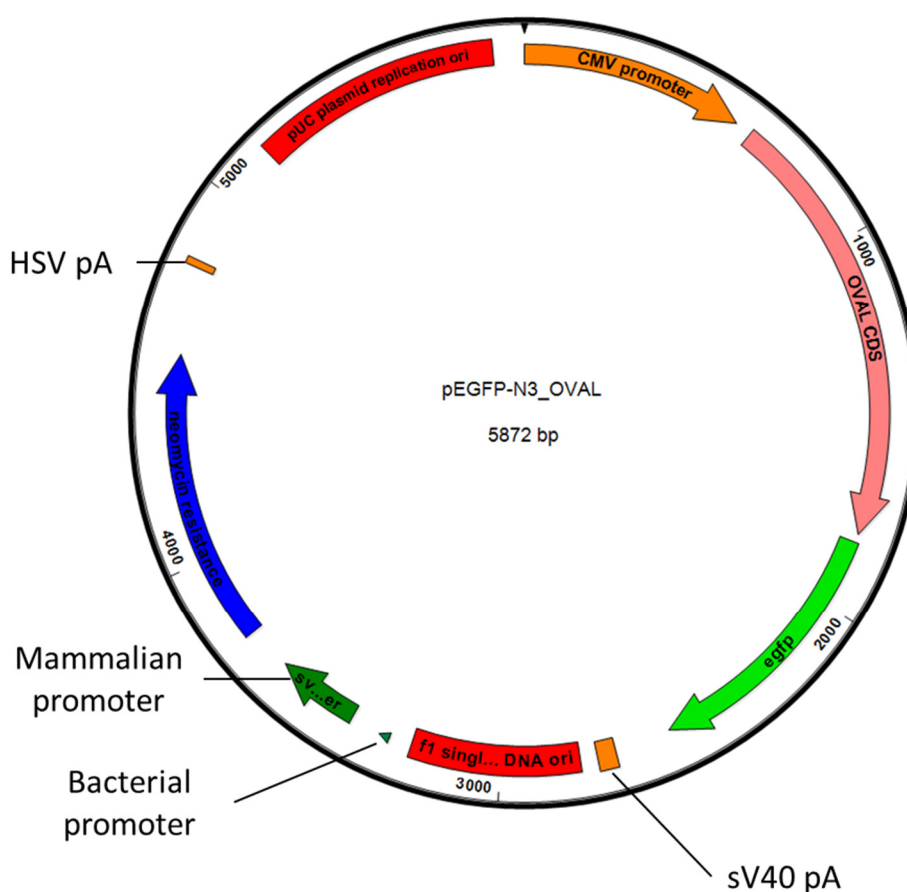
Figure A.2 - pEGFP-N3 OVA schematic.
Functional regions (clockwise from top) are: Cytomegalovirus (CMV) promoter; Ovalbumin gene; eGFP gene present in plasmid but not expressed; sV40 pA; Bacterial and mammalian promoter; Neomycin resistance gene; HSV pA; pUC origin of replication.

A.2.3 Expansion of construct in *E. coli*

To amplify the constructed plasmid, chemically-competent *E. coli* were used (XL10-Gold cells, Agilent Technologies). The vial was defrosted from -80ºC storage on ice, and 5μl of each ligated and re-ligated plasmid was added. After a brief agitation of the contents using

a pipette, the vial was left on ice for 30min. Following this, the cells were heat-shocked by placing in a water bath at 42ºC for 45 seconds before immediate return to ice for 3min. 250µl of super-rich agar broth was added to the vial, which was then incubated in a thermal mixer at 37ºC for 60min. The cells were streaked on two agar plates containing 25µg/ml kanamycin for selection of successfully transformed cells. One plate had 20µl of the broth streaked onto it; the remaining broth was centrifuged in a microcentrifuge at maximum speed (approx. 12000xg) for 30 seconds and the supernatant discarded. The pellet of bacteria was manually agitated to homogenise the concentration of bacteria in the remaining broth. This broth was then added undiluted to the agar plate in the event of minimal successful plasmid ligation. The plates were incubated at 37ºC overnight. From these plates, 12 clones were picked from the 20µl dilution plate, and were streaked onto new agar plates divided visually into 6 sections.

A.2.4 Validation of construct

The correct insertion of the ovalbumin cDNA was assessed by restriction enzyme digestion and gel electrophoresis as described previously. First, small colonies from each of the 12 sections were picked using a sterile pipette tip and added to 50µl distilled water. These colony samples were 'boiled' for 10min in a thermal cycler, and 1µl of this preparation was amplified using PCR using insert-spanning primers (**Table A**.2) as described previously and validated by electrophoresis on a 0.8% agarose gel.

Primer Name	Primer Sequence
CMV promoter (*Forward*)	5'- TGGCACCAAAATCAACGGGACT - 3'
eGFP (*Reverse*)	5'- CGTCGCCGTCCAGCTCGACCAG - 3'

Table A.2 - PCR primers used for plasmid validation.

As shown in **Figure A**.3**A**, from one plate of 6 clones, 4 clones successfully incorporated the 1.42kb ovalbumin cDNA into the plasmid as indicated by the presence of bands between 1kb and 1.5kb (lanes 1, and 3-5). These clones were selected for overnight culture in 5ml liquid agar broth supplemented with 25µg/ml kanamycin. The plasmid was extracted from the expanded colonies using the QiaPure MiniPrep system (Qiagen), as per the manufacturer's guidelines. To ensure the correct orientation of the insert within the plasmid, 3 restriction enzyme digests were prepared using the following enzyme mixes.

Ingredient	Volume (µl)/Concentration
Plasmid DNA	1ng
Restriction enzyme – PvuII, EcoRV + AvrII, NotI-HF	0.5
Reaction buffer	2
Double-distilled Nuclease-free Water	Up to 20

The samples were validated by electrophoresis on a 0.8% agarose gel as described previously.
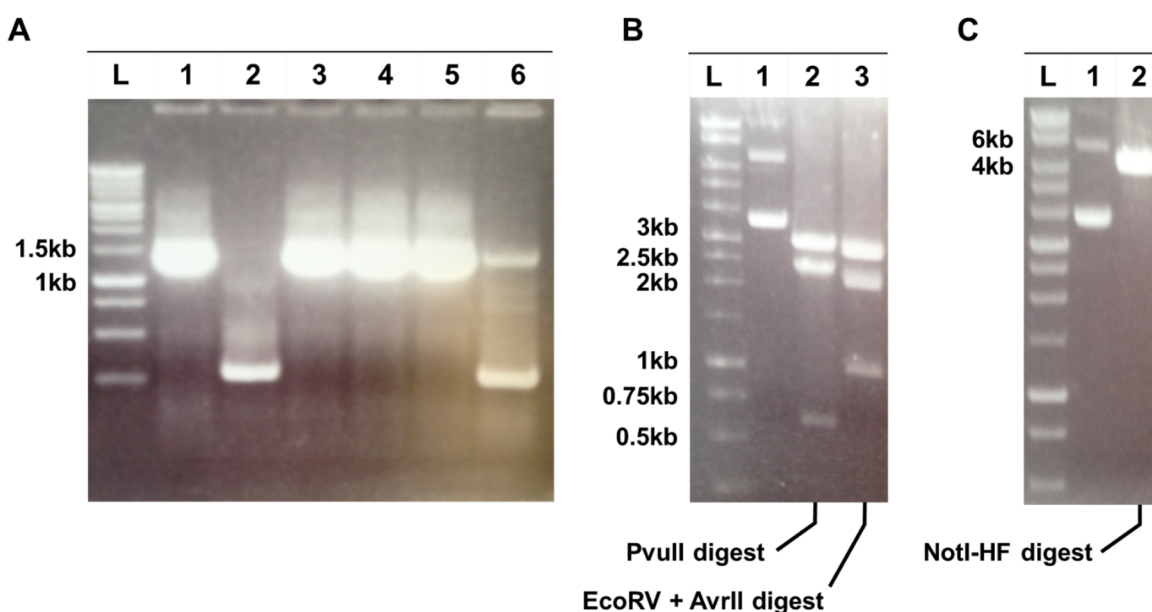
Figure A.3 - Validation of OVA plasmid.
A) Detection of ovalbumin cDNA insertion by site-spanning primers in 4 of 6 selected clones (lanes 1-6). B, C) Restriction enzyme digest with PvuII (B; lane 2), and EcoRV + AvrII (B; lane 3), or NotI-HF (C; lane 3) for selected clone (in B and C, lane 1 is undigested plasmid control).

To confirm the direction of the insert, three sets of restrictions were then performed to yield bands of known sizes. PvuII, which has three restriction sites on the plasmid construct, gave bands of 608bp, 2348bp and 2916bp (**Figure A**.3**B**). Similarly, the combination of EcoRV and AvrII restriction enzymes gave bands at 1015bp, 2113bp and 2744bp. NotI-HF was also used as it cut the plasmid only once, resulting in a full-sized band of 5.8kb total (**Figure A**.3**C**). The direction of the ovalbumin coding sequence was therefore determined to be correct in the plasmid. The full plasmid was also sequenced (Eurofin Genomics) for confirmation of the gene sequence and the absence of minor genetic changes known as single nucleotide polymorphisms (SNPs).

The selected clone was swabbed from the original plate and incubated at 37ºC in 5ml of agar broth supplemented with kanamycin, and subsequently expanded in 200ml of agar

broth in a conical flask. The final plasmid was extracted from the bacterial cells using the Qiagen EndoFree Plasmid Maxi Kit (Qiagen) as per the manufacturer's instructions and the concentration quantified by nanodrop.

A.2.5 Stable transfection of B16F10 cells

B16F10 cells were grown to 70-80% confluence in $25cm^3$ tissue culture flasks under normal culture conditions (described in **2.1**). The transfection reaction mixture was created by first adding 2µl Lipofectamine 2000 to 25µl Opti-MEM medium (Invitrogen). A second mixture was prepared by adding 500ng linearised plasmid DNA to 25µl Opti-MEM medium. These values had been previously determined by optimisation. B16F10 cells were transfected with both the ovalbumin plasmid construct described previously to induce production and presentation of ovalbumin epitopes, and the mRuby2 plasmid to make the cells express this fluorescent protein. Each plasmid was linearised as described previously using the enzymes in **Table A.3**.

Plasmid	Enzyme used for linearisation
pEGFP-N3-OVA	ApaL1
pEF6-mRuby2	Ssp1

Table A.3 - Restriction enzymes used for plasmid linearization.

The two mixtures were then combined by pipetting and incubated at room temperature for 5min to allow complex formation. The DNA-Lipofectamine 2000 complex was added into the flask in fresh DMEM, mixed by manual agitation to equally distribute the complexes, and then incubated under normal culture conditions. After 6 hours, the media was removed, the cells were washed with PBS and the media replaced. After 24 hours, the media was removed and replaced again. After a further 48 hours the cells were removed from the flask using trypsin as previously described and were split into 6 new $10cm^3$ culture dishes with media supplemented with the selection antibiotic. For the B16F10 cell line, both blasticidin (5µg/ml, Invitrogen) and G418 (2.5mg/ml, ThermoFisher Scientific) were used to maintain the mRuby2 and OVA plasmid, and concentrations were optimised by survival curve analysis (data not shown). Transfected cells were maintained under selection for up to 2 weeks until individual colonies were visible by eye. The media was replaced every 3-4 days as necessary.

A.2.6 Clonal selection of transfectants

To ensure homogenous expression of the transfected vector within the cell population, it was important to isolate colonies outgrowing from a single antibiotic-resistant cell. When the colonies were first visible by eye, they were visually isolated by drawing around the colony edges on the underside of the culture dish in waterproof pen. The media was removed from the dish using a pastette and the cells were washed once with PBS to remove loosely-adherent cells and debris. 5ml of PBS was then added to the culture dish. Individual colonies were removed from the dish by manually scraping the cells with a 10µl pipette tip and then were transferred into individual wells of a 48-well plate. New selection media was added to each well and the colonies allowed to grow to confluence before analysis. Transfected clones were also assessed for their growth compared to the untransfected B16F10 cell line, with clones growing very quickly being excluded from further analysis.

To quickly screen the colonies for presentation of ovalbumin, fully confluent colonies were prepared for flow cytometry by first lifting the cells using TryplE and washing in PEB as described previously. Cells were stained with 2µl of anti-SIINFEKL-MHC class I antibody conjugated to APC (BioLegend, clone: 25-D1.16), with untransfected B16F10 cells used as a control. This antibody binds the MHC class I-restricted ovalbumin epitope SIINFEKL in the context of MHC class I presentation. The samples were run on the MACSQuant and analysed using the FlowJo 10 software. A representative sample of the transfected clones is shown in **Figure A.4** below.
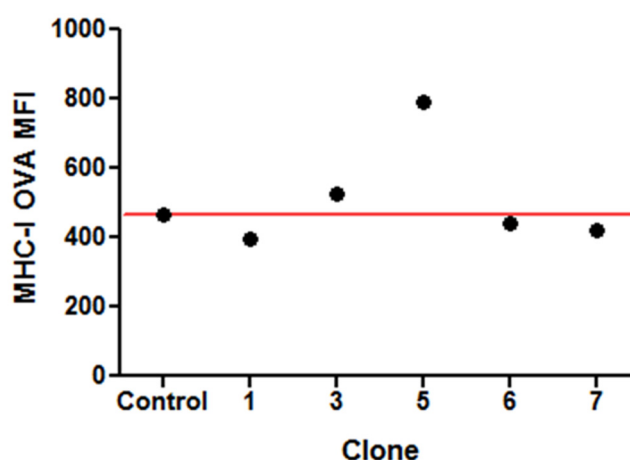
Figure A.4 - Clonal selection of B16F10.ova transfectants.
In this representative sample, only two clones expressed the ovalbumin protein fragment presented on MHC class I higher than the untransfected control cells (red line).

Several clones with high ovalbumin presentation were selected for continued use, with one primary clone selected for further validation before use and designated as B16F10.ova forthwith. Cells were routinely assessed for maintenance of transfected proteins by flow cytometry.

A.3 Characterisation of B16F10.ova

A.3.1 Gene expression by QPCR

Quantification of ovalbumin cDNA expression was done by QPCR. B16F10.ova cells were first lysed with RLT buffer containing β-mercaptoethanol. The RNA was then extracted using the RNeasy Mini Kit (Qiagen), as per manufacturer's instructions, including the on-column DNase digestion step using the RNase-free DNase kit (Qiagen). cDNA was generated from the RNA using the High Capacity RNA to cDNA Kit (Applied Biosystems) as per the manufacturer's instructions, including samples containing no RT enzyme as a control for genomic contamination. QPCR for gene expression was done as described in **2.4.4**, using the primers listed in **Table 2.2**.
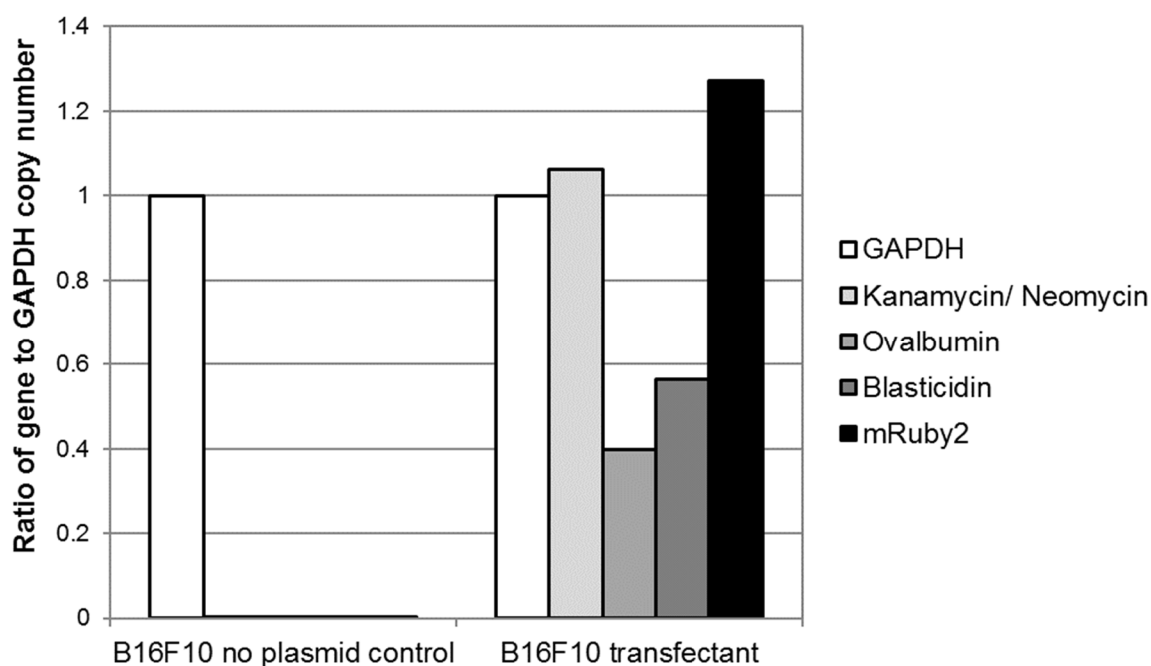
Figure A.5 - Expression of transfected genes in B16F10.ova cells by QPCR.
B16F10 transfectants were compared to the untransfected no-plasmid control and showed induction of expression of Ovalbumin and mRuby2 as desired, as well as the antibiotic resistance genes for Kanamycin/Neomycin and Blasticidin compared to the controls.

Expression levels of each transfected gene are variable compared to the housekeeping gene GAPDH, however **Figure A**.5 shows clearly the expression of the 4 genes contained within the plasmids used for transfection of the B16F10 cell line compared to the no plasmid control. Variability in the expression of individual genes may be a result of the genes being under the control of two different promotors, ovalbumin under the CMV promotor and mRuby2 under the Elongation Factor alpha (EFα) promotor, which may be expressed by B16F10 cells may be at different levels. The kanamycin/neomycin resistance cassette is part of the ovalbumin plasmid construct and allows the selection of bacterial clones through kanamycin or neomycin resistance as well as selection of eukaryotic cell clones through resistance to the antibiotic G418. The blasticidin resistance cassette is present in the mRuby2 construct and confers resistance to the antibiotic blasticidin in eukaryotic cells. The presence of transcripts of each transfected gene is a validation of successful transfection with both plasmids.

A.3.2 mRuby2 protein expression

To assess expression of the mRuby2 fluorophore, both fluorescent microscopy and flow cytometry were used. For microscopy, B16F10.ova cells were seeded into 4-well chamber slides (ThermoFisher Nunc) and grown to confluence under normal culture conditions. Once the cells had reached 70-80% confluence the media was removed, and the wells rinsed with PBS. 0.5ml of 4% PFA in PBS (v/v) was added to each chamber to fix cells and incubated for 20min at room temperature. After this the PFA was removed and the chambers rinsed with 0.5ml PBS. The chamber walls were manually removed from the slide, which was then allowed to dry at room temperature. The slides were mounted using Vectashield Hardset Antifade mounting medium (Vector Laboratories). The slides were assessed for cell fluorescence using an epifluorescent microscope; mRuby2 has λ_{ex} of 559nm and λ_{em} of 600 (Lam *et al.*, 2012). The images were captured and analysed using the Zen software. For flow cytometry, a sample of B16F10.ova cells in culture were removed during routine passaging, run on the LSRII (BD Biosciences) and analysed using the FlowJo 10 software.
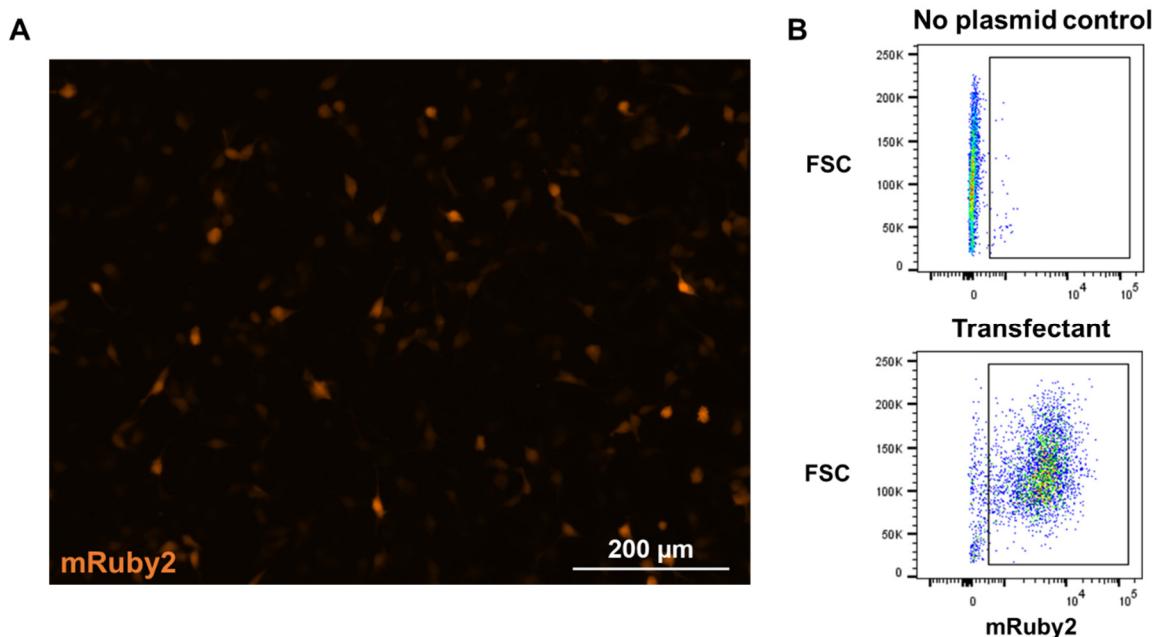
Figure A.6 - Validation of B16F10.ova mRuby2 expression using microscopy and flow cytometry.
Expression of the mRuby2 fluorescent protein was visible by microscopy (A) and by flow cytometry compared to the untransfected control cells (B).

mRuby2 expression by B16F10.ova transfectants is strong enough for the fluorophore to be visible by both microscopy and flow cytometry as seen in **Figure A.6**. The cell population does heterogeneously express the fluorophore however, and this is something that needs to be taken into consideration in future experiments. The mRuby2 fluorophore expression is also stable over routine passage (data not shown).

A.3.3 Ovalbumin protein expression

Assessing ovalbumin expression in the B16F10 transfected cell line was expected to be difficult because of the poor expression of both MHC class I and MHC class II molecules on tumour cells is well characterised and has been reported in the B16F10 cell line (Seliger *et al.*, 2001). The B16 model is a very commonly used tumour model and can still be targeted by CD8+ T cells *in vitro* and *in vivo*. To better understand the mechanism by which this is occurring, expression of MHC class I and II were tested following exposure to the inflammatory cytokine IFNγ.

B16F10 cells were seeded onto 24-well culture plates and allowed to grow to confluence under normal culture conditions. Once confluence had been reached, the media in the wells was removed and replaced with 1ml of media containing IFNγ at 20ng/ml or 50ng/ml, or

no IFNγ as a control. After 48 hours, the cells were prepared for flow cytometry by lifting with TrypLE and washing into PEB as described in **Chapter 2**. Cells were stained with 2μl of anti-H-2kb antibody conjugated to AF647 (BioLegend, clone: AF6-88.5) and anti-I-A/I-E antibody conjugated to AF488 (BioLegend, clone: M5/114.15.2). These antibodies stain MHC class I and II, respectively. The samples were run on the MACSQuant and analysed using the FlowJo 10 software.
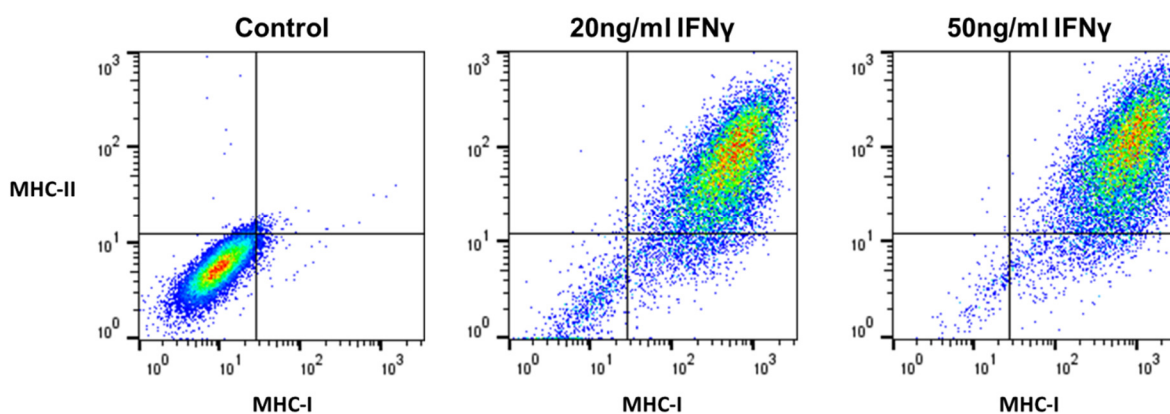
Figure A.7 - MHC class I and II expression of B16F10.ova cells under inflammatory conditions.
B16F10 cells were exposed to increasing concentrations of IFNγ and show a clear increase in the expression of both MHC class I and MHC class II.

As shown in **Figure A.7**, B16F10 cells are capable of upregulating MHC class I and II molecules during stimulation with as little as 20ng/ml IFNγ. General inflammation in the tumour microenvironment is likely to include IFNγ secretion by cells of the innate immune system such as NK cells, as well as by adaptive immune cells recruited to the site such as CD8+ T cells (Böhm *et al.,* 1998), suggesting a potential mechanism for tumour rejection.

A.3.4 CTL lysis assay

To confirm that B16F10.ova cells present the ovalbumin epitope using MHC, a T cell killing assay was performed using ovalbumin-specific T cells. These T cells were isolated from the lymph nodes and spleens of OT-I mice, a strain of genetically modified mice with CD8+ T cells recognising only the MHC class I-restricted epitope of ovalbumin, SIINFEKL. *In vitro*, this can be used to quantify the full potential T cell responses to a known antigen. To do this, T cells were isolated from OT-I mice and expanded as described previously in **2.5.3.2** and **2.6.5**.

After 7 days in culture, the cells were then collected using TrypLE for use. B16F10.ova cells were also collected from routine culture using TrypLE and plated on 12-well tissue culture plates at a concentration of $2x10^5$ B16F10.ova cells with T cells added at ratios of 1:5, 1:10, 1:20 and 1:40 in a total volume of 1ml complete RPMI/well. After 4 hours of culture, the cells were prepared for flow cytometry by lifting with TrypLE and washing into Annexin Binding Buffer (BioLegend) at a $1x10^6$ cells/ml. Cells were stained with 5μl of Annexin V conjugated to FITC (BioLegend) for 15min at room temperature, and 1μl of DRAQ7 (Biostatus) was added immediately prior to flow cytometry.
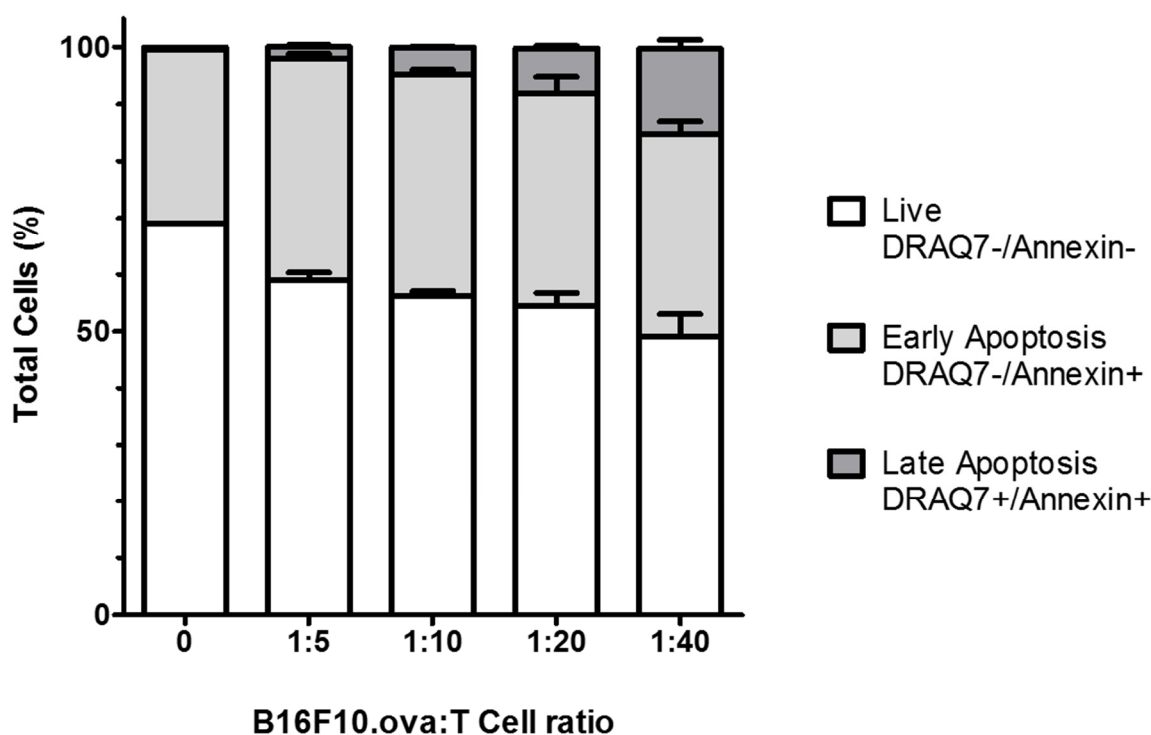
Figure A.8 - B16F10.ova targeting by activated antigen-specific T cells.
B16F10.ova cells were incubated with activated ova-specific T cells at increasing concentrations of T cells. Cells in culture were gated on expression of mRuby2 and Annexin V/DRAQ7 to distinguish cells undergoing early/late apoptosis; showing B16F10.ova cells undergo more apoptosis with increasing T cell concentration.

Annexin-V binds to phosphatidylserine (PS) on the cell membrane, which translocates to the extracellular membrane leaflet as the cell membrane loses its asymmetric architecture during early apoptosis. As apoptosis progresses, the cell membrane loses integrity and Annexin-V can also bind PS within the cell. DRAQ7, in contrast, binds double stranded DNA (dsDNA) which is only accessible for binding during late, and not early, apoptosis. A combination of Annexin-V and DRAQ7 staining can therefore be used to distinguish live cells from early and late apoptotic cells. As shown in **Figure A.8**, increasing the ratio of T

cells to B16F10.ova cells resulted in a dose-dependent T-cell mediated induction of apoptosis in the melanoma cells. Since all of the T cells present in the culture are specific for the SIINFEKL residue presented on MHC class I, B16F10.ova cells must both produce this protein endogenously and present it on the cell surface highly enough for recognition by T cells.

A.4 Conclusion

This Chapter details the process for construction of the ovalbumin plasmid for transfection of the B16F10 cell line, as well as the protocol used for the transfection of the cells. The cells were also transfected with mRuby2 to allow visualisation of the tumours *in vitro*. B16F10.ova cells were validated for successful transfection with the plasmids using QPCR for expression of the plasmid genes, and fluorescence microscopy and flow cytometry for expression of the proteins. The cells were also assessed functionally, by induction of apoptosis using antigen-specific T cells *in vitro*, showing that although MHC class I and II machinery is not highly expressed at rest, under inflammatory conditions the cells can be effectively targeted by the adaptive immune system. Taking these data together, the B16F10.ova cell line was successfully created and is a viable cancer model for this project.

List of References

Adam, C., King, S., Allgeier, T., Braumu, H., Lu, C., Mysliwietz, J., Kriegeskorte, A., Busch, D. H., Ro, M. and Mocikat, R. (2005) 'DC-NK cell cross talk as a novel CD4', *Blood*, 106(1), pp. 338–344.

Adema, G. J., Hartgers, F., Verstraten, R., de Vries, E., Marland, G., Menon, S., Foster, J., Xu, Y., Nooyen, P., McClanahan, T., Bacon, K. B. and Figdor, C. G. (1997) 'A dendritic-cell-derived C-C chemokine that preferentially attracts naive T cells', *Nature*, 387(6634), pp. 713–717.

Ahuja, S. S., Reddick, R. L., Sato, N., Montalbo, E., Kostecki, V., Zhao, W., Dolan, M. J., Melby, P. C. and Ahuja, S. K. (1999) 'Dendritic cell (DC)-based anti-infective strategies: DCs engineered to secrete IL-12 are a potent vaccine in a murine model of an intracellular infection', *Journal of Immunology*, 163(7), pp. 3890–3897.

Alegre, M., Frauwirth, K. A. and Thompson, C. B. (2001) 'T-cell regulation by CD28 and CTLA-4', *Nature Reviews Immunology*, 1, pp. 220–228.

Alvarez-Dominguez, C., Calderón-Gonzalez, R., Terán-Navarro, H., Salcines-Cuevas, D., Garcia-Castaño, A., Freire, J., Gomez-Roman, J. and Rivera, F. (2017) 'Dendritic cell therapy in melanoma', *Annals of Translational Medicine*, 5(19), pp. 386–386.

Anguille, S., Smits, E. L., Lion, E., van Tendeloo, V. F. and Berneman, Z. N. (2014) 'Clinical use of dendritic cells for cancer therapy', *Lancet Oncology*, 15, pp. e257–e267.

Anguille, S., Velde, A. L. Van De, Smits, E. L., Tendeloo, V. F. Van, Juliusson, G., Cools, N., Nijs, G., Stein, B., Lion, E., Van, A., Vandenbosch, I., Verlinden, A., Gadisseur, A. P., Wilfried, A., Muylle, L., Vermeulen, K., Maes, M., Deiteren, K., Malfait, R., Gostick, E., Lammens, M., Couttenye, M. M., Jorens, P., Goossens, H., Price, D. A., Ladell, K., Oka, Y., Fujiki, F., Sugiyama, H. and Berneman, Z. N. (2017) 'Dendritic cell vaccination as post-remission treatment to prevent or delay relapse in acute myeloid leukemia', *Blood*, 7.

Ansel, K. M. and Cyster, J. G. (2001) 'Chemokines in lymphopoiesis and lymphoid organ development', *Current Opinion in Immunology*, 13(2), pp. 172–179.

Bachem, A., Güttler, S., Hartung, E., Ebstein, F., Schaefer, M., Tannert, A., Salama, A.,

Movassaghi, K., Opitz, C., Mages, H. W., Henn, V., Kloetzel, P.-M., Gurka, S. and Kroczek, R. A. (2010) 'Superior antigen cross-presentation and XCR1 expression define human CD11c+ CD141+ cells as homologues of mouse CD8+ dendritic cells', *The Journal of Experimental Medicine*, 207(6), pp. 1273–1281.

Bajetto, A., Barbero, S., Bonavia, R., Piccioli, P., Pirani, P., Florio, T. and Schettini, G. (2001) 'Stromal cell-derived factor-1alpha induces astrocyte proliferation through the activation of extracellular signal-regulated kinases 1/2 pathway', *Journal of Neurochemistry*, 77(5), pp. 1226–1236.

Baker, J., Verneris, M. R., Ito, M., Shizuru, J. A. and Negrin, R. S. (2001) 'Expansion of cytolytic CD8+ natural killer T cells with limited capacity for graft-versus-host disease induction due to interferon gamma production', *Blood*, 97(10), pp. 2923–2931.

Banchereau, J., Palucka, A. K., Dhodapkar, M., Burkeholder, S., Taquet, N., Rolland, A., Taquet, S., Coquery, S., Wittkowski, K. M., Bhardwaj, N., Piniero, L., Steinman, R. M. and Fay, J. W. (2001) 'Immune and clinical responses in patients with metastatic melanoma to CD34+ progenitor-derived dendritic cell vaccine', *Cancer Research*, 61, pp. 6451–6458.

Barber, D. L., Wherry, E. J., Masopust, D., Zhu, B., Allison, J. P., Sharpe, A. H., Freeman, G. J. and Ahmed, R. (2006) 'Restoring function in exhausted CD8 T cells during chronic viral infection', *Nature*, 439(7077), pp. 682–687.

Bedrosian, I., Mick, R., Xu, S., Nisenbaum, H., Faries, M., Zhang, P., Cohen, P. A., Koski, G. and Czerniecki, B. J. (2003) 'Intranodal administration of peptide-pulsed mature dendritic cell vaccines results in superior CD8+T-cell function in melanoma patients', *Journal of Clinical Oncology*, 21(20), pp. 3826–3835.

Ben-Baruch, A. (2006) 'The multifaceted roles of chemokines in malignancy', *Cancer and Metastasis Reviews*, 25(3), pp. 357–371.

Benencia, F., Courrèges, M. C. and Coukos, G. (2008) 'Whole tumor antigen vaccination using dendritic cells: Comparison of RNA electroporation and pulsing with UV-irradiated tumor cells', *Journal of Translational Medicine*, 6(21).

Benteyn, D., Nuffel, A. M. T. Van, Corthals, J., Heirman, C., Neyns, B., Thielemans, K.

and Bonehill, A. (2012) 'Characterization of CD8+ T-cell responses in the peripheral blood and skin injection sites of melanoma patients treated with mRNA electroporated autologous dendritic cells (TriMixDC-MEL)', *BioMed Research International*, 2013.

von Bergwelt-Baildon, M. S., Popov, A., Saric, T., Chemnitz, J., Classen, S., Stoffel, M. S., Fiore, F., Roth, U., Beyer, M., Debey, S., Wickenhauser, C., Hanisch, F. and Schultze, J. L. (2006) 'CD25 and indoleamine 2,3-dioxygenase are up-regulated by prostaglandin E2 and expressed by tumor-associated dendritic cells in vivo: additional mechanisms of T-cell inhibition', *Blood*, 108(1), pp. 228–237.

Bernardini, G., Antonangeli, F., Bonanni, V. and Santoni, A. (2016) 'Dysregulation of chemokine/chemokine receptor axes and NK cell tissue localization during diseases', *Frontiers in Immunology*, 7, pp. 1–9.

Blackadar, C. B. (2016) 'Historical review of the causes of cancer', *World Journal of Clinical Oncology*, 7(1), p. 54.

Bloy, N., Pol, J., Aranda, F., Eggermont, A., Cremer, I., Fridman, W. H., Fučíková, J., Galon, J., Tartour, E., Spisek, R., Dhodapkar, M. V, Zitvogel, L., Kroemer, G. and Galluzzi, L. (2014) 'Trial watch: Dendritic cell-based anticancer therapy', *OncoImmunology*, 3(11).

Bogdan, C., Moll, H., Solbach, W. and Rollinghoff, M. (1990) 'Tumor necrosis factor-alpha in combination with interferon-gamma, but not with interleukin 4 activates murine macrophages for elimination of Leishmania major amastigotes', *European Journal of Immunology*, 20(5), pp. 1131–1135.

Böhm, W., Thoma, S., Leithäuser, F., Möller, P., Schirmbeck, R. and Reimann, J. (1998) 'T cell-mediated, IFN-γ-facilitated rejection of murine B16 melanomas', *Journal of Immunology*, 161, pp. 897–908.

Bol, K. F., Aarntzen, E. H. J. G., in 't Hout, F. E. M., Schreibelt, G., Creemers, J. H. A., Lesterhuis, W. J., Gerritsen, W. R., Grunhagen, D. J., Verhoef, C., Punt, C. J. A., Bonenkamp, J. J., de Wilt, J. H. W., Figdor, C. G. and de Vries, I. J. M. (2016) 'Favorable overall survival in stage III melanoma patients after adjuvant dendritic cell vaccination', *OncoImmunology*, 5(1), pp. 1–8.

Bol, K. F., Mensink, H. W., Aarntzen, E. H. J. G., Schreibelt, G., Keunen, J. E. E., Coulie, P. G., De Klein, A., Punt, C. J. A., Paridaens, D., Figdor, C. G. and De Vries, I. J. M. (2014) 'Long overall survival after dendritic cell vaccination in metastatic uveal melanoma patients', *American Journal of Ophthalmology*, 158(5), pp. 939–947.

Bol, K. F., Schreibelt, G., Gerritsen, W. R., Vries, I. J. M. De and Figdor, C. G. (2016) 'Dendritic cell-based immunotherapy: State of the art and beyond', *Clinical Cancer Research*, 22(8), pp. 1897–1907.

Boudreau, J. E., Bridle, B. W., Stephenson, K. B., Jenkins, K. M., Brunellière, J., Bramson, J. L., Lichty, B. D. and Wan, Y. (2009) 'Recombinant vesicular stomatitis virus transduction of dendritic cells enhances their ability to prime innate and adaptive antitumor immunity', *Molecular Therapy*, 17(8), pp. 1465–1472.

Bozza, S., Gaziano, R., Lipford, G. B., Montagnoli, C., Bacci, A., Di Francesco, P., Kurup, V. P., Wagner, H. and Romani, L. (2002) 'Vaccination of mice against invasive aspergillosis with recombinant Aspergillus proteins and CpG oligodeoxynucleotides as adjuvants', *Microbes and Infection*, 4(13), pp. 1281–1290.

Bozza, S., Perruccio, K., Montagnoli, C., Gaziano, R., Bellocchio, S., Burchielli, E., Nkwanyuo, G., Pitzurra, L., Velardi, A. and Romani, L. (2003) 'A dendritic cell vaccine against invasive aspergillosis in allogeneic hematopoietic transplantation', *Cell*, 102(10), pp. 3807–3814.

Bracci, L., Schiavoni, G., Sistigu, A. and Belardelli, F. (2014) 'Immune-based mechanisms of cytotoxic chemotherapy: Implications for the design of novel and rationale-based combined treatments against cancer', *Cell Death and Differentiation*, 21(1), pp. 15–25.

Brahmer, J. R., Tykodi, S. S., Chow, L. Q., Hwu, W. J., Topalian, S. L., Hwu, P., Drake, C. G., Camacho, L. H., Kauh, J., Odunsi, K., Pitot, H. C., Hamid, O., Bhatia, S., Martins, R., Eaton, K., Chen, S., Salay, T. M., Alaparthy, S., Grosso, J. F., Korman, A. J., Parker, S. M., Agrawal, S., Goldberg, S. M., Pardoll, D. M., Gupta, A. and Wigginton, J. M. (2012) 'Safety and activity of anti-PD-L1 antibody in patients with advanced cancer', *New England Journal of Medicine*, 366(26), pp. 2455–2465.

Bretscher, P. and Cohn, M. (1970) 'A theory of non-self discrimination', *Science*,

169(1964).

Le Brocq, M. L., Fraser, A. R., Cotton, G., Woznica, K., McCulloch, C. V, Hewit, K. D., McKimmie, C. S., Nibbs, R. J. B., Campbell, J. D. M. and Graham, G. J. (2014) 'Chemokines as novel and versatile reagents for flow cytometry and cell sorting', *Journal of Immunology*, 192, pp. 6120–6130.

Brown, C. E., Vishwanath, R. P., Aguilar, B., Starr, R., Najbauer, J., Aboody, K. S. and Jensen, M. C. (2007) 'Tumor-derived chemokine MCP-1/CCL2 is sufficient for mediating tumor tropism of adoptively transferred T cells', *The Journal of Immunology*, 179(5), pp. 3332–3341.

Brown, D., Fisher, T., Wei, C., Frelinger, J. and Lord, E. (2001) 'Tumours can act as adjuvants for humoral immunity', *Immunology*, 102(4), pp. 486–497.

van der Bruggen, P., Traversari, C., Chomez, P., Lurquin, C., Plaen, E. D. E., Van den Eynde, B., Knuth, A. and Boont, T. (1991) 'A gene encoding an antigen recognized by cytolytic T lymphocytes on a human melanoma', *Science*, 254(5048), pp. 1643–1648.

Busch, S., Acar, A., Magnusson, Y., Gregersson, P., Rydén, L. and Landberg, G. (2015) 'TGF-beta receptor type-2 expression in cancer-associated fibroblasts regulates breast cancer cell growth and survival and is a prognostic marker in pre-menopausal breast cancer', *Oncogene*, 34(1), pp. 27–38.

Butterfield, L. H. (2013) 'Dendritic cells in cancer immunotherapy clinical trials: Are we making progress?', *Frontiers in Immunology*, 4, pp. 3–9.

Butterfield, L. H., Ribas, A., Dissette, V. B., Amarnani, S. N., Vu, H. T., Oseguera, D., Wang, H.-J., Elashoff, R. M., McBride, W. H., Mukherji, B., Cochran, A. J., Glaspy, J. A. and Economou, J. S. (2003) 'Determinant spreading associated with clinical response in dendritic cell-based immunotherapy for malignant melanoma', *Clinical Cancer Research*, 9(3), pp. 998–1008.

Calabro, S., Liu, D., Gallman, A., Nascimento, M. S. L., Yu, Z., Zhang, T., Chen, P., Zhang, B., Gowthaman, U., Kirshnaswamy, J. K., Haberman, A. M., Williams, A. and Eisenbarth, S. C. (2016) 'Differential intrasplenic migration of dendritic cell subsets tailors adaptive immunity', *Cell Reports*, 16, pp. 2472–2485.

Cao, W. (2009) 'Molecular characterization of human plasmacytoid dendritic cells', *Journal of Clinical Immunology*, 29(3), pp. 257–264.

Carpentier, S., Vu Manh, T. P., Chelbi, R., Henri, S., Malissen, B., Haniffa, M., Ginhoux, F. and Dalod, M. (2016) 'Comparative genomics analysis of mononuclear phagocyte subsets confirms homology between lymphoid tissue-resident and dermal XCR1+DCs in mouse and human and distinguishes them from Langerhans cells', *Journal of Immunological Methods*, 432, pp. 35–49.

Carreno, B. M., Becker-Hapak, M., Huang, A., Chan, M., Alyasiry, A., Lie, W.-R., Aft, R. L., Cornelius, L. a., Trinkaus, K. M. and Linette, G. P. (2013) 'IL-12p70-producing patient DC vaccine elicits Tc1-polarized immunity', *Journal of Clinical Investigation*, 123(8), pp. 3383–3394.

Carreno, B. M., Magrini, V., Becker-hapak, M., Kaabinejadian, S., Hundal, J., Petti, A. A., Ly, A., Lie, W.-R., Hildebrand, W. H., Mardis, E. R. and Linette, G. P. (2015) 'A dendritic cell vaccine increases the breadth and diversity of melanoma neoantigen-specific T cells', *Science*, 348(6236), pp. 803–808.

Carson, D. A. and Lois, A. (1995) 'Cancer progression and p53', *The Lancet*, 346(8981), pp. 1009–1011.

Castle, J. C., Kreiter, S., Diekmann, J., Löwer, M., Van De Roemer, N., De Graaf, J., Selmi, A., Diken, M., Boegel, S., Paret, C., Koslowski, M., Kuhn, A. N., Britten, C. M., Huber, C., Türeci, Ö. and Sahin, U. (2012) 'Exploiting the mutanome for tumor vaccination', *Cancer Research*, 72(5), pp. 1081–1091.

Chaffer, C. L. and Weinberg, R. A. (2011) 'A perspective on cancer cell metastasis', *Science*, 331, pp. 1559–1565.

Chambers, C. A., Kuhns, M. S., Egen, J. G. and Allison, J. P. (2001) 'CTLA-4-mediated inhibition in regulation of T cell responses: Mechanisms and manipulation in tumor immunotherapy', *Annual Review of Immunology*, 19(1), pp. 565–594.

Chen, Y., Thai, P., Zhao, Y., Ho, Y., Desouza, M. M. and Wu, R. (2003) 'Stimulation of airway mucin gene expression by interleukin (IL)-17 through IL-6 paracrine/autocrine loop', *The Journal of Biological Chemistry*, 278(19), pp. 17036–17043.

Chiang, A. C. and Massagué, J. (2008) 'Molecular basis of metastasis', *New England Journal of Medicine*, 359(26), pp. 2814–2823.

Cisse, B., Caton, M. L., Lehner, M., Maeda, T., Scheu, S., Locksley, R., Holmberg, D., Zweier, C., Hollander, N. S. Den, Kant, S. G., Holter, W., Rauch, A., Zhuang, Y. and Reizis, B. (2008) 'Transcription factor E2-2 is an essential and specific regulator of plasmacytoid dendritic cell development', *Cell*, 135, pp. 37–48.

Constantino, J., Gomes, C., Falcao, A., Cruz, M. and Neves, B. (2016) 'Antitumour dendritic cell-based vaccines: lessons from 20 years of clinical trials and future perspectives', *Translational Research*, 168, pp. 74–95.

Constantino, J., Gomes, C., Falcão, A., Neves, B. M. and Cruz, M. T. (2017) 'Dendritic cell-based immunotherapy: A basic review and recent advances', *Immunologic Research*, 65(4), pp. 798–810.

Cooper, M. A., Fehniger, T. A. and Caligiuri, M. A. (2001) 'The biology of human natural killer-cell subsets', *Trends in Immunology*, 22(11), pp. 633–640.

Courau, T., Nehar-belaid, D., Florez, L., Levacher, B., Vazquez, T., Brimaud, F., Bellier, B. and Klatzmann, D. (2016) 'TGF- β and VEGF cooperatively control the immunotolerant tumor environment and the efficacy of cancer immunotherapies', *JCI Insight*, 1(9), pp. 1–16.

Crespo, J., Sun, H., Welling, T. H., Tian, Z. and Zou, W. (2013) 'T cell anergy, exhaustion, senescence and stemness in the tumor microenvironment', *Current Opinion in Immunology*, 25(2), pp. 214–221.

Curran, M. A., Montalvo, W., Yagita, H. and Allison, J. P. (2010) 'PD-1 and CTLA-4 combination blockade expands infiltrating T cells and reduces regulatory T and myeloid cells within B16 melanoma tumors', *Proceedings of the National Academy of Sciences*, 107(9), pp. 4275–4280.

Dankort, D., Curley, D. P., Cartlidge, R. A., Nelson, B., Anthony, N., Jr, W. E. D., You, M. J., Depinho, R. A. and Bosenberg, M. (2009) 'BRafV600E cooperates with Pten silencing to elicit metastatic melanoma', *Nature Genetics*, 41(5), pp. 544–552.

Delamarre, L., Holcombe, H. and Mellman, I. (2003) 'Presentation of exogenous antigens on major histocompatibility complex (MHC) class I and MHC class II molecules is differentially regulated during dendritic cell maturation', *The Journal of experimental medicine*, 198(1), pp. 111–22.

Diacovo, T. G., Blasius, A. L., Mak, T. W., Cella, M. and Colonna, M. (2005) 'Adhesive mechanisms governing interferon-producing cell recruitment into lymph nodes', *The Journal of Experimental Medicine*, 202(5), pp. 687–696.

DiLillo, D. J., Yanaba, K. and Tedder, T. F. (2010) 'B cells are required for optimal CD4+ and CD8+ T cell tumor immunity: therapeutic B cell depletion enhances B16 melanoma growth in mice', *Journal of Immunology*, 184(7), pp. 4006–4016.

Dillman, R. O. (2017) 'An update on the relevance of vaccine research for the treatment of metastatic melanoma', *Melanoma Management*, 4, pp. 203–215.

Dillman, R. O., Cornforth, A. N., Nistor, G. I., McClay, E. F., Amatruda, T. T. and Depriest, C. (2018) 'Randomized phase II trial of autologous dendritic cell vaccines versus autologous tumor cell vaccines in metastatic melanoma: 5-year follow up and additional analyses', *Journal for ImmunoTherapy of Cancer*, 6(19), pp. 1–10.

Dobrzanski, M. J., Reome, J. B. and Dutton, R. W. (1999) 'Therapeutic effects of tumor-reactive type 1 and type 2 CD8+ T cell subpopulations in established pulmonary metastases', *The Journal of Immunology*, 162(11), pp. 6671–6680.

Dohnal, A. M., Graffi, S., Witt, V., Eichstill, C., Wagner, D., Ul-Haq, S., Wimmer, D. and Felzmann, T. (2009) 'Comparative evaluation of techniques for the manufacturing of dendritic cell-based cancer vaccines', *Journal of Cellular and Molecular Medicine*, 13(1), pp. 125–135.

Domínguez, P. M., Ardavín, C., Dom, P. M. and Ardav, C. (2010) 'Differentiation and function of mouse monocyte-derived dendritic cells in steady state and inflammation', *Immunological Reviews*, 234(1), pp. 90–104.

Draube, A., Klein-González, N., Mattheus, S., Brillant, C., Hellmich, M., Engert, A. and von Bergwelt-Baildon, M. (2011) 'Dendritic cell based tumor vaccination in prostate and renal cell cancer: A systematic review and meta-analysis', *PLoS ONE*, 6(4).

Dubois, B., Massacrier, C., Vanbervliet, B., Fayette, J., Brière, F., Banchereau, J. and Caux, C. (1998) 'Critical role of IL-12 in dendritic cell-induced differentiation of naive B lymphocytes', *The Journal of Immunology*, 161, pp. 2223–2231.

Dunn, G. P., Bruce, A. T., Ikeda, H., Old, L. J. and Schreiber, R. D. (2002) 'Cancer immunoediting: from immuno-surveillance to tumor escape', *Nature Immunology*, 3(11), pp. 991–998.

Durgeau, A., Virk, Y., Corgnac, S. and Mami-Chouaib, F. (2018) 'Recent advances in targeting CD8 T-cell immunity for more effective cancer immunotherapy', *Frontiers in Immunology*, 9(14).

Dvorak H.F. (1987). 'Tumors: wounds that do not heal. Similarities between tumor stroma generation and wound healing', *New England Journal of Medicine* 315(26), pp. 1650-1659.

Dye, E. S. (1986) 'The antimetastatic function of concomitant antitumor immunity. II. Evidence that the generation of Ly-1+2+ effector T cells temporarily causes the destruction of already disseminated tumor cells', *Journal of Immunology*, 136(4), pp. 1510–1515.

Edlund, M., Sung, S. and Chung, L. W. K. (2004) 'Modulation of prostate cancer growth in bone microenvironments', *Journal of Cellular Biochemistry*, 91, pp. 686–705.

Eggermont, A. M. M. (2009) 'Immunostimulation versus immunosuppression after multiple vaccinations: The woes of therapeutic vaccine development', *Clinical Cancer Research*, 15(22), pp. 6745–6747.

Eggert, A. A. O., Schreurs, M. W. J., Boerman, O. C., Oyen, W. J. C., Boer, A. J. De, Punt, C. J. A., Figdor, C. G. and Adema, G. J. (1999) 'Biodistribution and vaccine efficiency of murine dendritic cells are dependent on the route of administration', *Cancer Research*, 59, pp. 3340–3345.

Elgueta, R., Benson, M. J., de Vries, V. C., Wasiuk, A., Guo, Y. and Noelle, R. J. (2013) 'Molecular mechanism and function of CD40/CD40L engagement in the immune system', *Immunological Reviews*, 229(1).

Emmanouilidis, N., Guo, Z., Dong, Y., Newton-West, M., Adams, A. B., Lee, E. D. H., Wang, J., Pearson, T. C., Larsen, C. P. and Newell, K. A. (2006) 'Immunosuppressive and

trafficking properties of donor splenic and bone marrow dendritic cells', *Transplantation*, 81(3), pp. 455–462.

Encke, J., Findeklee, J., Geib, J., Pfaff, E. and Stremmel, W. (2005) 'Prophylactic and therapeutic vaccination with dendritic cells against hepatitis C virus infection', *Clinical and Experimental Immunology*, 142(2), pp. 362–369.

Ersland, K., Wuthrich, M. and Klein, B. S. (2010) 'Dynamic interplay among monoctye-derived, dermal, and resident lymph node dendritic cells during the generation of vaccine immunity to fungi', *Cell Host & Microbe*, 7, pp. 474–487.

Eyles, J., Puaux, A. L., Wang, X., Toh, B., Prakash, C., Hong, M., Tan, T. G., Zheng, L., Ong, L. C., Jin, Y., Kato, M., Prévost-Blondel, A., Chow, P., Yang, H. and Abastado, J. P. (2010) 'Tumor cells disseminate early, but immunosurveillance limits metastatic outgrowth, in a mouse model of melanoma', *Journal of Clinical Investigation*, 120(6), pp. 2030–2039.

Faint, J. M., Annels, N. E., Curnow, S. J., Shields, P., Pilling, D., Hislop, A. D., Wu, L., Akbar, A. N., Buckley, C. D., Moss, P. A. H., Adams, D. H., Rickinson, A. B. and Salmon, M. (2001) 'Memory T cells constitute a subset of the human CD8+CD45RA+ pool with distinct phenotypic and migratory characteristics', *The Journal of Immunology*, 167(1), pp. 212–220.

Fearon, D. T., Manders, P. and Wagner, S. D. (2001) 'Arrested differentiation, the self-renewing memory lymphocyte, and vaccination', *Science*, 293(July), pp. 248–251.

Filaci, G., Contini, P., Fravega, M., Fenoglio, D., Azzarone, B., Julien-giron, M., Fiocca, R., Boggio, M., Necchi, V., Barbaro, A. D. L., Merlo, A., Rizzi, M., Ghio, M., Setti, M., Puppo, F., Zanetti, M. and Indiveri, F. (2002) 'Apoptotic DNA binds to HLA class II molecules inhibiting antigen presentation and participating in the development of anti-inflammatory functional behavior of phagocytic macrophages', *Human Immunology*, 64, pp. 9–20.

Fisher, B., Packard, B. S., Read, E. J., Carrasquillo, J. A., Carter, C. S., Topalian, S. L., Yang, J. C., Yolles, P., Larson, S. M. and Rosenberg, S. A. (1989) 'Tumor localization of adoptively transferred indium-111 labeled tumor infiltrating lymphocytes in patients with

metastatic melanoma', *Journal of Clinical Oncology*, 7(2), pp. 250–261.

Flynn, J. K. and Gorry, P. R. (2014) 'Stem memory T cells (TSCM)—their role in cancer and HIV immunotherapies', *Clinical & Translational Immunology*, 3(7), p. e20.

Fogg, D., Sibon, C., Miled, C., Jung, S., Aucouturier, P., Littman, D. R., Cumano, A. and Geissmann, F. (2006) 'A clonogenic bone marrow progenitor specific for macrophages and dendritic cells', *Science*, 311, pp. 83–87.

Fong, L., Brockstedt, D., Benike, C., Wu, L. and Engleman, E. G. (2001) 'Dendritic cells injected via different routes induce immunity in cancer patients', *The Journal of Immunology*, 166(6), pp. 4254–4259.

Fonteneau, J. F., Kavanagh, D. G., Lirvall, M., Sanders, C., Cover, T. L., Bhardwaj, N. and Larsson, M. (102AD) 'Characterization of the MHC class I crosspresentation pathway for cell associated antigens by human dendritic cells', *Blood*, (13), pp. 4448–4455.

Förster, R., Davalos-Misslitz, A. C. and Rot, A. (2008) 'CCR7 and its ligands: Balancing immunity and tolerance', *Nature Reviews Immunology*, 8, pp. 362–371.

Francia, G., Cruz-Munoz, W., Man, S., Xu, P. and Kerbel, R. S. (2011) 'Mouse models of advanced spontaneous metastasis for experimental therapeutics', *Nature Reviews Cancer*, 11(2), pp. 135–41.

Fransen, M. F., Arens, R. and Melief, C. J. M. (2013) 'Local targets for immune therapy to cancer: Tumor draining lymph nodes and tumor microenvironment', *International Journal of Cancer*, 132, pp. 1971–1976.

Fridlender, Z. G., Sun, J., Kim, S., Kapoor, V., Cheng, G., Ling, L., Worthen, G. S. and Albelda, S. M. (2009) 'Polarization of tumour-associated neutrophil (TAN) phenotype by TGFbeta: "N1" versus "N2" TAN', *Cancer Cell*, 16(3), pp. 183–194.

Fučíková, J., Rožková, D., Ulčová, H., Budinský, V., Sochorová, K., Pokorná, K., Bartůňková, J. and Špíšek, R. (2011) 'Poly I:C-activated dendritic cells that were generated in CellGro for use in cancer immunotherapy trials', *Journal of Translational Medicine*, 9(223), pp. 1–10.

Galluzzi, L., Senovilla, L., Vacchelli, E., Eggermont, A., Fridman, W. H., Galon, J., Sautès-Fridman, C., Tartour, E., Zitvogel, L. and Kroemer, G. (2012) 'Trial watch: Dendritic cell-based interventions for cancer therapy', *OncoImmunology*, 1(7), pp. 1111–1134.

García, F. and Routy, J. P. (2011) 'Challenges in dendritic cells-based therapeutic vaccination in HIV-1 infection. Workshop in dendritic cell-based vaccine clinical trials in HIV-1', *Vaccine*, 29(38), pp. 6454–6463.

Garetto, S., Sardi, C., Martini, E., Roselli, G., Morone, D., Angioni, R., Cianciotti, B. C., Trovato, A. E., Franchina, D. G., Castino, G. F., Vignali, D., Erreni, M., Marchesi, F., Rumio, C., Kallikourdis, M., Garetto, S., Sardi, C., Martini, E., Roselli, G., Morone, D., Angioni, R., Cianciotti, B. C., Trovato, A. E., Franchina, D. G., Castino, G. F., Vignali, D., Erreni, M., Marchesi, F., Rumio, C. and Kallikourdis, M. (2016) 'Tailored chemokine receptor modification improves homing of adoptive therapy T cells in a spontaneous tumor model', *Oncotarget*, 7(28), pp. 43010–43026.

Garg, A. D., Coulie, P. G., Van den Eynde, B. J. and Agostinis, P. (2017) 'Integrating next-generation dendritic cell vaccines into the current cancer immunotherapy landscape', *Trends in Immunology*, 38(8), pp. 577–593.

Garg, A. D., Vara Perez, M., Schaaf, M., Agostinis, P., Zitvogel, L., Kroemer, G. and Galluzzi, L. (2017) 'Trial watch: Dendritic cell-based anticancer therapy', *OncoImmunology*, 6(7).

Gattinoni, L., Lugli, E., Ji, Y., Pos, Z., Paulos, C. M., Quigley, M. F., Almeida, J. R., Gostick, E., Yu, Z., Carpenito, C., Wang, E., Douek, D. C., Price, D. A., June, C. H., Marincola, F. M., Roederer, M. and Restifo, N. P. (2012) 'A human memory T-cell subset with stem cell-like properties', *Nature Medicine*, 17(10), pp. 1290–1297.

Gay, C. L., DeBenedette, M. A., Tcherepanova, I. Y., Gamble, A., Lewis, W. E., Cope, A. B., Kuruc, J. D., McGee, K. S., Kearney, M. F., Coffin, J. M., Archin, N. M., Hicks, C. B., Eron, J. J., Nicolette, C. A. and Margolis, D. M. (2017) 'Immunogenicity of AGS-004 dendritic cell therapy in patients treated during acute HIV infection', *AIDS Research and Human Retroviruses*, 00(00), p. aid.2017.0071.

Geissler, K., Fornara, P., Lautenschläger, C., Holzhausen, H.-J., Seliger, B. and Riemann, D. (2015) 'Immune signature of tumor infiltrating immune cells in renal cancer', *OncoImmunology*, 4(1), p. e985082.

Geissmann, F., Jung, S. and Littman, D. R. (2003) 'Blood monocytes consist of two principal subsets with distinct migratory properties', *Immunity*, 19(1), pp. 71–82.

Gerard, C. and Rollins, B. J. (2001) 'Chemokines and disease', *Nature Immunology*, 2, pp. 108–115.

Golubovskaya, V. and Wu, L. (2016) 'Different subsets of T cells, memory, effector functions, and CAR-T immunotherapy', *Cancers*, 8(3).

Gorvel, L., Korenfeld, D. and Tung, T. (2017) 'Dendritic cell-derived IL-32alpha: A novel inhibitory cytokine of NK cell function', *Journal of Immunology*, 199.

Gourley, C., Michie, C. O., Roxburgh, P., Yap, T. A., Harden, S., Paul, J., Ragupathy, K., Todd, R., Petty, R., Reed, N., Hayward, R. L., Mitchell, P., Rye, T., Schellens, J. H. M., Lubinski, J., Carmichael, J., Kaye, S. B., Mackean, M. and Ferguson, M. (2010) 'Increased incidence of visceral metastases in Scottish patients with BRCA1/2-defective ovarian cancer: an extension of the ovarian BRCAness phenotype', *Journal of Clinical Oncology*, 28(15), pp. 2505–2511.

Governa, V., Trella, E., Mele, V., Tornillo, L., Amicarella, F., Cremonesi, E., Muraro, M. G., Xu, H., Droeser, R., Däster, S. R., Bolli, M., Rosso, R., Oertli, D., Eppenberger-Castori, S., Terracciano, L. M., Iezzi, G. and Spagnoli, G. C. (2017) 'The interplay between neutrophils and CD8+ T cells improves survival in human colorectal cancer', *Clinical Cancer Research*, 23(14), pp. 3847–3858.

Graddis, T. J., McMahan, C. J., Tamman, J., Page, K. J. and Trager, J. B. (2011) 'Prostatic acid phosphatase expression in human tissues', *International Journal of Clinical and Experimental Pathology*, 4(3), pp. 295–306.

Grazziutti, M., Przepiorka, D., Rex, J. H., Braunschweig, I. and Savary, C. A. (2001) 'Lymphocyte stimulation Dendritic cell-mediated stimulation of the in vitro lymphocyte response to Aspergillus', pp. 647–652.

Greenwald, R. J., Boussiotis, V. A., Lorsbach, R. B., Abbas, A. K., Sharpe, A. H. and Jude, S. (2001) 'CTLA-4 regulates induction of anergy in vivo', *Immunity*, 14, pp. 145–155.

Greter, M., Helft, J., Chow, A., Hashimoto, D., Mortha, A., Agudo-Cantero, J., Bogunovic, M., Gautier, E. L., Miller, J., Leboeuf, M., Lu, G., Aloman, C., Brown, B. D., Pollard, J. W., Xiong, H., Randolph, G. J., Chipuk, J. E., Frenette, P. S. and Merad, M. (2012) 'GM-CSF controls nonlymphoid tissue dendritic cell homeostasis but is dispensable for the differentiation of inflammatory dendritic cells', *Immunity*, 36(6), pp. 1031–1046.

Grewal, I. S. and Flavell, R. A. (1998) 'CD40 and CD154 in cell-mediated immunity', *Annual Review of Immunology*, 16, pp. 111–135.

Griffith, J. W., Sokol, C. L. and Luster, A. D. (2014) 'Chemokines and chemokine receptors: Positioning cells for host defence and immunity', *Annual Review of Immunology*, 32(1), pp. 659–702.

Grivennikov, S. I., Greten, F. R. and Karin, M. (2011) 'Immunity, inflammation and cancer', *Cell*, 140(6), pp. 883–899.

Gross, L. (1943). 'Intradermal immunization of C3H mice against a sarcoma that originated in an animal of the same line', *Cancer Research*, 3, pp. 326–33

Grotendorst, G. R., Rahmanie, H. and Duncan, M. R. (2004) 'Combinatorial signaling pathways determine fibroblast proliferation and myofibroblast differentiation', *The FASEB Journal*, 18(3), pp. 469–479.

Grouard, G., Rissoan, M. C., Filgueira, L., Durand, I., Banchereau, J. and Liu, Y. J. (1997) 'The enigmatic plasmacytoid T cells develop into dendritic cells with interleukin (IL)-3 and CD40-ligand', *The Journal of Experimental Medicine*, 185(6), pp. 1101–11.

Grundy, M. A., Zhang, T. and Sentman, C. L. (2007) 'NK cells rapidly remove B16F10 tumor cells in a perforin and interferon-gamma independent manner in vivo', *Cancer Immunology, Immunotherapy*, 56(8), pp. 1153–1161.

Guermonprez, P., Valladeau, J., Zitvogel, L., Théry, C. and Amigorena, S. (2002) 'Antigen presentation and T cell stimulation by dendritic cells', *Annual Review of Immunology*, 20, pp. 621–667.

Gulley, J. L., Madan, R. A. and Schlom, J. (2011) 'Impact of tumour volume on the potential efficacy of therapeutic vaccines', *Current Oncology*, 18(3), pp. 150–157.

Guy, T. V, Terry, A. M., Bolton, H. A., Hancock, D. G., Zhu, E., Brink, R., Mcguire, H. M. and Shklovskaya, E. (2016) 'Collaboration between tumor-specific CD4 + T cells and B cells in anti-cancer immunity', *Oncotarget*, 7(21).

Haessler, U., Pisano, M., Wu, M. and Swartz, M. A. (2011) 'Dendritic cell chemotaxis in 3D under defined chemokine gradients reveals differential response to ligands CCL21 and CCL19', *Proceedings of the National Academy of Sciences of the United States of America*, 108(14), pp. 5614–9.

Hagberg, N., Berggren, O., Leonard, D., Weber, G., Bryceson, Y. T., Alm, G. V., Eloranta, M.-L. and Ronnblom, L. (2011) 'IFN-alpha production by plasmacytoid dendritic cells stimulated with RNA-containing immune complexes is promoted by NK cells via MIP-1 beta and LFA-1', *The Journal of Immunology*, 186(9), pp. 5085–5094.

van den Ham, H.-J., Cooper, J. D., Tomasik, J., Bahn, S., Aerts, J. L., Osterhaus, A. D. M. E., Gruters, R. A. and Andeweg, A. C. (2018) 'Dendritic cell immunotherapy followed by cART interruption during HIV-1 infection induces plasma protein markers of cellular immunity and neutrophil recruitment', *PLoS ONE*, 13(2), pp. 1–17.

Hanahan, D. and Weinberg, R. A. (2000) 'The hallmarks of cancer', *Cell*, 100, pp. 57–70.

Hanahan, D. and Weinberg, R. A. (2011) 'Hallmarks of cancer: the next generation', *Cell*, 144(5), pp. 646–674.

Hanna, M. G., Hoover, H. C., Pinedo, H. M. and Finer, M. (2006) 'Active specific immunotherapy with autologous tumor cell vaccines for stage II colon cancer: logistics, efficacy, safety and immunological pharmacodynamics', *Human Vaccines*, 2(4), pp. 185–191.

Harlin, H., Meng, Y., Peterson, A. C., Zha, Y., Tretiakova, M., Slingluff, C., McKee, M. and Gajewski, T. F. (2009) 'Chemokine expression in melanoma metastases associated with CD8+ T cell recruitment', *Cancer Research*, 69(7), pp. 1–18.

Harrell, M. I., Iritani, B. M. and Ruddell, A. (2008) 'Lymph node mapping in the mouse',

Journal of Immunological Methods, 332(1–2), pp. 170–174. doi: 10.1016/j.jim.2007.11.012.

Hauser, M. A. and Legler, D. F. (2016) 'Common and biased signaling pathways of the chemokine receptor CCR7 elicited by its ligands CCL19 and CCL21 in leukocytes', *Journal of Leukocyte Biology*, 99(June), pp. 1–14.

Heink, S., Yogev, N., Garbers, C., Herwerth, M., Aly, L., Gasperi, C., Husterer, V., Croxford, A. L., Möller-hackbarth, K., Bartsch, H. S., Sotlar, K., Krebs, S., Regen, T., Blum, H., Hemmer, B., Misgeld, T., Wunderlich, T. F. and Hidalgo, J. (2017) 'Trans-presentation of IL-6 by dendritic cells is required for the priming of pathogenic Th17 cells', *Nature Immunology*, 18(1), pp. 74–88.

Helft, J., Böttcher, J., Chakravarty, P., Zelenay, S., Huotari, J., Schraml, B. U., Goubau, D. and Reis e Sousa, C. (2015) 'GM-CSF mouse bone marrow cultures comprise a heterogeneous population of CD11c+MHCII+ macrophages and dendritic cells', *Immunity*, 42(6), pp. 1197–1211.

Hieshima, K., Ohtani, H., Shibano, M., Izawa, D., Nakayama, T., Kawasaki, Y., Shiba, F., Shiota, M., Katou, F., Saito, T. and Yoshie, O. (2003) 'CCL28 has dual roles in mucosal immunity as a chemokine with broad-spectrum antimicrobial activity', *Journal of Immunology*, 170(3), pp. 1452–61.

Hilkens, C. M. U., Isaacs, J. D. and Thomson, A. W. (2010) 'Development of Dendritic Cell-Based Immunotherapy for Autoimmunity', *International Reviews of Immunology*, 29(2), p. 183.

Hobo, W., Strobbe, L., Maas, F. and Fredrix, H. (2013) 'Immunogenicity of dendritic cells pulsed with MAGE3 , Survivin and B-cell maturation antigen mRNA for vaccination of multiple myeloma patients', *Cancer Immunology, Immunotherapy*, 62, pp. 1381–1392.

Hodi, F. S., O'Day, S. J., McDermott, D. F., Weber, R. W., Sosman, J. A., Haanen, J. B., Gonzalez, R., Robert, C., Schadendorf, D., Hassel, J. C., Akerley, W., van den Eertwegh, A. J. M., Lutzky, J., Lorigan, P., Vaubel, J. M., Linette, G. P., Hogg, D., Ottensmeier, C. H., Lebbé, C., Peschel, C., Quirt, I., Clark, J. I., Wolchok, J. D., Weber, J. S., Tian, J., Yellin, M. J., Nichol, G. M., Hoos, A. and Urba, W. J. (2010) 'Improved survival with

ipilimumab in patients with metastatic melanoma', *New England Journal of Medicine*, 363(8), pp. 711–723.

Hoffman, P. C., Mauer, A. M. and Vokes, E. E. (2000) 'Lung cancer', *The Lancet*, 355, pp. 479–485.

Hoves, S., Ooi, C.-H., Wolter, C., Sade, H., Bissinger, S., Schmittnaegel, M., Ast, O., Giusti, A. M., Wartha, K., Runza, V., Xu, W., Kienast, Y., Cannarile, M. A., Levitsky, H., Romagnoli, S., De Palma, M., Rüttinger, D. and Ries, C. H. (2018) 'Rapid activation of tumor-associated macrophages boosts preexisting tumor immunity', *The Journal of Experimental Medicine*.

Hsu, F., Fagnoni, F., Benike, C., Liles, T., Czerwinski, D., Taidi, B., Engleman, E. and Levy, R. (1996) 'Vaccination of patients with B-cell lymphoma using autologous antigen-pulsed dendritic cells', *Nature Medicine*, 2(1), pp. 52–58.

Huang, A. Y., Golumbek, P., Ahmadzadeh, M., Jaffee, E., Pardoll, D. and Levitsky, H. (1994) 'Role of bone marrow-derived cells in presenting MHC class I-restricted tumor antigens', *Science*, 264(428), pp. 961–965.

Huang, Q., Liu, D., Majewski, P., Schulte, L. C., Korn, J. M., Young, R. A., Lander, E. S. and Haco (2001) 'The plasticity of dendritic cell responses to pathogens and their contents', *Science*, 294, pp. 870–875.

Hung, K., Hayashi, R., Lafond-Walker, A., Lowenstein, C., Pardoll, D. and Levitsky, H. (1998) 'The central role of CD4+ T cells in the antitumor immune response', *Journal of Experimental Medicine*, 188(12), pp. 2357–2368.

Idorn, M., Skadborg, S. K., Kellermann, L., Halldórsdóttir, H. R., Holmen Olofsson, G., Met, Ö. and thor Straten, P. (2018) 'Chemokine receptor engineering of T cells with CXCR2 improves homing towards subcutaneous human melanomas in xenograft mouse model', *OncoImmunology*.

Igarashi, T., Takahashi, H., Tobe, T., Suzuki, H., Mizoguchi, K., Nakatsu, H.-O. and Ito, H. (2002) 'Effect of tumor-infiltrating lymphocyte subsets on prognosis and susceptibility to interferon therapy in patients with renal cell carcinoma', *Urologia Internationalis*, 69(1), pp. 51–56.

Imai, K., Matsuyama, S., Miyake, S., Suga, K. and Nakachi, K. (2000) 'Natural cytotoxic activity of peripheral-blood lymphocytes and cancer incidence: an 11-year follow-up study of a general population', *The Lancet*, 356(9244), pp. 1795–1799.

Ishigami, S., Natsugoe, S., Tokuda, K., Nakajo, A., Che, X., Iwashige, H., Aridome, K., Hokita, S. and Aikou, T. (2000) 'Prognostic value of intratumoral natural killer cells in gastric carcinoma', *Cancer*, 88(3), pp. 577–583.

Ishiguro, T., Nakajima, M., Naito, M., Muto, T. and Tsuruo, T. (1996) 'Identification of genes differentially expressed in B16 murine melanoma sublines with different metastatic potentials identification of genes differentially expressed in B16 murine melanoma Sublines with Different Metastatic Potentials '', *Cancer Research*, 56, pp. 875–879.

Ito, T., Yang, M., Wang, Y.-H., Lande, R., Gregorio, J., Perng, O. A., Qin, X.-F., Liu, Y.-J. and Gilliet, M. (2007) 'Plasmacytoid dendritic cells prime IL-10–producing T regulatory cells by inducible costimulator ligand', *The Journal of Experimental Medicine*, 204(1), pp. 105–115.

Jablonska, J., Leschner, S., Westphal, K., Lienenklaus, S. and Weiss, S. (2010) 'Neutrophils responsive to endogenous IFN-b regulate tumor angiogenesis and growth in a mouse tumor model', *Journal of Clinical Investigation*, 120(4), pp. 1151–1164.

Jakubzick, C., Gautier, E. L., Gibbings, S. L., Sojka, D. K., Schlitzer, A., Johnson, T. E., Ivanov, S., Duan, Q., Bala, S., Condon, T., VanRooijen, N., Grainger, J. R., Belkaid, Y., Ma'ayan, A., Riches, D. W. H., Yokoyama, W. M., Ginhoux, F., Henson, P. M. and Randolph, G. J. (2013) 'Minimal differentiation of classical monocytes as they survey steady-state tissues and transport antigen to lymph nodes', *Immunity*. Elsevier Inc., 39(3), pp. 599–610.

Janssen, L. M. E., Ramsay, E. E., Logsdon, C. D. and Overwijk, W. W. (2017) 'The immune system in cancer metastasis: friend or foe?', *Journal for ImmunoTherapy of Cancer*, 5(1), pp. 1–14.

Jin, P., Han, T. H., Ren, J., Saunders, S., Wang, E., Marincola, F. M. and Stroncek, D. F. (2010) 'Molecular signatures of maturing dendritic cells: implications for testing the quality of dendritic cell therapies', *Journal of Translational Medicine*, 8, p. 4.

Jongmans, W., Tiemessen, D. M., Van Vlodrop, I. J. H., Mulders, P. F. A. and Oosterwijk, E. (2005) 'Th1-polarizing capacity of clinical-grade dendritic cells is triggered by ribomunyl but is compromised by PGE2: The importance of maturation cocktails', *Journal of Immunotherapy*, 28(5), pp. 480–487.

Jonuleit, H., Giesecke-Tuettenberg, A., Tüting, T., Thurner-Schuler, B., Stuge, T. B., Paragnik, L., Kandemir, A., Lee, P. P., Schuler, G., Knop, J. and Enk, A. H. (2001) 'A comparison of two types of dendritic cell as adjuvants for the induction of melanoma-specific T-cell responses in humans following intranodal injection', *International Journal of Cancer*, 93(2), pp. 243–251.

Kaech, S. M., Wherry, E. J. and Ahmed, R. (2002) 'Effector and memory T-Cell differentiation: Implications for vaccine development', *Nature Reviews Immunology*, 2(4), pp. 251–262.

Kakarla, S. and Gottschalk, S. (2015) 'CAR T cells for solid tumors: armed and ready to go?', *Cancer Journal*, 20(2), pp. 151–155.

Kamala, T. (2008) 'Hock immunization: a human alternative to mouse footpad injections', *Journal of Immunological Methods*, 328(1–2), pp. 204–214.

Kamphorst, A. O., Guermonprez, P., Dudziak, D. and Nussenzweig, M. C. (2010) 'Route of antigen uptake differentially impacts presentation by dendritic cells and activated monocytes', *The Journal of Immunology*, 185, pp. 3426–3435.

Kandoth, C., McLellan, M. D., Xie, M., Zhang, Q., Mcmichael, J. F., Wyczalkowski, M. A., Wendl, M. C., Ley, T. J., Wilson, R. K., Raphael, B. J. and Ding, L. (2013) 'Mutational landscape and significance across 12 major cancer types', *Nature*, 502(7471), pp. 333–339.

Kantoff, P. W., Higano, C. S., Shore, N. D., Berger, R., Small, E. J., Penson, D. F., Redfern, C. H., Ferrari, A. C., Dreicer, R., Sims, R. B., Xu, Y., Frohlich, M. W. and Schellhammer, P. F. (2010) 'Sipuleucel-T immunotherapy for castration-resistant prostate cancer', *New England Journal of Medicine*, 363(5), pp. 411–422.

Karrison, T. G., Donald, J. and Meier, P. (1999) 'Dormancy of mammary carcinoma after mastectomy', *Journal of the National Cancer Institute*, 91, pp. 80–85.

Kaser, A., Dunzendorfer, S., Offner, F. A., Ryan, T., Schwabegger, A., Cruikshank, W. W., Wiedermann, C. J. and Tilg, H. (1999) 'A role for IL-16 in the cross-talk between dendritic cells and T cells', *Journal of Immunology*, 163(6), pp. 3232–8.

Keir, M. E. and Sharpe, A. H. (2005) 'The B7/CD28 costimulatory family in autoimmunity', *Immunological Reviews*, 204, pp. 128–143.

Mac Keon, S., Ruiz, M. S., Gazzaniga, S. and Wainstok, R. (2015) 'Dendritic cell-based vaccination in cancer: Therapeutic implications emerging from murine models', *Frontiers in Immunology*, 6, pp. 1–18.

Kershaw, M.H., Wang, G., Westwood, J.A., Pachynoki, R.K., Tiffany, H.L., Marincola, F.M., Wang, E., Young, H.A., Murphy, P.M. and Hwu, P. (2002). 'Redirecting migration of t cells to chemokine secreted from tumors by genetic modification with CXCR2', *Human Gene Therapy,* 13(16), pp. 1971-1980.

Kirkwood, J. M., Butterfield, L. H., Tarhini, A. A. and Zarour, H. (2012) 'Immunotherapy of cancer in 2012', *CA: A Cancer Journal for Clinicians*, 62(5), pp. 309–335.

Kissenpfennig, A. and Malissen, B. (2006) 'Langerhans cells - Revisiting the paradigm using genetically engineered mice', *Trends in Immunology*, 27(3), pp. 132–139.

Klebanoff, C. a., Gattinoni, L. and Restifo, N. P. (2006) 'CD8+ T-cell memory in tumor immunology and immunotherapy', *Immunological Reviews*, 211, pp. 214–224.

Klebanoff, C. A., Gattinoni, L. and Restifo, N. P. (2012) 'Sorting through subsets: Which T-Cell populations mediate highly effective adoptive immunotherapy?', *Journal of Immunotherapy*, 35(9), pp. 651–660.

Klebanoff, C. A., Gattinoni, L., Torabi-Parizi, P., Kerstann, K., Cardones, A. R., Finkelstein, S. E., Palmer, D. C., Antony, P. A., Hwang, S. T., Rosenberg, S. A., Waldmann, T. A. and Restifo, N. P. (2005) 'Central memory self/tumor-reactive CD8+ T cells confer superior antitumor immunity compared with effector memory T cells', *Proceedings of the National Academy of Sciences*, 102(27), pp. 9571–9576.

Klebanoff, C. a, Finkelstein, S. E., Surman, D. R., Lichtman, M. K., Gattinoni, L., Theoret, M. R., Grewal, N., Spiess, P. J., Antony, P. a, Palmer, D. C., Tagaya, Y., Rosenberg, S. a,

Waldmann, T. a and Restifo, N. P. (2004) 'IL-15 enhances the in vivo antitumor activity of tumor-reactive CD8+ T cells', *Proceedings of the National Academy of Sciences*, 101(7), pp. 1969–1974.

Kline, J., Zhang, L., Battaglia, L., Cohen, K. S. and Gajewski, T. F. (2012) 'Cellular and molecular requirements for rejection of B16 melanoma in the setting of regulatory T cell depletion and homeostatic proliferation', *Journal of Immunology*, 188(6), pp. 2630–2642.

Koebel, C. M., Vermi, W., Swann, J. B., Zerafa, N., Rodig, S. J., Old, L. J., Smyth, M. J. and Schreiber, R. D. (2007) 'Adaptive immunity maintains occult cancer in an equilibrium state', *Nature*, 450, pp. 903–908.

Kohrgruber, N., Gröger, M., Meraner, P., Kriehuber, E., Petzelbauer, P., Brandt, S., Stingl, G., Rot, A. and Maurer, D. (2004) 'Plasmacytoid dendritic cell recruitment by immobilized CXCR3 ligands', *Journal of Immunology*, 173(11), pp. 6592–6602.

Koop, S., Macdonald, I. C., Luzzi, K., Schmidt, E. E., Morris, V. L., Grattan, M., Khokha, R., Chambers, A. F. and Groom, A. C. (1995) 'Fate of melanoma cells entering the microcirculation: over 80% survive and extravasate', *Cancer Research*, 55, pp. 2520–2524.

Krause, P., Bruckner, M., Uermösi, C., Singer, E., Groettrup, M., Daniel, F., Dc, W., Uermo, C. and Legler, D. F. (2009) 'Prostaglandin E2 enhances T-cell proliferation by inducing the costimulatory molecules OX40L, CD70, and 4-1BBL on dendritic cells', *Blood*, 113(113), pp. 2451–2460.

Kremer, V., Ligtenberg, M., Zendehdel, R., Seitz, C., Duivenvoorden, A., Wennerberg, E., Colón, E., Scherman-Plogell, A. H. and Lundqvist, A. (2017) 'Genetic engineering of human NK cells to express CXCR2 improves migration to renal cell carcinoma', *Journal for ImmunoTherapy of Cancer*, 5(1), pp. 1–13.

Krug, A., Uppaluri, R., Facchetti, F., Brigitte, G., Sheehan, K. C. F., Schreiber, R. D., Cella, M. and Colonna, M. (2002) 'IFN-producing cells respond to CXCR3 ligands in the presence of CXCL12 and secrete inflammatory chemokines upon activation', *The Journal of Immunology*, 169, pp. 6079–6083.

Kurachi, M., Kurachi, J., Suenaga, F., Tsukui, T., Abe, J., Ueha, S., Tomura, M., Sugihara,

K., Takamura, S., Kakimi, K. and Matsushima, K. (2011) 'Chemokine receptor CXCR3 facilitates CD8(+) T cell differentiation into short-lived effector cells leading to memory degeneration', *The Journal of Experimental Medicine*, 208(8), pp. 1605–20.

Kwak, M., Mu, L., Lu, Y., Chen, J. J., Wu, Y., Brower, K. and Fan, R. (2013) 'Single-cell protein secretomic signatures as potential correlates to tumor cell lineage evolution and cell-cell interaction', *Frontiers in Oncology*, 3, pp. 1–8.

Labarrière, N., Bretaudeau, L., Gervois, N., Bodinier, M., Bougras, G., Diez, E., Lang, F., Gregoire, M. and Jotereau, F. (2002) 'Apoptotic body-loaded dendritic cells efficiently cross-prime cytotoxic T lymphocytes specific for NA17-A antigen but not for Melan-A/MART-1 antigen', *International Journal of Cancer*, 101, pp. 280–286.

Langenkamp, A., Messi, M., Lanzavecchia, A. and Sallusto, F. (2000) 'Kinetics of dendritic cell activation: Impact on priming of TH1, TH2 and nonpolarized T cells', *Nature Immunology*, 1(4), pp. 311–316.

Langlet, C., Tamoutounour, S., Henri, S., Luche, H., Ardouin, L., Gregoire, C., Malissen, B. and Guilliams, M. (2012) 'CD64 expression distinguishes monocyte-derived and conventional dendritic cells and reveals their distinct role during intramuscular immunization', *The Journal of Immunology*, 188(4), pp. 1751–1760.

Lappin, M. B., Weiss, J. M., Delattre, V., Mai, B., Dittmar, H., Maier, C., Manke, K., Grabbe, S., Martin, S. and Simon, J. C. (1999) 'Analysis of mouse dendritic cell migration in vivo upon subcutaneous and intravenous injection', *Immunology*, 98(2), pp. 181–188.

Larregina, A. T., Morelli, A. E., Spencer, L. A., Logar, A. J., Watkins, S. C., Thomson, A. W. and Falo, L. D. (2001) 'Dermal-resident CD14+ cells differentiate into Langerhans cells', *Nature Immunology*, 2(12), pp. 1151–1158.

Larson, R. S. and Springer, T. A. (1990) 'Structure and function of leukocyte integrins', *Immunological Reviews*, (114), pp. 1037–1050.

Lee, A. W., Truong, T., Bickham, K., Fonteneau, J. F., Larsson, M., Da Silva, I., Somersan, S., Thomas, E. K. and Bhardwaj, N. (2002) 'A clinical grade cocktail of cytokines and PGE2 results in uniform maturation of human monocyte-derived dendritic cells: Implications for immunotherapy', *Vaccine*, 20, pp. 8–22.

Lelouard, H., Gatti, E., Cappello, F., Gresser, O., Camosseto, V. and Pierre, P. (2002) 'Transient aggregation of ubiquitinated proteins during dendritic cell maturation', *Nature*, 417, pp. 177–182.

Lennerz, V., Fatho, M., Gentilini, C., Frye, R. a, Lifke, A., Ferel, D., Wölfel, C., Huber, C. and Wölfel, T. (2005) 'The response of autologous T cells to a human melanoma is dominated by mutated neoantigens', *Proceedings of the National Academy of Sciences*, 102(44), pp. 16013–16018.

Lennon, P., Crotty, M. and Fenton, J. E. (2015) 'Infectious mononucleosis', *The British Medical Journal*, 250, pp. 29–32.

Lesterhuis, W. J., De Vries, I. J. M., Schreibelt, G., Lambeck, A. J. A., Aarntzen, E. H. J. G., Jacobs, J. F. M., Scharenborg, N. M., Van De Rakt, M. W. M. M., De Boer, A. J., Croockewit, S., Van Rossum, M. M., Mus, R., Oyen, W. J. G., Boerman, O. C., Lucas, S., Adema, G. J., Punt, C. J. A. and Figdor, C. G. (2011) 'Route of administration modulates the induction of dendritic cell vaccine-induced antigen-specific T cells in advanced melanoma patients', *Clinical Cancer Research*, 17, pp. 5725–5735.

Lim, D. S., Kim, J. H., Lee, D. S., Yoon, C. H. and Bae, Y. S. (2007) 'DC immunotherapy is highly effective for the inhibition of tumor metastasis or recurrence, although it is not efficient for the eradication of established solid tumors', *Cancer Immunology, Immunotherapy*, 56(11), pp. 1817–1829.

Lim, K., Hyun, Y.-M., Lambert-Emo, K., Capece, T., Bae, S., Miller, R., Topham, D. J. and Kim, M. (2015) 'Neutrophil trails guide influenza-specific CD8+ T cells in the airways', *Science*, 349(6252).

Liu, K., Victora, G. and Schwickert, T. (2009) 'In vivo analysis of dendritic cell development and homeostasis', *Science*, 324(April), pp. 392–397.

Liu, R., Lauridsen, H. M., Amezquita, R. A., Pierce, R. W., Jane-wit, D., Fang, C., Amanda, S., Kirkiles-smith, N. C., Gonzalez, A. L. and Pober, J. S. (2016) 'IL-17 promotes neutrophil-mediated immunity by activating microvascular pericytes and not endothelium', *The Journal of experimental medicine*, 197, pp. 2400–2408.

Lorenzo-Redondo, R., Fryer, H. R., Bedford, T., Kim, E., Archer, J., Kosakovsky Pond, S.

L., Chung, Y.-S., Penugonda, S., Chipman, J. G., Fletcher, C. V, Schacker, T. W., Malim, M. H., Rambaut, A., Haase, A. T., McLean, A. R. and Wolinsky, S. M. (2016) 'Persistent HIV-1 replication maintains the tissue reservoir during therapy', *Nature*, 530(7588), pp. 51–56.

Lu, W., Arraes, L. C., Ferreira, W. T. and Andrieu, J. M. (2004) 'Therapeutic dendritic-cell vaccine for chronic HIV-1 infection', *Nature Medicine*, 10(12), pp. 1359–1365.

Lucas, P. J., Negishi, I., Nakayama, K., Fields, L. E. and Loh, D. Y. (1995) 'Naive CD28-deficient T cells can initiate but not sustain an in vitro antigen-specific immune response.', *The Journal of Immunology*, 154, pp. 5757–5768.

Lundberg, K., Albrekt, A.-S., Nelissen, I., Santegoets, S., Gruijl, T. D. De, Gibbs, S. and Lindstedt, M. (2013) 'Transcriptional profiling of human dendritic cell populations and models - unique profiles of in vitro dendritic cells and implications on functionality and applicability', *PLoS ONE*, 8(1), p. e52875.

Luther, S. A., Tang, H. L., Hyman, P. L., Farr, A. G. and Cyster, J. G. (2000) 'Coexpression of the chemokines ELC and SLC by T zone stromal cells and deletion of the ELC gene in the plt/plt mouse', *Proceedings of the National Academy of Sciences*, 97(23), pp. 12694–12699.

Luther, S. a and Cyster, J. G. (2001) 'Chemokines as regulators of T cell differentiation.', *Nature Immunology*, 2(2), pp. 102–107.

Lutz, M. B., Strobl, H., Schuler, G. and Romani, N. (2017) 'GM-CSF monocyte-derived cells and Langerhans cells as part of the dendritic cell family', *Frontiers in Immunology*, 8, pp. 1–11.

Macke, L., Garritsen, H. S. P., Meyring, W., Hannig, H., Pägelow, U., Wörmann, B., Piechaczek, C., Geffers, R., Rohde, M., Lindenmaier, W. and Dittmar, K. E. J. (2010) 'Evaluating maturation and genetic modification of human dendritic cells in a new polyolefin cell culture bag system', *Transfusion*, 50(4), pp. 843–855.

Maglione, J. E., Moghanaki, D., Young, L. J. T., Manner, C. K., Ellies, L. G., Joseph, S. O., Nicholson, B., Cardiff, R. D. and MacLeod, C. L. (2001) 'Transgenic Polyoma Middle-T mice model premalignant mammary disease', *Cancer Research*, 61(22), pp. 8298–8305.

Malek, T. R. and Castro, I. (2010) 'Interleukin-2 receptor signaling: At the interface between tolerance and immunity', *Immunity*, 33(2), pp. 153–165.

Marelli-Berg, F. M., Cannella, L., Dazzi, F. and Mirenda, V. (2008) 'The highway code of T cell trafficking., *Journal of Pathology*, 214(2), pp. 179–189.

Margue, C., Dippel, W., Capesius, C., Mossong, J., Nathan, M., Giacchi, S., Scheiden, R. and Kieffer, N. (2006) 'Complete loss of PTEN expression as a possible early prognostic marker for prostate cancer metastasis', *International Journal of Cancer*, 120(6), pp. 1284–1292.

Markov, O. V, Mironova, N. L., Sennikov, S. V, Vlassov, V. V and Zenkova, M. A. (2015) 'Prophylactic dendritic cell-based vaccines efficiently inhibit metastases in murine metastatic melanoma', *PLoS ONE*, 10(9), pp. 1–21.

Marr, K. A. (2008) 'Fungal infections in hematopoietic stem cell transplant recipients', *Medical Mycology*, 46(4), pp. 293–302.

Marsland, B. J., Bättig, P., Bauer, M., Ruedl, C., Lässing, U., Beerli, R. R., Dietmeier, K., Ivanova, L., Pfister, T., Vogt, L., Nakano, H., Nembrini, C., Saudan, P., Kopf, M. and Bachmann, M. F. (2005) 'CCL19 and CCL21 induce a potent proinflammatory differentiation program in licensed dendritic cells', *Immunity*, 22(4), pp. 493–505.

Martin-Fontecha, A., Sebastiani, S., Höpken, U. E., Uguccioni, M., Lipp, M., Lanzavecchia, A. and Sallusto, F. (2003) 'Regulation of dendritic cell migration to the draining lymph node: impact on T lymphocyte traffic and priming', *Journal of Experimental Medicine*, 198(4), pp. 615–621.

Marzo, A. L., Lake, R. A., Lo, D., Sherman, L., McWilliam, A., Nelson, D., Robinson, B. W. and Scott, B. (1999) 'Tumor antigens are constitutively presented in the draining lymph nodes', *Journal of Immunology*, 162(10), pp. 5838–45.

Matheoud, D., Baey, C., Vimeux, L., Tempez, A., Valente, M., Louche, P., Le Bon, A., Hosmalin, A. and Feuillet, V. (2011) 'Dendritic cells crosspresent antigens from live B16 cells more efficiently than from apoptotic cells and protect from melanoma in a therapeutic model', *PloS One*, 6(4).

Matloubian, M., David, A., Engel, S., Ryan, J. E. and Cyster, J. G. (2000) 'A transmembrane CXC chemokine is a ligand for HIV-coreceptor', *Nature Immunology*, 1(4), pp. 298–304.

Matsuse, H., Yamagishi, T., Kodaka, N., Nakano, C., Fukushima, C., Obase, Y. and Mukae, H. (2017) 'Therapeutic modality of plasmacytoid dendritic cells in a murine model of Aspergillus fumigatus sensitized and infected asthma', *Allergy and Immunology*, 1(4), pp. 232–241.

Mckenna, H. J., Stocking, K. L., Miller, R. E., Brasel, K., De Smedt, T., Maraskovsky, E., Maliszewski, C. R., Lynch, D. H., Smith, J., Pulendran, B., Roux, E. R., Teepe, M., Lyman, S. D. and Peschon, J. J. (2000) 'Mice lacking flt3 ligand have deficient hematopoiesis affecting hematopoietic progenitor cells , dendritic cells , and natural killer cells', *Blood*, 95(11), pp. 3489–3497.

Melero, I., Hervas-Stubbs, S., Glennie, M., Pardoll, D. M. and Chen, L. (2007) 'Immunostimulatory monoclonal antibodies for cancer therapy', *Nature Reviews Cancer*, 7(2), pp. 95–106.

Melnikova, V. O., Bolshakov, S. V., Walker, C. and Ananthaswamy, H. N. (2004) 'Genomic alterations in spontaneous and carcinogen-induced murine melanoma cell lines', *Oncogene*, 23(13), pp. 2347–2356.

Merad, M., Ginhoux, F. and Collin, M. (2008) 'Origin, homeostasis and function of Langerhans cells and other langerin-expressing dendritic cells', *Nature Reviews Immunology*, 8(12), pp. 935–947.

Merad, M., Sathe, P., Helft, J., Miller, J. and Mortha, A. (2013) 'The dendritic cell lineage: ontogeny and function of dendritic cells and their subsets in the steady state and the inflamed setting.', *Annual review of immunology*, 31, pp. 563–604.

Miceli, M. H., Churay, T., Braun, T., Kauffman, C. A. and Couriel, D. R. (2017) 'Risk factors and outcomes of invasive fungal infections in allogeneic hematopoietic cell transplant recipients', *Mycopathologia*, 182(5–6), pp. 495–504.

Miller, A. B., Hoogstraten, B., Staquet, M. and Winkler, A. (1981) 'Reporting results of cancer treatment.', *Cancer*, 47(1), pp. 207–214.

Miller, E. and Bhardwaj, N. (2014) 'Advances in dendritic cell immunotherapies for HIV-1 infection', *Experimental Cell Research*, 14(11), pp. 1545–1549.

Moon, E. K., Carpenito, C., Sun, J., Wang, L. S., Predina, J., Jr, D. J. P., Riley, J. L., June, C. H. and Albelda, S. M. (2013) 'Expression of a functional CCR2 receptor enhances tumor localization and tumor eradication by retargeted human T cells expressing a mesothelin-specific chimeric antibody receptor', 17(14), pp. 4719–4730.

Morse, M. A., Niedzwiecki, D., Marshall, J. L., Garrett, C., Chang, D. Z., Aklilu, M., Crocenzi, T. S., Cole, D. J., Dessureault, S., Hobeika, A. C., Osada, T., Onaitis, M., Clary, B. M., Hsu, D., Devi, G. R., Bulusu, A., Annechiarico, R. P., Chadaram, V., Clay, T. M. and Lyerly, H. K. (2013) 'A randomized phase II study of immunization with dendritic cells modified with poxvectors encoding CEA and MUC1 compared with the same poxvectors plus GM-CSF for resected metastatic colorectal cancer', *Annals of surgery*, 258(6), pp. 879–86.

Mukherji, B., Chakraborty, N. G., Yamasaki, S., Okino, T., Yamase, H., Sporn, J. R., Kurtzman, S. K., Ergin, M. T., Ozols, J. and Meehan, J. (1995) 'Induction of antigen-specific cytolytic T cells in situ in human melanoma by immunization with synthetic peptide-pulsed autologous antigen presenting cells.', *Proceedings of the National Academy of Sciences*, 92(17), pp. 8078–82.

Muller, P. A. J. and Vousden, K. H. (2014) 'Mutant p53 in cancer: New functions and therapeutic opportunities', *Cancer Cell*, 25(3), pp. 304–317.

Mullins, D. W., Sheasley, S. L., Ream, R. M., Bullock, T. N. J., Fu, Y.-X. and Engelhard, V. H. (2003) 'Route of immunization with peptide-pulsed dendritic cells controls the distribution of memory and effector T cells in lymphoid tissues and determines the pattern of regional tumor control', *Journal of Experimental Medicine*, 198(7), pp. 1023–1034.

Muthuswamy, R., Mueller-Berghaus, J., Haberkorn, U., Reinhart, T. A., Schadendorf, D. and Kalinski, P. (2010) 'PGE2 transiently enhances DC expression of CCR7 but inhibits the ability of DCs to produce CCL19 and attract naive T cells', *Blood*, 116(9), pp. 1454–1459.

Neefjes, J., Jongsma, M. L. M., Paul, P. and Bakke, O. (2011) 'Towards a systems

understanding of MHC class I and MHC class II antigen presentation', *Nature Reviews Immunology*, 11, pp. 823–836.

Neller, M. A., López, J. A. and Schmidt, C. W. (2008) 'Antigens for cancer immunotherapy', *Seminars in Immunology*, 20(5), pp. 286–295.

Nestle, F. O. (2000) 'Dendritic cell vaccination for cancer therapy.', *Oncogene*, 19(56), pp. 6673–6679.

Nestle, F. O., Alijagic, S., Gilliet, M., Sun, Y., Grabbe, S., Dummer, R., Burg, G. and Schadendorf, D. (1998) 'Vaccination of melanoma patients with peptide- or tumor lysate-pulsed dendritic cells', *Nature Medicine*, 4(3), pp. 328–332.

Neubert, K., Lehmann, C., Heger, L., Baranska, A., Staedtler, A., Buchholz, V., Yamazaki, S., Heidkamp, G., Eissing, N., Zebroski, H., Nussenzweig, M., Nimmerjahn, F. and Dudziak, D. (2014) 'Antigen delivery to CD11c+CD8- dendritic cells induces protective immune responses against experimental melanoma in mice in vivo', *Journal of Immunology*, 192(12), pp. 5830–5838.

Nguyen, D. X., Bos, P. D. and Massagué, J. (2009) 'Metastasis: from dissemination to organ-specific colonization', *Nature Reviews Cancer*, 9, pp. 274–284.

Nibbs, R. J. and Graham, G. J. (2013) 'Immune regulation by atypical chemokine receptors', *Nature Reviews Immunology*, 13(11), pp. 815–829.

Nicolette, C. A., Healey, D., Tcherepanova, I., Whelton, P., Monesmith, T., Coombs, L., Finke, L. H., Whiteside, T. and Miesowicz, F. (2007) 'Dendritic cells for active immunotherapy: Optimizing design and manufacture in order to develop commercially and clinically viable products', *Vaccine*, 25.

O'Day, S. J., Hamid, O. and Urba, W. J. (2007) 'Targeting cytotoxic T-lymphocyte antigen-4 (CTLA-4): A novel strategy for the treatment of melanoma and other malignancies', *Cancer*, 110(12), pp. 2614–2627.

O'Garra, A., McEvoy, L. M. and Zlotnik, A. (1998) 'T-cell subsets: chemokine receptors guide the way', *Current Biology*, 8(18).

Ochando, J. C., Homma, C., Yang, Y., Hidalgo, A., Garin, A., Tacke, F., Angeli, V., Li, Y., Boros, P., Ding, Y., Jessberger, R., Trinchieri, G., Lira, S. A., Randolph, G. J. and Bromberg, J. S. (2006) 'Alloantigen-presenting plasmacytoid dendritic cells mediate tolerance to vascularized grafts', *Nature Immunology*, 7(6), pp. 652–662.

Okada, H., Kalinski, P., Ueda, R., Hoji, A., Kohanbash, G., Donegan, T. E., Mintz, A. H., Engh, J. A., Bartlett, D. L., Brown, C. K., Zeh, H., Holtzman, M. P., Reinhart, T. A., Whiteside, T. L., Butterfield, L. H., Hamilton, R. L., Potter, D. M., Pollack, I. F., Salazar, A. M. and Lieberman, F. S. (2011) 'Induction of CD8+ T-cell responses against novel glioma-associated antigen peptides and clinical activity by vaccinations with alpha-type 1 polarized dendritic cells and polyinosinic-polycytidylic acid stabilized by lysine and carboxymethylcellulose in patients with recurrent malignant glioma', *Journal of Clinical Oncology*, 29(3), pp. 330–336.

Ossendorp, F., Mengedé, E., Camps, M., Filius, R. and Melief, C. J. M. (1998) 'Specific T helper cell requirement for optimal induction of cytotoxic T lymphocytes against Major Histocompatibility Complex Class II negative tumors', *Journal of Experimental Medicine*, 187(5), pp. 693–702.

Otero, C., Groettrup, M. and Legler, D. F. (2006) 'Opposite fate of endocytosed CCR7 and its ligands: recycling versus degradation', *Journal of Immunology*, 177(4), pp. 2314–2323.

Ouwehand, K., Santegoets, S. J. A. M., Bruynzeel, D. P., Scheper, R. J., de Gruijl, T. D. and Gibbs, S. (2008) 'CXCL12 is essential for migration of activated Langerhans cells from epidermis to dermis', *European Journal of Immunology*, 38, pp. 3050–3059.

Overwijk, W. W. and Restifo, N. P. (2001) 'B16 as a mouse model for human melanoma', *Current Protocols in Immunology*, 20, pp. 1–33.

Palucka, A. K., Hideki, U., Fay, J. W. and Banchereau, J. (2007) 'Taming cancer by inducing immunity via dendritic cells', *Immunological Reviews*, 220, pp. 129–150.

Palucka, K. and Banchereau, J. (2013) 'Dendritic-Cell-Based therapeutic cancer vaccines', *Immunity*, 39(1), pp. 38–48.

Penna, G., Sozzani, S. and Adorini, L. (2001) 'Cutting Edge: Selective usage of chemokine teceptors by plasmacytoid dendritic cells', *Journal of Immunology*, 167(4), pp. 1862–1866.

Petit, S. J., Chayen, N. E. and Pease, J. E. (2008) 'Site-directed mutagenesis of the chemokine receptor CXCR6 suggests a novel paradigm for interactions with the ligand CXCL16', *European Journal of Immunology*, 38(8), pp. 2337–2350.

Piccioli, D., Sammicheli, C., Tavarini, S., Nuti, S., Frigimelica, E., Manetti, A. G. O., Nuccitelli, A., Aprea, S., Valentini, S., Borgogni, E., Wack, A. and Valiante, N. M. (2009) 'Human plasmacytoid dendritic cells are unresponsive to bacterial stimulation and require a novel type of cooperation with myeloid dendritic cells for maturation', *Blood*, 113, pp. 4232–4240.

Pollard, J. W. (2004) 'Tumour-educated macrophages promote tumour progression and metastasis', *Nature Reviews Cancer*, 4, pp. 223–229.

Poynard, T., McHutchison, J., Manns, M., Trepo, C., Lindsay, K., Goodman, Z., Ling, M. H. and Albrecht, J. (2002) 'Impact of pegylated interferon alfa-2b and ribavirin on liver fibrosis in patients with chronic hepatitis C', *Gastroenterology*, 122(5), pp. 1303–1313.

Precopio, M. L., Betts, M. R., Parrino, J., Price, D. A., Gostick, E., Ambrozak, D. R., Asher, T. E., Douek, D. C., Harari, A., Pantaleo, G., Bailer, R., Graham, B. S., Roederer, M. and Koup, R. A. (2007) 'Immunization with vaccinia virus induces polyfunctional and phenotypically distinctive CD8 [+] T cell responses', *The Journal of Experimental Medicine*, 204(6), pp. 1405–1416.

Prue, R. L., Vari, F., Radford, K. J., Tong, H., Hardy, M. Y., D'Rozario, R., Waterhouse, N. J., Rossetti, T., Coleman, R., Tracey, C., Goossen, H., Gounder, V., Crosbie, G., Hancock, S., Diaz-Guilas, S., Mainwaring, P., Swindle, P. and Hart, D. N. J. (2015) 'A phase I clinical trial of CD1c (BDCA-1)+ dendritic cells pulsed with HLA-A*0201 peptides for immunotherapy of metastatic hormone refractory prostate cancer', *Journal of Immunotherapy*, 38(2), pp. 71–76.

Qin, Z., Richter, G., Schuler, T., Ibe, S., Cao, X. and Blankenstein, T. (1998) 'B cells inhibit induction of T cell-dependent tumor immunity', *Nature Medicine*, 4(5), pp. 627–630.

Quillien, V., Moisan, A., Carsin, A., Lesimple, T., Lefeuvre, C., Adamski, H., Bertho, N., Devillers, A., Leberre, C. and Toujas, L. (2005) 'Biodistribution of radiolabelled human

dendritic cells injected by various routes', *European Journal of Nuclear Medicine and Molecular Imaging*, 32(7), pp. 731–741.

Randolph, G. J., Angeli, V. and Swartz, M. A. (2005) 'Dendritic-cell trafficking to lymph nodes through lymphatic vessels.', *Nature Reviews Immunology*, 5(8), pp. 617–28.

Randolph, G. J., Inaba, K., Robbiani, D. F., Steinman, R. M. and Muller, W. A. (1999) 'Differentiation of phagocytic monocytes into lymph node dendritic cells in vivo', *Immunity*, 11, pp. 753–761.

Ratzinger, G., Baggers, J., de Cos, M. A., Yuan, J., Dao, T., Reagan, J. L., Munz, C., Heller, G. and Young, J. W. (2004) 'Mature human Langerhans cells derived from CD34+ haematopoietic progenitors stimulate greater cytolytic T lymphocyte activity in the absence of bioactive IL-12p70, by either single peptide presentation or cross-priming, than do dermal-interstitial or monocyte-derived dendritic cells', *Journal of Immunology*, 173(4), pp. 2780–2791.

Ravandi, F. (2013) 'Relapsed acute myeloid leukemia: why is there no standard of care?', *Best Practice & Research: Clinical Haematology*, 26(3), pp. 253–259.

Redman, B. G., Alfred, E. C., Joel Whitfield, Peg Esper, Guihua Jiang, Thomas Braun, Blake Roessler and James, J. M. (2008) 'Phase Ib trial assessing autologous, tumor-pulsed dendritic cells as a vaccine administered with or without IL-2 in patients with metastatic melanoma', *Journal of Immunotherapy*, 31(6), pp. 591–598.

Restifo, N. P., Dudley, M. E. and Rosenberg, S. A. (2012) 'Adoptive immunotherapy for cancer: harnessing the T cell response', *Nature Reviews Immunology*. Nature Publishing Group, 12(4), pp. 269–281.

Ribas, A., Comin-Anduix, B., Chmielowski, B., Jalil, J., De La Rocha, P., McCannel, T. A., Ochoa, M. T., Seja, E., Villanueva, A., Oseguera, D. K., Straatsma, B. R., Cochran, A. J., Glaspy, J. A., Hui, L., Marincola, F. M., Wang, E., Economou, J. S. and Gomez-Navarro, J. (2009) 'Dendritic cell vaccination combined with CTLA4 blockade in patients with metastatic melanoma', *Clinical Cancer Research*, 15(19), pp. 6267–6276.

Ricupito, A., Grioni, M., Calcinotto, A., Michelini, R. H., Longhi, R., Mondino, A. and Bellone, M. (2013) 'Booster vaccinations against cancer are critical in prophylactic but

detrimental in therapeutic settings', *Cancer Research*, 73(12), pp. 3545–3554.

Ridgway, D. (2003) 'The first 1000 dendritic cell vaccinees', *Cancer Investigation*, 21(6), pp. 873–886.

Roberto, A., Castagna, L., Zanon, V., Bramanti, S., Crocchiolo, R., McLaren, J. E., Gandolfi, S., Tentorio, P., Sarina, B., Timofeeva, I., Santoro, A., Carlo-Stella, C., Bruno, B., Carniti, C., Corradini, P., Gostick, E., Ladell, K., Price, D. A., Roederer, M., Mavilio, D. and Lugli, E. (2015) 'Role of naive-derived T memory stem cells in T-cell reconstitution following allogeneic transplantation', *Blood*, 125(18), pp. 2855–2864.

Rogers, N. M., Isenberg, J. S. and Thomson, A. W. (2013) 'Plasmacytoid dendritic cells: No longer an enigma and now key to transplant tolerance?', *American Journal of Transplantation*, 13(5), pp. 1125–1133.

Rollins, B. J. (1997) 'Chemokines', *Blood*, 90(3), pp. 909–928.

Romani, N., Holzmann, S., Tripp, C. H., Koch, F. and Stoitzner, P. (2003) 'Langerhans cells - dendritic cells of the epidermis', *Apmis*, 111(7–8), pp. 725–740.

Rosenberg, S. A., Yang, J. C. and Restifo, N. P. (2004) 'Cancer immunotherapy: moving beyond current vaccines', *Nature Medicine*, 10(9), pp. 909–915.

Rosenberg, S. A., Yang, J. C., Sherry, R. M., Kammula, U. S., Marybeth, S., Phan, G. Q., Citrin, D. E., Restifo, N. P., Robbins, P. F., John, R., Morton, K. E., Laurencot, C. M., Steinberg, S. M., Donald, E. and Dudley, M. E. (2011) 'Durable complete responses in heavily pretreated patients with metastatic melanoma using T cell transfer immunotherapy', *Clinical Cancer Research*, 17(13), pp. 4550–4557.

Rot, A. and von Andrian, U. H. (2004) 'Chemokines in innate and adaptive host defense: basic chemokinese grammar for immune cells', *Annual Review of Immunology*, 22(1), pp. 891–928.

Routy, J. P., Boulassel, M.-R., Yassine-Diab, B., Nicolette, C. A., Healey, D., Jain, R., Landry, C., Yegorov, O., Tcherepanova, I. Y., Monesmith, T., Finke, L. and Sékaly, R.-P. (2010) 'Immunologic activity and safety of autologous HIV RNA-electroporated dendritic cells in HIV-1 infected patients receiving antiretroviral therapy', *Clinical Immunology*,

134(2), pp. 713–724.

Rowley, T. F. and Al-Shamkhani, A. (2004) 'Stimulation by soluble CD70 promotes strong primary and secondary CD8+ cytotoxic T cell responses in vivo', *The Journal of Immunology*, 172, pp. 6039–6046.

Roy, R. M. and Klein, B. S. (2012) 'Dendritic cells in anti-fungal immunity and vaccine design', *Cell Host & Microbe*, 11(5), pp. 436–446.

Ruffell, B., Chang-Strachan, D., Chan, V., Rosenbusch, A., Ho, C. M. T., Pryer, N., Daniel, D., Hwang, E. S., Rugo, H. S. and Coussens, L. M. (2014) 'Macrophage IL-10 blocks CD8+ T cell-dependent responses to chemotherapy by suppressing IL-12 expression in intratumoral dendritic cells', *Cancer Cell*, 26, pp. 623–637.

Sabado, R. L., Balan, S. and Bhardwaj, N. (2017) 'Dendritic cell-based immunotherapy', *Cell Research*, 27(1), pp. 74–95.

Sabado, R. L. and Bhardwaj, N. (2015) 'Dendritic-cell vaccines on the move', *Nature*, 519, pp. 300–301.

Saeki, H., Moore, A. M., Brown, M. J. and Hwang, S. T. (1999) 'Cutting Edge: Secondary Lymphoid- Tissue Chemokine (SLC) and CC Chemokine Receptor 7 (CCR7) participate in the emigration pathway of mature dendritic cells from the skin to regional lymph nodes.', *Journal of Immunology*, 162, pp. 2472–2475.

Salio, M., Cella, M., Vermi, W., Facchetti, F., Michael, J., Smith, C. L., Shepherd, D. and Colonna, M. (2003) 'Plasmacytoid dendritic cells prime IFN-y-secreting melanoma-specific CD8 lymphocytes and are found in primary melanoma lesions', *European Journal of Immunology*, 33, pp. 1052–1062.

Sallusto, F., Geginat, J. and Lanzavecchia, A. (2004) 'Central memory and effector memory T cell subsets: Function, generation and maitnenance', *Annual Review of Immunology*, 22, pp. 745–763.

Sallusto, F. and Lanzavecchia, A. (1994) 'Efficient presentation of soluble antigen by cultured human dendritic cells is maintained by granulocyte/macrophage colony-stimulating factor plus interleukin 4 and downregulated by tumour necrosis factor alpha.',

Journal of Experimental Medicine, 179, pp. 1109–1118.

Sallusto, F., Lenig, D., Forster, R., Lipp, M. and Lanzavecchia, A. (1999) 'Two subsets of memory T lymphocytes with distinct homing potentials', *Nature*, 401, pp. 708–712.

Sallusto, F., Palermo, B., Lenig, D., Miettinen, M., Matikainen, S., Julkunen, I., Forster, R., Burgstahler, R., Lipp, M. and Lanzavecchia, A. (1999) 'Distinct patterns and kinetics of chemokine production regulate dendritic cell function', *European Journal of Immunology*, 29(5), pp. 1617–1625.

Sallusto, F., Schaerli, P., Loetscher, P., Schaniel, C., Mackay, C. R., Qin, S. and Lanzavecchia, A. (1998) 'Rapid and coordinated switch in chemokine receptor expression during dendritic cell maturation', *European Journa of Immunology*, 28(9), pp. 2760–2769.

Salmon, H., Idoyaga, J., Rahman, A., Leboeuf, M., Remark, R., Jordan, S., Casanova-Acebes, M., Khudoynazarova, M., Agudo, J., Tung, N., Chakarov, S., Rivera, C., Hogstad, B., Bosenberg, M., Hashimoto, D., Gnjatic, S., Bhardwaj, N., Palucka, A. K., Brown, B. D., Brody, J., Ginhoux, F. and Merad, M. (2016) 'Expansion and activation of CD103+ dendritic cell progenitors at the tumor site enhances tumour responses to therapeutic PD-L1 and BRAF inhibtion', *Immunity*, 44, pp. 924–938.

Santos, P. M. and Butterfield, L. H. (2018) 'Dendritic cell–based cancer vaccines', *The Journal of Immunology*, 200(2), pp. 443–449.

Sathe, P., Pooley, J., Vremec, D., Mintern, J., Jin, J.-O., Wu, L., Kwak, J.-Y., Villadangos, J. A. and Shortman, K. (2011) 'The acquisition of antigen cross-presentation function by newly formed dendritic cells', *The Journal of Immunology*, 186, pp. 5184–5192.

Scandella, E., Men, Y., Gillessen, S., Förster, R. and Groettrup, M. (2002) 'Prostaglandin E2 is a key factor for CCR7 surface expression and migration of monocyte-derived dendritic cells', *Blood*, 100, pp. 1354–1361.

Schaft, N., Dörrie, J. and Nettelbeck, D. M. (2006) 'Nucleic Acid Transfer', in Lutz, M. B., Romani, N., and Steinkasserer, A. (eds) *Handbook of Dendritic Cells. Biology, Diseases and Therapies.* 3rd edn. Weinheim: Wiley-VCH, pp. 1143–1171.

Schaft, N., Dörrie, J., Thumann, P., Beck, V. E., Müller, I., Schultz, E. S., Kämpgen, E.,

Dieckmann, D. and Schuler, G. (2005) 'Generation of an optimized polyvalent monocyte-derived dendritic cell vaccine by transfection defined RNAs after rather than before maturation', *The Journal of Immunology*, 174, pp. 3087–3097.

Schmid, M. a, Takizawa, H., Baumjohann, D. R., Saito, Y. and Manz, M. G. (2000) 'Bone marrow dendritic cell progenitors sense pathogens via Toll-like receptors and subsequently migrate to inflamed lymph nodes', *Blood*, 118(18), pp. 4829–4840.

Schreibelt, G., Bol, K. F., Westdorp, H., Wimmers, F., Aarntzen, E. H. J. G., Boer, T. D., Rakt, M. W. M. M. Van De, Scharenborg, N. M., Boer, A. J. De, Pots, J. M., Olde, M. A. M., Oorschot, T. G. M. Van, Tel, J., Winkels, G., Petry, K., Blokx, W. A. M., Rossum, M. M. Van, Welzen, M. E. B., Mus, R. D. M., Croockewit, S. A. J., Koornstra, R. H. T., Jacobs, J. F. M., Kelderman, S., Blank, C. U., Gerritsen, W. R. and Punt, C. J. A. (2016) 'Effective clinical responses in metastatic melanoma patients after vaccination with primary myeloid dendritic cells', *Clinical Cancer Research*, 22(9), pp. 2155–2167.

Schreibelt, G., Tel, J., Sliepen, K. H. E. W. J., Benitez-Ribas, D., Figdor, C. G., Adema, G. J. and de Vries, I. J. M. (2010) 'Toll-like receptor expression and function in human dendritic cell subsets: Implications for dendritic cell-based anti-cancer immunotherapy', *Cancer Immunology, Immunotherapy*, 59, pp. 1573–1582.

Schreiber, R. D., Old, L. J. and Smyth, M. J. (2011) 'Cancer immunoediting: Integrating immunity's roles in cancer suppression and promotion.', *Science*, 331, pp. 1565–1571.

Schuler-Thurner, B., Dieckmann, D., Keikavoussi, P., Bender, A., Maczek, C., Jonuleit, H., Röder, C., Haendle, I., Leisgang, W., Dunbar, R., Cerundolo, V., von Den Driesch, P., Knop, J., Bröcker, E. B., Enk, A., Kämpgen, E. and Schuler, G. (2000) 'Mage-3 and influenza-matrix peptide-specific cytotoxic T cells are inducible in terminal stage HLA-A2.1+ melanoma patients by mature monocyte-derived dendritic cells', *Journal of Immunology*, 165(6), pp. 3492–6.

Seder, R. A., Darrah, P. A. and Roederer, M. (2008) 'T-cell quality in memory and protection: Implications for vaccine design', *Nature Reviews Immunology*, 8(4), pp. 247–258.

Seliger, B., Wollscheid, U., Momburg, F., Cells, B. M., Blankenstein, T. and Huber, C.

(2001) 'Characterization of the Major Histocompatibility Complex Class I deficiencies in B16 melanoma cells', *Cancer Research*, 61, pp. 1095–1099.

Seré, K., Baek, J. H., Ober-Blöbaum, J., Müller-Newen, G., Tacke, F., Yokota, Y., Zenke, M. and Hieronymus, T. (2012) 'Two distinct types of Langerhans cells populate the skin during steady state and inflammation', *Immunity*, 37, pp. 905–916.

Seth, S., Oberdorfer, L., Hyde, R., Hoff, K., Thies, V., Worbs, T., Schmitz, S. and Forster, R. (2011) 'CCR7 essentially contributes to the homing of plasmacytoid dendritic cells to lymph nodes under steady-state as well as inflammatory conditions', *The Journal of Immunology*, 186(6), pp. 3364–3372.

Shankaran, V., Ikeda, H., Bruce, A. T., White, J. M., Swanson, P. E., Old, L. J. and Schreiber, R. D. (2001) 'IFN gamma and lymphocytes prevent primary tumour development and shape tumour immunogenicity', *Nature*, 410, pp. 1107–1111.

Sharpe, A. H. and Freeman, G. J. (2002) 'The B7-CD28 superfamily', *Nature Reviews Immunology*, 2, pp. 26–28.

Shi, C. and Pamer, E. G. (2014) 'Monocyte recruitment during infection and inflammation', *Nature Reviews Immunology*, 11(11), pp. 762–774.

Shklovskaya, E., Terry, A. M., Guy, T. V, Buckley, A., Bolton, H. A., Zhu, E., Holst, J. and de St Groth, B. F. (2016) 'Tumour-specific CD4 T cells eradicate melanoma via indirect recognition of tumour-derived antigen', *Immunology and Cell Biology*, 94, pp. 1–40.

Shortman, K. and Naik, S. H. (2007) 'Steady-state and inflammatory dendritic-cell development', *Nature Reviews Immunology*, 7(1), pp. 19–30.

Siegal, F. P., Kadowaki, N., Shodell, M., Fitzgerald-Bocarsly, P., Shah, K., Ho, S., Antonenko, S. and Liu, Y.-J. (1999) 'The nature of the principal type I interferon-producing cells in human blood', *Science*, 284, pp. 1835–1837.

Siegel, P. M., Hardy, W. R. and Muller, W. J. (2000) 'Mammary gland neoplasia: Insights from transgenic mouse models', *BioEssays*, 22(6), pp. 554–563.

Slepnev, V. I. and De Camilli, P. (2000) 'Accessory factors in clathrin-dependent synaptic vesicle endocytosis', *Nature Reviews Neuroscience*, 1(3), pp. 161–172.

Small, E. J., Fratesi, P., Reese, D. M., Strang, G., Laus, R., Peshwa, M. V and Valone, F. H. (2000) 'Immunotherapy of hormone refractory prostate cancer with antigen-loaded dendritic cells', *Journal of Clinical Oncology*, 18(23), pp. 3894–3903.

Small, E. J., Schellhammer, P. F., Higano, C. S., Redfern, C. H., Nemunaitis, J. J., Valone, F. H., Verjee, S. S., Jones, L. A. and Hershberg, R. M. (2006) 'Placebo-controlled phase III trial of immunologic therapy with Sipuleucel-T (APC8015) in patients with metastatic, asymptomatic hormone refractory prostate cancer', *Journal of Clinical Oncology*, 24(19), pp. 3089–3094.

Snijders, A., Kalinski, P., Hilkens, C. M. U. and Kapsenberg, M. L. (1998) 'High-level IL-12 production by human dendritic cells requires two signals', *International Immunology*, 10(11), pp. 1593–1598.

Söbirk, S. K., Mörgelin, M., Egesten, A., Bates, P., Shannon, O. and Collin, M. (2013) 'Human chemokines as antimicrobial peptides with direct parasiticidal effect on Leishmania mexicana in vitro.', *PLoS ONE*, 8(3).

Song, N., Guo, H., Ren, J., Hao, S. and Wang, X. (2018) 'Synergistic anti-tumor effects of dasatinib and dendritic cell vaccine onmetastatic breast cancer in a mouse model', *Oncology Letters*, 15(5), pp. 6831–6838.

Sozzani, S., Vermi, W., Del Prete, A. and Facchetti, F. (2010) 'Trafficking properties of plasmacytoid dendritic cells in health and disease', *Trends in Immunology*, 31(7), pp. 270–277.

Spiekstra, S. W., Toebak, M. J., Sampat-Sardjoepersad, S., van Beek, P. J., Boorsma, D. M., Stoof, T. J., von Blomberg, B. M. E., Scheper, R. J., Bruynzeel, D. P., Rustemeyer, T. and Gibbs, S. (2005) 'Induction of cytokine (interleukin-1alpha and tumor necrosis factor-alpha) and chemokine (CCL20, CCL27, and CXCL8) alarm signals after allergen and irritant exposure', *Experimental Dermatology*, 14(2), pp. 109–116.

Spranger, S., Spaapen, R. M., Zha, Y., Williams, J., Meng, Y., Ha, T. T. and Gajewski, T. F. (2013) 'Up-regulation of PD-L1, IDO, and Tregs in the melanoma tumor

microenvironment is driven by CD8+ T cells', *Science Translational Medicine*, 5(200).

Stein, J. V. and Nombela-Arrieta, C. (2005) 'Chemokine control of lymphocyte trafficking: A general overview', *Immunology*, 116(1), pp. 1–12.

Steinman, R. M. and Cohn, Z. A. (1973) 'Identification of a novel cell type in peripheral lymphoid organs of mice.', *The Journal of Experimental Medicine*, 137, pp. 1142–1162.

Takeuchi, S. and Furue, M. (2007) 'Dendritic cells -ontogeny-', *Allergology international*, 56(3), pp. 215–223.

Teft, W. A., Kirchhof, M. G. and Madrenas, J. (2006) 'A molecular perspective of CTLA-4 function', *Annual Review of Immunology*, 24(1), pp. 65–97.

Tel, J., Aarntzen, E. H. J. G., Baba, T., Schreibelt, G., Schulte, B. M., Benitez-ribas, D., Boerman, O. C., Croockewit, S., Oyen, W. J. G., Rossum, M. Van, Winkels, G., Coulie, P. G., Punt, C. J. A., Figdor, C. G. and de Vries, I. J. M. (2013) 'Natural human plasmacytoid dendritic cells induce antigen-specific T cell responses in melanoma patients', *Cancer Research*, 73(3), pp. 1063–1076.

Thommen, D. S. and Schumacher, T. N. (2018) 'T cell dysfunction in cancer', *Cancer Cell*, 33(4), pp. 547–562.

Thurner, B., Haendle, I., Röder, C., Dieckmann, D., Keikavoussi, P., Jonuleit, H., Bender, A., Maczek, C., Schreiner, D., Driesch, P. V. Den, Bröcker, E. B., Steinman, R. M., Enk, A., Kämpgen, E. and Schuler, G. (1999) 'Vaccination with Mage-3A1 peptide-pulsed mature monocyte-derived dendritic cells expands specific cytotoxic T cells and induces regression of some metastases in advanced stage IV melanoma', *Journal of Experimental Medicine*, 190(11), pp. 1669–1678.

Timmons, J. J., Cohessy, S. and Wong, E. T. (2016) 'Injection of syngeneic murine melanoma cells to determine their metastatic potential in the lungs', *Journal of Visualized Experiments*, (111), pp. 4–7.

Trinchieri, G. (2003) 'Interleukin-12 and the regulation of innate resistance and adaptive immunity', *Nature Reviews Immunology*, 3(2), pp. 133–146.

Valladeau, J., Ravel, O., Dezutter-dambuyant, C., Moore, K., Kleijmeer, M., Liu, Y., Vincent, C., Schmitt, D., Davoust, J., Caux, C., Lebecque, S. and Saeland, S. (2000) 'Langerin, a novel C-type lectin specific to Langerhans cells, is an endocytic receptor that induces the formation of Birbeck granules', *Immunity*, 12, pp. 71–81.

Vanbervliet, B., Homey, B., Durand, I., Massacrier, C., Smina, A.-Y., Bouteiller, O. De, Vicari, A. and Caux, C. (2002) 'Sequential involvement of CCR2 and CCR6 ligands for immature dendritic cell recruitment: Possible role at inflamed epithelial surfaces.', *European Journal of Immunology*, 32, pp. 231–242.

Varol, C., Vallon-Eberhard, A., Elinav, E., Aychek, T., Shapira, Y., Luche, H., Fehling, H. J., Hardt, W. D., Shakhar, G. and Jung, S. (2009) 'Intestinal lamina propria dendritic cell subsets have different origin and functions', *Immunity*, 31(3), pp. 502–512.

Veglia, F. and Gabrilovich, D. I. (2017) 'Dendritic cells in cancer: The role revisited', *Current Opinion in Immunology*, 45, pp. 43–51.

Veldhoen, M., Hocking, R. J., Atkins, C. J., Locksley, R. M. and Stockinger, B. (2006) 'TGFbeta in the context of an inflammatory cytokine milieu supports de novo differentiation of IL-17-producing T cells', *Immunity*, 24, pp. 179–189.

Velten, F. W., Rambow, F., Metharom, P. and Goerdt, S. (2007) 'Enhanced T-cell activation and T-cell-dependent IL-2 production by CD83+, CD25high, CD43highhuman monocyte-derived dendritic cells', *Molecular Immunology*, 44(7), pp. 1555–1561.

Verdijk, P., Aarntzen, E. H. J. G., Lesterhuis, W. J., Boullart, A. C. I., Kok, E., Van Rossum, M. M., Strijk, S., Eijckeler, F., Bonenkamp, J. J., Jacobs, J. F. M., Blokx, W., Vankrieken, H. J. M., Joosten, I., Boerman, O. C., Oyen, W. J. G., Adema, G., Punt, C. J. A., Figdor, C. G. and De Vries, I. J. M. (2009) 'Limited amounts of dendritic cells migrate into the T-cell area of lymph nodes but have high immune activating potential in melanoma patients', *Clinical Cancer Research*, 15(7), pp. 2531–2540.

Vesely, M. D., Kershaw, M. H., Schreiber, R. D. and Smyth, M. J. (2011) 'Natural innate and adaptive immunity to cancer', *Annual Review of Immunology,* 29, pp. 235-271.

Vik-Mo, E. O., Nyakas, M., Mikkelsen, B. V, Moe, M. C., Due-Tønnesen, P., Suso, E. M. I., Sæbøe-Larssen, S., Sandberg, C., Brinchmann, J. E., Helseth, E., Rasmussen, A., Lote,

K., Aamdal, S., Gaudernack, G., Kvalheim, G. and Langmoen, I. A. (2013) 'Therapeutic vaccination against autologous cancer stem cells with mRNA-transfected dendritic cells in patients with glioblastoma', *Cancer Immunology & Immunotherapy*, 62, pp. 1499–1509.

Villablanca, E. J. and Mora, J. R. (2008) 'A two-step model for Langerhans cell migration to skin-draining LN', *European Journal of Immunology*, 38, pp. 2975–2980.

Villadangos, A. and Heath, W. R. (2005) 'Life cycle, migration and antigen presenting functions of spleen and lymph node dendritic cells : Limitations of the Langerhans cells paradigm', *Seminars in Immunology*, 17, pp. 262–272.

Villadangos, J. A. and Schnorrer, P. (2007) 'Intrinsic and cooperative antigen-presenting functions of dendritic-cell subsets in vivo', *Nature Reviews Immunology*, 7(7), pp. 543–555.

Villadangos, J. A. and Young, L. (2008) 'Antigen-presentation properties of plasmacytoid dendritic cells', *Immunity*, 29(3), pp. 352–361.

Villegas, F. R., Coca, S., Villarrubia, V. G., Jiménez, R., Chillón, M. J., Jareño, J., Zuil, M. and Callol, L. (2002) 'Prognostic significance of tumor infiltrating natural killer cells subset CD57 in patients with squamous cell lung cancer', *Lung Cancer*, 35(1), pp. 23–28.

Voigtländer, C., Rößner, S., Cierpka, E., Theiner, G., Wiethe, C., Menges, M., Schuler, G. and Lutz, M. B. (2006) 'Dendritic cells matured with TNF can be further activated in vitro and after subcutaneous injection in vivo which converts their tolerogenicity into immunogenicity', *Journal of Immunotherapy*, 29(4), pp. 407–415.

de Vries, I. J. M., Eggert, A. a O., Scharenborg, N. M., Vissers, J. L. M., Lesterhuis, W. J., Boerman, O. C., Punt, C. J. a, Adema, G. J. and Figdor, C. G. (2002) 'Phenotypical and functional characterization of clinical grade dendritic cells', *Journal of Immunotherapy*, 25(5), pp. 429–438.

de Vries, I. J. M., Krooshoop, D. J., Scharenborg, N. M., Lesterhuis, W. J., Diepstra, J., van Muijen, G. N., Strijk, S. P., Ruers, T. J., Boerman, O. C., Oyen, W. J., Adema, G. J., Punt, C. J. and Figdor, C. G. (2003) 'Effective migration of antigen-pulsed dendritic cells to lymph nodes in melanoma patients is determined by their maturation state', *Cancer Research*, 63, pp. 12–17.

de Vries, I. J. M., Lesterhuis, W. J., Scharenborg, N. M., Engelen, L. P. H., Ruiter, D. J., Gerritsen, M.-J. P., Croockewit, S., Britten, C. M., Torensma, R., Adema, G. J., Figdor, C. G. and Punt, C. J. A. (2003) 'Maturation of dendritic cells is a prerequisite for inducing immune responses in advanced melanoma patients', *Clinical Cancer Research*, 9(14), pp. 5091–100.

Vrisekoop, N., Drylewicz, J., Van Gent, R., Mugwagwa, T., Van Lelyveld, S. F. L., Veel, E., Otto, S. A., Ackermans, M. T., Vermeulen, J. N., Huidekoper, H. H., Prins, J. M., Miedema, F., de Boer, R. J., Tesselaar, K. and Borghans, J. A. M. (2015) 'Quantification of naive and memory T-cell turnover during HIV-1 infection', *AIDS*, 29(16), pp. 2071–2080.

Vyas, J. M., Van der Veen, A. G. and Ploegh, H. L. (2008) 'The known unknowns of antigen processing and presentation', *Nature Reviews Immunology*, 8, pp. 607–618.

Wang, Y., Szretter, K. J., Vermi, W., Gilfillan, S., Rossini, C., Cella, M., Barrow, A. D., Diamond, M. S. and Colonna, M. (2012) 'IL-34 is a tissue-restricted ligand of CSF1R required for the development of Langerhans cells and microglia', *Nature Immunology*, 13(8), pp. 753–760.

Weber, C., Weber, K. S. C., Klier, C., Gu, S., Wank, R., Horuk, R. and Nelson, P. J. (2001) 'Specialized roles of the chemokine receptors CCR1 and CCR5 in the recruitment of monocytes and Th1-like/CD45RO+ T cells.', *Blood*, 97(4), pp. 1144–1146.

Weber, M., Hauschild, R., Schwarz, J., Moussion, C., de Vries, I., Legler, D. F., Luther, S. A., Bollenbach, T., Sixt, M., Middleton, J., Bao, X., Alon, R., Butcher, E. C., Picker, L. J., Wei, S. H., Parker, I., Miller, M. J., Cahalan, M. D., Castellino, F., Ehrlich, L. I. R., Oh, D. Y., Weissman, I. L., Lewis, R. S., Boldajipour, B., Okada, T., McDonald, B., Alvarez, D., Vollmann, E. H., Andrian, U. H. von, Pflicke, H., Sixt, M., Förster, R., Link, A., Britschgi, M. R., Favre, S., Luther, S. A., Baluk, P., Levchenko, A., Iglesias, P. A., Schumann, K., Hirose, J., Paz, J. L. de, Müller, P., Schier, A. F., Bax, M., Vliet, S. J. van, Litjens, M., García-Vallejo, J. J., Kooyk, Y. van, Uchimura, K., Lämmermann, T., Petrie, R. J., Doyle, A. D., Yamada, K. M., Rot, A., Salanga, C. L., Handel, T. M., Haessler, U., Pisano, M., Wu, M., Swartz, M. A., Bélisle, J. M., Correia, J. P., Wiseman, P. W., Kennedy, T. E. and Costantino, S. (2013) 'Interstitial dendritic cell guidance by haptotactic chemokine gradients', *Science*, 339(6117), pp. 328–32.

Weigelt, B., Peterse, J. L. and Veer, L. J. Van (2005) 'Breast cancer metastasis: markers and models', *Nature Reviews Cancer*, 5, pp. 591–602.

Wendland, M., Czeloth, N., Mach, N., Malissen, B., Kremmer, E., Pabst, O. and Fo, R. (2007) 'CCR9 is a homing receptor for plasmacytoid dendritic cells to the small intestine', 104(15), pp. 1–6.

Wesley, J. D., Whitmore, J., Trager, J. and Sheikh, N. (2012) 'An overview of sipuleucel-T: Autologous cellular immunotherapy for prostate cancer', *Human Vaccines and Immunotherapeutics*, 8(4), pp. 512–519.

West, M. A., Prescott, A. R., Eskelinen, E. L., Ridley, A. J. and Watts, C. (2000) 'Rac is required for constitutive macropinocytosis by dendritic cells but does not control its downregulation', *Current Biology*, 10(14), pp. 839–848.

Whiteside, T. L. (2008) 'The tumor microenvironment and its role in promoting tumor growth', *Oncogene*, 27(45), pp. 5904–5912.

Wilgenhof, S., Corthals, J., Heirman, C., Van Baren, N., Lucas, S., Kvistborg, P., Thielemans, K. and Neyns, B. (2016) 'Phase II study of autologous monocyte-derived mRNA electroporated dendritic cells (TriMixDC-MEL) plus ipilimumab in patients with pretreated advanced melanoma', *Journal of Clinical Oncology*, 34(12), pp. 1330–1338.

Wimmers, F., De Haas, N., Scholzen, A., Schreibelt, G., Simonetti, E., Eleveld, M. J., Brouwers, H. M. L. M., Beldhuis-Valkis, M., Joosten, I., De Jonge, M. I., Gerritsen, W. R., De Vries, I. J. M., Diavatopoulos, D. A. and Jacobs, J. F. M. (2017) 'Monitoring of dynamic changes in keyhole limpet hemocyanin (KLH)-specific B cells in KLH-vaccinated cancer patients', *Scientific Reports*, 7, pp. 1–9.

Wyckoff, J., Wang, W., Lin, E. Y., Wang, Y., Pixley, F., Stanley, E. R., Graf, T., Pollard, J. W., Segall, J. and Condeelis, J. (2004) 'A paracrine loop between tumor cells and macrophages is required for tumor cell migration in mammary tumors', *Cancer Research*, 64, pp. 7022–7029.

Wykes, M., Pombo, A. and Jenkins, C. (2018) 'Dendritic cells interact directly with naive B lymphocytes to transfer antigen and initiate class switching in a primary T-dependent response', *Journal of Immunology*, 161, pp. 1313–1319.

Xing, F., Wang, J., Hu, M., Yu, Y., Chen, G. and Liu, J. (2011) 'Comparison of immature and mature bone marrow-derived dendritic cells by atomic force microscopy', *Nanoscale Research Letters*, 6, pp. 1–9.

Yang, S., Liu, F., Wang, Q. J., Rosenberg, S. A. and Morgan, R. A. (2011) 'The shedding of CD62L (L-selectin) regulates the acquisition of lytic activity in human tumor reactive T lymphocytes', *PLoS ONE*, 6(7).

Zabaleta, A., D'Avola, D., Echeverria, I., Llopiz, D., Silva, L., Villanueva, L., Riezu-Boj, J. I., Larrea, E., Pereboev, A., Lasarte, J. J., Rodriguez-Lago, I., Iñarrairaegui, M., Sangro, B., Prieto, J. and Sarobe, P. (2015) 'Clinical testing of a dendritic cell targeted therapeutic vaccine in patients with chronic hepatitis C virus infection', *Molecular Therapy - Methods & Clinical Development*, 2, p. 15006.

Zarour, H. M. (2016) 'Reversing T-cell dysfunction and exhaustion in cancer', *Clinical Cancer Research*, 22(8), pp. 1856–1864.

Zernecke, A., Liehn, E. A., Gao, J. L., Kuziel, W. A., Murphy, P. M. and Weber, C. (2006) 'Deficiency in CCR5 but not CCR1 protects against neointima formation in atherosclerosis-prone mice: Involvement of IL-10', *Blood*, 107(11), pp. 4240–4243.

Zhou, Y., Zhang, Y., Yao, Z., Moorman, J. P. and Jia, Z. (2012) 'Dendritic cell-based immunity and vaccination against hepatitis C virus infection', *Immunology*, 136(4), pp. 385–396.

Zigmond, E., Varol, C., Farache, J., Elmaliah, E., Satpathy, A. T., Friedlander, G., Mack, M., Shpigel, N., Boneca, I. G., Murphy, K. M., Shakhar, G., Halpern, Z. and Jung, S. (2012) 'Ly6Chi monocytes in the inflamed colon give rise to proinflammatory effector cells and migratory antigen-presenting cells', *Immunity*, 37(6), pp. 1076–1090.

Zlotnik, A. and Yoshie, O. (2000) 'Chemokines: a new classification system and their role in immunity', *Immunity*, 12(3), pp. 121–127.

Zobywalski, A., Javorovic, M., Frankenberger, B., Pohla, H., Kremmer, E., Bigalke, I. and Schendel, D. J. (2007) 'Generation of clinical grade dendritic cells with capacity to produce biologically active IL-12p70', *Journal of Translational Medicine*, 5, pp. 1–16.